Mellin-Barnes representations for multiloop Feynman integrals with applications to 2-loop electroweak Z boson studies

Dissertation
zur Erlangung des Doktorgrades
des Departments Physik
der Universität Hamburg

vorgelegt von
Ievgen Dubovyk

Hamburg
2019

Gutachter der Dissertation:	Prof. Dr. Sven-Olaf Moch Dr. Tord Riemann
Zusammensetzung der Prüfungskommission:	Prof. Dr. Sven-Olaf Moch Dr. Tord Riemann Prof. Dr. Robin Santra Prof. Dr. Elisabetta Gallo Dr. Jürgen Reuter
Vorsitzender des Prüfungsausschusses:	Prof. Dr. Robin Santra
Datum der Disputation:	14 Oct 2019
Vorsitzender des Fach-Promotionsausschusses:	Prof. Dr.Michael Potthoff
Leiter des Fachbereichs PHYSIK:	Prof. Dr. Wolfgang Hansen
Dekan der MIN-Fakultät:	Prof. Dr. Heinrich Graener

Eidesstattliche Versicherung

Hiermit versichere ich an Eides statt, die vorliegende Dissertationsschrift selbst verfasst und keine anderen als die angegebenen Hilfmittel und Quellen benutzt zu haben. Die eingereichte schriftliche Fassung entspricht der auf dem elektronischen Speichermedium. Die Dissertation wurde in der vorgelegten oder einer ähnlichen Form nicht schon einmal in einem früheren Promotionsverfahren angenommen oder als ungenügend beurteilt.

HK, 25.07.2019 Ievgen Dubovyk

Acknowledgments

Firstly, I would like to express my sincere gratitude to my advisor Dr. Tord Riemann for his continuous support during my Ph.D. study and related research, for his patience, motivation, and immense knowledge.

Besides my advisor, I would like to thank my collaborators Prof. Dr. Ayres Freitas and Prof. Dr. Janusz Gluza for help and discussions during our common projects. Especially to Janusz for his precious support without which it would be impossible to complete this research.

My sincere thank also goes to Prof. Dr. Sven-Olaf Moch for his great help during the final stage of preparation of this thesis.

Finally, I thank my officemate and collaborator Dr. Johann Usovitsch for stimulating discussions.

This work was supported by a research grant of Deutscher Akademischer Austauschdienst (DAAD) and by Deutsches Elektronensychrotron DESY.

Abstract

The calculation of radiative corrections beyond one loop level within the Standard Model of gauge interactions is necessary for precision phenomenological studies. Namely, the knowledge of higher order effects in physical observables constitutes the solid ground in search for potential and elusive non-standard Elementary Particle Physics. It also helps in deeper understanding of the Standard Model itself, and Quantum Field Theory in general.

The thesis is devoted to the development of methods and tools for the evaluation of complicated one- to three-loop massive tensor Feynman integrals using Mellin-Barnes representations and their application to the two-loop Z-boson decay studies.

In particular, a `Mathematica` package `PlanarityTest` has been created which tests planarity of a given integral, an important step in automatizing calculations which involves thousands of integrals. Second, the `AMBRE` project has been further developed for an automated construction of Mellin-Barnes integrals, optimized for minimal dimensionality of massive vertex Feynman integrals at the two- and three- loop levels. Here the bottleneck were non-planar diagrams, treated now with a dedicated use of the Cheng-Wu theorem. Finally, the numerical integration of multidimensional `MB` integrals in Minkowskian regions is carried out using the `MBnumerics` package. Altogether, the here developed `MB` packages define a huge step in a new direction of calculating effectively some classes of Feynman integrals.

Thanks to these developments and with support of the independent and to a large extent complementary method of sector decomposition, the 2-loop Feynman integrals for the so-called bosonic electroweak two-loop corrections to the fermionic Z-boson partial widths Γ_f, the Z-peak hadronic cross-section σ_{peak} and the Z-pole asymmetries for lepton pairs A_l and b-quarks A_b have been calculated. In this way it became possible to complete the electroweak two-loop corrections to the Z boson pseudoobservables.

The method and results presented here give a chance for the precise calculation of the Standard Model corrections to the Z boson pseudoobservables beyond the 2-loop level. This accuracy level of theoretical calculations will be needed in order not to limit the physical interpretation of the measurements at future electron-positron colliders.

Zusammenfassung

Für phänomenologische Präzisionsstudien ist die Berechnung von Strahlungskorrekturen jenseits des Einschleifenniveaus im Standardmodell der Eichwechselwirkungen notwendig. Die Effekte höherer Schleifen-Ordnungen in physikalischen Observablen bilden die Grundlage bei der Suche nach möglicherweise vorhandenen und schwer fassbaren Phänomenen jenseits des Standardmodells der Elementarteilchenphysik. Ihr Studium hilft auch beim tieferen Verständnis des Standardmodells selbst, wie auch dem der Quantenfeldtheorie allgemein.

Die Dissertation widmet sich der Entwicklung von Methoden und Tools zur Berechnung von komplizierten massiven Tensor-Feynmanintegralen mit ein bis drei Schleifen unter Verwendung von Mellin-Barnes-Darstellungen und ihrer Anwendung auf Z-Boson-Zerfallsstudien mit Zwei-Schleifen-Genauigkeit.

Insbesondere wurde das Mathematica-Paket PlanarityTest erstellt, mit dem die Planarität eines gegebenen Integrals getestet werden kann, ein wichtiger Schritt bei der Automatisierung von Berechnungen mit tausenden von Integralen.

Zweitens wurde das AMBRE-Projekt für die automatische Konstruktion von Mellin-Barnes (MB)-Integralen minimaler Dimensionalität für massive Vertex-Feynmanintegrale mit zwei und drei Schleifen weiterentwickelt. Problematisch waren hier nicht-planare Integrale, die nun mit einem dedizierten Gebrauch des Theorems von Cheng und Wu behandelt werden.

Schließlich wird die numerische Integration von mehrdimensionalen MB-Integralen direkt in der (problematischen) Minkowski-Kinematik mit dem MBnumerics-Paket durchgeführt.

Insgesamt definieren die hier entwickelten Mellin-Barnes-Softwarepakete einen entscheidenden Fortschritt bei Ausarbeitung einer neue Methode der effektiven Berechnung einiger Klassen von Feynman-Integralen jenseits des Einschleifenniveaus, zudem in der Minkowski-Kinematik. Dank dieser Entwicklungen, und unter Anwendung einer anderen, unabhängigen und weitgehend komplementären Methode, der Sektorzerlegung von Feynmanintegralen, konnten die 2-Schleifen-Feynmanintegrale für so genannte bosonische elektroschwache Zwei-Schleifen-Korrekturen der fermionischen Z-Boson-Partialbreiten Γ_f, des Z-Peak-Wirkungsquerschnitts σ^{peak} und die Asymmetrien A_l, A_b für Leptonen und b-quarks berechnet werden.

Mit den Resultaten der Dissertation wurde die Berechnung der elektroschwachen Zwei-Schleifen-Korrekturen für die Pseudo-Observablen des Z-Bosons abgeschlossen.

Die hier vorgestellte Methode und die bisherigen Resultate stellen zugleich eine Grundlage dar für die Berechnung der Standardmodell-Korrekturen zu den Pseudo-Observablen des Z-Bosons jenseits des 2-Schleifen-Niveaus. Dieses theoretische Genauigkeitsniveau ist erforderlich, um die physikalische Interpretation von Messungen an zukünftigen Electron-Positron-Beschleunigern nicht einzuschränken.

List of papers

This thesis is based on the following papers and conference contributions:

1. A. Blondel, et al., Standard Model Theory for the FCC-ee: The Tera-Z, in: Mini Workshop on Precision EW and QCD Calculations for the FCC Studies: Methods and Techniques. CERN, Geneva, Switzerland, January 12-13, 2018. (Contributions to the Chapter B and sections E.3, E.4). arXiv:1809.01830.

2. J. Usovitsch, I. Dubovyk, T. Riemann, MBnumerics: Numerical integration of Mellin-Barnes integrals in physical regions, PoS LL2018 (2018) 046. arXiv:1810.04580.

3. I. Dubovyk, A. Freitas, J. Gluza, T. Riemann, J. Usovitsch, Complete electroweak two-loop corrections to Z boson production and decay, Phys. Lett. B783 (2018) 86–94. arXiv:1804.10236, doi:10.1016/j.physletb.2018.06.037.

4. I. Dubovyk, A. Freitas, J. Gluza, T. Riemann, J. Usovitsch, Electroweak Bosonic 2-loop Corrections to the Z-pole Precision Observables, Acta Phys. Polon. B48 (2017) 2321. doi:10.5506/APhysPolB.48.2321.

5. I. Dubovyk, J. Gluza, T. Jelinski, T. Riemann, J. Usovitsch, New prospects for the numerical calculation of Mellin-Barnes integrals in Minkowskian kinematics, Acta Phys. Polon. B48 (2017) 995. arXiv:1704.02288, doi:10.5506/APhysPolB.48.995.

6. I. Dubovyk, A. Freitas, J. Gluza, T. Riemann, J. Usovitsch, 30 years, some 700 integrals, and 1 dessert, or: Electroweak two-loop corrections to the Z$\bar{b}$b vertex, PoS LL2016 (2016) 075. arXiv:1610.07059, doi:10.22323/1.260.0075.

7. I. Dubovyk, A. Freitas, J. Gluza, T. Riemann, J. Usovitsch, The two-loop electroweak bosonic corrections to $\sin^2\theta^{\rm b}_{\rm eff}$, Phys. Lett. B762 (2016) 184–189. arXiv:1607.08375, doi:10.1016/j.physletb.2016.09.012.

8. I. Dubovyk, J. Gluza, T. Riemann, J. Usovitsch, Numerical integration of massive two-loop Mellin-Barnes integrals in Minkowskian regions, PoS LL2016 (2016) 034. arXiv:1607.07538, doi:10.22323/1.260.0034.

9. I. Dubovyk, J. Gluza, T. Riemann, Non-planar Feynman diagrams and Mellin-Barnes representations with `AMBRE 3.0`, J. Phys. Conf. Ser. 608 (1) (2015) 012070. doi:10.1088/1742-6596/608/1/012070.

10. J. Blümlein, I. Dubovyk, J. Gluza, M. Ochman, C. G. Raab, T. Riemann, C. Schneider, Non-planar Feynman integrals, Mellin-Barnes representations, multiple sums, PoS LL2014 (2014) 052. arXiv:1407.7832, doi:10.22323/1.211.0052.

11. K. Bielas, I. Dubovyk, J. Gluza, T. Riemann, Some Remarks on Non-planar Feynman Diagrams, Acta Phys. Polon. B44 (11) (2013) 2249–2255. arXiv:1312.5603, doi:10.5506/APhysPolB.44.2249.

Contents

Chapter 1

Introduction

Progress in physics relies heavily on increasing the precision of our statements about physical phenomena. Otherwise it would be impossible to identify yet uncharted areas of research or scrutinize experimental findings. For this reason a deeper and more precise understanding of the well established and basic theory of elementary particles, known as the Standard Model (SM) of particle physics [1–4] is needed. We know already much about the Standard Model. It comprises three of the four known basic interactions, while gravity is still out of a correct quantum description. The Standard Model determines a definite number of elementary particles. In 2012, it proved to be finally consistent by the discovery of a scalar particle: the Higgs boson, found at the Large Hadron Collider (LHC) at CERN [5, 6]. The search for this elusive particle was strongly guided by precise calculations derived from the Standard Model. In contemporary particle physics most of the experimental groups are searching for signals of New Physics. But these, if being there, cannot be recognized if the so-called well-known Standard Model is not understood with absolute safety in the actual set-up. And so it is no wonder that many of the New Physics searches are, in the essence, a highly advanced analysis of data in the Standard Model. This is exactly where this Phd thesis is placed, developing new tools and methods for the calculation of radiative corrections in Quantum Field Theory, used in the end in a non-trivial two-loop electroweak Standard Model calculation of radiative corrections to the Z-boson decay.

Calculation of radiative corrections has a long tradition and hits foundations of Quantum Electrodynamics in first instant [7, 8]. Historically it began in the late fourties of the last century when the $2s - 2p$ shift in the energy level of the hydrogen atom was measured by Lamb and Retherford [9]. For the first time the role of radiative corrections in precise measurements was evident - in this specific case the self-energy of a bound electron revealed its nature in Bethe's calculation [10]. Just several months later, Schwinger's calculation of the electron's magnetic moment explained the measured deviations from Dirac's predictions due to another radiative effect: the QED one-loop vertex [11]. Several decades later radiative corrections became essential in precise tests of the renormalizable SM.

The first non-trivial study of electroweak (EW) loop effects was the calculation of the large quadratic top quark mass contribution to the Z and W propagators at one-loop order [12]. The complete one-loop corrections to the Z decay parameters were derived in [13–16]. Through the years of LEP and SLC studies, the effects of EW corrections

became visible in global fits of the SM parameters [17–20]. Global fits to EW precision measurements allowed to predict the mass of the top quark and the Higgs boson prior to their discoveries at Tevatron in 1995 [21,22] and at the LHC in 2012 [6]. The first proposal was [23].

Feynman diagrams at the NNLO level depend on complicated integrals which in turn depend on many masses and kinematical invariants, hard to solve analytically. We know already that elliptic functions can appear here, see the contributions of S. Weinzierl, J. Henn, V. Smirnov in [24]. There is no closed mathematical theory for their solution beyond the NLO approximation. To calculate the NNLO Feynman integrals, technically, we consider concepts taken from complex analysis and formulated by the mathematicians R. H. Mellin and E. W. Barnes at the turn of 20th century [25,26]. Their method of integral representations in the complex plane, translated properly to the modern description of Feynman integrals by Symanzik polynomials [27,28] offers a way to solve many classes of Feynman integrals that describe scattering processes of quantum particles, in particular higher-order perturbative effects.

Mellin-Barnes (`MB`) representations are used in particle physics to describe Feynman diagrams in a complex plain [27]. The method has been applied in many projects. For instance, in [29] `MB` integrals have been used for the direct numerical calculation of electroweak corrections in the Minkowskian region. In [30–32] the method of direct calculation of the phase-space and angular integrals have been developed by this method. Finally, in [33] `MB` representations have been transformed to the form of constraint Dirac delta function and parametric integrals instead of nested sums. Public packages for `MB` integral representations can be found at the hepforge site MBtools [34].

In this thesis suitable methods and algorithms for the `MB` studies are developed and implemented to the calculation of subtle quantum effects at Z-boson decay [35–38]. This process was one of the most important decays studied at LEP (Large Electron-Positron collider) at CERN where millions of such events were observed. In establishing the SM, studies of the Z boson effects were especially important. This particle was being produced resonantly at the first Large Electron-Positron collider (LEP1) with an at that time huge statistics of about 10^6 events. Its decays generated various particles studied in great detail. This allowed to determine many of the electroweak parameters very precisely; sometimes about a factor of 100 better than before.

In 2013 a European Strategy was established for particle physics which states that "There is a strong scientific case for an electron-positron collider, complementary to the LHC, that can study properties of Higgs boson and other particles with unprecedented precision and whose energy can be upgraded" [39].

When it will be built, it will have a comparable impact like LEP1, because the new high-luminosity machines will be again more accurate in measurements as LEP was, this time by a factor 20-100. Such huge shrinkage of errors can be typically 10-30 times smaller than the present level of theory errors [40]. That is why theoretical calculations must improve considerably and three-loop (NNNLO) calculations become a "must" for the future high-luminosity lepton colliders [24,41]. It is a final goal for a next decade or so in theory, which we would like to accomplish in the calculation of Standard Model effects at the three-loop order of perturbative Quantum Field Theory in Z-boson decay studies. This gigantic

level of accuracy gives corrections to physical electroweak observables at the less than per mil level. Such corrections are sensitive to the masses of the top quark, the gauge bosons $W^{\pm}, Z^0$, the Higgs boson, and, potentially, new virtual states of matter which go beyond the Standard Model. Then, there is no wonder that the study of the Z-boson resonance is considered as an option in future colliders.

The Z resonance is formed by electron-positron collisions at a center-of-mass energy around 91 GeV. Up to 5×10^{12} Z-boson decays are planned to be observed at projected future e^+e^- machines (ILC, CEPC, FCC-ee) running at the Z-boson resonance [42–47]. These statistics are several orders of magnitude larger than at LEP and would lead to very accurate experimental measurements of EWPOs if the systematic experimental error can be hold appropriately small too. This in turn means, that theoretical predictions must be also very precise, of the order of 3- to 4-loop QCD and EW effects [40].

In this thesis a substantial step in this direction has been made. First, some new, advanced tools are developed for multiloop integrals evaluation within the MB approach. Second, thanks to them, the two-loop calculation of the most difficult bosonic two-loop diagrams to the Z-boson decay [36, 38] are worked out. In this way the Standard Model electroweak two-loop corrections are completed and now the focus can be directed on the next, NNNLO order of loop calculation.

Outline of the Thesis

This thesis is organized as follows. In the next chapter, the basics of the electroweak theory in the context of Z-boson decay studies are given. In chapter 3 the present status of methods of loop calculations is discussed. In chapters 4 and 5 the main results of the PhD thesis are given. Namely, in chapter 4 optimal ways of construction of MB representations are discussed, while in chapter 4 results for the calculation of parameters connected with Z-boson physics are presented. In the last chapter 6 a summary and an outline of further studies are discussed. In the Appendix additional material is gathered, namely, in sections 7.1 and 7.2 notations for the packages AMBREv3 and PlanarityTest are specified. In section 7.3 classes of two-loop Z-boson Feynman diagrams are shown and the complete set of the evaluated MB integrals for the Z-boson leptonic decay is tabularized. The thesis finishes with the bibliography.

Chapter 2

Standard Model of electroweak interactions and Z-boson physics

2.1 Emergence of the $SU(2)_L \times U(1)_Y$ gauge group of electroweak interactions

In 2018 we have celebrated 50 years of emergence of the Standard Model of electroweak interactions [48]. The fundamental work in which the $SU(2)_L \times U(1)_Y$ gauge group appeared for the first time is by S. Weinberg [4]. Not accidently, it was titled "A Model of Leptons", because a primary concern at that time was about leptons, the number of lepton families as well as their interactions and the understanding of the mass spectrum. For that, spontaneous symmetry breaking with emergence of Goldstone bosons which can be eliminated by introducing gauge fields was a crucial idea. At that time it was not clear if such a model, based on the $SU(2)_L \times U(1)_Y$ gauge group, is renormalizable. In the two and half pages paper by Weinberg we can find the remark that "The model may be renormalizable" and a question: "if this model is renormalizable, what happens when we extend it to include the couplings of $\vec{A}_\mu$ and B_μ to the hadrons?" Renormalizability of the model with massive gauge bosons was worked out in 1972 [49, 50]. However, if Z-bosons are necessary and do exist in nature was still not clear. Z-bosons were considered also in another seminal paper by S.L. Glashow [2], who found considerations on "partial symmetries" academic, "without decisive experimental consequence". The solution came in 1973 with the Gargamelle experiment at CERN, where neutral currents have been detected [51], indicating indirectly the necessity for neutral gauge bosons. This discovery marked the real emergence of the SM, where the experiment has chosen the correct path offered by theory, based on the $SU(2)_L \times U(1)_Y$ gauge group. This is not a minimal solution. E.g. the $O(3)$ group gives 3 degrees of freedom, without need for another neutral boson, apart from the photon. Having it at hand, with a proof that the theory is renormalizable and the neutral currents exist, a further natural consequence of research progress was to find $W^\pm$ and Z bosons directly in experiments. The discovery of the W and Z bosons came ten years later in proton-antiproton collisions by the UA1 and UA2 collaborations at CERN in Geneva [52–55]. In 1984 Carlo Rubbia shared the Nobel Prize in Physics with Simon van der Meer "for their decisive contributions to the large project, which led to the discovery of the field particles W

and Z, communicators of weak interaction" [56]. What followed, a dedicated and detailed study of the gauge boson physics was a subject of the Large Electron-Positron LEP collider project at CERN [57, 58] as well as of the SLAC Linear Collider project in the USA, which both started operation in 1989 [59].

Since 1989 the LEP accelarator worked for seven years in the Z-resonance region of center of mass energy around 91 GeV (within plus minus 3 GeV around the Z pole), accumulating some 17 million Z-boson decays [60].

The recorded experimental data allowed for a detailed investigation of the electroweak sector of the SM. For that, from the theoretical side, a precise calculation of radiative corrections to the parameters of the SM is needed. The first non-trivial study of electroweak (EW) loop effects was the calculation of the large quadratic top quark mass contribution to the Z and W propagators at one-loop order [12]. A few years later, the on-shell renormalization scheme as it is used today [61–63] and the notion of effective weak mixing angles [64–66] were introduced, and the scheme was used for calculations of the $W^{\pm}$ and Z boson masses [67]. The complete one-loop corrections to the Z decay parameters were derived in Refs. [13–16], and those to the $W^{\pm}$ width in Refs. [15, 68, 69]. Through the years of LEP and SLC studies, the effects of EW corrections became visible in global fits of the SM parameters [17–20]. Global fits to EW precision measurements allowed to predict the mass of the top quark and the Higgs boson prior to their discoveries at Tevatron in 1995 [21, 22] and at the LHC in 2012 [6].

To make these precise findings in the electroweak sector of the SM theory possible properly, many issues must be investigated, one of them are extractions of the background connected with pure QED effects (radiated photons), also known as deconvolution. Similarly, the issue of initial final interference and contributions of box-type diagrams to Z-boson cross-sections vertices, co-existence of photon and Z-boson exchange in e^+e^- collision must be understood properly. The methodology of disentangling pure QED corrections from pure electroweak corrections at the amplitude level, summing up soft photon effects to infinite order (exponentiation) and adding QED collinear non-soft corrections order by order (independently of the EW part) is well known and numerically implemented in the KKMC program [70]. This program includes so far QED non-soft corrections to second order and pure EW corrections up to first order (with some 2nd order EW improvements, QCD etc.) using the weak library DIZET [71] of ZFITTER [72]. For recent discussions of these issues, also in the context of experimental demands of future accelerators, see [40]. The global fits [60] were done with ZFITTER.

In the next section definitions of so-called electroweak pseudo-observables (EWPOs) are given. The prefix "*pseudo-* underlines the fact that they are extracted and deconvoluted from initial physical data in the sense just mentioned above. Pseudo-observables make it possible to focus on theoretical calculations, order by order in perturbation theory, of pure electroweak and QCD virtual effects.

2.2 Z-boson physics and EWPOs

The LEP data allowed to determine a large amount of electroweak observables with very high precision through measurements of the Z line-shape and of cross section asymmetries,

joined by high-precision parity-violating asymmetries measured at the SLC [60].

The Z-boson properties are determined from measurements of fermion pair production in electron-positron e^+e^- collisions, $e^+e^- \to f\bar{f}$, on the Z-pole, i.e., for $\sqrt{s} \sim 91$ GeV. To isolate the physics of the Z-boson, the typical set of EWPOs is defined in terms of the deconvoluted cross-section $\sigma_f(s)$, where the effect of initial- and final-state photon radiation and from s-channel photon and double-boson (box) exchange has been removed.

We consider the following set of quantities, at LEP coded in the ZFITTER programme [72–74]:

$$\sigma^0_{\rm had} = \sigma[e^+e^- \to \text{hadrons}]_{s=M_Z^2}, \tag{2.1}$$

$$\Gamma_Z = \sum_f \Gamma[Z \to f\bar{f}], \tag{2.2}$$

$$R_\ell = \frac{\Gamma[Z \to \text{hadrons}]}{\Gamma[Z \to \ell^+\ell^-]}, \quad \ell = e, \mu, \tau, \tag{2.3}$$

$$R_q = \frac{\Gamma[Z \to q\bar{q}]}{\Gamma[Z \to \text{hadrons}]}, \quad q = u, d, s, c, b. \tag{2.4}$$

The remaining EWPOs are cross section asymmetries, measured at the Z pole. The forward-backward asymmetry is defined as

$$A^f_{\rm FB} = \frac{\sigma_f\left[\theta < \frac{\pi}{2}\right] - \sigma_f\left[\theta > \frac{\pi}{2}\right]}{\sigma_f\left[\theta < \frac{\pi}{2}\right] + \sigma_f\left[\theta > \frac{\pi}{2}\right]}, \tag{2.5}$$

where θ is the scattering angle between the incoming e^- and the outgoing f. It can be approximately written as a product of two terms (for more precise discussion, see [40, 75])

$$A^f_{\rm FB} = \frac{3}{4}\mathcal{A}_e\mathcal{A}_f, \tag{2.6}$$

with

$$\mathcal{A}_f = \frac{2\Re e\frac{v_f}{a_f}}{1 + \left(\Re e\frac{v_f}{a_f}\right)^2} = \frac{1 - 4|Q_f|\sin^2\theta^{\rm f}_{\rm eff}}{1 - 4|Q_f|\sin^2\theta^{\rm f}_{\rm eff} + 8(Q_f\sin^2\theta^{\rm f}_{\rm eff})^2}. \tag{2.7}$$

The $\sin^2\theta^{\rm f}_{\rm eff}$ defined above,

$$\frac{v_f}{a_f} = 1 - 4|Q_f|\sin^2\theta^{\rm f}_{\rm eff}, \tag{2.8}$$

describes the ratio of the vector and axial-vector couplings of an (on-shell) Z boson to fermions. This definition is called the *effective weak mixing angle*, henceforth denoted as $\sin^2\theta^{f,\rm eff}_W$. It gathers the net contributions from the radiative corrections to the ratio v_f/a_f.

It is one of several possible definitions, two other ones considered in theory are described by

(i) the ratio of the two gauge couplings,

$$g'/g = c_W/s_W, \tag{2.9}$$

usual in the $\overline{\rm MS}$ renormalization scheme.

(ii) the ratio of two gauge boson (on-shell) masses,

$$s_W^2 = 1 - \frac{M_W^2}{M_Z^2}. \tag{2.10}$$

There are various renormalization schemes connected with the above choices. We will consider (ii), corrected by radiative corrections, in chapter 5 where results for $\sin^2\theta_W^{b,\rm eff}$ will be given.

The most precise measurements of $A_{\rm FB}^f$ have been obtained for leptonic and bottom-quark final states (f $= \ell$, b). In the presence of polarized electron beams, one can also measure the parity-violating left-right asymmetry

$$A_{\rm LR}^f \;=\; \frac{\sigma_f\,[P_e<0] - \sigma_f\,[P_e>0]}{\sigma_f\,[P_e<0] + \sigma_f\,[P_e>0]} = \mathcal{A}_e|P_e|. \tag{2.11}$$

Here P_e denotes the polarization degree of the incident electrons where $P_e < 0$ ($P_e > 0$) refers to left-handed (right-handed) polarizations, respectively. Since $A_{\rm FB}^f$ and $A_{\rm LR}^f$ are defined as normalized asymmetries, they do not depend on (parity conserving) initial- and final-state QED and QCD radiation effects. Here it is assumed that any issues related to the determination of the experimental acceptance have been evaluated and unfolded using Monte-Carlo methods.

As in this thesis we will discuss complete results for the 2-loop EW corrections to $\sin^2\theta_{\rm eff}^{\rm f}$ and other EWPOs defined in (2.1)-(2.4), let us sketch shortly connection between $A_{\rm FB}^f$ and σ_f in (2.5) and $\sin^2\theta_{\rm eff}^{\rm f}$ and the effective vector v_f and axial a_f couplings, and inspect (2.7) more carefully.

First, asymmetries like $A_{\rm FB}^f$ or $A_{\rm LR}^f$ are defined through de-convoluted cross sections σ_f. Writing σ_f in terms of amplitudes, ratio of v_f and a_f couplings emerges in (2.7). For a calculation of EWPOs (2.1)-(2.4), v_f and a_f must be known separately.

These couplings are understood as effective, built up from loop diagrams corresponding to perturbative order by order terms of the Z-boson decay amplitude. This is schematically shown in Fig.2.12. The $V_\mu^{Zb\bar b}$ represents an effective Z-boson form factor.

$$V_\mu^{Zb\bar b} = \gamma_\mu[v_b(s) + \; a_b(s)\gamma_5] = \cdots + \overbrace{\underbrace{\quad + \quad}_{\rm planar,non-planar}}^{\rm fermionic,bosonic} + \cdots \tag{2.12}$$

We should stress that the scheme presented here is highly simplified, as initial-final factorization of vertices in the $e^+e^- \to f\bar f$ process is assumed in (2.6). This is only true at

tree level as already 1-loop box diagrams make a non-separable connection between initial and final states. In addition the photon exchange disturbs the picture of the pure Z-boson resonance[1]. However, these effects were under control at LEP [77]. That state of the art presumable will be not enough for a precise determination of EWPOs at FCC-ee. For more details see [40].

Due to the above approximations, the EWPOs are related to the effective vector and axial-vector couplings of the Z boson to a fermion type f, v_f and a_f. These, in turn, are related to the weak mixing angle according to

$$\frac{v_f}{a_f} = 1 - 4|Q_f| \sin^2 \theta_W^{f,\mathrm{eff}} \equiv 1 - 4|Q_f| s_W^2 \, \kappa_f^Z, \tag{2.13}$$

where from now on (2.10) holds. The $s_W^2 = 1 - M_W^2/M_Z^2$ is the on-shell weak mixing angle, and κ_f^Z captures the effect of radiative corrections (in Born approximation, $\kappa_f^B = 1$). The form factor κ_f^Z was introduced by A. Sirlin [61, 64]. Even though s_W^2 is not a (pseudo-)observable in itself, it is a useful quantity for discussions of the EWPOs with higher order corrections.

In (2.12) so-called fermionic corrections are mentioned. These include the self-energy insertions of fermionic loops. Bosonic diagrams are these without such closed fermion looops. Planar and non-planar diagrams will be discussed in chapter 4 where MB integral representations of Feynman diagrams will be investigated.

	$\delta\Gamma_Z$ [MeV]	δR_l [10^{-4}]	δR_b [10^{-5}]	$\delta \sin^2\theta^{\mathrm{l}}_{\mathrm{eff}}$ [10^{-6}]	$\delta \sin^2\theta^{\mathrm{b}}_{\mathrm{eff}}$ [10^{-5}]	$\delta\sigma^0_{\mathrm{had}}$ [pb]
Present EWPO errors						
EXP1	2.3	250	66	160	1600	37
TH1	0.5	50	15	45	5	6
FCC-ee-Z EWPO error estimations						
EXP2	0.1	10	$2 \div 6$	6	70	4

Table 2.1: Present total experimental errors EXP1 [60] and, estimated in 2014 [78–80], theoretical errors TH1 for selected EW observables. EXP2 gives corresponding experimental error estimations for the FCC-ee Z-resonance mode, see Tab. 1 in [40].

Tab. 2.1 shows the FCC-ee experimental goals for the basic EWPOs. As is evident from the table, the theoretical uncertainties of the current results TH1 are safely below the current experimental errors EXP1. Typically, present errors are at the level of permill or less, e.g. exact value for Γ_Z is 2495.2 MeV, error EXP1 is 2.3 MeV [60] while future FCC-ee-Z experimental goal is determination of Γ_Z with precision of 0.1 MeV. Exact numbers for other EWPOs can be found in [40]. Note that the presently estimated theoretical error (0.5 MeV) is five times larger than the expected FCC-ee-Z accuracy (0.1 MeV). This error is without taking into account the calculated in this thesis two-loop α^2_{bos}. For how the situation changes after that is discussed in chapter 5. Theoretical error estimations take

[1] Thinking about new physics possibilities, additional hard terms may come from potential Z-prime s-channel contributions which should be formally considered with care [40, 76].

into account some ways in which so far not calculated higher order radiative corrections are guessed. This will be also discussed in more details in chapter 5.

Chapter 3

Analytical and numerical methods of loop calculations

Many of the computer languages were developed initially to help particle physics calculations [81]. It started basically with numerical programs like `FORTRAN` (1957, John Backus, IBM) and algebraic software as `Reduce` (started in 1963 by Anthony Hearn), Schoonschip (started in 1967 by Martinus J. G. Veltman) or the now widely used `Form` package (initial released in 1989 by Jos Vermaseren). For historical introduction on numerical and algebra systems and software development, see [81].

Perturbative calculation techniques developed rapidly in the last decades, both due to the immense computer power available, and also due to the better mathematical understanding of the theory of Feynman integrals. Nonetheless, there is still an important lack on the theory side of solutions which make possible the mass production of electroweak massive results at the so-called NNLO level. More and better universal tools and packages for numerical and analytical calculations are also needed [40].

In this chapter we summarize recent developments and strategies in calculations of higher order radiative corrections.

Since the 1980s, many multiloop methods to calculate higher order corrections in particle physics have been developed, based on tree-duality, generalized unitarity, reductions at the integrand level, improved diagrammatic approach and recursion relations applied to higher-rank tensor integrals, simultaneous numerical integration of amplitudes over the phase space and the loop momentum, contour deformations, expansions by regions, sector-decomposition, dispersion relations, differential equations, summation of series, Mellin-Barnes representations, and so on. Many methods aim at direct Feynman integral calculations. For general reviews see [24, 27, 82–85].

To solve the integrals, analytical methods can be used, though they exhibit natural limitations when sophisticated integrals with many parameters appear. Such a situation takes place in gauge theories like the electroweak-QCD Standard Model. However, concerning analytical approaches to Feynman integrals, we should especially appreciate recent progress in the differential equation method [86–89], which got a push in 2013 [90] followed by latest corresponding software and ideas [28, 91–95]. Here further progress in developing integration-by-parts (IBP) concepts is also very important [96, 97].

The problem to be solved here is a topic of considerable complexity and importance at the frontier of theoretical high energy physics: *The numerical evaluation of complicated massive beyond one-loop Feynman integrals in Minkowskian space-time.* We aim at shifting the numerically well controlled quantum loop order, usually from NLO (next-to leading order) in electroweak physics with several mass scales and/or many external legs to NNLO (next-to-next-to leading order). So far a lot has been done for that at NLO order. Many NLO programs allow to consider processes automatically and in a numerical way. Different systems and libraries of reductions of $(2 \to n)$ amplitudes have been developed, like FeynArts/FormCalc, [98, 99], CutTools, [100], Blackhat, [101], Helac-1loop, [102], NGluon, [103], Samurai, [104], Madloop, [105], Golem95C, [106], GoSam, [107], OpenLoops, [108], PJFry [109]. Some of them are necessarily supported by basic one-loop integral libraries FF, OneLOop, QCDloop, Collier [110–113].

Going beyond the one-loop calculations in Minkowskian regions, the situation is quite different. Minkowskian regions means: The physical kinematical conditions, which are met in e^+e^- colliders. There are technical obstructions in the calculation of Feynman integrals in this setting due to threshold effects, singularities, on-shellness or several mass parameters involved. The convergence of the numerical evaluation of amplitudes in this physical regime is a hard challenge. With increasing number of loops and increasing number of mass and momentum scales, it becomes more difficult to compute these corrections analytically, or even semi-analytically. Certainly non-analytical methods will become even more important in the future.

There are presently only few public programs for the numerical integration of integrals beyond the NLO level. `NICODEMOS` [114] is based on contour deformations. There are also complete programs dedicated specifically to the precise calculation of two-loop self-energy diagrams [115, 116].

In 2014 the only advanced automatic numerical two-loop method in Minkowskian kinematics was sector decomposition [117, 118], where a complex contour deformation of the Feynman parameter integrals is implemented in the publicly available numerical packages `FIESTA 3` [119] (since 2013) and `SecDec 2` [120] (since 2012), followed by pySecDec [121]. However, working during last years on the completion of two-loop corrections to the Z-boson decay, we observed serious convergence problems for some classes of integrals both with `SecDec` and `FIESTA`, which enforced us to go in another direction. The integrals calculated are very challenging. There are (i) up to four dimensionless scales at $s = M_Z^2$ with a variance of masses M_Z, M_W, m_t, M_H involved and (ii) intricate threshold and on-shell effects where contour deformation fails. To tackle these problems, the semi-numerical approach to the calculation of Feynman integrals based on Mellin-Barnes representations has been developed. In our calculations MB method is used with many suitable packages gathered in what we call the MB-suite. An important part of our MB-suite is the `AMBRE` project. It includes among others the construction of MB representations [36, 122–124]) and the recognition of planarity of Feynman diagrams [125, 126] with the corresponding packages `Mathematica AMBRE.m` and `PlanarityTest.m`. They are the heart of the developed procedure. For the extraction of ϵ-singularities in dimensional regularization of multiloop integrals, the `MB.m` [127] and MBresolve.m [128] packages are used. As they offer also the possibility of numerical integrations in Euclidean kinematics, they are used also

as a numerical cross check of analytical results for multiloop integrals. In our calculations the new numerical Mellin-Barnes (MB) approach to the calculation of multiloop and massive Feynman integrals is used, with the MB package `MBnumerics.m` [129, 130], section E6 in [40]. This package has being developed in the last years and is devoted to the direct calculation of MB integrals in Minkowskian kinematics, solving so far untouchable regions of precision physics. Most of the mentioned packages can be found at the hep-forge web page `MBtools` [34]. The main concern of this thesis is about developing MB-integral representations with some numerical ideas, worked out by the author during last years. Details will be presented in the next two chapters.

Let us finally remark that there is large activity in the field and other methods are also under development [40]. Let us mention direct numerical calculations of Feynman integrals in d=4 [131–136] or calculations based on the unitarity method, with first two-loop numerical evaluations [137,138]. There are also efforts to understand space of functions related to Feynman multiloop integrals, which go beyond harmonic polylogarithms [40].

For more details on methods and tools in multi-loop calculations,see recent reports [40, 139] and further references therein.

Chapter 4

Construction of Mellin-Barnes representations

4.1 Introduction

The Mellin-Barnes transformation of multidimensional Feynman integrals to multivariable complex contour integrations [25, 26] has been used in many particle physics calculations. In the first applications [140, 141] this kind of transformation has been applied directly to propagators in the loop integrals, changing "momenta^2–mass^2" terms into ratios of momenta and masses in the complex plane. Nowadays, a more efficient and systematic treatment of multiloop integrals goes by expressing Feynman integrals by the Symanzik polynomials F and U [34, 82, 122, 123, 127, 128, 141–145], for which the general MB formula is applied

$$\begin{aligned}\frac{1}{(A_1+\ldots+A_n)^\lambda} &= \frac{1}{\Gamma(\lambda)}\frac{1}{(2\pi i)^{n-1}}\int_{c_1-i\infty}^{c_1+i\infty} dz_1\cdots\int_{c_2-i\infty}^{c_2+i\infty} dz_2\ldots dz_n \prod_{i=2}^{n} A_i^{z_i} \\ &\times A_1^{-\lambda-z_2-\ldots-z_n}\Gamma(\lambda+z_2+\ldots+z_n)\prod_{i=2}^{n}\Gamma(-z_i). \qquad (4.1)\end{aligned}$$

In what follows, we will call (4.1) the MB-master formula.

As we can see, n additive terms lead to $n-1$ complex integrals. The A_i terms correspond to kinematical parameters of the integral. A typical simple example is the 1-dimensional singular part of the 1-loop massive QED vertex [36, 127, 146], which has the following form $\sim \int dz(-s)^{-z}\Gamma^3(-z)\Gamma(1+z)\Gamma^{-1}(-2z)$. Choosing properly the contour of integration can make the annoying oscillatory behavior of the term $(-s)^{-z}$ small and controllable (for $s>0$, so Minkowskian kinematic [35, 36]). Furthermore, the Gamma functions Γ exhibit singularities either, and make the task of integral evaluations highly non-trivial. These are typical problems when treating MB integrals numerically.

The construction of MB integrals through Symanzik polynomials is automatized in the AMBRE project [36, 122–124]. Using it with MB.m or MBresolve.m, IR and UV divergences can be extracted and regulated multidimensional MB integrals are obtained [82]. On the webpage [147] more auxiliary packages with examples related to MB calculations can be found.

AMBRE is the project devoted to the efficient and automatic construction of Mellin-Barnes representations of Feynman multiloop integrals in $d = n - 2\epsilon$ dimensions, $n \in \mathbb{Z}$. In the main parts it includes: (i) Proper treatment of non-planar diagrams with up to three loops; (ii) Treatment of tensor integrals. It is still a developing project. It helps to solve Feynman integrals converted into MB form analytically, numerically, or in more complex cases semi-analytically.

In [122] the basic Mathematica toolkit AMBRE has been described which derives Mellin-Barnes (MB) representations for Feynman integrals in $d = 4 - 2\varepsilon$ dimensions. It can be applied for tadpoles as well as for multi-leg multi-loop scalar and tensor integrals. However, this package works fine only for planar Feynman diagrams as it uses a loop-by-loop approach (LA) where Feynman parameter integrations and the Mellin-Barnes basic relation (Eq.(1) in [122]) which changes sums of terms into integrals over complex space are made subsequently for each internal momenta of the Feynman integrals. In a planar case, there is no mismatch, and after each step, in the next step the effective (planar) diagram appears. In additions, the LA has an advantage because at each step we consider actually one loop subloops, so $U = 1$ results automatically, and we have to care only about polynomial F which should be factorized in the most efficient way in order to arrive a minimal dimension of the constructed MB integral.

In nonplanar cases, the situation is more complicated. Here not necessarily after each step well defined connected diagrams can be drawn. As a consequence, not all vertices conserve momenta [126]. That is why in this case a more natural is an approach where F and U polynomials are treated in one shot for all internal momenta, however, this global approach (GA) has the price that F and U polynomials are more complicated. Still, the GA approach to F and U polynomials has an important property: The polynomials are homogeneous functions of the Feynman parameters of some given degree, depending on the underlying topology. So, we can systematically rescale Feynman variables and in turn, change Dirac's delta function under the integral which defines the area of the integrand. In this case, the Dirac delta function can be used on a restricted subset of Feynman parameters [148]. This is, in fact, the Cheng-Wu theorem [82]. The problem is for which variables the factorization of the polynomials will be most efficient leading to the smallest number of terms and finally, leading to the lowest dimensionality of the MB complex integrals.

In practice, a choice between the LA and GA strategies for a given integral aiming at the lowest MB dimensionality of integrals seems not to be unique. For instance, in a massless case of the non-planar two-loop diagram, a minimal fourfold MB representation was derived starting from the global Feynman parameter representation [143]. On the other hand, in the massive case, it appears that the LA is more efficient, an eightfold MB representation can be obtained [149]. In this case none less than a tenfold MB representation is known if we start from global Feynman parameters [149]. As discussed there and in [150], those representations may differ also as far as the regularization of singularities is concerned. This is another subtlety which shows up after a construction of MB representations in real applications.

Taking into account all the above details, it is clear why it is not easy to get a general and efficient program for the construction of a broad class of MB representations.

The MB-suite comprises several tools and the calculational procedure goes for dimen-

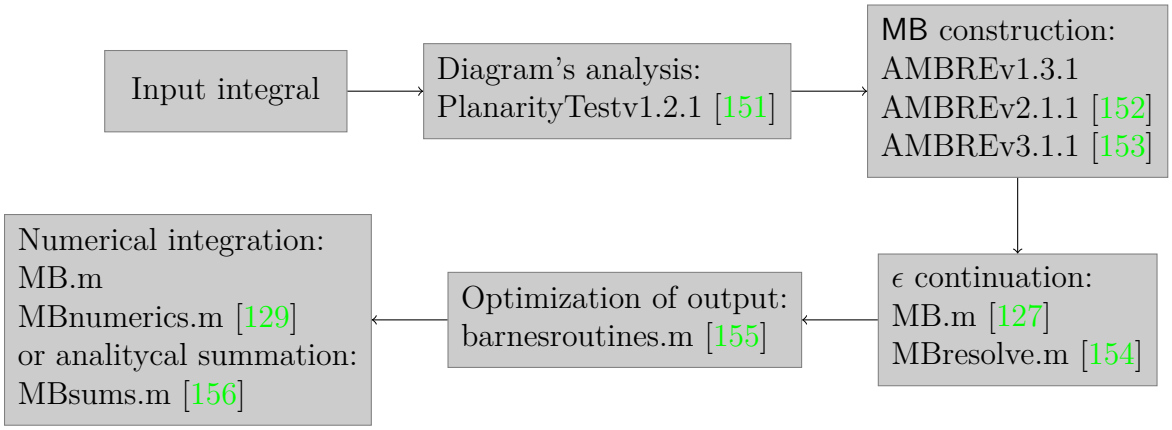

Figure 4.1: The operational sequence of the MB-suite. This flowchart shows the main steps and the correponding software to produce a Mellin-Barnes representation of a Feynman integral and perform its numerical or analytical solution.

sionally regulated Feynman integrals in the momentum space like this:

(i) Transform Feynman integrals into those expressed by Feynman parameters (textbook knowledge).

(ii) Use a proper version of the `AMBRE` package [36, 122, 123, 157] controlled for automation procedures by the `PlanarityTest.m` package [125, 126] – transform them into Mellin-Barnes integrals, valid at initial parameters which include a finite shift ϵ of dimension, $d = 4 - 2\epsilon$, and with original integration paths parallel to the imaginary axis.

(iii) Use `MB.m` or `MBresolve.m` [127, 128] – perform an analytical continuation in ϵ, approaching small ϵ.

(iv) — expand the Mellin-Barnes integrals as series in small ϵ;

(v) Use `barnesroutines.m` from the MBtools web page [147] — perform simplifications using Barnes lemmas.

(vi) At this stage the original representation of the Feynman integral in terms of several finite `MB`-integrals has been formulated. One may now start to calculate them, either analytically or numerically, or in a mixed approach.

In sufficiently complicated situations, only numerics can be applied.

(vii) Use `MBnumerics.m` [158] to perform parametric integrations of the `MB`-integrals along the paths defined in step (iii), thereby applying a variety of techniques: integration variable transformations, reparameterizations, contour deformations, contour shifts and whatsoever. For the parameter integrations, CUHRE of the package CUBA [159] is used.

All these details are the subject of this thesis and their developments are described in the next sections.

To some extent, we gave descriptions of AMBRE details before in [35–37]. Useful, important MB literature is [29, 35–37, 83, 122, 123, 126–128, 143, 146, 148, 151–156, 160–172].

4.2 Feynman parameterization and related issues

In this section we will show the equivalence of Feynman and Schwinger parametrizations, consider properties of Feynman graphs with the F and U Symanzik polynomials, introduce the Cheng-Wu theorem, a very useful theorem in the GA in the construction of MB representations. Further, tensor integrals are introduced in a form which is translated into AMBRE. Then, the issue of planarity identification of given integral is discussed, examples of the PlanarityTest package will be given in Appendix 7.2. Next subsections deal with MB constructions within the LA and GA. An efficient application of first and second Barnes lemmas is discussed. Then specific 2-loop and 3-loop examples of MB integral constructions will be given, with focus on the Z-boson two-loop and three-loop cases. Finally, the numerical integration of MB integrals is discussed.

4.2.1 Feynman and Schwinger parameters

A general Feynman loop integral $G(X)$ can be defined in $d = 4 - 2\epsilon$ dimensions, in the sense of dimensional regularization, in the following way

$$G(X) = \frac{1}{(i\pi^{d/2})^L} \int \frac{d^d k_1 \dots d^d k_L \, X(k_1, \dots, k_L)}{D_1^{\nu_1} \dots D_i^{\nu_i} \dots D_N^{\nu_N}}, \tag{4.2}$$

where the L denotes number of loops and D_i stands for particles propagators, which can have in principle arbitrary powers ν_i. $X(k_1, \dots, k_L)$ is a tensor numerator of some rank. In particular, in case of a scalar integral $X = 1$.

A single Feynman propagator D_i is of the form

$$D_i = q_i^2 - m_i^2 + i\delta = \left[\sum_{l=1}^{L} c_i^l k_l + \sum_{e=1}^{E} d_i^e p_e\right]^2 - m_i^2 + i\delta, \tag{4.3}$$

where k_l and p_e are internal and external momenta respectively. The c_i^l, $d_i^e \in [-1, 1]$ are integer coefficients and depend on a particular topology.

To proceed further we introduce here a generalized Feynman parameters representation

$$\frac{1}{D_1^{n_1} D_2^{n_2} \dots D_N^{n_N}} = \frac{\Gamma(n_1 + \dots + n_N)}{\Gamma(n_1) \dots \Gamma(n_N)} \int_0^1 dx_1 \dots \int_0^1 dx_N \frac{x_1^{n_1-1} \dots x_N^{n_N-1} \delta(1 - x_1 - \dots - x_m)}{(x_1 D_1 + \dots + x_N D_N)^{N_\nu}} \tag{4.4}$$

with $N_\nu = n_1 + \dots + n_N$.

In parallel to this one can also use a so called Schwinger or α-parameter representation

$$\frac{1}{D_1^{n_1} D_2^{n_2} \dots D_N^{n_N}} = \frac{i^{-N_\nu}}{\Gamma(n_1) \dots \Gamma(n_N)} \int_0^\infty d\alpha_1 \dots \int_0^\infty d\alpha_N \alpha_1^{n_1-1} \dots \alpha_N^{n_N-1} e^{i[\alpha_1 D_1 + \dots + \alpha_N D_N]}. \tag{4.5}$$

Here it will be useful to show connection between these two representation; we will use it later in order to prove some important relations. Using the identity

$$1 = \int\limits_0^\infty \frac{d\lambda}{\lambda} \delta\left(1 - \frac{1}{\lambda}\sum_{i=1}^N \alpha_i\right) \tag{4.6}$$

and changing variables from α_i to $\alpha_i = \lambda x_i$, one can find

$$\frac{1}{D_1^{n_1} D_2^{n_2} \dots D_N^{n_N}} = \frac{i^{-N_\nu}}{\Gamma(n_1)\dots\Gamma(n_N)} \int\limits_0^\infty dx_1 \dots \int\limits_0^\infty dx_N \, x_1^{n_1-1} \dots x_N^{n_N-1} \times \int\limits_0^\infty d\lambda \lambda^{N_\nu - 1} \delta\left(1 - \sum_{i=1}^N x_i\right) e^{i\lambda \sum\limits_{i=1}^N x_i D_i}. \tag{4.7}$$

Integrating over λ we come to the Feynman parameters representation

$$\frac{1}{D_1^{n_1} D_2^{n_2} \dots D_N^{n_N}} = \frac{\Gamma(n_1 + \dots + n_N)}{\Gamma(n_1)\dots\Gamma(n_N)} \int\limits_0^\infty dx_1 \dots \int\limits_0^\infty dx_N \frac{x_1^{n_1-1} \dots x_N^{n_N-1} \delta(1 - \sum\limits_{i=1}^N x_i)}{\left(\sum\limits_{i=1}^N x_i D_i\right)^{N_\nu}}. \tag{4.8}$$

Note that all x_i are positive while the sum of x_i must be unity. Therefore the integration region can be limited:

$$0 < x_i < 1 \;\; \Leftrightarrow \;\; 0 < x_i < \infty.$$

Let us now consider the momentum dependent function

$$m^2(\vec{x}) = x_1 D_1 + \dots + x_i D_i + \dots + x_N D_N = k_i M_{ij} k_j - 2 Q_j k_j + J \tag{4.9}$$

with a M – $(L \times L)$-matrix, $Q = Q(x_i, p_e)$ – an L-vector and $J = J(x_i x_j, m_i^2, p_{e_i} p_{e_j})$.

Before integration over loop momenta one has to perform several preparatory steps:

- Shift momenta in order to remove linear terms in k,

$$k \to k + M^{-1} Q \Rightarrow m^2 = kMk - QM^{-1}Q + J. \tag{4.10}$$

  Shifts leave the integrals unchanged.

- Wick rotations – transform Minkowskian space into Euclidean for all loop momenta:

$$k_0 \to i k_0; \;\; k_j \to k_j (1 \leqslant j \leqslant d-1) \Rightarrow k^2 \to -k^2; \;\; d^d k \to i d^d k.$$

- Diagonalization of the matrix M:

$$k^\dagger M k = (V(x)k)^\dagger V(x) M V(x)^{-1} V(x) k; \;\; k(x) = V(x) k;$$

$$V M V^{-1} = M_{\text{diag}}; \;\; (V^\dagger = V^{-1})$$

$$kMk \Rightarrow k(x)M_{\rm diag}k(x) = \sum_{i=1}^{L} \alpha_i k_i^2(x).$$

The operation leaves integrals unchanged.

After such manipulations the function m^2 has the following form:

$$m^2 = -\sum_{i=1}^{L} \alpha_i k_i^2 - QM^{-1}Q + J.$$

- Rescale of k_i:

$$k_i \to \sqrt{\alpha_i} k_i \Rightarrow d^d k_i \to (\alpha_i)^{-d/2} d^d k_i \quad \text{and} \quad \prod_{i=1}^{L} \alpha_i = \det M.$$

Finally, we obtain

$$G(X) = (-1)^{N_\nu}(i)^L (\det M)^{-d/2} \frac{\Gamma(N_\nu)}{\prod\limits_{i=1}^{N} \Gamma(n_i)} \int dx_1 \dots dx_N \int \frac{Dk_1 \dots Dk_L}{\left(\sum\limits_{i=1}^{L} k_i^2 + QM^{-1}Q - J\right)^{N_\nu}}$$

or

$$G(X) = \frac{(i)^{L-N_\nu}(\det M)^{-d/2}}{\prod\limits_{i=1}^{N} \Gamma(n_i)} \int d\alpha_1 \dots d\alpha_N \int Dk_1 \dots Dk_L \; e^{-i\left(\sum\limits_{i=1}^{L} k_i^2 + QM^{-1}Q - J\right)},$$

with $Dk = \dfrac{d^d k}{i\pi^{d/2}}$.

Now the integration over loop momenta can be done in a simple way

$$i^L \int \frac{Dk_1 \dots Dk_L}{\left(\sum\limits_{i=1}^{L} k_i^2 + \mu^2(x)\right)^{N_\nu}} = \frac{\Gamma\left(N_\nu - \frac{d}{2}L\right)}{\Gamma(N_\nu)} \frac{1}{(\mu^2(x))^{N_\nu - \frac{dL}{2}}}, \tag{4.11}$$

$$\int Dk_1 \dots Dk_L e^{-i\left(\sum\limits_{i=1}^{L} k_i^2 + \mu^2(\alpha)\right)} = (-i)^{-Ld/2} e^{-i\mu^2(\alpha)}, \tag{4.12}$$

with $\mu^2(x) = QM^{-1}Q - J$. The final result is

$$G(X) = \frac{(-1)^{N_\nu}\Gamma\left(N_\nu - \frac{d}{2}L\right)}{\prod\limits_{i=1}^{N} \Gamma(n_i)} \int \prod_{j=1}^{N} dx_j \; x_j^{n_j - 1} \delta(1 - \sum_{i=1}^{N} x_i) \frac{U(x)^{N_\nu - d(L+1)/2}}{F(x)^{N_\nu - dL/2}} \tag{4.13}$$

or

$$G(X) = \frac{(i)^{L-N_\nu}(detM)^{-d/2}}{\prod\limits_{i=1}^{N} \Gamma(n_i)} \int \prod_{j=1}^{N} d\alpha_j \; \alpha_j^{n_j - 1} e^{-i\frac{F(\alpha)}{U(\alpha)}}, \tag{4.14}$$

where we introduced two Feynman graph polynomials U and F

$$m^2 = kMk - 2Qk + J \Leftrightarrow \; U = \det M,$$
$$F = -\det M \; J + QM^T Q. \tag{4.15}$$

4.2.2 Graph polynomials and their properties

The functions U and F are called graph polynomials. They are polynomials in the Feynman parameters and have the following properties:

- They are homogeneous in the Feynman parameters, U is of degree L, F is of degree $L+1$.
- U is linear in each Feynman parameter. If all internal masses are zero, then also F is linear in each Feynman parameter.
- In expanded form each monomial of U has a coefficient $+1$.

Sometimes one calls U the first Symanzik polynomial and F the second Symanzik polynomial of the graph.

As shown above U and F can be calculated in an algebraic way from the structure of propagators for a given Feynman diagram using (4.15). In parallel, these polynomials can be also derived from the topology of the underlying graph.

To explain the graphical method of construction graph polynomials one needs first to introduce some basic definitions:

- Spanning tree T for the graph G
  sub-graph with the following properties:
  - T contains all the vertices of G
  - the number of loops in T is zero
  - T is connected

  T can be obtained from G by deleting L edges (L – number of loops in G).
- Spanning k–forest $\mathcal{T}_k$ for the graph G
  has the same properties as T but it is not required that a spanning forest is connected.
  F can be obtained from G by deleting $L+k-1$ edges.

If $\mathcal{T}$ is the set of all spanning forests of G and $\mathcal{T}_k$ is set of spanning k-forests of G when

$$\mathcal{T} = \bigcup_{k=1}^{r} \mathcal{T}_k \quad (r - \text{number of vertices}).$$

Each element of $\mathcal{T}_k$ has k connected components $(T_1, \ldots, T_k)$. As a P_{T_i} we denote a set of external momenta attached to T_i for a given k–forest. Depending on the "direction" of external momenta (are they incoming or outgoing) they enter to the P_{T_i} with a different relative sign.

The graph polynomials U and F can be obtained from the spanning trees and the spanning 2–forests of a graph G in the following way:

$$U = \sum_{T \in \mathcal{T}_1} \prod_{e_i \notin T} x_i, \tag{4.16}$$

$$F = -\sum_{(T_1,T_2)\in\mathcal{T}_2}\left(\prod_{e_i\notin(T_1,T_2)} x_i\right)\left(\sum_{p_i\in P_{T_1}} p_i\right)\left(\sum_{p_j\in P_{T_2}} p_j\right) + U\sum_{i=1}^{n} x_i m_i^2 = F_0 + U\sum_{i=1}^{n} x_i m_i^2. \tag{4.17}$$

Examples for non-planar vertex are shown in Figs. (4.2) and (4.3).

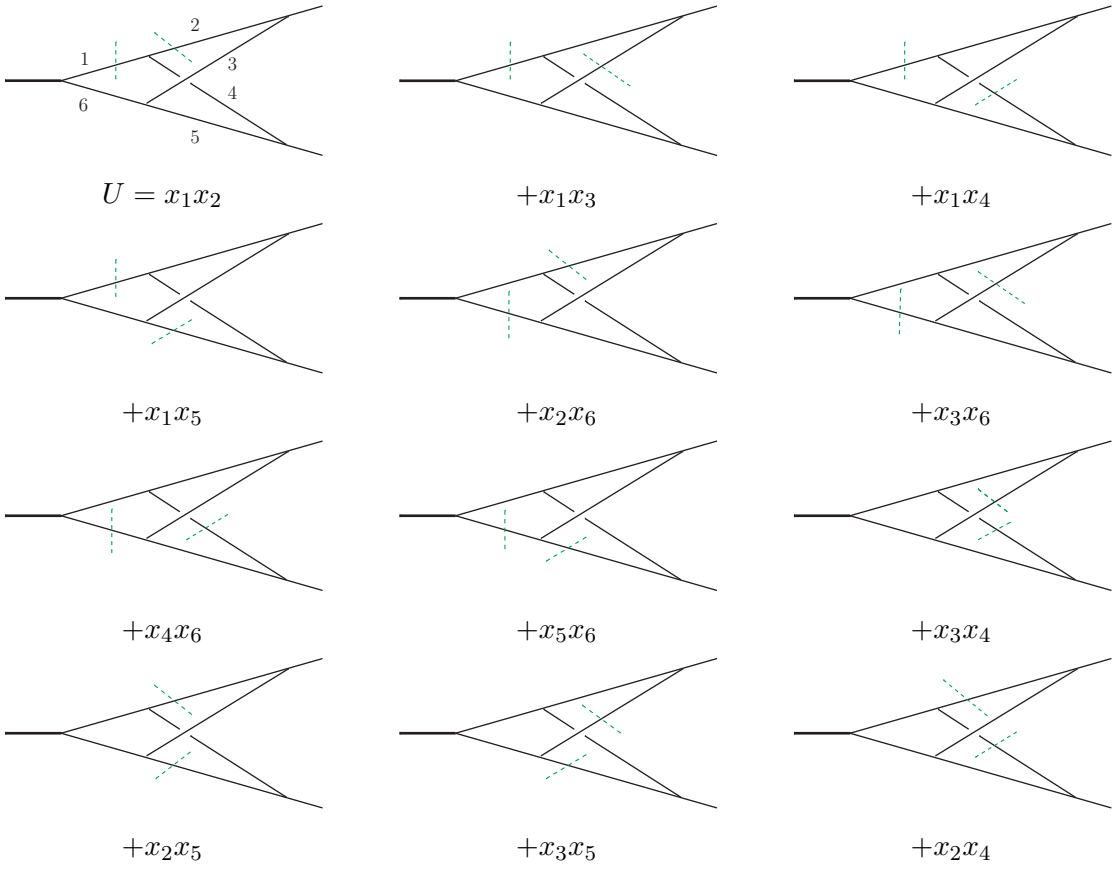

Figure 4.2: Example: Construction of the U polynomial for the non-planar massless vertex.

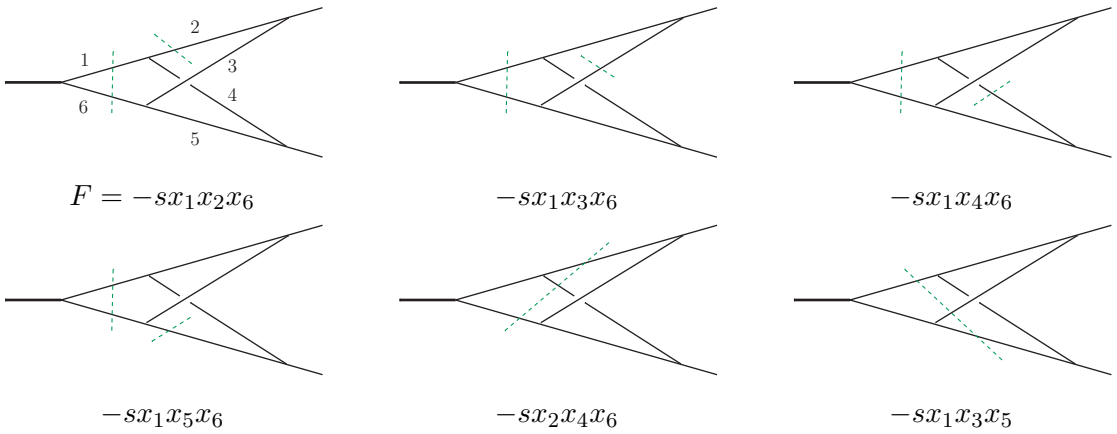

Figure 4.3: Example: Construction of the F polynomial for the non-planar massless vertex.

4.2.3 Cheng–Wu theorem

For the Feynman parameter representation (4.13) the Cheng–Wu (CW) theorem states that the same formula holds with the delta function $\delta(1-\sum\limits_{i=1}^{N} x_i)$ replaced by

$$\delta\left(\sum_{i\in\Omega} x_i - 1\right), \tag{4.18}$$

where Ω is an arbitrary subset of the lines $1,\ldots,L$, when the integration over the rest of the variables, i.e. for $i \notin \Omega$, is extended to the integration from zero to infinity.

One can prove this theorem in a simple way starting from the alpha representation using

$$1 = \int\limits_0^\infty \frac{d\lambda}{\lambda}\delta\left(1-\frac{1}{\lambda}\sum_{i=1}^{N}\alpha_i\right) \Leftrightarrow 1 = \int\limits_0^\infty \frac{d\lambda}{\lambda}\delta\left(1-\frac{1}{\lambda}\sum_{i\in\Omega}\alpha_i\right)$$

and change variables from α_i to $\alpha_i = \lambda x_i$ as shown above.

Let us stress that this theorem holds not only for Feynman diagrams with standard propagators but also for diagrams with various linear propagators.

4.2.4 Feynman parameterization and tensor integrals

In Section 4.2.1 the procedure of construction of a Feynman parameterization for scalar integrals was shown. It can be simply extended to the general case when the numerator is a tensor of rank R in the integration variables:

$$X(k_1,\ldots,k_L) \;=\; k_{l_1}^{\mu_1}\cdots k_{l_R}^{\mu_R}. \tag{4.19}$$

To make this one just has to treat properly the numerator after momenta shifts (4.10) keeping in mind that in the last step of integration (4.11) integrals with an odd number of k_i^μ vanish and integrals with an even number are proportional to a symmetrized product of the metric tensors $q^{\mu\nu}$.

Finally, the momentum integral is replaced by Feynman parameter integrals

$$\begin{aligned} G_L[X] \;=\; & \frac{(-1)^{N_\nu}}{\Gamma(\nu_1)\ldots\Gamma(\nu_N)}\int\prod_{i=1}^{N} dx_i x_i^{\nu_i-1}\delta(1-\sum_{i=1}^{N}x_i)\;\frac{U^{N_\nu-\frac{d}{2}(L+1)-R}}{F^{N_\nu-\frac{d}{2}L}} \\ & \times\sum_{r=0}^{R}\frac{1}{(-2)^{\frac{r}{2}}}\Gamma\left(N_\nu-dL/2-r/2\right)\;F^{\frac{r}{2}}\left\{\mathcal{A}_r^{[\mu_1,\ldots,\mu_r}\mathcal{P}_{R-r}^{\mu_{r+1},\ldots,\mu_R]}\right\}. \end{aligned} \tag{4.20}$$

The object $\mathcal{A}_r\mathcal{P}_{R-r}$ contains the tensor structure due to its two elements

$$\mathcal{A}_0 \;=\; 1, \tag{4.21}$$

$$\mathcal{A}_r \;=\; 0 \quad \text{for odd } r>0, \tag{4.22}$$

$$\mathcal{A}_r^{\mu_1\cdots\mu_r} \;=\; \tilde{g}^{\mu_1\mu_2}\cdots\tilde{g}^{\mu_{r-1}\mu_r}, \tag{4.23}$$

and

$$\mathcal{P}_0 = 1, \tag{4.24}$$

$$\mathcal{P}_r^{\mu_1\cdots\mu_r} = \mathcal{P}^{\mu_1}\ldots\mathcal{P}^{\mu_r}, \tag{4.25}$$

where we left out in the notations the indices related to the loop numbering, because they are fixed by (4.19) when the Lorentz indices are defined:

$$\tilde{g}^{\mu_1\mu_2} \equiv \left(\tilde{M}_L{}^{-1}\right)_{l_1 l_2} g^{\mu_1\mu_2}, \tag{4.26}$$

$$\mathcal{P}^{\mu_i} \equiv \sum_{l=1}^{L} \left(\tilde{M}_L\right)_{l_i l} Q_l^{\mu_i}. \tag{4.27}$$

The product $\left\{\mathcal{A}_r^{[\mu_1,\ldots,\mu_r}\mathcal{P}_{R-r}^{\mu_{r+1},\ldots,\mu_R]}\right\}$ is completely symmetrized in Lorentz indices. For example, in the case $\mathcal{A}_2\mathcal{P}_2$ this means

$$\begin{aligned}\mathcal{A}_2^{[\mu\nu}\mathcal{P}_2^{\lambda\rho]} = {} & \mathcal{A}_2^{\mu\nu}\mathcal{P}_2^{\lambda\rho} + \mathcal{A}_2^{\mu\lambda}\mathcal{P}_2^{\nu\rho} + \mathcal{A}_2^{\nu\lambda}\mathcal{P}_2^{\mu\rho} \\ & + \mathcal{A}_2^{\mu\rho}\mathcal{P}_2^{\nu\lambda} + \mathcal{A}_2^{\nu\rho}\mathcal{P}_2^{\mu\lambda} + \mathcal{A}_2^{\lambda\rho}\mathcal{P}_2^{\mu\nu}.\end{aligned} \tag{4.28}$$

More explicitly, the numerator $T(k_1^{\mu_1}k_2^{\mu_2})$ corresponds to the two terms

$$\mathcal{A}_0\mathcal{P}_2^{\mu_1\mu_2} = P^{\mu_1}P^{\mu_2} \tag{4.29}$$

and, with a different numerical factor (see (4.20)),

$$\mathcal{A}_2^{\mu_1\mu_2}\mathcal{P}_0^{\mu_1\mu_2} = \tilde{g}^{\mu_1\mu_2}. \tag{4.30}$$

For one-loop integrals, the matrix M is trivial, $M_1 = \tilde{M}_1 = 1$, which leads to $U = \det M = 1$ and $F(x) = -J + Q^2$ [1]. Eq.(4.20) then becomes

$$G_1(T_R) = \frac{(-1)^{N_\nu}}{\prod_{i=1}^N \Gamma(\nu_i)} \int \prod_{i=1}^N dx_i x_i^{\nu_i-1}\delta(1-\sum_{j=1}^N x_j) \sum_{r=0}^R \frac{\Gamma\left(n-\frac{d+r}{2}\right)}{(-2)^{\frac{r}{2}}F^{n-\frac{d+r}{2}}} \left\{\mathcal{A}_r\mathcal{P}_{R-r}\right\}^{[\mu_1,\ldots,\mu_R]}, \tag{4.31}$$

and in case of a tensor of rank 2, we get for the sum in (4.20)

$$T(k_1^{\mu_1}k_1^{\mu_2}) \to \Gamma(N_\nu - d/2)\left[Q^{\mu_1}Q^{\mu_2} - \frac{1}{2(N_\nu - d/2 - 1)}\, F\, g^{\mu_1\mu_2}\right]. \tag{4.32}$$

The general expressions, as well as the examples, agree with [123]. For one-loop tensors, equivalent expressions are also given in [83].

The additional terms arising from the *tensorial* structure of the L-loop Feynman integrals are polynomials in the x_i.

[1] Sometimes it is useful to rewrite $F(x) \to -(\sum x_i)J + Q^2$, which keeps F to be a bi-linear function of the x_i.

4.3 Planarity of Feynman diagrams

4.3.1 Planar and non-planar diagrams

Non-planar Feynman diagrams arise naturally from perturbative quantum field theory. They are interesting for many reasons. A graph is *planar* if it can be drawn on a surface (sphere) without intersections. A *non-planar* graph is a graph that is not planar. From the graph-theoretical point of view, many constructions and theorems are formulated only for planar graphs. It is interesting to note that in the so-called 't Hooft limit of SU (N) with coupling g, where $N \to \infty$, $g^2 N = \text{const}$, only planar diagrams survive. Thus one could argue that (non-)planarity is not of purely technical, graph theoretical character, but rather it is a significant ingredient with a physical interpretation in the above limit.

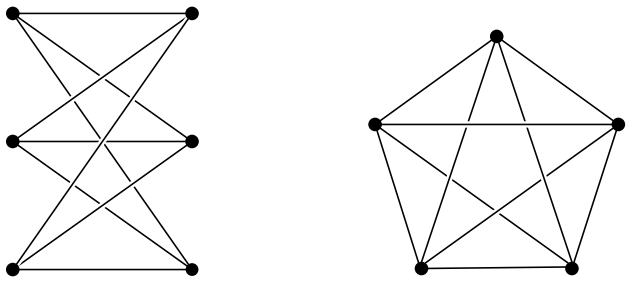

Figure 4.4: The simplest non-planar Kuratowski graphs.

Formally, any Feynman diagram G can be considered as a graph and thus subjected to graph-theoretical methods. Moreover, labeling all edges of G by momenta makes G a network flow, which is not necessarily unique. Consequently, it can make some redundant problems on the way to find effective analytical or numerical solutions to a given Feynman diagram. This is especially true if we want to make general programs which use some methods to solve Feynman integrals. We focus here on one technical aspect. Given a Feynman diagram G, is it possible to decide the planarity of G only upon its propagators? The question could be rewritten in a more general way: Is it possible to decide the planarity of a network flow only upon its flows? The answer is important considering e.g. computer algebra methods in particle physics. We faced the problem when working on the upgrade of the `AMBRE` package [152, 153], where different methods are applied in order to construct an optimal, low-dimensional Mellin–Barnes representation of G depending on its planarity (work in progress). In general, the available graph-theoretical methods to recognize planarity of a graph rely mainly on its geometry, like the Kuratowski theorem, that claims that a graph G is planar if it does not contain a subgraph that is a subdivision of $K_{3,3}$ or K_5 [172], see Fig. 4.4.

When no geometry of G is given, it is hard to decide about subgraphs of G. This is the case of `AMBRE`, where only propagators are given. As we will show, the answer to the question is positive.

Here one of the methods is described, elaborated by the author of this thesis. It is based on adjacency of the Laplacian matrix of a given graph. Another approach is based on the

twistor methods and dual variables. Details of this method can be found in [126].

Now we will describe the second method.

4.3.2 Planarity and dual graphs

A *dual* to a graph is constructed by drawing vertices inside the faces (including the external face) and connecting vertices that correspond to adjacent faces (Fig. 4.5).

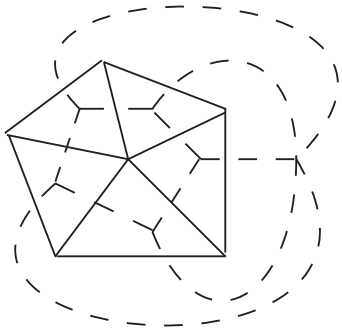

Figure 4.5: Given graph (solid line) and its dual (dashed line). Such duals can be defined only for planar graphs, hence we have one of the ways to find planarity of a given diagram.

To say that a Feynman diagram G is (non-)planar, one defines the *adjoint* diagram G^* (Fig. 4.6). It is constructed from G by attaching all external lines to an auxiliary vertex [172]. We say that a Feynman diagram G is planar iff G^* is planar.

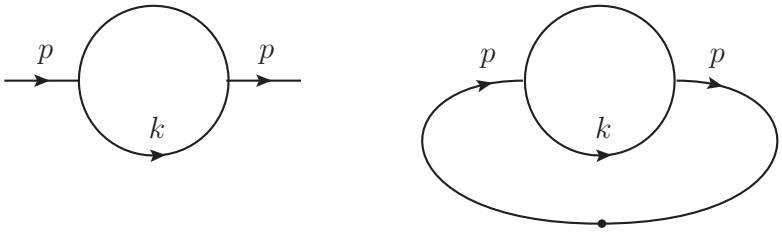

Figure 4.6: A Feynman diagram (left) and its adjoint (right).

Let G be a connected $l-$loop Feynman diagram, $\{p_1, ..., p_m\}$ be the set of external momenta, $\{e_1, ..., e_n\}$ be the set of edges in G (neglecting external lines), $\{k_1, ..., k_n\}$ be the set of corresponding momentum flows in G, and $\{v_1, ..., v_r\}$ be the set of vertices in G. Then there holds [171]

$$r = n - l + 1. \tag{4.33}$$

Hence given the number of edges (flows) and loops, the number of vertices r can be derived from (4.33). After introducing Feynman parameters $x_1, ..., x_n$, one defines the Laplacian matrix L of a graph G as an $r \times r$ matrix with entries

$$L_{ij} = \begin{cases} \sum\limits_{k=1}^{n} x_k & \text{if } i = j,\ e_k \text{ is attached to } v_i,\ e_k \text{ is not a self-loop,} \\ -\sum\limits_{k=1}^{n} x_k & \text{if } i \neq j,\ e_k \text{ connects } v_i, v_j. \end{cases} \tag{4.34}$$

The elements of L are calculated in a few steps. Diagonal elements L_{ii} are obtained by deciding which Feynman parameters x_k are attached to v_i. Vertices are divided into external (attached to external lines) and internal ones. Note that only vertices of degree 3 and 4 are allowed[2]. Thus the conditions are of the form

$$\text{for external vertices: } \pm k_a \pm k_b = \pm p_e \text{ or } \pm k_a \pm k_b \pm k_c = \pm p_e,$$

$$\text{for internal vertices: } \pm k_a \pm k_b = \pm k_c \text{ or } \pm k_a \pm k_b \pm k_c = \pm k_d,$$

where $a, b, c, d \in \{1, ..., n\}$, $e \in \{1, ..., m\}$. The flows that fulfill the above relations contribute to diagonal elements of L. Furthermore, off-diagonal elements L_{ij} are obtained by deciding Feynman parameters x_k that connect vertices v_i, v_j. Observe that such x_k's have to be both in L_{ii} and L_{jj}, thus the intersection of elements in L_{ii} and L_{jj} is non-empty and gives exactly these x_k's. In the case of many edges connecting v_i, v_j, they shrink to one edge, thus giving exactly one x_k (hence $\sum x_k \to x_k$).
In order to obtain a more familiar form of L, understandable to `Mathematica` software [173], redefine L by

$$L_{ij} = \begin{cases} \deg(v_i) & \text{if } i = j, \\ -1 & \text{if } i \neq j \text{ and } v_i, v_j \text{ are adjacent}, \end{cases}$$

where $\deg(v_i)$ is the degree of v_i. The above definition is derived from (4.34) by substituting $x_k \to 1$. Then L can be written as

$$L = D - A, \tag{4.35}$$

where $D = \text{diag}(\deg(v_1), ..., \deg(v_r))$ is a degree matrix and A is the adjacency matrix given by

$$A_{ij} = \begin{cases} 1 & \text{if } i \neq j \text{ and } v_i, v_j \text{ are adjacent}, \\ 0 & \text{otherwise}. \end{cases}$$

The final part of the algorithm is to create the adjoint diagram G^*.[3] The Laplacian matrix L^* of G^* is build upon L by extending it by one row and one column corresponding to v_{r+1}. Clearly $\deg(v_{r+1}) = m$ and extra 1's appear in the $(r+1)^{th}$ column and $(r+1)^{th}$ row at the elements corresponding to external vertices. Thus, from (4.35) the adjacency matrix $A^* = D^* - L^*$ is obtained. Eventually, given A^*, the function `PlanarQ` of the `Mathematica` package `Combinatorica` yields the answer for the question of planarity of a Feynman diagram G. In fact, given the matrix A^* it is possible to draw a given diagram with `Mathematica` by using the function `AdjacencyGraph`.

How to call and use the `PlanarityTest` package is shown in Appendix 7.2. More instructive examples for planarity recognition using the described algorithm are given in [151].

[2] For more general applications like gravity, the algorithm should be improved.
[3] In the case of vacuum diagrams, G^* is the same as G by definition.

4.4 MB-representations of Feynman integrals and Barnes lemmas

The basic relation for constructing MB-representations of Feynman integrals is the following Barnes formula

$$\frac{1}{(A+B)^\lambda} = \frac{1}{\Gamma(\lambda)}\frac{1}{2\pi i}\int_{-i\infty}^{i\infty} dz\, \frac{A^z}{B^{\lambda+z}}\Gamma(-z)\Gamma(\lambda+z). \tag{4.36}$$

The integration path is such that poles of the Gamma function with argument $\lambda + z$ are separated from poles of the Gamma function with argument $-z$. This can be achieved when the position of the contour on the real axis is chosen such that real parts of both Gamma functions are positive. The contour is usually, but not necessarily, a straight line parallel to the imaginary axes.

Equation (4.36) can be generalized to any amount of terms in the denominator, as given by the MB-master formula (4.1). This formula can be applied to the Feynman parameter representation (4.13) or (4.20). Different strategies of this procedure will be discussed in the next sections, but finally graph polynomials are split into pieces and the integration over Feynman parameters can be easily done by using the relation

$$\int_0^1 \prod_{i=1}^N dx_i\; x_i^{n_i-1}\; \delta(1-x_1-\ldots-x_N) = \frac{\Gamma(n_1)\ldots\Gamma(n_N)}{\Gamma\left(n_1+\ldots+n_N\right)}, \tag{4.37}$$

which is a generalization of the Euler formula

$$\int_0^1 dx\, x^{\alpha_1-1}(1-x)^{\alpha_2-1} = \frac{\Gamma(\alpha_1)\Gamma(\alpha_2)}{\Gamma(\alpha_1+\alpha_2)}. \tag{4.38}$$

In the most general form an MB representation consists of integrals of the form

$$\frac{1}{(2\pi i)^r}\int_{-i\infty}^{+i\infty}\cdots\int_{-i\infty}^{+i\infty}\prod_i^r dz_i\; \mathbf{F}(Z,S,\epsilon)\frac{\prod_{j=1}^{N_n}\Gamma(\Lambda_j)}{\prod_{k=1}^{N_d}\Gamma(\Lambda_k)}. \tag{4.39}$$

$$\begin{aligned}\mathbf{F}\text{ depends on: }& Z-\text{set of integration variables whose length is usually smaller than } r,\\ & S-\text{set of kinematic parameters and masses;}\\ \Lambda_i:\ & \text{linear combinations of } z_i \text{ and } \epsilon, \text{ e.g. } \Lambda_i = \sum_l \alpha_{il} z_l + \gamma_i + \delta_i\epsilon.\end{aligned} \tag{4.40}$$

In practice F is a product of elements of S raised to some powers as shown below,

$$\mathbf{F} \sim \prod_k X_k^{\sum_i(\alpha_{ki}z_i+\gamma_k+\delta_k\epsilon)}, \tag{4.41}$$

where $\alpha_{ij}, \gamma_i, \delta_i \in Z$ and X_k are ratios of kinematical invariants and masses, e.g., $X = \left\{-\frac{s}{m_1^2}, \frac{m_1^2}{m_2^2}, \frac{s}{t}, \ldots\right\}$.

The dimensionality of the representation r is the most crucial point for practical application of the method. Of course, it depends on the way in which the Barnes formula was applied to graph polynomials, see next sections. Besides these different approaches, the dimensionality of the representation can be decreased by analytical integration over free z-variables ("free" means they do not appear in powers of X ratios in (4.41)) using the following two identities

$$\frac{1}{2\pi i}\int_{-i\infty}^{i\infty} dz\Gamma(a+z)\Gamma(b+z)\Gamma(c-z)\Gamma(d-z) = \frac{\Gamma(a+c)\Gamma(a+d)\Gamma(b+c)\Gamma(b+d)}{\Gamma(a+b+c+d)}, \quad (4.42)$$

and

$$\frac{1}{2\pi i}\int_{-i\infty}^{i\infty} dz\frac{\Gamma(a+z)\Gamma(b+z)\Gamma(c+z)\Gamma(d-z)\Gamma(e-z)}{\Gamma(f+z)} = \frac{\Gamma(a+d)\Gamma(a+e)\Gamma(b+d)\Gamma(b+e)\Gamma(c+d)\Gamma(c+e)}{\Gamma(a+b+d+e)\Gamma(a+c+d+e)\Gamma(b+c+d+e)}, \quad (4.43)$$

with

$$a+b+c+d+e = f. \quad (4.44)$$

They are called first and second Barnes lemmas, respectively.

A direct application of Barnes lemmas is limited by the structure of the MB-representation. A more efficient way to decrease the dimensionality of MB-representation is to perform a transformation of variables in such a way that Barnes lemmas can be applied. Such an approach has been implemented in the package barnesroutines.m [155] for MB-integrals with fixed contours which appear after the expansion of the MB-representation in ϵ. It performs a search for suitable transformations with restrictions to absolute values of matrix elements for this transformation.

After ϵ expansion, due to the lack of the ϵ parameter, the program has more freedom in applying condition (4.44) in searching for the application of the second Barnes lemma and in some cases allows to decrease noticeably the dimensionality of MB-integrals. However, this approach has also some disadvantages when comparing to the general MB-representation without expansion in ϵ. First, the application of Barnes lemmas to MB-integrals with fixed contours is more complicated and may lead finally to a large number of MB-integrals. Second, starting with the ϵ expansion from a high dimensional MB-representation we get in general a bigger cascade of integrals than starting from a representation where dimensionality was already decreased by Barnes lemmas. That is why in the new upcoming AMBREv.4.0, searching for the application of Barnes lemmas will go in two steps: without and with ϵ expansion. In the second step barnesroutines.m is applied. In what follows we describe how to perform searching of transformations for applying Barnes lemmas in the first step, which results in a clear answer if such transformation is possible or not. Together with barnesroutines.m it dramatically decreases the dimensionality of the resulting MB integrals, especially with increasing number of loops. This strategy gives the minimal number of dimensions for MB-integrals.

We start the procedure by encoding the z-dependence of Gamma functions in a MB-representation (4.39) in a matrix form

$$M_\Gamma Z = \begin{bmatrix} \alpha_{ij}(\text{numerator}) \\ \dots\dots\dots\dots\dots\dots \\ \alpha_{ij}(\text{denominator}) \end{bmatrix} \begin{pmatrix} z_1 \\ \vdots \\ z_r \end{pmatrix}. \tag{4.45}$$

M_Γ is a rectangular $(N_n + N_d) \times r$ matrix whose upper part contains α-coefficients (4.40) from the numerator in (4.39) and whose bottom part contains analogous α-coefficients from the denominator in (4.39). Z is an r-vector of integration variables. Now, any linear variable transformation can be represented as

$$M_\Gamma Z = M_\Gamma U^{-1} U Z = M_\Gamma U^{-1} Z', \;\; Z' = UZ, \tag{4.46}$$

with a non-singular $r \times r$ transformation matrix U. $M_\Gamma U^{-1}$ encodes a new z structure of Gamma functions. Barnes lemmas can be applied if columns in $M_\Gamma U^{-1}$ have specific "signatures". For the first Barnes lemma elements in a column from $N_n + 1$ to $N_n + N_d$ must be equal to 0 and elements from 1 to N_n must contain the set $\{1, 1, -1, -1\}$ while all others must be also equal to 0. This can be formulated in terms of overdetermined systems of linear equations

$$M_\Gamma X = \{B_1\}. \tag{4.47}$$

X is an unknown r-vector representing a column in U^{-1} and $\{B_1\}$ is a set of all possible right hand sides. For general N_n one has $\dfrac{3N_n!}{4!(N_n-4)!}$ different r.h.s.

Because systems are overdetermined they may have no solutions at all. This means that there are no transformations leading to the Barnes' first lemma. If some number of solutions n_s is found, one can proceed further with the construction of the matrix U^{-1}. Each solution represents a column in the matrix and can be placed on any position starting from the diagonal U^{-1}. The procedure of replacing columns in a diagonal matrix by our solutions continues until the matrix becomes singular. After all these transformations, the maximal amount of added columns before the matrix becomes singular gives the number of integrations which can be done with the help of Barnes' first lemma.

The situation with Barnes' second lemma is more complicated because from the beginning it has a restriction on arguments of involved Gamma functions, see (4.44). First, ignoring this restriction one should check if it is possible to get a "signature" of Barnes' second lemma in the new matrix $M_\Gamma U^{-1}$. This can be again formulated in terms of systems of equations

$$M_\Gamma X = \{B_2\}, \tag{4.48}$$

where elements of the r.h.s. from $N_n + 1$ to $N_n + N_d$ must have one element equal to 1 and all other elements equal to 0 in all possible combinations. This bottom part of $\{B_2\}$ should be combined with a top part (elements from 1 to N_n) where a set $\{1, 1, 1, -1, -1\}$ is placed in all possible positions while the residual elements are equal to 0. Alltogether this gives $\dfrac{10N_dN_n!}{5!(N_n-5)!}$ different r.h.s. As before we take only solutions which give non-singular matrix, and in a next step we check the condition (4.44) for Barnes' second lemma. The

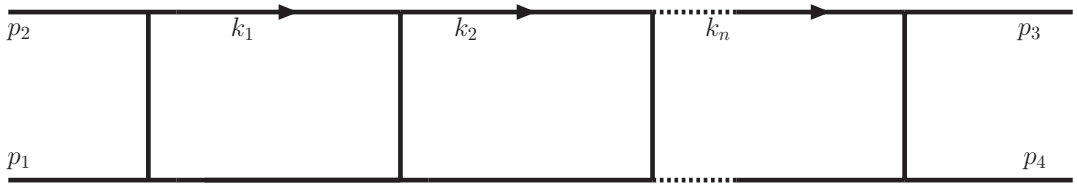

Figure 4.7: n-loop ladder diagram with $k_1, ..., k_n$ internal and $p_1, ..., p_4$ external momenta.

Dimensions of planar ladder MB integrals	Massless cases				Massive (QED) cases			
Number of loops (L)	1	2	3	4	1	2	3	4
No Barnes first lemma (BFL)	1	4	7	10	3	8	13	18
With BFL	1	4	7	10	2 (1+1)	6 (4+2)	10 (7+3)	14 (10+4)

Table 4.1: Optimal results for ladder diagrams defined in Fig.(4.7): Dim(massive case) = Dim(massless case) + #loops.

search for transformations for both lemmas can be performed recursively until no solution can be found. The resulting dimensionality also depends on the order in which the search is performed. Searching for a transformation for the second lemma can be successful after a search and application of the first lemma and vice-versa. The efficiency of this procedure will be shown in the next sections.

4.5 Loop–by–loop approach

As mentioned in the introduction to this chapter the LA uses the advantages of the MB method in application to one loop Feynman diagrams there U can be always set equal to one and only the F polynomial matters. Within this approach, each subloop of a multiloop diagram is treated separately in an iterative way. Aspects of derivation MB representations, such as the order of integration, simplifications of a result via Barnes lemmas, etc., using the LA are discussed in [122, 123] and a lot of instructive examples can be found in [124]. For planar cases the automatic construction of MB representations by the LA (AMBRE v1.3.1 and v2.1.1) seems to be optimal, see, for example QED ladder diagrams shown in Fig.(4.7) and Tab.(4.1).

To illustrate the method in more detail we show several examples which appear in the context of two loops electroweak Z-boson studies. We concentrate on such issues as threshold identification, the presence of many different masses and application of the LA to non-planar diagrams.

The first example is a planar two-loop vertex shown in Fig. (5.1(b)) in the next chapter. Lines with masses $m_1 = m_3 = m_6 = M_Z$, $m_2 = M_H$ and $m_4 = m_5 = 0$ correspond to the integral 3 of the type "xh0w" for which numerical results are presented in the Appendix

7.3. The integral representation of this diagram is the following:

$$I_3^{xh0w} = \int d^dk_1 d^dk_2 \frac{1}{(k_1^2 - M_H^2)((k_1-k_2)^2 - M_Z^2)(k_2^2 - M_Z^2)} \times \frac{1}{(k_1+p_1)^2(k_2+p_1)^2((k_1+p_1+p_2)^2 - M_Z^2)} \tag{4.49}$$

with $p_1^2 = p_2^2 = 0$ and $(p_1+p_2)^2 = s$.

The minimal MB dimentionality for this integral can be obtained if one integrates first over the subloop triangle, see Fig.(4.8), and then over remaining propagators, so the order of integration is $k_2 \to k_1$. For the first iteration we have

$$I_3^{xh0w}(1) = \int d^dk_2 \frac{1}{((k_1-k_2)^2 - M_Z^2)(k_2^2 - M_Z^2)(k_2+p_1)^2}. \tag{4.50}$$

The F polynomial corresponding to this integral is

$$F_{(1)}(\vec{x}) = M_Z^2 x_1 + M_Z^2 x_2 - k_1^2 x_1 x_2 - (k_1+p_1)^2 x_1 x_3. \tag{4.51}$$

The linear dependence on Feynman parameters for M_Z^2 terms takes place due to the fact that $U = 1$. The MB representation for this subloop can be written as

$$\begin{aligned} R_{(1)} =& (-1)^{2-\epsilon-z_1-z_2}(M_Z^2)^{z_1+z_2}(k_1^2)^{-z_3}((k_1+p_1)^2)^{-1-\epsilon-z_1-z_2-z_3}\Gamma(-z_1)\Gamma(-\epsilon-z_2)\Gamma(-z_2) \\ & \Gamma(-\epsilon-z_1-z_2-z_3)\Gamma(-z_3)\Gamma(1+z_2+z_3)\Gamma(1+\epsilon+z_1+z_2+z_3) \\ & /\Gamma(1-2\epsilon-z_1-z_2). \end{aligned} \tag{4.52}$$

Integrations over z-variables in a complex plane are assumed.

In the next stage we integrate over the remaining loop momentum k_1

$$I_3^{xh0w}(2) = \int d^dk_1 \frac{1}{(k_1^2)^{z_3}(k_1^2 - M_H^2)((k_1+p_1)^2)^{2+\epsilon+z_1+z_2+z_3}((k_1+p_1+p_2)^2 - M_Z^2)}. \tag{4.53}$$

This integral has four propagators and the powers of k_1^2 and $(k_1+p_1)^2$ are complex. One notices that during the first step it is possible to modify F by the term $\pm M_H^2 x_1 x_2$ and get in the next iteration only one propagator $k_1^2 - M_H^2$ in complex power. Such modification has an unpleasant side effect, the MB representation for that modified F function will have a term $(-M_H^2)^z$ which forces the integration to be always of "Minkowskian" type. In fact, the propagators in (4.53) can be represented as a vertex diagram where propagators k_1^2 and $k_1^2 - M_H^2$ are combined into one line as shown in Fig.(4.8) and this doesn't bring any complication for further computation.

The F polynomial for the final iteration is

$$F_{(2)}(\vec{x}) = M_H^2 x_2 + M_Z^2 x_4 - s x_1 x_4 - s x_2 x_4, \tag{4.54}$$

and we end up with a six dimensional MB representation:

$$\begin{aligned} R_3^{xh0w} =& (M_H^2)^{z_4}(M_Z^2)^{z_{125}}(-s)^{-2-2\epsilon-z_{1245}}\Gamma(-z_1)\Gamma(-\epsilon-z_2)\Gamma(-z_2)\Gamma(-\epsilon-z_{123})\Gamma(1+z_{23}) \\ & \Gamma(1+\epsilon+z_{123})\Gamma(-1-2\epsilon-z_{124})\Gamma(-z_4)\Gamma(-z_5)\Gamma(-1-2\epsilon-z_{1256}) \\ & \Gamma(-z_6)\Gamma(-z_3+z_6)\Gamma(2+2\epsilon+z_{12456})/\Gamma(1-2\epsilon-z_{12})\Gamma(-3\epsilon-z_{1245}). \end{aligned} \tag{4.55}$$

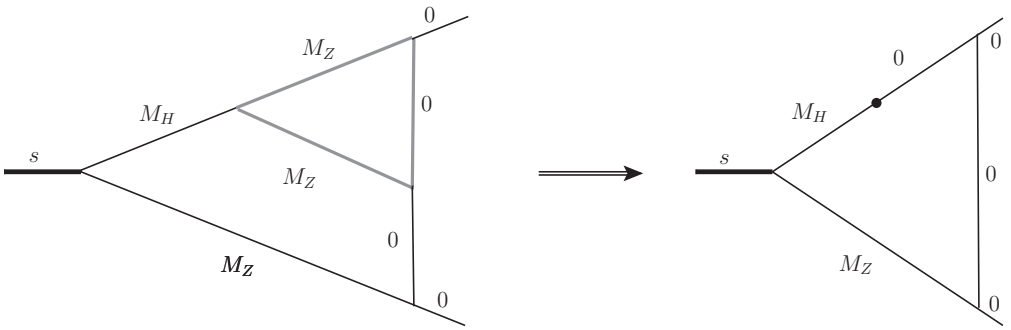

Figure 4.8: Example of the LA, first iteration – triangle subloop (in gray), second – four propagators effectively combined into a vertex.

Let's now concentrate on further simplifications of this representation. Already at the stage of F polynomials one can see that, for example, $F_{(1)}(\vec{x})$ can be rewritten in the form

$$F^{(1)}(\vec{x}) = M_Z^2(x_1 + x_2) - k_1^2 x_1 x_2 - (k_1 + p_1)^2 x_1 x_3 \tag{4.56}$$

and x_1+x_2 can be considered as one term and the MB formula can be applied recursively first to the F polynomial as a whole and then to the term $x_1 + x_2$. This always allows to apply Barnes' first lemma to a z-variable used in the MB transformation of the sum $x_1 + x_2$. It is similar to collecting full squares of sums of Feynman parameters as described in [122]. This feature is connected with the structure of formulas (4.1) and (4.37) and with the fact that corresponding z-variables do not appear in exponents of kinematical invariants or masses.

Another way to achieve the same result without factorizing linear terms is to remove as many as possible z-variables out of exponents of invariants and masses and then to check for Barnes' first lemma. Such a procedure can be done by a simple linear shift of one of z variables. Usually, we have a combination $\sum_{j=i_1}^{i_N} \alpha_j z_j$ in the exponent of one of the invariants and $-\sum_{j=i_1}^{i_N} \alpha_j z_j$ in the exponent of another one and also this combination doesn't appear in other exponents. Having such combination one can make a shift $z_{i_1} \to z_{i_1} - \sum_{j=i_2}^{i_N} \alpha_j z_j$ and check Barnes' first lemma for all variables $z_{i_2} \dots z_{i_N}$.

This algorithm is implemented in AMBRE and for our example (4.55), after the shift $z_1 \to z_1 - z_2 - z_5$, Barnes' first lemma is applied for variables z_2 and z_6 giving a 4-dimensional final representation[4].

For Euclidian kinematics ($s < 0$), an MB integral corresponding to this representation can be easily evaluated using MB.m [127]. In Minkoskian region ($s > 0$) the computation of an MB integral with a negative number raised to some complex power becomes more complicated, details will be discussed in Sec. (4.7).

The Feynman integral (4.49) has a physical threshold at the point $s = M_Z^2$. This means that for $s > M_Z^2$ in becomes complex valued. The requirement to obtain a minimal possible dimensionality makes this property invisible in the representation. Substituting

[4]In this case z_2 responds for the factorization in the term $M_Z^2(x_1+x_2)$ and z_6 - in the term $-sx_4(x_1+x_2)$ in $F_{(2)}(\vec{x})$. z_6 doesn't appear in exponents automatically by construction.

the U polynomial back to $F_{(2)}(\vec{x})$ in the term $M_Z^2 x_4$ we can rewrite (4.54) as follow

$$F_{(2)}(\vec{x}) = M_H^2 x_2 + (M_Z^2 - s)x_1 x_4 + (M_Z^2 - s)x_2 x_4 + M_Z^2 x_3 x_4 + M_Z^2 x_4^2. \tag{4.57}$$

This expression leads to a 5-dimensional representation but the term $(M_Z^2 - s)$ is now separated and numerical integration with `MB.m` can be for sure done in the interval $s < M_Z$. Moreover, exactly at the threshold the term $M_Z^2 - s$ can be dropped out, the representation is 4-dimensional and has a purely Euclidian form

$$\begin{aligned} R_{3,thr}^{xh0w} =& (M_H^2)^{z_4}(M_Z^2)^{-2-2\epsilon-z_4}\Gamma(-z_1)\Gamma(-\epsilon - z_2)\Gamma(-z_2)\Gamma(-\epsilon - z_{123})\Gamma(-z_3)\Gamma(1 + z_{23}) \\ & \Gamma(1 + \epsilon + z_{123})\Gamma(-1 - 3\epsilon - z_{12} + z_3 - 2z_4)\Gamma(-1 - 2\epsilon - z_{124})\Gamma(-z_4) \\ & \Gamma(1 + z_4)\Gamma(2 + 2\epsilon + z_{124})/\Gamma(1 - 2\epsilon - z_{12})\Gamma(-3\epsilon - z_{124})\Gamma(1 - \epsilon + z_3 - z_4). \end{aligned} \tag{4.58}$$

This example shows that the construction of optimal representations relies not only on the dimensionality but also on a kinematical point where they are evaluated.

Another example is a non-planar two-loop vertex shown in Fig. (5.1(c)) in the next chapter. Propagators with masses $m_1 = m_2 = m_3 = m4 = m5 = 0$ and $m_6 = M_Z$ correspond to the integral 15 of the type "0h0w" presented in Appendix 7.3. The integral representation in this case is

$$I_{15}^{0h0w} = \int d^d k_1 d^d k_2 \frac{1}{k_1^2 (k_1 - k_2)^2 k_2^2 ((k_1 - k_2 + p_1)^2 - M_Z^2)(k_2 + p_2)^2 (k_1 + p_1 + p_2)^2}. \tag{4.59}$$

The main purpose of the example is to show difficulties related to the application of the `LA`to non-planar diagrams.

As before we start with a one-loop subdiagram, the order of integrations again chosen is as $k_2 \to k_1$. In contrast to the previous example, we don't have any triangle subdiagram and have started from the 4-propagators box integral

$$I_{15}^{0h0w}(1) = \int d^d k_2 \frac{1}{(k_1 - k_2)^2 (k_2)^2 ((k_1 - k_2 + p_1)^2 - M_Z^2)(k_2 + p_2)^2}, \tag{4.60}$$

which has a more complicated $F_{(1)}(\vec{x})$ function:

$$\begin{aligned} F_{(1)}(\vec{x}) =& - k_1^2 x_1 x_2 - ((k_1 + p_1)^2 - M_Z^2)x_2 x_3 - (k_1 + p_2)^2 x_1 x_4 - (k_1 + p_1 + p_2)^2 x_3 x_4 \\ & + M_Z^2 x_3 (x_1 + x_3 + x_4). \end{aligned} \tag{4.61}$$

More problems appear when we go to the integration over loop momenta k_1

$$\begin{aligned} I_{15}^{0h0w}(2) = \int d^d k_1 & \frac{1}{((k_1)^2)^{1-z_1}((k_1 + p_1)^2 - M_Z^2)^{-z_3}((k_1 + p_2)^2)^{-z_5}} \\ & \times \frac{1}{((k_1 + p_1 + p_2)^2)^{3+\epsilon+z_{123456}}}. \end{aligned} \tag{4.62}$$

In (4.62) the propagators do not form a diagram with conserved momentum flow. Propagators $(k_1)^2((k_1 + p_1)^2 - M_Z^2)(k_1 + p_1 + p_2)^2$ correspond to a 1-loop vertex diagram but $(k_1 + p_2)^2$ must be considered as an artificial numerator. The `AMBRE` packages can work

with numerators in form of propagators raised to some negative integer powers, see [124], the final result is equal to one obtained by expanding such numerators and treating in the usual way, but this is possible only for integers powers. In non-planar case the exponent is complex.

After the k_1 integration $F_{(2)}(\vec{x})$ looks like

$$F_{(2)}(\vec{x}) = M_Z^2 x2 + 2s x_2 x_3 - 2s x_1 x_4, \tag{4.63}$$

and the final 6-dimensional representation can be written in the form[5]

$$\begin{aligned} R_{15}^{0h0w} =& \frac{1}{(-2s)^{2+2\epsilon}}(-1)^{z_8}\left(\frac{M_Z^2}{-2s}\right)^{z_2}\Gamma(-z_1)\Gamma(-1-2\epsilon-z_{13})\Gamma(1+z_{13})\Gamma(-1-\epsilon-z_{15}) \\ & \Gamma(1+z_{15})\Gamma(2+\epsilon+z_{1235}-z_7)\Gamma(-z_7)\Gamma(-z_2+z_7)\Gamma(-1-\epsilon-z_{123}+z_7) \\ & \Gamma(-1-2\epsilon-z_{128})\Gamma(1-\epsilon+z_{135}-z_{78})\Gamma(-z_8)\Gamma(2+2\epsilon+z_{28})\Gamma(-z_5+z_8) \\ & \Gamma(-z_3+z_{78})/\Gamma(-2\epsilon)\Gamma(1-z_1)\Gamma(-3\epsilon-z_2)\Gamma(3+\epsilon+z_{1235}-z_7) \\ & \Gamma(-1-2\epsilon-z_{123}+z_7). \end{aligned} \tag{4.64}$$

The main disadvantage of this representation is the factor $(-1)^{z_8}$ which forces the integral to be always of Minkowskian type.

By construction this representation is correct and in principle can be used for the evaluation of the integral but due to its Minkowskian form it cannot be checked by `MB.m`directly. In the next sections, we will describe another approach to construct physically valid and checkable representations for all types of non-planar diagrams.

4.6 Global approach

The second possibility to construct an `MB` representation for a given Feynman integral is to integrate simultaneously over all loop momenta. In this case $U(\vec{x})$ is not equal to 1 anymore. A naive way to construct a representation is to apply the `MB`-master formula (4.1) to both $U(\vec{x})$ and $F(\vec{x})$ polynomials and then try to simplify the result using Barnes lemmas. However, in this way, one faces several problems. First, after integration over Feynman parameters, one always gets $\Gamma(0)$ in the denominator. This happens precisely because of the homogeneity of the original Feynman parameters representation. An option to regulate this singularity is to shift the exponent of one of the Feynman parameters by arbitrary δ and then take the limit $\delta \to 0$, before doing the analytic continuation in the dimensional parameter $\epsilon \to 0$. One should stress that shifting the original exponents of propagators $n_i \to n_i + \eta$, similar to what we do in case of irreducible numerators, does not help because $\Gamma(0)$ appears automatically and it does not depend on powers of propagators n_i. Second, even at two-loop level, the amount of terms in $U(\vec{x})$ and $F(\vec{x})$ is quite large; the number of `MB` integrations is equal to the number of terms in a polynomial, minus one, see (4.1). It leads to a very high-dimensional `MB` representation for which it is difficult to catch all possible simplifications by Barnes lemmas.

[5] after ϵ-expansion only 5-dimensional `MB` integrals remain.

To show how to avoid such a complication we will start this section with a detailed explanation of one of the first successful implementations of the global approach to a non-trivial Feynman integral, namely, the non-planar massless double box [143]. Later we will show how to extend this approach to any two-loop diagram. Finally, we will show a generalization of the GA to the case of three-loop integrals.

Let us consider a non-planar massless two loop box diagram, Fig.(4.9), with on-shell external legs ($p_i^2 = 0$). We define an integral for this diagram as (all external momenta p_i

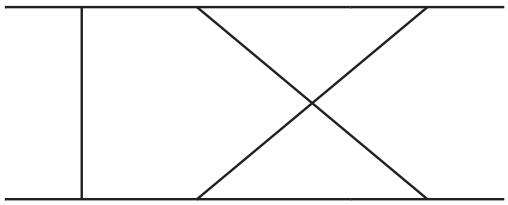

Figure 4.9: The non-planar double box topology.

are incoming in cyclic notation):

$$B_7^{NP} = \iint d^dk_1 d^dk_2 \frac{1}{[(k_1+k_2+p_1+p_2)^2]^{n_1}[(k_1+k_2+p_2)^2]^{n_2}[(k_1+k_2)^2]^{n_3}} \frac{1}{[(k_1-p_3)^2]^{n_4}[(k_1)^2]^{n_5}[(k_2-p_4)^2]^{n_6}[(k_2)^2]^{n_7}}. \quad (4.65)$$

An explicit form of the Symanzik polynomials for this integral is

$$U(x) = x_1x_2 + x_1x_4 + x_2x_4 + x_1x_5 + x_2x_5 + x_2x_6 + x_4x_6 + x_5x_6 + x_1x_7 + x_4x_7 + x_5x_7 + x_6x_7 \quad (4.66)$$

and

$$F(x) = -s\ x_1x_2x_5 - s\ x_1x_3x_5 - s\ x_2x_3x_5 - u\ x_2x_4x_6 - s\ x_3x_5x_6 - t\ x_1x_4x_7 - s\ x_3x_5x_7 - s\ x_3x_6x_7. \quad (4.67)$$

Changing sums of monomials in x into products using the MB-master formula (4.1) leads to an 18-fold MB-integral (11 and 7 complex variables come from U and F, respectively). Certainly, it can be better, if U and F are factorized properly. The factorization proposed in [143] looks as follows

$$U(x) = (x_1+x_6)(x_2+x_7) + (x_3+x_4+x_5)(x_1+x_2+x_6+x_7), \quad (4.68)$$

$$F(x) = -t\ x_1x_4x_7 - u\ x_2x_4x_6 - s\ x_1x_2x_5 - s\ x_3x_6x_7 - s\ x_3x_5(x_1+x_2+x_6+x_7), \quad (4.69)$$

where the longest factorized term has four Feynman parameters $x_1 + x_2 + x_6 + x_7$.

Now we can apply the CW theorem, keeping in the δ-function the longest factorized subset of Feynman parameters, so it can be dropped out from the Symanzik polynomials, and the integral becomes

$$B_7^{NP} = \frac{(-1)^{N_\nu}\Gamma\left(N_\nu - d\right)}{\Gamma(n_1)\ldots\Gamma(n_N)} \int\limits_0^\infty dx_3dx_4dx_5 \int\limits_0^1 dx_3dx_4dx_5\delta(1-(x_1+x_2+x_6+x_7)) \\ \frac{((x_1+x_6)(x_2+x_7)+x_3+x_4+x_5)^{N_\nu-\frac{3d}{2}}}{(-t\ x_1x_4x_7 - u\ x_2x_4x_6 - s\ x_1x_2x_5 - s\ x_3x_6x_7 - s\ x_3x_5)^{N_\nu-d}}. \quad (4.70)$$

In the next step we apply the MB relation to U and F not expanding the term $(x_1+x_6)(x_2+x_7)$:

$$B_7^{NP} = \frac{(-1)^{N_\nu}}{\Gamma(n_1)\ldots\Gamma(n_N)} \int\limits_{-i\infty}^{i\infty} dz_1\ldots dz_2 \int dx_1\ldots dx_7\ (-s)^{-N_\nu+d-z_2-z_3}(-t)^{z_2}(-u)^{z_3} \\ \times \Gamma(-z_1)\Gamma(-z_2)\Gamma(-z_3)\Gamma(-z_4)\Gamma(N_\nu-d+z_1+z_2+z_3+z_4) \\ \times x_1^{-N_\nu+d-z_1-z_2-z_3}x_2^{z_2+z_3}x_3^{-N_\nu+d-z_2-z_3-z_4}x_4^{z_1+z_3}x_5^{z_2+z_4}x_6^{z_1+z_2}x_7^{z_3+z_4} \\ \times (x_3+x_4+x_5+(x_1+x_6)(x_2+x_7))^{N_\nu-\frac{3d}{2}}. \quad (4.71)$$

To perform the integration over Cheng-Wu variables we can use iteratively the following integration formula

$$\int\limits_0^\infty dx\ x^{z_1}(x+y)^{z_2} = \frac{y^{1+z_1+z_2}\Gamma(1+z_1)\Gamma(-1-z_1-z_2)}{\Gamma(-z_2)}. \quad (4.72)$$

In the last step we apply the MB-master relation (4.1) to the terms (x_1+x_6) and (x_2+x_7). As we know from the previous section, the corresponding z-variables can be removed using first Barnes lemma. Finally, we end up with a 4-dimensional MB representation,

$$B_7^{NP} = \frac{(-1)^{N_\nu}}{\Gamma(n_1)\ldots\Gamma(n_7)} \int\limits_{-i\infty}^{i\infty} dz_1\ldots dz_4(-s)^{4-2\epsilon-N_\nu-z_{23}}(-t)^{z_3}(-u)^{z_2} \\ \frac{\Gamma(-z_1)\Gamma(-z_2)\Gamma(-z_3)\Gamma(-z_4)\Gamma(2-\epsilon-n_{45})\Gamma(2-\epsilon-n_{67})}{\Gamma(4-2\epsilon-n_{4567})\Gamma(n_{45}+z_{1234})\Gamma(n_{67}+z_{1234})\Gamma(6-3\epsilon-N_\nu)} \\ \Gamma(n_2+z_{23})\Gamma(n_4+z_{24})\Gamma(n_5+z_{13})\Gamma(n_6+z_{34})\Gamma(n_7+z_{12})\Gamma^3(-2+\epsilon+n_{4567}+z_{1234}) \\ \Gamma(4-2\epsilon-n_{124567}-z_{123})\Gamma(4-2\epsilon-n_{234567}-z_{234})\Gamma(-4+2\epsilon+N_\nu+z_{1234}), \quad (4.73)$$

with notations $z_{i\ldots j\ldots k} = z_i + \ldots + z_j + \ldots + z_k$ and $n_{i\ldots j\ldots k} = n_i + \ldots + n_j + \ldots + n_k$.

4.6.1 Two-loop integrals

To generalize the steps given in the previous section, let's consider the two-loop skeleton diagram in Fig. (4.10a). To get any two-loop diagram one has to attach external lines/legs

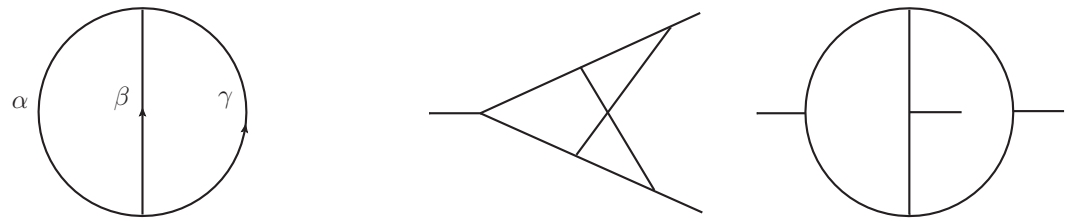

(a) (b)

Figure 4.10: Two-loop skeleton diagrams.

to lines and/or vertices of the skeleton diagram. For example, to get a non-planar two-loop vertex diagram one has to attach one external leg to each line on the skeleton diagram Fig. (4.10b); the two-loop planar box can be obtained by attaching two external legs to line α and two external legs to line γ; non-planar double-box - attach two legs to line α and one leg to each of lines β and γ; etc. Lines α, β and γ in the skeleton diagram sometimes are called chains [170].

For the loop momenta k_1 and k_2, all propagators belonging to one of the chains contain only one of the following combination of loop momenta - k_1, k_2 and $k_1 + k_2$ (or $k_1 - k_2$, depending on the orientation of momentum flow in chains), plus corresponding external momenta depending on the topology. Let now introduce the following transformation of the Feynman parameters belonging to each chain:

$$\{\vec{x}\}_i : \quad x_k \to v_i \xi_{ik} \quad \times \delta\left(1 - \sum_{k=1}^{\eta_i} \xi_{ik}\right), \tag{4.74}$$

where i denotes the chain index and $k \in [1, \eta_i]$, with η_i - the number of propagators in the chain. The δ-function keeps the number of variables unchanged.

Now the integration over Feynman parameters looks as follow:

$$\int_0^1 \prod_{i=1}^{N} dx_i \; \delta\left(1 - \sum_{i=1}^{N} x_i\right) \to \int_0^1 \prod_{i=1}^{3} dv_i v_i^{\eta_i - 1} \; \delta\left(1 - \sum_{i=1}^{3} v_i\right) \int_0^1 \prod_{i=1}^{3} \prod_{k=1}^{\eta_i} d\xi_{ik} \; \prod_{i=1}^{3} \delta\left(1 - \sum_{k=1}^{\eta_i} \xi_{ik}\right). \tag{4.75}$$

This transformation dramatically simplifies graph polynomials.
Utilizing the δ-functions $\prod_{i=1}^{3} \delta\left(1 - \sum_{k=1}^{\eta_i} \xi_{ik}\right)$, the first the Symanzik polynomial for any two-loop diagram becomes

$$U(\vec{x}) \to U(\vec{v}) = v_1 v_2 + v_2 v_3 + v_1 v_3. \tag{4.76}$$

The second Symanzik polynomial has more complicated structure and depends on a definite topology.

As an illustration, lets consider a two-loop non-planar vertex, whose U and F are represented on Figs. (4.2) and (4.3). The corresponding Feynman integral is

$$\iint d^d k_1 d^d k_2 \frac{1}{[k_1^2]^{n_1}[(p_1 - k_1)^2]^{n_2}[(p_1 - k_1 - k_2)^2]^{n_3}} \frac{1}{[(p_2 + k_1 + k_2)^2]^{n_4}[(p_2 + k_2)^2]^{n_5}[k_2^2]^{n_6}}. \tag{4.77}$$

The momentum dependent function $m^2(\vec{x})$, see (4.9), and the parameters transformations for the integral are the following

$$\begin{array}{rcll} m^2(\vec{x}) & = & x_1(p_1-k_1-k_2)^2 & x_1 \to v_1\xi_{11} \\ & + & x_2(p_2+k_1+k_2)^2 & x_2 \to v_1\xi_{12} \\ & + & x_3(k_1)^2 & x_3 \to v_2\xi_{21} \\ & + & x_4(p_1-k_1)^2 & x_4 \to v_2\xi_{22} \\ & + & x_5(p_2+k_2)^2 & x_5 \to v_3\xi_{31} \\ & + & x_6(k_2)^2 & x_6 \to v_3\xi_{32}. \end{array} \tag{4.78}$$

After the transformation, U is equal to (4.76) and F is

$$F = -s\xi_{11}\xi_{22}\xi_{31}v_1v_2v_3 - s\xi_{12}\xi_{21}\xi_{32}v_1v_2v_3 - s\xi_{31}\xi_{32}v_1v_3^2 - s\xi_{31}\xi_{32}v_2v_3^2. \tag{4.79}$$

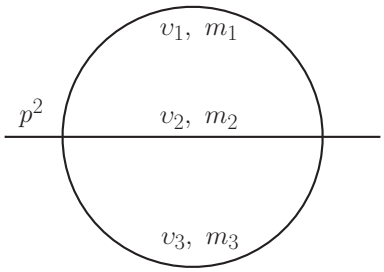

Figure 4.11: The sunrise diagram.

Looking on the homogeneity of variables v and ξ in (4.79) we can see that the CW theorem can be applied only to the v variables. For any 2-loop diagram the graph polynomials U and F can be represented in the form corresponding to the so-called sunrise diagram Fig. (4.11), where p^2 and m_i^2 depend on ξ_{ik} and the kinematical invariants (S) of the initial diagram:

$$G(X) \sim \int \prod d\xi_{ik}\delta\left(1-\sum_k \xi_{ik}\right) \\ \int d^dk_1 d^dk_2 \frac{1}{[k_1^2-m_1^2(S,\xi_{ik})]^{n_1}[k_2^2-m_2^2(S,\xi_{ik})]^{n_2}[(p+k_1+k_2)^2-m_3^2(S,\xi_{ik})]^{n_3}}. \tag{4.80}$$

In case of a massless non-planar vertex (4.77):

$$p^2 = -s(\xi_{12}\xi_{22}\xi_{31} + \xi_{12}\xi_{21}\xi_{32} - \xi_{31}\xi_{32}), \tag{4.81}$$

$$m_1^2 = -s\xi_{31}\xi_{32}, \quad m_2^2 = m_3^2 = 0. \tag{4.82}$$

There are only three possibilities to choose a subset in $\delta\left(1-\sum_{i=1}^3 v_i\right)$ in order to use the CW theorem. This choice depends on the structure of F, from v_1+v_2, v_2+v_3 or v_1+v_3 one should take the combination which makes F as simple as possible. In case of (4.79) it is v_1+v_2, so we have

$$U = v_3 + v_1v_2, \tag{4.83}$$

$$F = -s\xi_{11}\xi_{22}\xi_{31}v_1v_2v_3 - s\xi_{12}\xi_{21}\xi_{32}v_1v_2v_3 - s\xi_{31}\xi_{32}v_1v_3^2. \tag{4.84}$$

Applying the MB-master formula to F and integrating over v_3 we get a two-fold MB-integral:

$$V_6^{NP} = (-1)^{N_\nu}(-s)^{4-2\epsilon-N_\nu}\int\limits_{-i\infty}^{i\infty} dz_1 dz_2$$
$$\frac{\Gamma(2-\epsilon-n_{12})\Gamma(2-\epsilon-n_{56})\Gamma(4-2\epsilon-n_{12356}-z_1)\Gamma(-z_1)\Gamma(n_1+z_1)}{\Gamma(n_1)\Gamma(n_2)\Gamma(n_3)\Gamma(n_4)\Gamma(n_5)\Gamma(4-2\epsilon-n_{1256})\Gamma(n_6)\Gamma(n_5+z_1)}$$
$$\frac{\Gamma(-z_2)\Gamma(n_2+z_2)\Gamma(n_6+z_2)\Gamma(-4+2\epsilon+N_\nu+z_{12})}{\Gamma(8-4\epsilon-2n_{1256}-n_{34}-z_{12})\Gamma(n_{12}+z_{12})\Gamma(n_{56}+z_{12})\Gamma(4-2\epsilon-n_{12456}-z_2)}. \quad (4.85)$$

In case of massive diagrams, namely when some of the propagators have masses m_i^2, the best option is to not to expand the term $U\sum x_i m_i^2$ and apply (4.1) to F, considering U as an independent variable. Adding a mass parameter to one of the propagators in the non-planar vertex results only in one additional MB integration.

However, for example in case of the non-planar QED double box, see Fig.(4.65) with $p_i^2 = m^2$ and masses m^2 in propagators 1, 3, 4 and 7, the calculation will lead to the appearance of a "pseudo" Minkowskian factor $(-m^2)^{z_i}$ in the MB-representation, which restricts this approach. Expanding the term $U(\vec{x})\sum x_i m_i^2$, all $-m^2 x_i x_j$ contributions are removed but this leads to a dramatic increasing of terms. In the massive case, U is the same as in (4.68) and the corresponding F polynomial is

$$F(\vec{x}) = F_0(\vec{x}) - m^2(...) + U(\vec{x})m^2(x_2+x_3+x_5+x_6), \quad (4.86)$$

where $-m^2(...)$ has 24 terms and is not shown here. After simplifications, the mass dependent part can be represented as

$$+ m^2((x_2+x_7)(x_3+x_5+x_7)^2 + x_1(x_2+x_3+x_5)^2 + x_4(x_2+x_6)^2$$
$$+ x_6(x_3+x_5)^2 + x_2^2(x_3+x_5+x_6) + x_6^2(x_3+x_5)). \quad (4.87)$$

As in the LA, we collect full squares of sums of Feynman parameters and make a simple factorization in the last two terms.[6] Using transformation (4.74) and applying recursively Barnes formula (4.1) to linear combinations of parameters in (4.87) one can get a 15-dimensional MB representation. Such a high dimensionality shows that for problems where the term $\sum_i U m_i^2 x_i$ must be expanded other techniques should be developed.

In parallel, making an MB representation in the LA, one gets an 8-dimensional representation, see, e.g., [149], which points to the applicability of the loop-by-loop approach also to non-planar diagrams.

4.6.2 Generalization to 3-loop integrals

At the three-loop level, the situation becomes more complicated. Now we have two generating diagrams Fig. (4.12), see [170], which have different properties.

[6] in the AMBRE package linear combinations of Feynman parameters can be replaced by the FX[...] function.

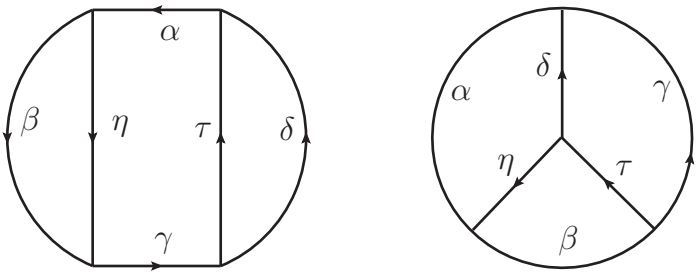

Figure 4.12: Basic skeleton generating diagrams for the 3-loop topologies discussed in [170].

The diagram on the left side of Fig. (4.12) and all its derivatives can be cut into two one-loop pieces. Propagators corresponding to the diagrams can have besides three different loop momenta only two different combinations of two of them (three different loop momenta in one propagator normally do not appear). Because chains (a) and (b) carry the same internal momenta they can be considered as one chain, so the total amount of v-variables in the transformation rules (4.74) is five. Typical examples of this type of diagrams for the box topologies are depicted in Fig. (4.13).

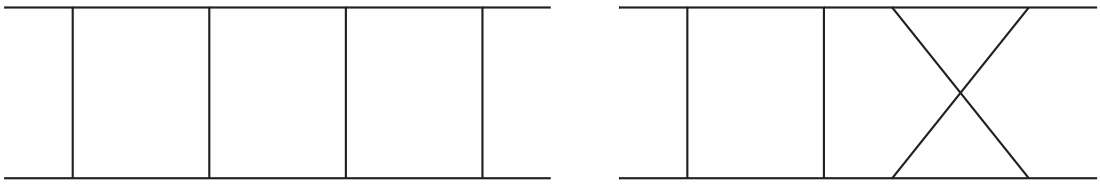

Figure 4.13: The 3-loop box topologies obtained from the left skeleton diagram in Fig. (4.12) have the same U polynomial structure.

After a transformation of variables, all diagrams up to replacing of indices have a U polynomial in the following form:

$$U = v_1v_2v_3 + v_1v_2v_4 + v_2v_3v_4 + v_1v_2v_5 + v_1v_3v_5 + v_2v_3v_5 + v_1v_4v_5 + v_3v_4v_5. \tag{4.88}$$

Many diagrams of this type have planar sub-loops and can be treated in a different way, see the next section.

The diagram on the right side in Fig. (4.12) can not be divided into two one loop pieces. Its propagators have all three different combinations of two loop momenta and number of v-variables is six. This skeleton generates the most complicated non-planar topologies, see for example Fig. (4.14) and Fig. (4.22k).

All child diagrams have now again the same U function in the form

$$\begin{aligned} U &= v_1v_2v_3 + v_1v_2v_4 + v_1v_3v_4 + v_1v_2v_5 + v_1v_3v_5 + v_2v_3v_5 + v_2v_4v_5 + v_3v_4v_5 \\ &+ v_1v_2v_6 + v_2v_3v_6 + v_1v_4v_6 + v_2v_4v_6 + v_3v_4v_6 + v_1v_5v_6 + v_3v_5v_6 + v_4v_5v_6. \end{aligned} \tag{4.89}$$

Figure 4.14: The 3-loop box topologies obtained from the right skeleton diagram in Fig. (4.12) and have another U polynomial structure.

As in the two-loop case, further simplification can be done with the help of the CW theorem [148,174]. The shortest form of U can be obtained if we choose three CW variables. An analysis of the form of U shows that that there are four different possibilities to choose CW variables. For (4.89) one of them is

$$\int_0^\infty dv_2 dv_3 dv_4 \int_0^1 dv_1 dv_5 dv_6 \delta(1 - v_1 - v_5 - v_6), \tag{4.90}$$

which gives

$$U_{CW} = v_2v_3 + v_2v_4 + v_3v_4 + v_1v_2v_5 + v_1v_3v_5 + v_1v_2v_6 + v_1v_4v_6 + v_1v_5v_6 + v_3v_5v_6 + v_4v_5v_6 \tag{4.91}$$

and reduces the number of terms in U from 16 to 10.

One of possible ways to make the integration over suitable CW variables is to use the following factorization trick:

$$U_{CW} = v_2(v_3 + v_4 + v_1v_5) + v_3(v_4 + v_1v_5) + v_1v_6(v_2 + v_5) + v_4v_6(v_1 + v_5) + v_3v_5v_6. \tag{4.92}$$

There are six different possibilities to get four terms in U and altogether we have 24 variants to choose Cheng-Wu variables and factorize U. A final choice is based, first, on a minimization of the amount of terms in F and, second, on the presence in F of the same factorization patterns as in (4.92) for U.

Now, to construct the MB representation as in the two-loop case we do not have to necessarily expand mass terms in F (see the previous section). Similarly, it is not necessary to expand any factorized combination which corresponds to the pattern in (4.92). After applying (4.1) to U and F we can integrate recursively the polynomials over v_3 and then over v_4 using (4.72). The integration over v_2 can be also done by (4.72). Finally, we apply again (4.1) to the term $v_1 + v_5$. In the end this MB integration can be removed by first Barnes lemma, see the discussion in Sec. 4.5. As one can see within this algorithm the U polynomial itself gives already 4 MB integrations. And because F is usually more complicated function and potentially can give even more MB integrations the resulting MB representation can be very high dimensional. This is a natural limitation of the method. As a rule of thumb, the GA usually gives optimal representations if from the beginning Length[U] $\leq$ Length[F]. However, here we would like to show an example where the GA together with an appropriate usage of Barnes lemmas applied to a planar 3 loop diagram gives the resulting dimensionality equal to the one obtained by the LA.

```
{((-s)^(-3 eps))
   Gamma[-z1] Gamma[-z2] Gamma[3 eps + z1 + z2]
   Gamma[-z3] Gamma[-z4] Gamma[1 + z1 + z4]
   Gamma[-z5] Gamma[1 - 3 eps + z3 + z5]
   Gamma[1 - eps + z1 + z3 + z4 + z5]
   Gamma[-2 + 3 eps - z1 - z2 - z3 - z4 - 2 z5 - z6]
   Gamma[-1 + eps - z2 - z5 - z6]
   Gamma[-1 + 3 eps - z3 - z5 - z6]
   Gamma[1 + z2 + z6] Gamma[2 - 4 eps + z3 + z4 + z5 + z6]
   Gamma[2 - 2 eps + z1 + z2 + z3 + z4 + z5 + z6 - z7]
   Gamma[-z7] Gamma[-z1 - z4 + z7] Gamma[1 - 2 eps + z5 + z7])/
   (Gamma[2 - 4 eps] Gamma[-z1 - z4]
   Gamma[2 - 3 eps + z1 + z3 + z4 + z5]
   Gamma[-1 + 3 eps - z2 - z3 - 2 z5 - z6]
   Gamma[2 - eps + z1 + z2 + z3 + z4 + z5 + z6])}
```

Figure 4.15: MB representation for the diagram in Fig. (7.4) obtained by the GA.

Let us consider now the diagram in Fig. (7.4). The LA method gives here 4-dimensional MB representation, see section E4 in [40]. This diagram corresponds to the right skeleton diagram in Fig. (4.12) with two external legs attached to vertices on the circle, so variable transformation of the type (4.74) is not needed. The U polynomial has the same structure as in (4.92), corresponding F polynomial can be simplified to the following form:

$$F = -sv_3v_4v_6(v_1 + v_5) - sv_2v_3(v_4 + v_1v_5) - sv_1v_3v_6(v_2 + v_5). \tag{4.93}$$

This means three additional MB integrations plus 4 integrations which come from the U polynomial. The resulting 7-dimensional output from AMBREv3.2 is shown in Fig. (4.15), for simplicity the powers of all propagators are set to 1.

The integration over z7 corresponds to the term v_1+v_5 and can be immediately removed with the help of 1st Barnes lemma. In the next step the following simplification is possible. Making the shift z6 -> z6 - z3 - z2, one can apply 1st Barnes lemma to the variable z2 and 2nd Barnes lemma to the variable z3, obtaining a 4-dimensional representation as in case of the LA. This shift was found using the algorithm described in Sec.(4.4).

To complete this section and the discussion of the GA method for 3-loop cases we present a strategy of choosing CW variables and a factorization for the first type of 3-loop diagrams in Fig. (4.13). Because here we have only five v-variables, the optimal choice is to consider two CW variables. For (4.88) this leads to

$$\int_0^\infty dv_1dv_2 \int_0^1 dv_3dv_4dv_5\delta(1 - v_3 - v_4 - v_5) \tag{4.94}$$

and

$$U_{CW} = v_1v_2 + v_2v_3v_4 + v_1v_3v_5 + v_2v_3v_5 + v_1v_4v_5 + v_3v_4v_5. \tag{4.95}$$

This operation reduces the number of terms in U from 8 to 6. As in the previous case, there are also 4 possibilities to choose CW variables. A factorization scheme to integrate

over CW variables can be the following:

$$U_{CW} = v_2(v_1 + v_3v_4) + v_3v_5(v_2 + v_4) + v_1v_5(v_3 + v_4). \tag{4.96}$$

Due to the smaller number of variables and terms there are now only 4 possibilities to factorize U. All other steps are the same as in the case of the second type of 3-loop diagrams, see Fig. (4.14).

In the next section we introduce a so-called hybrid method which for many cases can help to avoid complications when using the GA at the 3-loop level.

4.6.3 Limitations and the hybrid approach

At the three-loop level, we can also try to combine all the advantages of the approaches described above. A general scheme is shown in Figs. (4.16) and (4.17). In the first case, Fig. (4.16), we start with the LA and integrate over one of the loop momenta. After that the obtained effective two-loop diagram is treated by the GA. In the second case, Fig. (4.17), we go in the opposite direction, first, we apply the GA to a two-loop sub-diagram, basically a non-planar one, and the remaining one-loop integral is processed in a simple way by the LA.

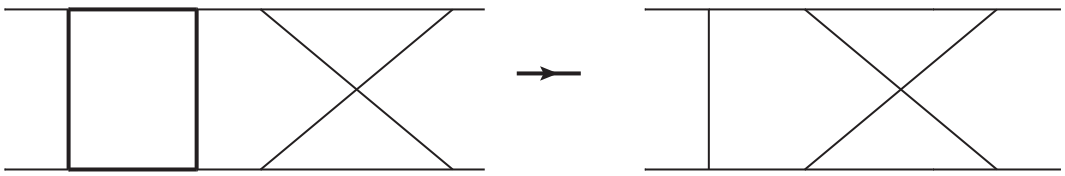

Figure 4.16: Hybrid approach. The LA is applied first – H ($1 \to 2$).

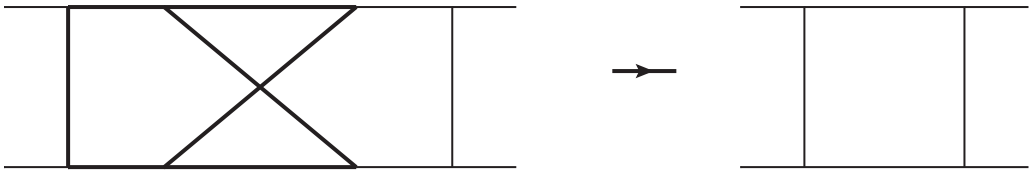

Figure 4.17: Hybrid approach. The GA is applied first – H ($2 \to 1$).

Here we present several examples which show the potential of the methods for specific topologies.

The first example is a non-planar vertex shown in Fig. (4.18). As was mentioned before the combination of three different loop momenta in one propagator usually does not take place, they appear here due to the procedure of generation of diagrams using FeynArts. A "normal" form can be obtained by a simple shift, $k_3 \to k_3 + k_2$. In this particular case that plays no role because in the first iteration the momentum k_1 circulates only in the one-loop sub-diagram shown in bold, and for the GA, in the second iteration the momentum flow is

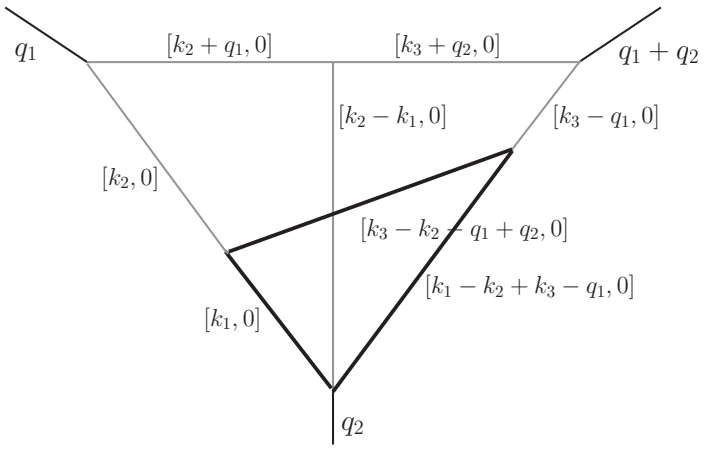

Figure 4.18: Hybrid method, example I. The bold lines show the choice of the one-loop sub-diagram in the first step of `H` ($1 \to 2$).

```
PR[k1, 0, n1] PR[-k1 + k2, 0, n2] PR[k2, 0, n3] PR[k2 + q1, 0, n4]
PR[k3 + q2, 0, n5] PR[k3 - q1, 0, n6] PR[-k2 + k3 - q1 + q2, 0, n7]
PR[k1 - k2 + k3 - q1, 0, n8]

--iteration nr: 1 with momentum: k1

F polynomial during this iteration
-PR[k2,0] X[1] X[2]-PR[k2-k3+q1,0] X[1] X[3]-PR[k3-q1,0] X[2] X[3]

PR[k2, 0, nz3] PR[k3 - q1, 0, nz6] PR[k2 + q1, 0, n4] PR[k3 + q2, 0,n5]
PR[-k2 + k3 - q1 + q2, 0, n7] PR[k2 - k3 + q1, 0, z]
```

Figure 4.19: Partial output of the `AMBRE` program illustrating the `H` ($1 \to 2$) method for the diagram in Fig. (4.18).

not important. At this point one should stress that the momentum flow plays a significant role for the hybrid approach and the `LA` – each loop momentum should go through a minimal possible topological construction. For example, due to some specific construction procedure k_1 could appear in more than three propagators. In this case a preliminary shift of loop momenta is needed for a successful application of the hybrid method.

As shown in Fig. (4.19), after a first integration one gets a 2-dimensional representation. The remaining six propagators (see the last line) correspond to the 2-loop non-planar vertex, so the final representation is 4-dimensional. The dimensionality for this diagram is also shown in Tab. 4.2.

The second example illustrating the opposite direction of the method is shown in Figs. (4.20) and (4.21). In the first iteration the two-loop non-planar vertex effectively has two off-shell external legs, so after transformation (4.74), in contrast to the non-planar vertex from Sec. 4.6.1, one gets a 6-dimensional representation. The remaining three propagators

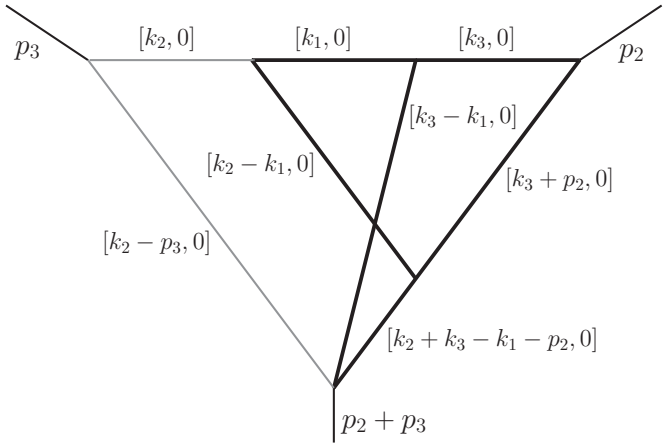

Figure 4.20: Hybrid method, example II. The bold lines show the choice of the two-loop sub-diagram in the first step of `H` ($2 \to 1$).

```
PR[k1, 0, n8] PR[k2, 0, n6] PR[-k1 + k2, 0, n7] PR[k3, 0, n5]
PR[-k1 + k3, 0, n3] PR[k3 + p2, 0, n4] PR[-k1 + k2 + k3 + p2, 0, n2]
PR[k2 - p3, 0, n1]

--iteration nr: 1 with momentum: {k1, k3}

F polynomial during this iteration
-PR[k2, 0] x[1] x[2] x[3] - PR[k2, 0] x[1] x[2] x[4] -
PR[k2, 0] x[2] x[3] x[4] - PR[k2, 0] x[1] x[2] x[5] -
PR[k2 + p2, 0] x[2] x[4] x[5] - PR[k2, 0] x[1] x[2] x[6] -
PR[k2 + p2, 0] x[1] x[3] x[6] - PR[k2 + p2, 0] x[1] x[4] x[6] -
PR[k2 + p2, 0] x[2] x[4] x[6] - PR[k2 + p2, 0] x[3] x[4] x[6] -
PR[k2, 0] x[1] x[5] x[6] - PR[k2 + p2, 0] x[4] x[5] x[6]

PR[k2, 0, nz6] PR[k2 - p3, 0, n1] PR[k2 + p2, 0, z]
```

Figure 4.21: Partial output of the `AMBRE` program illustrating the `H` ($2 \to 1$) method for the diagram in Fig. (4.20).

form one-loop vertex and give no additional `MB` integration. See also Tab.4.2.

To summarize the discussion of the hybrid method we would like to show in Tab. 4.2 dimensionalities and exact approaches which give optimal results for typical non-planar topologies which can appear in future 3-loop $Z \to f\bar{f}$ studies shown in Fig. (4.22).

At 4-loops, complexity of U and F leaves almost no possibility to construct reasonable representation using the `GA`. The hybrid method opens a possibility to construct `MB` representations beyond 3 loops, see for example for one of the possible implementations in [175].

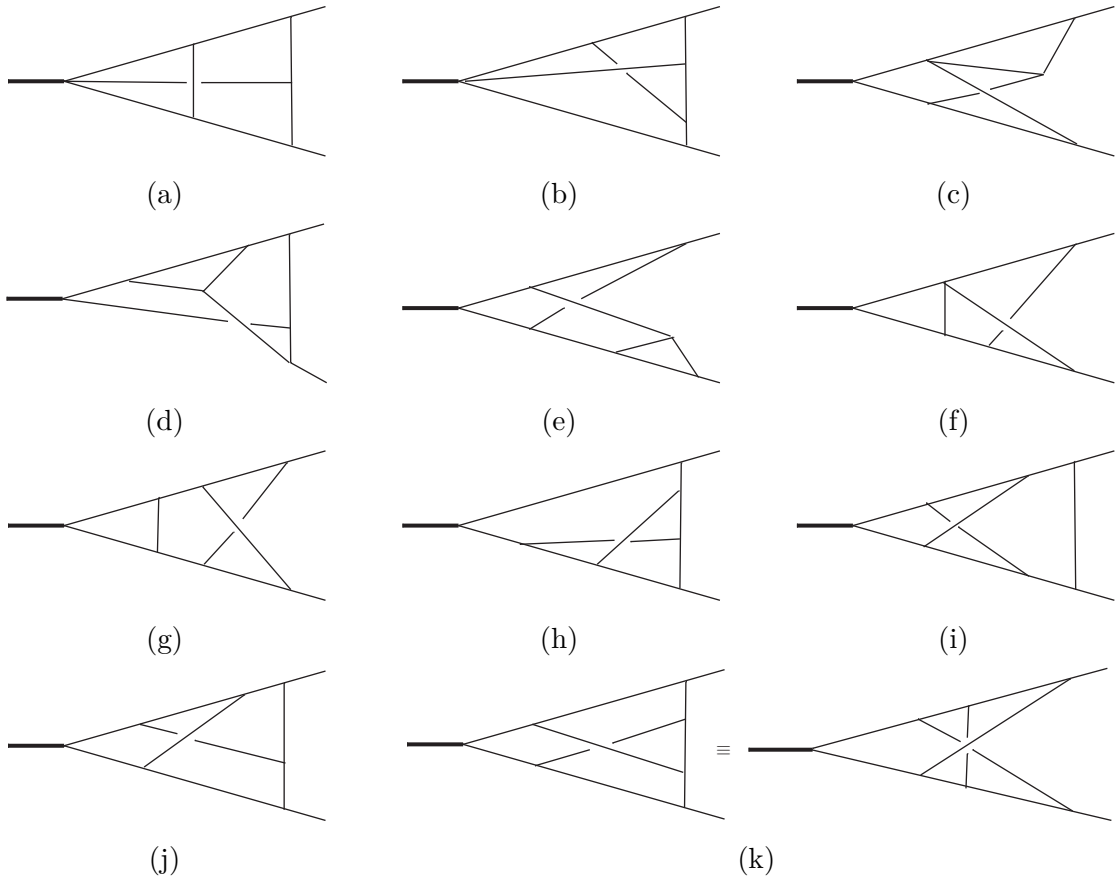

Figure 4.22: General non-planar 3-loop electroweak SM topologies for the $Z \to f\bar{f}$ vertex. Diagrams correspond to those mentioned in Tab. 5.9.

diagram	MB dimensionality	method
fig. 4.22a	4	H $(1 \to 2)$
fig. 4.22b	6	H $(2 \to 1)$
fig. 4.22c	4	H $(1 \to 2)$
fig. 4.22d	4	H $(1 \to 2)$
fig. 4.22e	4	H $(1 \to 2)$
fig. 4.22f	4	H $(1 \to 2)$
fig. 4.22g	4	H $(1 \to 2)$
fig. 4.22h	8	H $(2 \to 1)$
fig. 4.22i	10	H $(2 \to 1)$
fig. 4.22j	12	H $(1 \to 2)$
fig. 4.22k	12	H $(1 \to 2)$

Table 4.2: Dimensionalities and type of hybrid method used for the non-planar diagrams shown in Fig.4.22.

4.7 Numerical integration of MB integrals

The general form of the MB representation shown in Eq. (4.39) is well defined if real parts of all Γ-functions are positive (equivalent to the separation of all right poles of Γ-functions from all left ones). This can be achieved by the proper choice of real parts for all integration variables z_{i0} together with ϵ. $1/\epsilon^i$ poles are extracted making an analytical continuation $\epsilon \to 0$, and collecting residues corresponding to crossings poles of Γ-functions.

The final form of MB integrals suited to numerical integration is obtained by Laurent expansions around $\epsilon = 0$ and can be represented as follows:

$$I = \frac{1}{(2\pi i)^r} \int\limits_{-i\infty+z_{10}}^{+i\infty+z_{10}} \cdots \int\limits_{-i\infty+z_{r0}}^{+i\infty+z_{r0}} \prod_i^r dz_i \, \mathbf{F}(Z,S) \frac{\prod\limits_{j=1}^{N_n} \Gamma(\Lambda_j)}{\prod\limits_{k=1}^{N_d} \Gamma(\Lambda_k)} f_\psi(Z). \tag{4.97}$$

Notations are the same as in Eq. (4.39) but now it doesn't depend on ϵ. The positions of contours are fixed by z_{i0}. The part $f_\psi(Z)$ may depend on poly-gamma functions and constants like Eulergamma γ_E or is equal to 1 if the corresponding Feynman integral has no $1/\epsilon^i$ poles.

To understand the problems one faces during numerical integrations of MB integrals, one has first to study the asymptotic behavior of integrands. The main building blocks of MB integrals are Gamma and poly-gamma functions which have the following asymptotics for large arguments $|z| \to \infty$

$$\Gamma(z)_{|z|\to\infty} = \sqrt{2\pi} e^{-z} z^{z-\frac{1}{2}} \left[1 + \frac{1}{12z} + \frac{1}{288z^2} + \dots\right], \tag{4.98}$$

$$\begin{aligned}
\psi(z)_{|z|\to\infty} &= \ln z - \frac{1}{2z} - \frac{1}{12z^2} + \dots \\
\psi'(z)_{|z|\to\infty} &= \frac{1}{z} + \frac{1}{2z^2} + \frac{1}{6z^3} + \dots \\
\psi''(z)_{|z|\to\infty} &= -\frac{1}{z^2} - \frac{1}{z^3} + \dots \\
\psi^{(3)}(z)_{|z|\to\infty} &= \frac{2}{z^3} + \dots \\
&\dots \quad .
\end{aligned} \tag{4.99}$$

Let's now consider a definite example, namely the $1/\epsilon^2$ pole of the integral 5 of the class **0h0w** shown in App. 7.3

$$I^{0h0w}_{5,\epsilon^{-2}} = \frac{1}{2s} \frac{1}{2\pi i} \int\limits_{-i\infty-\frac{1}{2}}^{+i\infty-\frac{1}{2}} \left(\frac{M_Z^2}{-s}\right)^z \frac{\Gamma^3(-z)\Gamma(1+z)}{\Gamma^2(1-z)}. \tag{4.100}$$

We are interested only in the leading term of the expansion for big $|z|$. It is evident that the poly-gamma functions as well as the linear fractional part of the asymptotic of gamma functions do not contribute, and we are looking only on the $e^{-z} z^{z-\frac{1}{2}}$ part of the

Stirling formula (4.98). It is easy to see that e^{-z} parts from different functions cancel each other. This is a general property of MB representations and can be extended to any multi-dimensional integral. Based on that the asymptotic behavior of MB integrals is determined only by the $z^{z-\frac{1}{2}} = e^{(z-\frac{1}{2})\ln z}$ part of Eq. (4.98).

For the example (4.100) the ratio of Gamma functions, which we will call a "core" of the MB representation is in the limit $|z| \to \infty$

$$\frac{\Gamma^3(-z)\Gamma(1+z)}{\Gamma^2(1-z)} \xrightarrow{|z|\to\infty} e^{z(\ln z - \ln(-z)) + \frac{1}{2}\ln z - \frac{5}{2}\ln(-z)}. \tag{4.101}$$

Here one should notice that independent of the contour of integration, the following relation holds: $\ln z - \ln(-z) = i\pi\,\mathrm{sign}(\Im m\, z)$.

In case of practical applications, as mentioned above, the integration contour is a straight line parallel to the imaginary axis, so $z = z_0 + i\,t,\ \ t \in (-\infty, \infty)$ and the core of MB integral (4.100) in the limit $|z| \to \infty \Leftrightarrow t \to \pm\infty$ can be represented as

$$\frac{\Gamma^3(-z)\Gamma(1+z)}{\Gamma^2(1-z)} \longrightarrow e^{-\pi|t|}\frac{1}{|t|^2} \tag{4.102}$$

and is a well-behaved and non-oscillating function.[7]

Now lets look on the kinematics term $\left(\frac{M_Z^2}{-s}\right)^z$. In the Euclidean case $s < 0$, this factor gives only oscillations which are well damped by the $e^{-\pi|t|}$. In the Minkowskian case $s \to s + i\delta\,(s > 0)$, where $i\delta$ comes from the propagator definition and is needed to choose the proper branch of the logarithm,

$$\left(\frac{M_Z^2}{-s}\right)^z = e^{z\ln(-\frac{M_Z^2}{s} + i\,\delta)} \longrightarrow e^{i\,t\ln\frac{M_Z^3}{s}} e^{-\pi t},\, s > 0. \tag{4.103}$$

As one can see, $e^{-\pi|t|}$ and $e^{-\pi t}$ cancel each other when $t \to -\infty$ and oscillations are not damped any more by an exponential factor. Moreover it may happen that an exponent α in the fractional part $\frac{1}{|t|^\alpha}$ of the limit (4.102) (in our example $\alpha = 2$) is not big enough to guarante the convergence of the integral (see, e.g., Sec. (3.4) in [127]). This is the main problem of numerical integration of MB integrals for physical kinematics.

One of the ways to avoid the described problem is to perform a deformation of the integration path in a way then the overall exponential damping factor is restored. Presently two different approaches are known. The first one is based on the rotation of integration contours for all variables by the same angle: $z_i = z_{i0} + (i+\theta)t_i$. This approach is described in [29] and works well for certain integrals, but is not general. A second approach is based on more advanced deformations of contours $z_i = z_{i0} + f_i(t_1, ..., t_n) + it_i$ which allow also to improve the smoothness of the integrand but, at the present moment, it works only for one-dimensional integrals, see [146].

Here we would like to discuss methods of integrations of MB integrals without contour deformations. In practice for numerical integrations some external libraries like CUBA are

[7] This can be also extended to any multi-dimensional integral and is valid only for contours parallel to the imaginary axis.

used. Usually the integration over infinite intervals requires theirs transformation into finite ones (for example in `CUBA` it is the interval $[0,1]$). In the package `MB.m` such transformation is done in the following way

$$t_i \to \ln\left(\frac{x_i}{1-x_i}\right), \quad dt_i \to \frac{dx_i}{x_i(1-x_i)}. \tag{4.104}$$

In case of example (4.100), the limit $t \to -\infty$ is equivalent to $x \to 0$ and in this limit the integrand behaves like

$$\frac{1}{x\ \ln^2 x} \xrightarrow{x\to 0} \infty. \tag{4.105}$$

This singularity is integrable but prevents reaching a high accuracy result. As an alternative one can transform the integration interval $(-\infty,\infty)$ into $[0,1]$ differently:

$$t_i \to \tan\left(\pi(x_i-\frac{1}{2})\right), \quad dt_i \to \frac{\pi dx_i}{\cos^2\left(\pi(x_i-\frac{1}{2})\right)}. \tag{4.106}$$

The corresponding limit now is

$$\frac{1}{\sin^2\left(\pi(x_i-\frac{1}{2})\right)} \xrightarrow{x\to 0} 1, \tag{4.107}$$

and the integration can be easily performed. One should stress that with the new type of transformation imaginary parts of arguments of Gamma functions grow much faster than with ln-type transformation. At some moment Gamma functions in the denominator become equal to 0, numerically. To avoid this problem we compute the core of `MB` integral in the following way:

$$\frac{\prod_{j=1}^{N_n}\Gamma(\Lambda_j)}{\prod_{k=1}^{N_d}\Gamma(\Lambda_k)} = \mathrm{Exp}\left(\sum_{j=1}^{N_n}\ln\Gamma(\Lambda_j) - \sum_{k=1}^{N_d}\ln\Gamma(\Lambda_k)\right), \tag{4.108}$$

where $\ln\Gamma$ denotes the log-gamma function (see, e.g., `CernLib` documentation).

The transition from one- to multi-dimensional integrals quite often is not a trivial task. Let's consider the integral 2 of the class **0h0w**, see App. 7.3. It has a 3-dimensional representation which can be written in two different forms:

$$\begin{aligned} I^{0h0w}_{2,I} =& \frac{1}{s^2}\frac{1}{(2\pi i)^3}\int_{-i\infty-\frac{47}{37}}^{i\infty-\frac{47}{37}} dz_1 \int_{-i\infty-\frac{44}{211}}^{i\infty-\frac{44}{211}} dz_2 \int_{-i\infty-\frac{176}{235}}^{i\infty-\frac{176}{235}} dz_3 \left(-\frac{s}{M_Z^2}\right)^{-z_1} \Gamma(-1-z_1)\Gamma(2+z_1) \\ & \Gamma(-1-z_{12})\Gamma(-z_2)\Gamma^2(1+z_{12}-z_3)\Gamma(-z_3)\Gamma(1+z_3)\Gamma^2(-z_1+z_3)\Gamma(-z_{12}+z_3) \\ & /\Gamma(-z_1)\Gamma(1-z_2)\Gamma(1-z_1+z_3) \end{aligned} \tag{4.109}$$

and

$$I_{2,II}^{0h0w} = \frac{1}{s^2}\frac{1}{(2\pi i)^3}\int\limits_{-i\infty-\frac{47}{37}}^{i\infty-\frac{47}{37}} dz_1 \int\limits_{-i\infty-\frac{139}{94}}^{i\infty-\frac{139}{94}} dz_2 \int\limits_{-i\infty-\frac{176}{235}}^{i\infty-\frac{176}{235}} dz_3 \left(-\frac{s}{M_Z^2}\right)^{-z_1} \Gamma(-1-z_1)\Gamma(2+z_1)$$
$$\Gamma(-1-z_2)\Gamma(z_1-z_2)\Gamma(1+z_2-z_3)^2\Gamma(-z_3)\Gamma(1+z_3)\Gamma(-z_1+z_3)^2\Gamma(-z_2+z_3)$$
$$/\Gamma(-z_1)\Gamma(1+z_1-z_2)\Gamma(1-z_1+z_3). \qquad (4.110)$$

The first integral is obtained using the MB-suite Fig. (4.1). The second – by the shift $z_2 \to z_2 - z_1$, from the first result. The difference between the two expressions is in their asymptotic behavior. Eq. (4.109) has the cancellation of the overall dumping factor along the line $t_1 = -t_2 = t$, $t_3 = 0$, and Eq. (4.110) - along the t_1-axis ($t_1 = t$, $t_2 = t_3 = 0$). Numerical results for both integrals obtained with different combinations of transformations (4.104) and (4.106) are compared with an analytical solution in Tab. 4.3. In the table MB1 corresponds to the numerical integration of Eq. (4.109), where mapping into the integration interval $[0, 1]$ is performed by the tan-type of transformation (4.106) for all variables. MB2 - integration of Eq. (4.109), tan-mapping for t_1 and t_2, ln-mapping (4.104) for t_3. MB3 - Eq. (4.110) with tan-mapping for all variables. MB4 - Eq. (4.110), tan-mapping for t_1 and ln-mapping for the remaining variables. MB5 - Eq. (4.109), ln-mapping for all variables. All integrations are done by the CUHRE routine from the CUBA library. Maximum number of integrand evaluations allowed was set to 10^7. The absolute error reported by the routine is at the level of 10^{-8}. MB6 - the same as MB5 but integration is done by the VEGAS routine with an error estimation of $\sim 10^{-4}$.

As one can see from Tab. (4.3) a sufficient numerical accuracy was obtained only in the case MB4. This shows that the direct integration of MB integrals is possible but limited by several factors. First, the best accuracy is achieved when the cancellation of the exponential damping factor happens along one of the axes in the integration space. In the case of integrals with more than one scale, a cancellation takes place in multiple directions or in some sector of the integration space and getting a high accuracy result becomes much more complicated. Second, as in the case of one-dimensional integrals, exponent α in $\frac{1}{|t|^\alpha}$ in the asymptotical expansion along the direction of the damping factor cancellation may be not big enough for a good convergence. In a multi-dimensional case in contrast to the one-dimensional case, this problem can be solved by shifts of integration contours $z_i \to z_{i0} + s_i + it_i$, $s_i \in Z$. An appropriate set of $\{s_i\}$ allows to increase α. For example, in case of the integral (4.110), taking $z_3 \to -176/235 - 1 + it_3$, one can get $\alpha = 881/235$ instead of $646/235$. In addition to the shifted integral, contributions from the residues must be added. The additional terms are MB integrals with one integration less and hence simpler to evaluate.

If shifts can help to change asymptotical behavior, the cancellation of the damping factor in some integration subspace is a general feature of multi-scale integrals and cannot be fixed.

For the calculation of two-loop corrections to EWPOs, a new method of calculation of MB integrals was used. It is based on properties of MB integrals described above and its main feature is that by shifts of integration contours $\{s_i\}$ one can not only change the asymptotic behavior of the integrand but also make the absolute value of the integral

	$s = 1$	
AB	$-1.\mathbf{199526183135}$	$+5.\mathbf{567365907880}i$
MB1	$-1.\mathbf{19952}5259137$	$+5.\mathbf{56736}7419371i$
MB2	$-1.\mathbf{19952}4318757$	$+5.\mathbf{567365}298565i$
MB3	$-1.\mathbf{19952}6239547$	$+5.\mathbf{567365}843910i$
MB4	$-1.\mathbf{199526183}168$	$+5.\mathbf{56736590}7904i$
MB5	NaN	
MB6	$-1.\mathbf{20}4597845834$	$+5.\mathbf{567}518701898i$
	$s = 2$	
AB	$-1.\mathbf{842298196087}$	$+3.\mathbf{325738275614}i$
MB1	$-1.\mathbf{842}171254543$	$+3.\mathbf{32573}0490241i$
MB2	$-1.\mathbf{842}031171736$	$+3.\mathbf{325}621842247i$
MB3	$-1.\mathbf{84229819}1312$	$+3.\mathbf{32573}8333870i$
MB4	$-1.\mathbf{84229819}8430$	$+3.\mathbf{32573827}9891i$
MB5	NaN	
MB6	$-1.\mathbf{842}950555639$	$+3.\mathbf{324}950811982i$

Table 4.3: Numerical results for the integral 2 in Tab. 7.2 for two different values of s and $M_Z^2 = 1$. AB - analytical solution [176]. MB1-MB6 – numerical integration of the corresponding MB integrals.

	$s = 1$	
AB	$-5.\mathbf{46318633201975}$	$+3.\mathbf{83353434712221}i$
MB	$-5.\mathbf{46318633201}924$	$+3.\mathbf{83353434712}128i$
	$s = 2$	
AB	$-2.\mathbf{01402077672107}$	$+2.\mathbf{06704179425209}i$
MB	$-2.\mathbf{01402077672}170$	$+2.\mathbf{06704179425}242i$

Table 4.4: Numerical results for integral 43 in Tab. 7.2 for two different values of s and $M_Z^2 = 1$. AB - analytical solution [177]. MB - numerical integration of the corresponding representation is performed by the MB.m package.

negligibly small. A low accuracy of the result for the shifted integral plays no role in this case. This procedure is applied recursively to lower dimensional integrals which appear after shifts. The algorithm is implemented in the package MBnumerics.m, for more details see [130].

As a conclusion, one should notice that for some Feynman integrals the MB-suite works without MBnumerics and any additional tricks because even in the Minkowskian case a cancellation of the damping factor does not happen and the integrand of the corresponding MB integral has always Euclidean-like asymptotic by default. As an example, Tab. 4.4 shows a result for the integral 43 of the class **0h0w** (see App. 7.3) obtained just with the MB.m package.

Chapter 5

Z-boson resonance physics: 2–loop electroweak results and future projections

5.1 Introduction

Historically, the complete one-loop corrections to the Z-pole EWPOs were calculated for the first time in [13]. Over the next three decades many groups with many methods determined partial 2- and 3-loop corrections to EWPOs.

Already for the precision achieved at LEP and SLC, the calculation of loop corrections beyond the one-loop order was necessary to keep theory uncertainties under control. Specifically, these included two-loop $\mathcal{O}(\alpha\alpha_s)$ [178–182] and fermionic $\mathcal{O}(\alpha^2)$ [79, 80, 166, 183–194] corrections to the Fermi constant, which can be used to predict the W-boson mass, and to the Z-pole parameters. Here α refers an electroweak loop order, whereas "fermionic" denotes contributions from diagrams with at least one closed fermion loop. In addition, leading three- and four-loop results, enhanced by powers of the top Yukawa coupling y_t, were obtained at order $\mathcal{O}(\alpha_t\alpha_s^2)$ [195, 196], $\mathcal{O}(\alpha_t^2\alpha_s)$, $\mathcal{O}(\alpha_t^3)$ [197, 198], and $\mathcal{O}(\alpha_t\alpha_s^3)$ [199–201], where $\alpha_t = y_t^2/(4\pi)$.

While the numerical effects of the bosonic two-loop corrections are relatively small compared to the current experimental precision from LEP and SLC, their inclusion will become mandatory for future e^+e^- colliders, see TH1 in Tab. 2.1. Thus the computation of the full two-loop corrections for all Z-pole EWPOs is an important goal and the results are included in this thesis.

For the EW two-loop corrections, the calculation of the fermionic contributions was a natural first step, since these are numerically enhanced by the numbers of flavors and colors and by powers of y_t. Moreover, the fermionic two-loop diagrams are relatively simpler than the full set. For example, the latter includes non-planar vertex topologies, which are absent in the former. The remaining bosonic two-loop corrections to the Fermi constant and the leptonic effective weak mixing angle, $\sin^2\theta^\ell_{\text{eff}}$, have subsequently been presented in [78, 202–207], and more recently also for the weak mixing angle in the $b\bar{b}$ channel [37] and the remaining bosonic $\mathcal{O}(\alpha^2)$ contributions to the Z-boson total and partial widths, and

the hadronic Z-peak cross-section within the SM. The result has been published recently in [38].

5.2 $Z \to b\bar{b}$ decay: asymmetries and $\sin^2\theta^{\rm b}_{\rm eff}$

The unfolded Z-peak forward-backward asymmetry $A_{\rm FB}^{b\bar{b},0}$ and forward-backward left-right asymmetry $A_{\rm FB,LR}^{b\bar{b},0}$ can be written, in an approximation with neglecting non-factorisable terms [40], as

$$A_{\rm FB}^{b\bar{b},0} = \tfrac{3}{4} A_{\rm e} A_{\rm b}, \qquad\qquad A_{\rm FB,LR}^{b\bar{b},0} = \tfrac{3}{4} P_{\rm e} A_{\rm b}, \tag{5.1}$$

where $P_{\rm e}$ is the electron polarization and

$$A_{\rm b} = \frac{2\ \Re e\,\frac{v_{\rm b}}{a_{\rm b}}}{1+\left(\Re e\,\frac{v_{\rm b}}{a_{\rm b}}\right)^2} \quad = \quad \frac{1-4|Q_b|\sin^2\theta^{\rm b}_{\rm eff}}{1-4|Q_b|\sin^2\theta^{\rm b}_{\rm eff}+8Q_b^2\left(\sin^2\theta^{\rm b}_{\rm eff}\right)^2}. \tag{5.2}$$

The right part of (5.2) follows from the definition

$$\sin^2\theta^{\rm b}_{\rm eff} = \frac{1}{4|Q_b|}\left(1-\Re e\,\frac{v_{\rm b}}{a_{\rm b}}\right), \tag{5.3}$$

where $Q_b = -1/3$. Technically, the calculation of $A_{\rm b}$ rests on the calculation of the vertex form factor $V_\mu^{Zb\bar{b}}$, whose vector and axial-vector components can be obtained using the projection operations

$$v_{\rm b}(k^2) = \frac{1}{2(2-D)k^2}\,{\rm Tr}[\gamma^\mu \not{p}_1\, V_\mu^{Zb\bar{b}}\, \not{p}_2], \tag{5.4}$$

$$a_{\rm b}(k^2) = \frac{1}{2(2-D)k^2}\,{\rm Tr}[\gamma_5\,\gamma^\mu \not{p}_1\, V_\mu^{Zb\bar{b}}\, \not{p}_2], \tag{5.5}$$

where $D = 4-2\epsilon$ is the space-time dimension and $p_{1,2}$ are the momenta of the external b-quarks, and $k = p_1 + p_2$. As a result, only scalar integrals remain after projection, but they may contain non-trivial combinations of scalar products in the numerator. More specifically, we calculated here the bosonic two-loop contribution to the (complex) ratio $v_{\rm b}(M_Z^2)/a_{\rm b}(M_Z^2)$. It should be noted that in this thesis all external on-shell fermions in the Z-boson decay (leptons and quarks) are assumed to be massless.

It should be noted that the determination of the pseudo-observables in Eq. (5.1) from true observables requires carefully written interfaces for the unfolding and subtraction of QED, QCD and box contributions, and other contributions not contained in the pseudo-observables [72, 77]. In fact, the interfaces implemented in `ZFITTER` [72–74] have proven to be adequate for an analysis of Z-pole pseudo-observables at the $\mathcal{O}(\alpha^2)$ level [207]. This is a highly non-trivial issue which deserves further studies in the case of higher precision foreseen in the future e^+e^- colliders. The experimental values for $A_{\rm b}$ and $\sin^2\theta^{\rm b}_{\rm eff}$ from a global fit to the LEP and SLC data are [60, 208]:

$$A_{\rm b} = 0.899 \pm 0.013, \qquad\qquad \sin^2\theta^{\rm b}_{\rm eff} = 0.281 \pm 0.016. \tag{5.6}$$

The Standard Model prediction for the effective weak mixing angle can be written as

$$\sin^2\theta^{\rm b}_{\rm eff} = \left(1-\frac{M_W^2}{M_Z^2}\right)(1+\Delta\kappa_{\rm b}), \tag{5.7}$$

where $\Delta\kappa_{\rm b}$ contains the contributions from radiative corrections.

These can be embedded for any f-flavour, at the 2-loop renormalization level, in the following form [207]

$$\begin{aligned}\sin^2\theta^f_{\rm eff} &\equiv \left(1-\frac{\bar{M}_W^2}{\bar{M}_Z^2}\right)\Re e\left\{1+\Delta\bar{\kappa}^f_Z(M_Z^2)\right\} \\ &= \left(1-\frac{\bar{M}_W^2}{\bar{M}_Z^2}\right)\Re e\left\{1+\frac{a_f^{(1)}\,v_f^{(0)}-v_f^{(1)}\,a_f^{(0)}}{a_f^{(0)}(a_f^{(0)}-v_f^{(0)})}\right|_{k^2=M_Z^2} \\ &\quad + \left.\frac{a_f^{(2)}\,v_f^{(0)}\,a_f^{(0)}-v_f^{(2)}\,(a_f^{(0)})^2-(a_f^{(1)})^2\,v_f^{(0)}+a_f^{(1)}\,v_f^{(1)}\,a_f^{(0)}}{(a_f^{(0)})^2(a_f^{(0)}-v_f^{(0)})}\right|_{s=M_Z^2}\Bigg\},\end{aligned} \tag{5.8}$$

where $\sin^2\theta^f_{\rm eff}$ is related directly to vector and axial couplings

$$\bar{\kappa}^f_Z(s) = \frac{1}{4|Q_f|\sin^2\theta_W}\left(1-\frac{v_f(s)}{a_f(s)}\right), \tag{5.9}$$

The barred quantities refer to the pole scheme where $\bar{M}_Z$ is defined as the real part of the pole of the S matrix. The problem is a relation between experimental parametrization of the Z-resonance and its proper theoretical description. In general, the shape of the Z-resonance can be parametrized by an s-dependent K factor [40]

$$K_Z(s) = (1+i\bar{\Gamma}_Z/\bar{M}_Z)^{-1}\,\frac{s}{s-\bar{M}_Z^2+i\bar{M}_Z\bar{\Gamma}_Z}. \tag{5.10}$$

In many analyses of the LEP era, it was assumed that the Z width is s-dependent, because it is a result of renormalizing the Z boson self energy, which depends on s. Due to the absence of production thresholds around the Z peak, one finds to a very good level of precision:

$$K_Z(s) = \frac{s}{s-M_Z^2+iM_Z\Gamma_Z(s)}, \qquad \Gamma_Z(s) = \frac{s}{M_Z^2}\,\Gamma_Z. \tag{5.11}$$

Both definitions are related [209]:

$$\bar{M}_Z = M_Z\Big/\sqrt{1+\Gamma_{\rm Z}^2/M_Z^2} \approx M_Z - \frac{1}{2}\,\frac{\Gamma_Z^2}{M_Z}, \tag{5.12}$$

$$\bar{\Gamma}_Z = \Gamma_{\rm Z}\Big/\sqrt{1+\Gamma_{\rm Z}^2/M_Z^2} \approx \Gamma_Z - \frac{1}{2}\,\frac{\Gamma_Z^3}{M_Z^2}. \tag{5.13}$$

Numerically, this leads to $\overline{M}_{\rm Z} \approx M_Z - 34$ MeV and $\overline{\Gamma}_{\rm Z} \approx \Gamma_{\rm Z} - 0.9$ MeV.

This situation may be seen also in the following way [40]. The amplitude for $e^+e^- \to f\bar{f}$ near the Z pole, $\sqrt{s} \approx M_Z$ can be written in a theoretically well-defined way as a Laurent expansion around the complex pole $s_0 \equiv \overline{M}_{\mathrm{Z}}^2 - i\overline{M}_{\mathrm{Z}}\overline{\Gamma}_{\mathrm{Z}}$,

$$\mathcal{A}[e^+e^- \to f\bar{f}] = \frac{R}{s - s_0} + S + (s - s_0)S' + \ldots, \tag{5.14}$$

where $\overline{M}_{\mathrm{Z}}$ and $\overline{\Gamma}_{\mathrm{Z}}$ are the on-shell mass and width of the Z boson, respectively. According to eq. (5.14), the approximate line shape of the cross-section near the Z pole is given by $\sigma \propto [(s - \overline{M}_{\mathrm{Z}}^2)^2 + \overline{M}_{\mathrm{Z}}^2\overline{\Gamma}_{\mathrm{Z}}^2]^{-1}$. It is important to note that this differs from the line shape used in experimental analyses, which is of the form $\sigma \propto [(s - M_Z^2)^2 + s^2\Gamma_Z^2/M_Z^2]^{-1}$. As a result, the parameters in eq. (5.14) differ from the experimental mass M_Z and width Γ_Z from LEP by a fixed factor [209]:

$$\begin{aligned} \overline{M}_{\mathrm{Z}} &= M_Z \Big/ \sqrt{1 + \Gamma_{\mathrm{Z}}^2/M_Z^2}\,, \\ \overline{\Gamma}_{\mathrm{Z}} &= \Gamma_{\mathrm{Z}} \Big/ \sqrt{1 + \Gamma_{\mathrm{Z}}^2/M_Z^2}\,. \end{aligned} \tag{5.15}$$

5.3 Z-boson decay widths, branching ratios, hadronic peak cross section

The total width, $\overline{\Gamma}_{\mathrm{Z}}$, can be extracted from the condition that the Z propagator has a pole at $s = s_0$, leading to

$$\overline{\Gamma}_{\mathrm{Z}} = \frac{1}{\overline{M}_{\mathrm{Z}}} \mathrm{Im}\, \Sigma_{\mathrm{Z}}(s_0), \tag{5.16}$$

where $\Sigma_{\mathrm{Z}}(s)$ is the transverse part of the Z self-energy. Using the optical theorem, it can also be written as [80, 194]

$$\overline{\Gamma}_{\mathrm{Z}} = \sum_f \overline{\Gamma}_f, \tag{5.17}$$

$$\overline{\Gamma}_f = \frac{N_c^f \overline{M}_{\mathrm{Z}}}{12\pi} \Big[\mathcal{R}_{\mathrm{V}}^f F_{\mathrm{V}}^f + \mathcal{R}_{\mathrm{A}}^f F_{\mathrm{A}}^f \Big]_{s=\overline{M}_{\mathrm{Z}}^2}. \tag{5.18}$$

At 2-loop accuracy, it is not necessary to distinguish between barred and un-barred masses in the radiative corrections, since $\overline{M}_Z^2 - M_Z^2 = \mathcal{O}(\alpha^2)$ [207].

Here the sum runs over all fermion types besides the top quark, $f = e, \mu, \tau, \nu_e, \nu_\mu, \nu_\tau, u, d, c, s, b$, and $N_c^f = 3(1)$ for quarks (leptons). The radiator functions $\mathcal{R}_{\mathrm{V,A}}$ capture the effect of final-state QED and QCD corrections. They are known up to $\mathcal{O}(\alpha_{\mathrm{s}}^4)$ and $\mathcal{O}(\alpha^2)$ for massless external fermions and $\mathcal{O}(\alpha_{\mathrm{s}}^3)$ for the kinematic mass corrections [210–212]. For the results shown in this thesis, the explicit form given in the appendix of [80] has been used.

The remaining radiative corrections are IR finite and contained in the form factors $F_{\mathrm{V,A}}^f$. These include massive EW corrections as well as mixed EW–QCD and EW–QED corrections. The bosonic two-loop contributions, which are of interest for this thesis, contribute

according to [80]:

$$F^f_{\mathrm{V}(2)} = 2\,\mathrm{Re}\,(v_{f(0)}v_{f(2)}) + |v_{f(1)}|^2 - v^2_{f(0)}\Big[\mathrm{Re}\,\Sigma'_{\mathrm{Z}(2)} - (\mathrm{Re}\,\Sigma'_{\mathrm{Z}(1)})^2\Big] - 2\,\mathrm{Re}\,(v_{f(0)}v_{f(1)})\,\mathrm{Re}\,\Sigma'_{\mathrm{Z}(1)}\,, \tag{5.19}$$

$$F^f_{\mathrm{A}(2)} = 2\,\mathrm{Re}\,(a_{f(0)}a_{f(2)}) + |a_{f(1)}|^2 - a^2_{f(0)}\Big[\mathrm{Re}\,\Sigma'_{\mathrm{Z}(2)} - (\mathrm{Re}\,\Sigma'_{\mathrm{Z}(1)})^2\Big] - 2\,\mathrm{Re}\,(a_{f(0)}a_{f(1)})\,\mathrm{Re}\,\Sigma'_{\mathrm{Z}(1)}\,, \tag{5.20}$$

where v_f and a_f are the effective vector and axial-vector couplings, respectively, which include $Zf\bar{f}$ vertex corrections and Z–γ mixing contributions. Σ'_{Z} denotes the derivative of Σ_{Z}, and the loop order is indicated by the subscript (n).

It should be pointed out that v_f, a_f and Σ_Z as defined above include γ–Z mixing contributions, *i. e.*

$$v_f(s) = v^{\mathrm{Z}}_f(s) - v^{\gamma}_f(s)\,\frac{\Sigma_{\gamma\mathrm{Z}}(s)}{s+\Sigma_{\gamma\gamma}(s)}\,, \tag{5.21}$$

$$a_f(s) = a^{\mathrm{Z}}_f(s) - a^{\gamma}_f(s)\,\frac{\Sigma_{\gamma\mathrm{Z}}(s)}{s+\Sigma_{\gamma\gamma}(s)}\,, \tag{5.22}$$

$$\Sigma_{\mathrm{Z}}(s) = \Sigma_{\mathrm{ZZ}}(s) - \frac{[\Sigma_{\gamma\mathrm{Z}}(s)]^2}{s+\Sigma_{\gamma\gamma}(s)}\,. \tag{5.23}$$

Here v^{Z}_f and a^{Z}_f are the one-particle irreducible $Zf\bar{f}$ vector and axial-vector vertex contributions, respectively, whereas v^{γ}_f and a^{γ}_f are their counterpart for the $\gamma f\bar{f}$ vertex. Furthermore, $\Sigma_{V_1V_2}$ denotes the one-particle irreducible V_1–V_2 self-energy.

Another important quantity is the hadronic peak cross section, σ^0_{had}, which is defined as the total cross section for $e^+e^- \to (Z) \to$ hadrons for $s = M^2_Z$, after removal of s-channel photon exchange and box diagram contributions, as well as after the de-convolution of initial-state and initial-final interference QED effects [19, 60]. The impact of the bosonic two-loop vertex corrections on σ^0_{had} is given by [80, 194]

$$\sigma^0_{\mathrm{had}(2)} = \sum_{f=u,d,c,s,b} \frac{12\pi}{\overline{M}^2_{\mathrm{Z}}}\left[\frac{\overline{\Gamma}_{e(0)}\overline{\Gamma}_{f(2)} + \overline{\Gamma}_{e(2)}\overline{\Gamma}_{f(0)}}{\overline{\Gamma}^2_{\mathrm{Z}(0)}} - 2\frac{\overline{\Gamma}_{e(0)}\overline{\Gamma}_{f(0)}}{\overline{\Gamma}^2_{\mathrm{Z}(0)}}\overline{\Gamma}^2_{\mathrm{Z}(2)}\right]. \tag{5.24}$$

The form factors $F^f_{\mathrm{V,A}}$ are understood to include appropriate counterterms such that they are UV finite. All calculations shown here are made in the on-shell renormalization scheme, which defines all particle masses in terms of their (complex) propagator poles and the electromagnetic coupling in terms of the photon-electron vertex in the Thomson limit. A more detailed discussion of the relevant counterterms can be found in [191].

5.4 The complete 2-loop results

As a consequence of the renormalization scheme, the EW corrections are organized as a series in the electromagnetic coupling α, rather than the Fermi constant G_μ. Instead, G_μ

will be used to compute M_W within the SM, including appropriate two-loop and partial higher-loop corrections. After this step, the remaining input parameters for the prediction of the Z coupling form factors are M_Z, M_H, m_t, G_μ, α, α_s and $\Delta\alpha$. Here $\Delta\alpha$ captures the running of the electromagnetic coupling induced by light fermion loops. It is defined through $\alpha(M_Z^2) = \alpha(0)/(1-\Delta\alpha)$, where $\alpha(q^2)$ is the coupling at scale q^2. The contribution from leptons to $\Delta\alpha$ can be computed perturbatively and is known at the three-loop level [213], $\Delta\alpha_\mathrm{lept}(M_Z) = 0.0314976$. On the other hand, the quark contribution is non-perturbative at low scales and thus is commonly derived from experimental data. For recent evaluations of $\Delta\alpha^{(5)}_\mathrm{had}$, see [214–216]. As a reference value, $\Delta\alpha^{(5)}_\mathrm{had} = 0.02750$ is used in this work.

Though in principle Γ_Z and Γ_W are calculable quantities, they are needed as initial inputs to convert M_Z and M_W to the complex pole scheme, see eq. (5.15). Furthermore, the radiator functions $\mathcal{R}^f_{\mathrm{V,A}}$ depend on b-quark ($m_\mathrm{b}^{\overline{\mathrm{MS}}}$), c-quark ($m_\mathrm{c}^{\overline{\mathrm{MS}}}$) and $\tau-$lepton kinematic fermion mass effects in the final state, whereas the masses of electron, muon, neutrinos, and $u/d/s$ quarks can be taken as zero to a very good approximation. In contrast to all other masses in this work, the $\overline{\mathrm{MS}}$ masses are used for the bottom and charm quarks, since their on-shell counterparts are poorly defined.

All the numerical results discussed below are based on the input parameters gathered in Tab. 5.1.

Parameter	Value	Range
M_Z	91.1876 GeV	$\pm$0.0042 GeV
Γ_Z	2.4952 GeV	-
M_W	80.385 GeV	$\pm$0.030 GeV
Γ_W	2.085 GeV	-
M_H	125.1 GeV	$\pm$5.0 GeV
m_t	173.2 GeV	$\pm$4.0 GeV
$m_\mathrm{b}^{\overline{\mathrm{MS}}}$	4.20 GeV	-
$m_\mathrm{c}^{\overline{\mathrm{MS}}}$	1.275 GeV	-
m_τ	1.777 GeV	-
$m_e, m_\mu, m_u, m_d, m_s$	0	-
$\Delta\alpha$	0.05900	$\pm$0.0050
$\alpha_\mathrm{s}(M_Z)$	0.1184	$\pm$0.0005
G_μ	1.16638×10^{-5} GeV^{-2}	-

Table 5.1: Input parameters used in the numerical analysis, taken from [213, 217, 218].

5.4.1 $Z \to b\bar{b}$ decay and $\sin^2\theta^\mathrm{b}_\mathrm{eff}$

With the defined input values, the *bosonic* electroweak two-loop corrections amount to

$$\Delta\kappa_\mathrm{b}^{(\alpha^2,\mathrm{bos})} = -0.9855 \times 10^{-4}. \tag{5.25}$$

Order	Value $[10^{-4}]$	Order	Value $[10^{-4}]$
α	468.945	$\alpha_t^2\alpha_s$	1.362
$\alpha\alpha_s$	−42.655	α_t^3	0.123
$\alpha_t\alpha_s^2$	−7.074	α_{ferm}^2	3.866
$\alpha_t\alpha_s^3$	−1.196	α_{bos}^2	−0.986

Table 5.2: Comparison of different orders of radiative corrections to $\Delta\kappa_b$, using the input parameters in Tab. 5.1.

This result can be compared to the already known corrections: one-loop contributions [13, 14], *fermionic* electroweak two-loop corrections [79], $\mathcal{O}(\alpha\alpha_s)$ QCD corrections [178–182], [219–224], and partial higher-order corrections of orders $\mathcal{O}(\alpha_t\alpha_s^2)$ [195, 196], $\mathcal{O}(\alpha_t\alpha_s^3)$ [199–201], $\mathcal{O}(\alpha^2\alpha_t)$ and $\mathcal{O}(\alpha_t^3)$ [197, 198]. The numerical values for the corresponding contributions are listed in Tab. 5.2.

For varying input parameters, the new result is best expressed in terms of a simple fitting formula,

$$\Delta\kappa_b^{(\alpha^2,\text{bos})} = k_0 + k_1 c_H + k_2 c_t + k_3 c_t^2 + k_4 c_H c_t + k_5 c_W, \tag{5.26}$$

with

$$\begin{aligned} c_H &= \log\left(\frac{M_H}{M_Z}\times\frac{91.1876\text{ GeV}}{125.1\text{ GeV}}\right), \quad c_t = \left(\frac{m_t}{M_Z}\times\frac{91.1876\text{ GeV}}{173.2\text{ GeV}}\right)^2 - 1, \\ &\qquad\qquad c_W = \left(\frac{M_W}{M_Z}\times\frac{91.1876\text{ GeV}}{80.385\text{ GeV}}\right)^2 - 1. \end{aligned} \tag{5.27}$$

Fitting this formula to the full numerical result, the coefficients are obtained as

$$\begin{aligned} &k_0 = -0.98605\times10^{-4}, \quad k_1 = 0.3342\times10^{-4}, \quad k_2 = 1.3882\times10^{-4}, \\ &k_3 = -1.7497\times10^{-4}, \quad k_4 = -0.4934\times10^{-4}, \quad k_5 = -9.930\times10^{-4}. \end{aligned} \tag{5.28}$$

This parameterization reproduces the full calculation with average and maximal deviations of 5×10^{-8} and 1.2×10^{-7}, respectively, for the input parameter ranges indicated in Tab. 5.1.

Combining this result with the already known corrections (see above) the currently most precise prediction for $\sin^2\theta_{\text{eff}}^b$ is obtained. Additionally, one free parameter can be eliminated by using the Standard Model prediction of M_W from the Fermi constant G_μ. The W-boson mass has been calculated previously including the same perturbative higher order contributions as listed above [205]. To a very good approximation, this result can be written as

$$\sin^2\theta_{\text{eff}}^b = s_0 + d_1 L_H + d_2 L_H^2 + d_3\Delta_\alpha + d_4\Delta_t + d_5\Delta_t^2 + d_6\Delta_t L_H + d_7\Delta_{\alpha_s} + d_8\Delta_t\Delta_{\alpha_s} + d_9\Delta_Z \tag{5.29}$$

with

$$\begin{aligned} &L_H = \log\left(\frac{M_H}{125.7\text{ GeV}}\right), \quad \Delta_t = \left(\frac{m_t}{173.2\text{ GeV}}\right)^2 - 1, \quad \Delta_Z = \frac{M_Z}{91.1876\text{ GeV}} - 1, \\ &\Delta_\alpha = \frac{\Delta\alpha}{0.0059} - 1, \qquad \Delta_{\alpha_s} = \frac{\alpha_s}{0.1184} - 1. \end{aligned} \tag{5.30}$$

Here $\Delta\alpha$ is the shift of the electromagnetic fine structure constant due to light fermion loops between the scales $q^2 = 0$ and M_Z^2. The best-fit numerical values for the coefficients are given by

$$\begin{aligned} s_0 = 0.232704, \quad & d_1 = 4.723 \times 10^{-4}, \quad d_2 = 1.97 \times 10^{-4}, \quad d_3 = 2.07 \times 10^{-2}, \\ & d_4 = -9.733 \times 10^{-4}, \quad d_5 = 3.93 \times 10^{-4}, \quad d_6 = -1.38 \times 10^{-4}, \\ & d_7 = 2.42 \times 10^{-4}, \quad d_8 = -8.10 \times 10^{-4}, \quad d_9 = -0.664. \end{aligned} \tag{5.31}$$

With these values, the formula (5.29) approximates the full result with average and maximal deviations of 2×10^{-7} and 1.3×10^{-6}, respectively, within the ranges in Tab. 5.1.

The complete set of two-loop integrals required for this calculation can be divided into several categories. For the renormalization counterterms one needs two-loop self-energies with Minkowskian external momentum, $p^2 = M_i^2 + i\varepsilon$, $M_i = M_W$, M_Z. In addition, there are two-loop vertex integrals with one non-vanishing external momentum squared, $s = M_Z^2 + i\varepsilon$. Two-loop self-energy integrals and vertex integrals with self-energy subloops have been computed using the dispersion relation techniques described in Refs. [207, 225, 226]. The remaining two-loop vertex integrals with triangle subloops amount to some 700 integrals, with tensor rank $R \leq 3$, Minkowskian external momentum, and up to three dimensionless parameters per integral, from the set M_i^2/M_Z^2, where $M_\mathrm{H}^2, M_W^2, m_\mathrm{t}^2$, besides $M_i^2 = M_Z^2 + i\varepsilon$. The aim was an accuracy of eight significant digits. A variety of integrals were calculated already for the leptonic Z boson asymmetry parameter A_e. Here, up to two dimensionless parameters had to be treated [78, 207, 227]. In view of the larger number of scales encountered in the $Zb\bar{b}$ vertex, a fully numerical strategy was applied here.

No reduction to a minimal set of master integrals (MIs) was attempted, except for simple cancellations of numerator and denominator terms. One might perform a standard reduction to MIs, which could reduce the number of integrals by about a factor of ten. From the point of view of performance of the project as a whole, this is no important gain in efficiency, because the time of calculating the integrals is not a limiting factor. However, for cases with many different mass scales, coefficient terms in integral reductions can become very large, which makes this approach cumbersome from a technical point of view. Furthermore, using the program KIRA [97], it has been observed that the numerical treatment of the coefficient terms becomes difficult for some integrals with propagators of mass M_Z at the kinematical point $s = M_Z^2 + i\varepsilon$. At the same time, we know that a number of MIs will remain to be evaluated numerically. The techniques developed for them can relatively easily be applied to the complete set of (unreduced) integrals, thus obviating the need for integral reductions.

For *Euclidean kinematics* all the needed integrals can be evaluated straightforwardly with sector decomposition, using the packages `FIESTA` and `SecDec`. One obtains Feynman parameter integrals with 4 or 5 dimensions. For *Minkowskian kinematics* the numerical SD method still works well for most of the integrals, although there were some problematic cases connected with integrals represented by diagrams in Fig. 5.1:

(i) For 16 single-scale six-propagator integrals with one massive line and $s = M_Z^2 + i\epsilon$, no result at all was obtained with sector decomposition: see Fig. 5.1 (b) with $m_4 = M_Z$, (c) with $m_1 = M_Z$, (d) with $m_5 = M_Z$. The corresponding MB-representations are at most 3-dimensional.

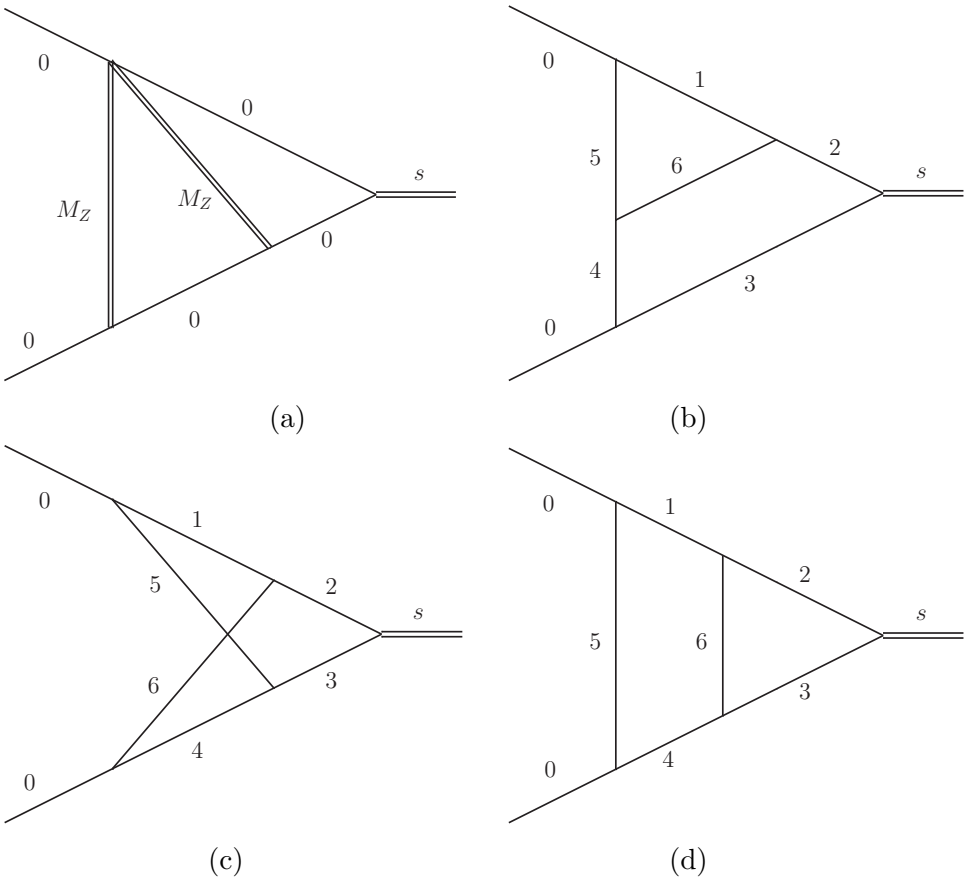

Figure 5.1: Samples of Feynman integral topologies for the $Z\bar{b}b$ vertex calculated with high accuracy with the MB method.

(ii) For 12 single-scale six-propagator integrals with two massive lines and $s = M_Z^2 + i\epsilon$, results with only few significant digits were achieved with sector decomposition: see Fig. 5.1 (b) with $m_1 = m_4 = M_Z$, (c) with $m_1 = m_4 = M_Z$, (d) with $m_5 = m_6 = M_Z$. The corresponding MB-representations are at most 4-dimensional.

(iii) For 26 planar integrals with zero threshold and $s = M_Z^2 + i\epsilon$, the number of integration points had to be increased up to several millions to reach a numerical accuracy of few digits with sector decomposition: see Fig. 5.1 (b) with $m_4 = M_Z$ or $m_4 = 0$ and $m_1 = M_W, m_\mathrm{t}$ and $m_5 = m_6 = m_\mathrm{t}, M_W$, (d) with $m_1 = M_Z$, where $m_2 = M_W, m_\mathrm{t}$ and $m_3 = m_6 = m_\mathrm{t}, M_W$. The corresponding MB-representations are at most 4-dimensional.

(iv) For 8 planar integrals with zero threshold and $s = M_Z^2 + i\epsilon$, the number of integration points had to be increased to about 80 millions in order to determine six significant digits with sector decomposition: see Fig. 5.1 (d) with $m_5 = m_6 = M_W, m_\mathrm{t}$ and $m_1 = m_2 = m_\mathrm{t}, M_W$, and also with $m_5 = M_Z$ and $m_6 = M_W, m_\mathrm{t}$ and $m_2 = m_3 = m_\mathrm{t}, M_W$. The corresponding MB-representations are at most 5-dimensional.

Using the Mellin-Barnes method, at least 8 significant digits were achieved for all integrals

Γ_i [MeV]	Γ_e	Γ_ν	Γ_d	Γ_u	Γ_b	Γ_Z
Born	81.142	160.096	371.141	292.445	369.562	2420.19
$\mathcal{O}(\alpha)$	2.273	6.174	9.717	5.799	3.857	60.22
$\mathcal{O}(\alpha\alpha_s)$	0.288	0.458	1.276	1.156	2.006	9.11
$\mathcal{O}(\alpha_t\alpha_s^2,\ \alpha_t\alpha_s^3,\ \alpha_t^2\alpha_s,\ \alpha_t^3)$	0.038	0.059	0.191	0.170	0.190	1.20
$\mathcal{O}(N_f^2\alpha^2)$	0.244	0.416	0.698	0.528	0.694	5.13
$\mathcal{O}(N_f\alpha^2)$	0.120	0.185	0.493	0.494	0.144	3.04
$\mathcal{O}(\alpha_{bos}^2)$	0.017	0.019	0.059	0.058	0.167	0.51

Table 5.3: Contributions of different orders in perturbation theory to the partial and total Z widths. A fixed value of M_W has been used as input, instead of G_μ. N_f and N_f^2 refer to corrections with one and two closed fermion loops, respectively, whereas α_{bos}^2 denotes contributions without closed fermion loops. Furthermore, $\alpha_t = y_t^2/(4\pi)$. In all rows the radiator functions $\mathcal{R}_{V,A}$ with known contributions through $\mathcal{O}(\alpha_s^4)$, $\mathcal{O}(\alpha^2)$ and $\mathcal{O}(\alpha\alpha_s)$ are included.

in this list, with exclusion of the last item where we obtain an accuracy of 6 digits.

5.4.2 Partial Z-boson decay widths

Let us start presenting results for a fixed value of M_W as input, instead of calculating M_W from G_μ. This illustrates the impact of the newly completed $\mathcal{O}(\alpha_{bos})^2$ corrections more clearly. Table 5.3 shows the contributions from different loop orders to the SM prediction of various partial Z widths. As is evident from the table, the complete two-loop EW corrections are significant and larger than the current experimental uncertainty (EXP1 for Γ_Z in Tab. 2.1). The newly calculated bosonic corrections $\mathcal{O}(\alpha_{bos}^2)$ are smaller but still noteworthy. They amount to half of all known leading three-loop QCD corrections $\mathcal{O}(\alpha_t\alpha_s^2,\ \alpha_t\alpha_s^3,\ \alpha_t^2\alpha_s,\ \alpha_t^3)$, even though the QCD contributions are potentially enhanced by effects connected with powers of α_s, α_t and $N_f > 1$.

Table 5.4 shows the SM predictions obtained if one uses G_μ as an input to compute M_W, based on the results of [190, 191, 202–205]. Each line of the table adds an additional order of perturbation theory, using the same order for the $Zf\bar{f}$ vertex corrections and the calculation of the W mass.

The $\mathcal{O}(\alpha_{bos}^2)$ correction to Γ_Z, corresponding to the difference between the last two rows in Table 5.4, amounts to 0.34 MeV, which is more than three times larger than its previous estimation [80] and it is about 15 times the aim of $\Gamma_Z \sim 0.1$ MeV for FCC-ee Tera-Z [40]. An updated discussion on how this knowledge changes the theoretical error estimations will be given in section 5.5.

5.4.3 Z-boson decay branching ratios

The experimental results from LEP and SLC are typically not presented in terms of partial widths for the different final states. Instead, this information is captured in the form of

	Γ_Z [GeV]	σ^0_{had} [nb]
Born	2.53601	41.6171
$+ \mathcal{O}(\alpha)$	2.49770	41.4687
$+ \mathcal{O}(\alpha\alpha_s)$	2.49649	41.4758
$+ \mathcal{O}(\alpha_t\alpha_s^2, \alpha_t\alpha_s^3, \alpha_t^2\alpha_s, \alpha_t^3)$	2.49560	41.4770
$+ \mathcal{O}(N_f^2\alpha^2, N_f\alpha^2)$	2.49441	41.4883
$+ \mathcal{O}(\alpha_{bos}^2)$	2.49475	41.4896

Table 5.4: Results for Γ_Z and σ^0_{had}, with M_W calculated from G_μ, order of perturbation theory indicated in each line. The complete radiator functions $\mathcal{R}_{V,A}$ are included.

	R_ℓ	R_c	R_b
Born	21.0272	0.17306	0.21733
$+ \mathcal{O}(\alpha)$	20.8031	0.17230	0.21558
$+ \mathcal{O}(\alpha\alpha_s)$	20.7963	0.17222	0.21593
$+ \mathcal{O}(\alpha_t\alpha_s^2, \alpha_t\alpha_s^3, \alpha_t^2\alpha_s, \alpha_t^3)$	20.7943	0.17222	0.21593
$+ \mathcal{O}(N_f^2\alpha^2, N_f\alpha^2)$	20.7512	0.17223	0.21580
$+ \mathcal{O}(\alpha_{bos}^2)$	20.7516	0.17222	0.21585

Table 5.5: Results for the ratios R_ℓ, R_c and R_b, with M_W calculated from G_μ to the same order as indicated in each line. In all cases, the complete radiator functions $\mathcal{R}_{V,A}$ are included.

various branching ratios. The most relevant ones are

$$R_\ell \equiv \Gamma_{had}/\Gamma_\ell, \qquad R_c \equiv \Gamma_c/\Gamma_{had}, \qquad R_b \equiv \Gamma_b/\Gamma_{had}, \tag{5.32}$$

where $\Gamma_\ell = \frac{1}{3}(\Gamma_e + \Gamma_\mu + \Gamma_\tau)$, and Γ_{had} is the partial width into hadronic final states, which at the parton level is equivalent to $\sum_q \Gamma_q$ $(q = u, d, c, s, b)$.

In addition, the hadronic peak cross-section (5.24) is, to a good approximation, defined as the ratio of partial widths and the total Z width.

Numerical results for σ^0_{had} and the ratios in (5.32) are given in Tab. 5.4 and Tab. 5.5, respectively, for different orders of radiative corrections. These quantities are less sensitive to higher loop effects than Γ_Z, since there is a partial cancellation between the corrections in the numerators and denominators of the ratios. Thus the influence of the new bosonic corrections on all branching ratios R_ℓ, R_c, R_b and on σ^0_{had} is about 0.02% or less, which is far below the current experimental errors: $R_\ell = 20.767 \pm 0.025$, $R_c = 0.1721 \pm 0.0030$, $R_b = 0.21629 \pm 0.00066$, and $\sigma^0_{had} = 41.541 \pm 0.037$ nb [60]. However, these are at the level of sensitivity of proposed measurements of R_b at future e^+e^- colliders [42–45], see EXP2 in Tab. 2.1.

5.4.4 Overall parameterization formulae

The tables above only contain numbers for a single benchmark point. Let us estimate now parametric errors connected with uncertainty in direct determination of input parameters. It will be done by presenting the results for a range of input values conveniently expressed in terms of simple parameterization formulae. The coefficients of these formulae have been fitted to the full calculation results on a grid that spans the currently allowed experimental ranges for each input parameter. Here the full calculation includes all higher-order corrections listed at the introduction section 5.1 for the partial widths, branching ratios and the peak cross-sections, and with M_W calculated from G_μ to the same precision. The parameterization formula for all EWPOs is written in the form:

$$X = X_0 + c_1 L_\mathrm{H} + c_2 \Delta_\mathrm{t} + c_3 \Delta_{\alpha_\mathrm{s}} + c_4 \Delta_{\alpha_\mathrm{s}}^2 + c_5 \Delta_{\alpha_\mathrm{s}} \Delta_\mathrm{t} + c_6 \Delta_\alpha + c_7 \Delta_\mathrm{Z}, \tag{5.33}$$

where

$$L_\mathrm{H} = \log \frac{M_\mathrm{H}}{125.7\ \mathrm{GeV}}, \quad \Delta_\mathrm{t} = \left(\frac{m_\mathrm{t}}{173.2\ \mathrm{GeV}}\right)^2 - 1, \qquad \Delta_{\alpha_\mathrm{s}} = \frac{\alpha_\mathrm{s}(M_Z)}{0.1184} - 1,$$
$$\Delta_\alpha = \frac{\Delta\alpha}{0.059} - 1, \quad \Delta_\mathrm{Z} = \frac{M_Z}{91.1876\ \mathrm{GeV}} - 1.$$

As before, M_H, M_Z, m_t and $\Delta\alpha$ are defined in the on-shell scheme, using the s-dependent width scheme for M_Z (to match the published experimental values), while α_s is defined in the $\overline{\mathrm{MS}}$ scheme. The dependence on m_b, m_c and m_τ is negligible within the allowed ranges for these quantities.

Observable	X_0	c_1	c_2	c_3	c_4	c_5	c_6	c_7	max. dev.
$\Gamma_{e,\mu}$ [MeV]	83.983	−0.061	0.810	−0.096	−0.01	0.25	−1.1	286	< 0.001
Γ_τ [MeV]	83.793	−0.060	0.810	−0.095	−0.01	0.25	−1.1	285	< 0.001
Γ_ν [MeV]	167.176	−0.071	1.26	−0.19	−0.02	0.36	−0.1	504	< 0.001
Γ_u [MeV]	299.993	−0.38	4.08	14.27	1.6	1.8	−11.1	1253	< 0.002
Γ_c [MeV]	299.916	−0.38	4.08	14.27	1.6	1.8	−11.1	1253	< 0.002
$\Gamma_{d,s}$ [MeV]	382.828	−0.39	3.83	10.20	−2.4	0.67	−10.1	1470	< 0.002
Γ_b [MeV]	375.889	−0.36	−2.14	10.53	−2.4	1.2	−10.1	1459	< 0.006
Γ_Z [MeV]	2494.74	−2.3	19.9	58.61	−4.0	8.0	−56.0	9273	< 0.012
R_ℓ [10^{-3}]	20751.6	−7.8	−37	732.3	−44	5.5	−358	11696	< 0.1
R_c [10^{-3}]	172.22	−0.031	1.0	2.3	1.3	0.38	−1.2	37	< 0.01
R_b [10^{-3}]	215.85	0.029	−2.92	−1.32	−0.84	0.032	0.72	−18	< 0.01
σ^0_had [pb]	41489.6	1.6	60.0	−579.6	38	7.3	85	−86011	< 0.1

Table 5.6: Coefficients for the parameterization formula (5.33) for various observables (X) within the ranges as given in Tab. 5.1. The formulae approximate the full results with maximal deviations given in the last column.

The fit values of the coefficients for the different EWPOs are given in Tab. 5.6. With these parameters, the formulae provide very good approximations to the full results within the ranges as given in Tab. 5.1, with maximal deviations as quoted in the last column of Tab. 5.6. As can be seen from the latter, the accuracies of the fit formulae are sufficient for the forseeable future concerning parametric errors. Ranges of input parameters should decrease in future, either [40].

5.5 Theoretical error estimations beyond 2-loop order

The EWPOs discussed in the last sections can be predicted within the SM order by order in perturbation series using $G_{\rm F}$ (or $\alpha(M_Z)$), $\alpha_s(M_Z)$, M_Z, $M_{\rm H}$ and $m_{\rm t}$ as inputs. As discussed in previous sections, the radiative corrections in these predictions are currently known including two-loop corrections. At 2-loop order it has been found that the α^2_{bos} 2-loop correction is important, as exemplified for $\sin^2\theta^{\rm b}_{\rm eff}$. It stabilizes the theoretical error at the 10^{-4} level of accuracy and is at the level of one quarter of the fermionic ones [37].

In [40,228,229] it was estimated how the theoretical uncertainty will likely be reduced *if* the following 3-loop calculations become available: complete $\mathcal{O}(\alpha\alpha_{\rm s}^2)$ corrections, fermionic $\mathcal{O}(\alpha^2\alpha_{\rm s})$ corrections, double-fermionic $\mathcal{O}(\alpha^3)$ corrections, and leading four-loop corrections enhanced by the top Yukawa coupling.

δ_1 :	δ_2 :	δ_3 :	δ_4 :	δ_5 :	$\delta\Gamma_Z$ [MeV]
$\mathcal{O}(\alpha^3)$	$\mathcal{O}(\alpha^2\alpha_{\rm s})$	$\mathcal{O}(\alpha\alpha_{\rm s}^2)$	$\mathcal{O}(\alpha\alpha_{\rm s}^3)$	$\mathcal{O}(\alpha^2_{bos})$	$=\sqrt{\sum_{i=1}^5\delta_i^2}$
TH1 (estimated error limits from geometric series of perturbation)					
0.26	0.3	0.23	0.035	0.1	0.5
TH1-new (estimated error limits from geometric series of perturbation)					
0.2	0.21	0.23	0.035	$< 10^{-4}$	0.4

δ'_1 :	δ'_2 :	δ'_3 :	δ_4 :		$\delta\Gamma_Z$ [MeV]
$\mathcal{O}(N_f^{\leq 1}\alpha^3)$	$\mathcal{O}(\alpha^3\alpha_{\rm s})$	$\mathcal{O}(\alpha^2\alpha_{\rm s}^2)$	$\mathcal{O}(\alpha\alpha_{\rm s}^3)$		$\sqrt{\delta_1'^2+\delta_2'^2+\delta_2'^3+\delta_4^2}$
TH2 (extrapolation through prefactor scaling)					
0.04	0.1	0.1	0.035	10^{-4}	0.15

Table 5.7: The theoretical error estimates TH1 for Γ_Z, as given in [80, 85], and updates taking into account the newly completed $\mathcal{O}(\alpha^2_{\rm bos})$) corrections TH1-new [38]. TH2 is a projection into the future, assuming $\delta_{2,3}$ and the fermionic parts of δ_1 to be known.

The results are given in Tab. 5.7 for the study case of Z-boson decay width. As is

evident from the table, in order to match the anticipated precision at the future, most demanding collider FCC-ee, substantial improvements in the SM theory predictions are necessary, including electroweak 3-loop effects. In Tab. 5.8 estimations for more EWPOs are given, under the assumption that 3-loop and leading 4-loop contributions are known (TH3). Estimations are based on geometric series and prefactor arguments. From the past it is known that these methods are enough to judge on the order of missing higher order results. We should pay attention to the fact that theory error evaluations are always to be taken with a grain of salt and they can differ from the actual calculations even by factors 3-5. Such situation has been observed in our context in [38]. It can be seen when we compare estimations for the Z-boson decay width (TH1 value of 0.1 MeV in Tab. 5.7) with its actual calculation based on different input parameters in Tables 5.3 and 5.4 (0.51 MeV and 0.35 MeV, respectively). That is why a theory calculation should have a precision tag at least a factor of 5 better than the corresponding experimental errors discussed for the FCC-ee. There is no other way around but to make calculations of higher loop effects, ideally with at least two independent ways or teams.

As is discussed in detail in [40], assuming that 3-loop EW and mixed EW/QCD radiative corrections with leading higher order QCD terms are known, future theory predictions will not limit physics studies. For this aim, calculations must be done with at least two digits accuracy (10%) for precision Z-boson EWPOs.

FCC-ee-Z EWPO error estimations				
	$\delta\Gamma_Z$ [MeV]	δR_l [10^{-4}]	δR_b [10^{-5}]	$\delta \sin^2\theta^{\rm l}_{\rm eff}$ [10^{-5}]
EXP2 [230]	0.1	10	$2 \div 6$	6
TH1-new	0.4	60	10	45
TH2	0.15	15	5	15
TH3	< 0.07	< 7	< 3	< 7

Table 5.8: Comparison of experimental FCC-ee precision goals for selected EWPOs (EXP2, from Table 2.1) to various scenarios for theory error estimations. TH1-new is the current theory error based on extrapolations through geometric series. TH2 is an estimate of the theory error (using prefactor scalings), assuming that electroweak 3-loop corrections are known. TH3 denotes a scenario where also the dominant 4-loop QCD corrections are available. Since reliable quantative estimates of TH3 are not possible at this point, only conservative upper bounds on the theory error are given.

Let us now discuss the prospects for computing the missing three-loop EW contributions. At three loops, diagrams can involve all massive EW particles. One of the most challenging planar 3-loop $Z \to b\bar{b}$ diagram to be solved includes 6 massive (Z,W,W,W,t,H) and three massless (b,b,A) propagators, see Fig. 5.2. Transforming the diagram to the corresponding MB representation with `AMBREv3.1.1`, an 8-dimensional MB integral emerges. The same dimension has the corresponding integral obtained with the SD method. This dimensionality can be then treated numerically with available methods; such integrals were carried out in our 2-loop project [37]. For a smaller number of massive propagators the

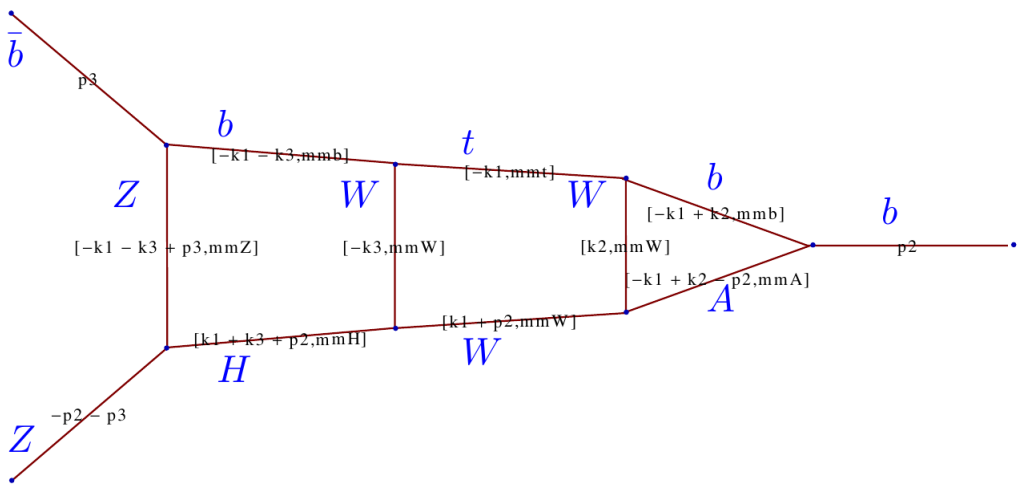

Figure 5.2: A 3-loop contribution to the $Z \to bb$ vertex which involves all heaviest SM massive particles. Diagram generated using `PlanarityTest.m`.

situation is even better, in favor of the MB method. For instance, for the same planar topology with massive propagators (H,Z) and massles propagators (b,b,b,b,b,A,A), we get a 6-dimensional MB integral and the SD integral remains 8-dimensional. These examples show also the complementarity of both methods [123]. It is worth to stress that only one of the methods, either MB or SD, is not enough, if we keep the demand of high accuracy of at least 8-digits.

There are two basic factors which play a role in estimation of theoretical errors: the number of Feynman diagrams (or, correspondingly, the number of Feynman integrals) and the precision with which single Feynman integrals can be calculated. Some basic bookkeeping concerning the number of diagram topologies and different types of diagrams is given in Tab. 5.9. First, let us compare the known number of diagram topologies and individual diagrams at two loops and three loops. Comparing the genuine three-loop fermionic diagrams, which are simpler than the bosonic ones, to the already known two-loop bosonic diagrams, there is about an order of magnitude difference in their number: 17580 (13104) diagrams for $Z \to bb$ ($Z \to e^+e^-$) at $\mathcal{O}(\alpha^3_{\rm ferm})$ versus 964 (766) at $\mathcal{O}(\alpha^2_{\rm bos})$. In general, however, the number of diagrams is of course not equivalent to the number of integrals to be calculated. At $\mathcal{O}(\alpha^3_{\rm ferm})$ we expect $\mathcal{O}(10^3) - \mathcal{O}(10^4)$ distinct three-loop Feynman integrals before a reduction to a basis, because different classes of diagrams often share parts of their integral basis.

Second, the accuracy with which three-loop diagrams can be calculated must be estimated. For the two-loop bosonic vertex integrals, results have been obtained with a high level of accuracy, which was 8 digits in mose cases and at least 6 digits for the few worst integrals. The final accuracy of the complete results for the bosonic two-loop corrections to the EWPOs was at the level of four digits [37, 38]. To achieve this goal, the Feynman integrals have been calculated numerically, directly in the Minkowskian region, with two main approaches: (i) `SD` implemented in the packages `FIESTA 3` [119] and `SecDec 3` [231], and (ii) `MB` integrals as implemented in the package `MBsuite` [36, 122, 123, 126, 163, 164]. Because fermionic three-loop diagrams are technically not much more complicated than two-loop

$Z \to b\bar{b}$			
Number of topologies	1 loop	2 loops	3 loops
	1	$14 \to^{(A)} 7 \to^{(B)} 5$	$211 \to^{(A)} 84 \to^{(B)} 51$
Number of diagrams	15	$2383 \to^{(A,B)} 1114$	$490387 \to^{(A,B)} 120472$
Fermionic loops	0	150	17580
Bosonic loops	15	964	102892
Planar / Non-planar	15 / 0	981/133	84059/36413
QCD / EW	1 / 14	98 / 1016	10386/11086
$Z \to e^+e^-, \ldots$			
Number of topologies	1 loop	2 loops	3 loops
	1	$14 \to^{(A)} 7 \to^{(B)} 5$	$211 \to^{(A)} 84 \to^{(B)} 51$
Number of diagrams	14	$2012 \to^{(A,B)} 880$	$397690 \to^{(A,B)} 91472$
Fermionic loops	0	114	13104
Bosonic loops	14	766	78368
Planar / Non-planar	14 / 0	782/98	65487/25985
QCD / EW	0 / 14	0 / 880	144/91328

Table 5.9: Number of topologies and diagrams for $Z \to f\bar{f}$ decays in the Feynman gauge. Statistics for planarity, QCD and EW type diagrams is also given. (A) and (B) denote statistics after elimination of tadpoles, products of lower level diagrams and topological symmetries of diagrams.

bosonic integrals (e.g in the case of self-energy insertions the dimensionality of MB integrals increases only by one), an overall two-digit precision for the final phenomenological results seems to be within reach already now. This estimate is based on present knowledge and available methods and tools [40]. It will be also interesting to study how IBP reductions by `KIRA` [97], the most efficient presently tool for integrals reductions, along with a dispersion method [232, 233] can help and complement with so far used by us `MB` and `SD` methods in Z-boson EWPOs analysis.

Chapter 6

Summary and outlook

The method of integral representations in the complex plane by Mellin-Barnes methods allows us nowadays to treat many classes of complicated Feynman integrals, which are fundamental for the calculation of higher order perturbative effects in particle physics. In this Thesis suitable methods and algorithms are developed and implemented for the numerical prediction of fine effects which can be tested experimentally.

As announced in the title of the thesis, the automatic and optimized constructions of MB integrals is a key feature for the completion of the electroweak two-loop calculation of the most difficult bosonic corrections to the Z-boson decay.

Summarizing, the outcome of this PhD thesis is two-fold.

First, driven by needs of new methods and tools in precise calculation of higher orders radiative corrections, the automate packages have been developed to deal with Mellin-Barnes integrals. Here new software was developed `PlanarityTest` `AMBRE` which make it possible to construct Mellin-Barnes representations in an automatic way. Many details had to be solved concerning identification of planarity of Feynman diagram. This step is important as amplitudes of Feynman diagrams are generated automatically with the computer algebra package `FeynArts` in our calculational framework and efficient evaluation towards minimal dimensional complex MB integrals depends on planarity of given diagram. Supplemented by additional MB tools `MB.m` `MBresolve.m` `barnesroutines.m` , resulting MB integrals are evaluated numerically directly in Minkowskian kinematics by the `MBnumerics.m` package. In this Thesis the package `AMBREv4.0` is discussed with Barnes lemma implementations in a way which minimizes number of `MB` dimensions of constructed `MB`-integral representations. The numerical approach of MB integrations has being developed since 2015 with conceptual insights from the author of this thesis. For the numerical integrations, the `CUHRE` routine of the `CUBA` library are used.

It should be stressed that in calculations the second numerical method of sector decomposition has been also used. These two methods appeared to be to a large extend complementary.

Second, as an outcome of the thesis the software developed has been tested heavily in the real and demanding calculation of two-loop bosonic electroweak radiative corrections to

the Z-boson decay. These are the most difficult two-loop integrals as they involve all heavy SM particles resulting in many-scale (up to four) Feynman integrals. In addition, they include also non-planar diagrams, all the simpler fermionic two-loop diagrams are purely planar.

The results obtained improved the accuracy of EWPO predictions. They allow also to estimate and understand in a better way the issue of theoretical intrinsic errors. The main upshot of all these considerations is that: (i) In order to meet the experimental precision of the FCC-ee Tera-Z for EWPOs, even electroweak 3-loop calculations of the $Zf\bar{f}$-vertex will be needed, comprising the loop orders $\mathcal{O}(\alpha\alpha_s^2), \mathcal{O}(N_f\alpha^2\alpha_s), \mathcal{O}(N_f^2\alpha^3)$ and corresponding QCD 4-loop terms; (ii) future calculations of the higher order terms would meet the experimental FCC-ee-Z demands if they are performed with a 10 percent accuracy, corresponding to 2 significant digits; (iii) The central techniques for the electroweak loop calculations will be numerical. This is due to the number of scales involved. A further development and refinement of available methods and tools and the creation of new tools based on completely new ideas are nevertheless welcome. The future looks very prospective and fascinating from this, theoretical point of view. In order to reveal new effects and explore particle physics in yet deeper levels of accuracy, a progress in theoretical methods and techniques is unavoidable. The improved precision will provide a platform for deep tests of the quantum structure of nature and unprecedented sensitivity to heavy or super-weakly coupled new physics.

Chapter 7

Appendix

7.1 The package AMBREv3: examples

The branch AMBREv3 of the AMBRE software implements the GA to construct MB representations for 2- and 3-loop Feynman diagrams including various scalar products in the numerator. The syntax of the package is similar to previous versions of AMBRE, see, e.g., [122]. A minimal input for construction of MB representations is a definition of the integral and of the kinematical invariants

```
invariants = {invariants as a rule};
MBreprNP[{numerator}, {denominator}, {internal momenta}];
```

Figure 7.1: The input of the AMBREv3 package.

The variable invariants contains rules which identify scalar products of external momenta. The command MBreprNP defines a given integral and returns the corresponding MB representation. Its arguments are as follows:

- numerator: scalar products of external and internal momenta {k1*p1,k2^2,...}.
- propagators: product of propagators of the form PR[q,m,n1]$\equiv (q^2 - m^2)^{-n_1}$.
- internal momenta: list of internal momenta.

Other functions and options of the package are:

- SimplifyFpoly[...]; – should be called before MBreprNP, as an argument it takes a list of rules which can be used to simplify the F polynomial. For example, in case of the non-planar massless 2-loop box 4.65 this is SimplifyFpoly[s+t+u->0];
- Fauto[0] – as in previous versions of AMBRE it allows user to modify the F polynomial by hand changing the variable fupc. Should be called after MBreprNP.
- d – is used to change space-time dimension $D = d - 2\varepsilon$. By default d=4.

- `BarnesLemma[repr,1,Shifts->True/Fals]` and `BarnesLemma[repr,2,Shifts->True/Fals]` – function tries to apply first and second Barnes lemmas to a given `MB` representation respectively, for more details see [122].

An example for a non-planar vertex with one massive line is presented below. For more examples visit [124].

```
invariants = {p1^2 -> 0, p2^2 -> 0, p1*p2 -> s/2};

d = 6 - 2 eps;(* by default d=4-2 eps *)

res = MBreprNP[{1}, {PR[k1, 0, n1] PR[k1 - k2, 0, n2] PR[k2, 0, n3]
PR[k1 - k2 + p1, m, n4] PR[k2 + p2, 0, n5] PR[k1 + p1 + p2, 0, n6]}, {k1, k2}]
Fauto::mode: F polynomial will be calculated in AUTO mode.
In order to use MANUAL mode execute Fauto[0].

Upoly = x[1] x[2]+x[1] x[3]+x[2] x[3]+x[1] x[4]+x[3] x[4]+x[1] x[5]+x[2] x[5]
+x[4] x[5]+x[2] x[6]+x[3] x[6]+x[4] x[6]+x[5] x[6]
Fpoly = m^2 Upoly x[4]-s x[1] x[4] x[5]-s x[1] x[2] x[6]-s x[1] x[3] x[6]
-s x[2] x[3] x[6]-s x[1] x[4] x[6]-s x[1] x[5] x[6]

{((-1)^(n1+n2+n3+n4+n5+n6) (m^2)^z1 (-s)^(6-2 eps-n1-n2-n3-n4-n5-n6-z1)
Gamma[3-eps-n3-n5] Gamma[3-eps-n2-n4-z1] Gamma[-z1] Gamma[3-eps-n1-n6-z2] Gamma[-z2]
Gamma[6-2 eps-n2-n3-n4-n5-n6-z1-z3] Gamma[6-2 eps-n1-n2-n3-n5-n6-z2-z3]
Gamma[6-2 eps-n1-n2-n3-n4-n6-z1-z2-z3] Gamma[-z3] Gamma[n2+z3] Gamma[n3+z3]
Gamma[n6+z2+z3] Gamma[-6+2 eps+n1+n2+n3+n4+n5+n6+z1+z2+z3])/(Gamma[n1] Gamma[n2]
Gamma[n3] Gamma[n4] Gamma[n5] Gamma[n6] Gamma[6-2 eps-n2-n3-n4-n5-z1]
Gamma[9-3 eps-n1-n2-n3-n4-n5-n6-z1] Gamma[6-2 eps-n1-n3-n5-n6-z2]
Gamma[6-2 eps-n1-n2-n4-n6-z1-z2])}
```

Figure 7.2: An example of usage of the `AMBREv3` package.

7.2 The package `PlanarityTest`: examples

The package `PlanarityTest.m` requires the `AMBRE` package in order to avoid redefinition of propagators. The simplest call is shown in Fig.(7.3). The function `PlanarityTest` returns `True` if the diagram is planar and `False` otherwise.

```
PlanarityTest[propagators, internal momenta]
```

Figure 7.3: The input function of the `PlanarityTest.m` package.

The arguments are as follows:

- `propagators:` product of propagators of the form `PR[q,m,n1]`$\equiv (q^2 - m^2)^{-n_1}$.
- `internal momenta:` list of internal momenta. All external momenta assumed are to be incoming.

The last optional argument in the function allows to insert additional options, the possibilities are:

- `PrintResult -> True/False:` turns on/off printing of the text message "The Diagram is planar/non-planar" (default value - `True`).
- `TestAlgorithm -> 1 or 2:` allows to change testing algorithm (default value – 1); 1 - for Method I, 2 - for Method II (see above).
- `DrawGraph -> True/False:` turns on/off drawing of the input diagram (default value – `False`). Drawing function is based on Method I.
- `VertexLegNum -> 4 or 5:` allows to change the maximal degree of vertices for Method I (default value - 4).

```
PlanarityTest[{PR[k1, 0, n1] PR[k2, 0, n2] PR[k3, 0, n3]
PR[k1 + k3, 0, n4] PR[k2 + k3, 0, n5] PR[k2 - k1 + q, 0, n6]},
{k1, k2, k3}, DrawGraph -> True];
The Diagram
is planar.
```

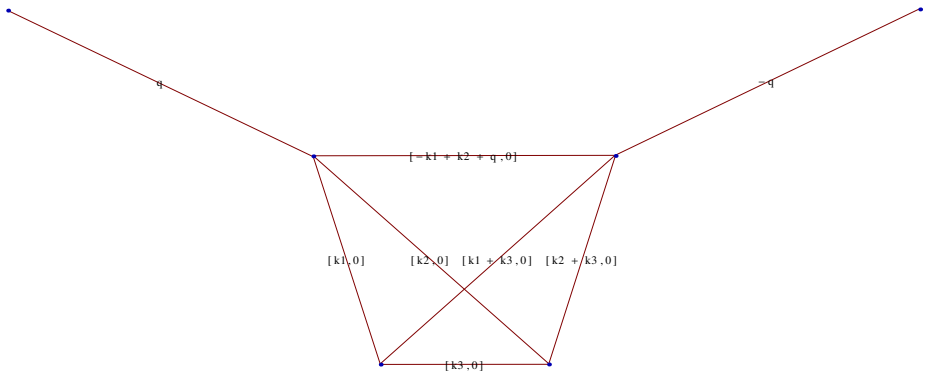

Figure 7.4: Example of usage of the `PlanarityTest.m` package.

The diagram in Fig.(7.4) is planar but by default it is drawn with crossing of edges. Using build-in `Mathematica` functionality it can be transformed into a clear planar form, Fig.(7.5).

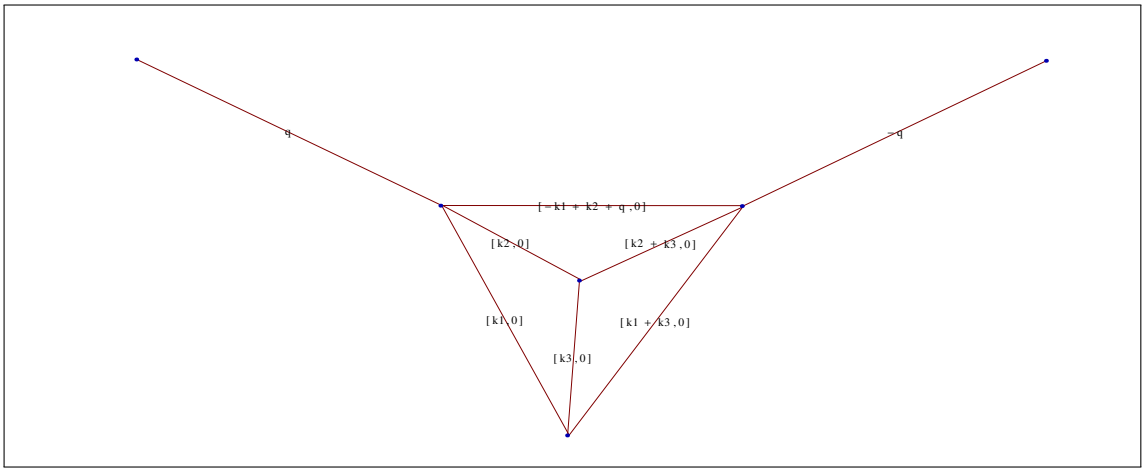

Figure 7.5: The diagram from Fig. 7.4 in a clear planar form.

7.3 Classes of Z-boson decay 2-loop diagrams

In this section, we will show integral definitions and numerical results obtained with the help of the sector decomposition method. In the equations below different combinations of momenta are shown as they appear in propagators of integrals corresponding to the $Z \to b\bar{b}$ vertex

$$\begin{aligned} q_1 &= k_1 \\ q_2 &= k_1 - k_2 \\ q_3 &= k_2 \\ q_4 &= k_2 + p_1 \\ q_5 &= k_1 - p_2 \\ q_6 &= k_1 + p_1 \\ q_7 &= k_1 + p_1 + p_2 \\ q_8 &= k_1 + p_2 \\ q_9 &= k_2 + p_2 \\ q_{10} &= k_1 - k_2 + p_1 \\ q_{11} &= k_2 + p_1 + p_2 \\ q_{12} &= k_1 - p_1 \\ q_{13} &= k_1 - k_2 + p_2 \end{aligned} \tag{7.1}$$

The integrals are separated into 6 different classes. Classes differ by the massive particles which appear in intermediate states:

- **xh0w** – 16 integrals, contains M_H and M_Z;
- **0h0w** – 100 integrals, contains M_Z only;
- **xhxw0z** – 53 integrals, contains m_t, M_H, M_W;

- **xhxwxz** – 65 integrals, contains m_t, M_H, M_W and M_Z;
- **0hxwxt0z** – 232 integrals, contains M_H, M_W;
- **0hxwxtxz** – 239 integrals, contains M_H, M_W and M_Z;

Results shown here were obtained using the `SecDec-3.0.9` program [231]. If some results are equal to X, this means that `nan` or `inf` was obtained. One should stress that the new version `pySecDec` [121] can work with such cases and gives at least few digits of accuracy.

Nr.	denominator	numerator
1	$q_1^2(q_2^2-M_Z^2)q_3^2(q_4^2-M_Z^2)(q_5^2-M_Z^2)$ $= 0.29794309685\epsilon^0$	k_1p_1
2	$q_1^2(q_2^2-M_Z^2)q_3^2(q_4^2-M_Z^2)(q_5^2-M_Z^2)$ $= 0.29794309685\epsilon^0$	k_2p_2
3	$(q_1^2-M_H^2)(q_2^2-M_Z^2)(q_3^2-M_Z^2)q_4^2q_6^2(q_7^2-M_Z^2)$ $= 0.507443225\mathbf{6}\epsilon^0$	1
4	$(q_1^2-M_H^2)(q_2^2-M_Z^2)(q_3^2-M_Z^2)(q_7^2-M_Z^2)q_8^2q_9^2$ $= 0.507443225\mathbf{6}\epsilon^0$	1
5	$(q_1^2-M_H^2)(q_2^2-M_Z^2)(q_3^2-M_Z^2)q_4^2(q_7^2-M_Z^2)$ $= 0.211371101\mathbf{2}\epsilon^0$	k_1p_1
6	$(q_1^2-M_H^2)(q_2^2-M_Z^2)(q_3^2-M_Z^2)q_4^2(q_7^2-M_Z^2)$ $= 0.309014750\mathbf{6}\epsilon^0$	k_2p_2
7	$(q_1^2-M_H^2)(q_2^2-M_Z^2)(q_3^2-M_Z^2)(q_7^2-M_Z^2)q_9^2q_{10}^2$ $= 0.403548763\mathbf{3}\epsilon^0$	1
8	$(q_1^2-M_H^2)(q_2^2-M_Z^2)(q_3^2-M_Z^2)(q_7^2-M_Z^2)q_9^2$ $= 0.290858281\mathbf{6}\epsilon^0$	k_1p_1
9	$(q_1^2-M_H^2)(q_2^2-M_Z^2)(q_3^2-M_Z^2)(q_7^2-M_Z^2)q_9^2$ $= 0.309014750\mathbf{6}\epsilon^0$	k_2p_1
10	$(q_1^2-M_Z^2)(q_2^2-M_H^2)(q_3^2-M_Z^2)q_4^2q_5^2$ $= 0.414313849\mathbf{45}\epsilon^0$	k_1p_1
11	$(q_1^2-M_Z^2)q_2^2q_3^2(q_4^2-M_Z^2)(q_7^2-M_H^2)$ $= 0.236191663\mathbf{45}\epsilon^0$	k_1p_1
12	$(q_1^2-M_Z^2)q_2^2q_3^2(q_7^2-M_H^2)(q_9^2-M_Z^2)$ $= 0.31771895704\mathbf{9}\epsilon^0$	k_1p_1
13	$(q_1^2-M_H^2)(q_2^2-M_Z^2)(q_3^2-M_Z^2)q_4^2q_6^2(q_7^2-M_Z^2)$ $= 0.170787890\mathbf{2}\epsilon^0$	k_2p_2
14	$(q_1^2-M_H^2)(q_2^2-M_Z^2)(q_3^2-M_Z^2)(q_7^2-M_Z^2)q_8^2q_9^2$ $= 0.170787890\mathbf{2}\epsilon^0$	k_2p_1
15	$(q_1^2-M_H^2)(q_2^2-M_Z^2)(q_3^2-M_Z^2)(q_7^2-M_Z^2)q_9^2q_{10}^2$ $= 0.124804125\mathbf{5}\epsilon^0$	k_1p_1
16	$(q_1^2-M_H^2)(q_2^2-M_Z^2)(q_3^2-M_Z^2)(q_7^2-M_Z^2)q_9^2q_{10}^2$ $= 0.0436166553\mathbf{7}\epsilon^0$	$(k_1p_1)(k_1p_1)$

Table 7.1: Integral definitions and numerical results for the class **xh0w** of $Z \to b\bar{b}$ integrals.

Nr.	denominator	numerator
1	$q_1^2q_2^2q_3^2q_4^2(q_6^2-M_Z^2)q_7^2$ $= X\epsilon^0 + X\epsilon^{-1} + X\epsilon^{-2}$	1
2	$q_1^2q_2^2(q_3^2-M_Z^2)q_4^2(q_6^2-M_Z^2)q_7^2$ $= (1.20\mathbf{9} + 5.57\mathbf{7}i)\epsilon^0$	1
3	$q_1^2q_2^2q_3^2q_4^2(q_6^2-M_Z^2)$ $= 1.085600275\epsilon^0$ $0.1875\epsilon^{-1}$ $0.125\epsilon^{-2}$	k_2p_2
4	$q_1^2q_2^2q_3^2(q_4^2-M_Z^2)q_5^2$ $= (6.8061675\mathbf{84} - 0.i)\epsilon^0$ $1.249999999\epsilon^{-1}$ $0.25\epsilon^{-2}$	k_1p_1
5	$q_1^2q_2^2q_3^2(q_4^2-M_Z^2)q_5^2$ $= 0.8276092911\mathbf{5}\epsilon^0$ $0.322467033\mathbf{4}\epsilon^{-1}$	k_2p_2
6	$q_1^2q_2^2q_3^2q_4^2(q_5^2-M_Z^2)$ $= 0.8276092911\mathbf{5}\epsilon^0$ $0.322467033\mathbf{4}\epsilon^{-1}$	k_1p_1
7	$q_1^2q_2^2q_3^2q_7^2(q_8^2-M_Z^2)q_9^2$ $= X\epsilon^0 + X\epsilon^{-1} + X\epsilon^{-2}$	1
8	$q_1^2q_2^2(q_3^2-M_Z^2)q_7^2(q_8^2-M_Z^2)q_9^2$ $= (1.20\mathbf{9} + 5.57\mathbf{7}i)\epsilon^0$	1
9	$q_1^2q_2^2q_3^2(q_8^2-M_Z^2)q_9^2$ $= 1.085600275\epsilon^0$ $0.1875\epsilon^{-1}$ $0.125\epsilon^{-2}$	k_2p_1
10	$q_1^2q_2^2q_3^2q_4^2q_7^2$ $= (3.06842955\mathbf{2} + 5.167712779\mathbf{9}i)\epsilon^0$ $0.822467033\mathbf{5}\epsilon^{-1}$	k_1p_1
11	$q_1^2q_2^2q_3^2q_4^2q_7^2$ $= (3.664465268\mathbf{5} - 2.68626885\mathbf{6}i)\epsilon^0$ $(0.427532966\mathbf{5} - 1.57079632\mathbf{7}i)\epsilon^{-1}$ $0.25\epsilon^{-2}$	k_2p_2
12	$q_1^2(q_2^2-M_Z^2)q_3^2q_4^2q_7^2$ $= (1.821367\mathbf{2} - 1.58240792\mathbf{7}i)\epsilon^0$ $(0. - 0.606789763\mathbf{5}i)\epsilon^{-1}$	k_1p_1
13	$q_1^2q_2^2q_3^2(q_4^2-M_Z^2)q_7^2$ $= (0.136519\mathbf{51} + 1.160964\mathbf{13}i)\epsilon^0$	k_1p_1
14	$q_1^2(q_2^2-M_Z^2)q_3^2(q_4^2-M_Z^2)q_7^2$ $= (0.39238285\mathbf{9} + 0.74563885\mathbf{2}i)\epsilon^0$	k_1p_1
15	$q_1^2q_2^2q_3^2q_7^2q_9^2(q_{10}^2-M_Z^2)$ $= X\epsilon^0 + X\epsilon^{-1} + X\epsilon^{-2}$	1

16	$q_1^2q_2^2q_3^2q_7^2q_9^2$ $= (3.911797366\mathbf{8} + 0.798082285\mathbf{9}i)\epsilon^0$ $(0.12701874\mathbf{1} - 1.013060063\mathbf{}i)\epsilon^{-1}$ $0.161233516\mathbf{7}\epsilon^{-2}$	k_1p_1
17	$q_1^2q_2^2q_3^2q_7^2q_9^2$ $= (3.664465268\mathbf{5} - 2.686268856\mathbf{}i)\epsilon^0$ $(0.427532966\mathbf{5} - 1.570796327\mathbf{}i)\epsilon^{-1}$ $0.2\mathbf{5}\epsilon^{-2}$	k_2p_1
18	$q_1^2(q_2^2 - M_Z^2)q_3^2q_7^2q_9^2$ $= (1.658299397 - 1.957941886\mathbf{}i)\epsilon^0$ $(0.122981259\mathbf{2} - 0.685138431\mathbf{5}i)\epsilon^{-1}$	k_1p_1
19	$q_1^2(q_2^2 - M_Z^2)q_3^2q_7^2q_9^2$ $= (1.148976\mathbf{49} - 1.582407\mathbf{95}i)\epsilon^0$ $(0.177532966\mathbf{6} - 0.606789763\mathbf{5}i)\epsilon^{-1}$	k_2p_1
20	$q_1^2q_2^2q_3^2q_7^2(q_9^2 - M_Z^2)$ $= (0.050810691 + 1.300549\mathbf{28}i)\epsilon^0$	k_1p_1
21	$q_1^2q_2^2q_3^2q_7^2(q_9^2 - M_Z^2)$ $= (0.2451727\mathbf{5} + 1.0876746\mathbf{1}i)\epsilon^0$	k_2p_1
22	$q_1^2(q_2^2 - M_Z^2)q_3^2q_7^2(q_9^2 - M_Z^2)$ $= (0.4904638\mathbf{19} + 0.764910\mathbf{4}i)\epsilon^0$	k_1p_1
23	$q_1^2(q_2^2 - M_Z^2)q_3^2q_7^2(q_9^2 - M_Z^2)$ $= (0.44767620\mathbf{7} + 0.562392166\mathbf{}i)\epsilon^0$	k_2p_1
24	$q_1^2q_2^2q_3^2q_7^2q_{11}^2$ $= 1.803085354\mathbf{5}\epsilon^0$	k_1p_1
25	$q_1^2(q_2^2 - M_Z^2)q_3^2q_7^2q_{11}^2$ $= (0.901542677 + 1.291928195\mathbf{}i)\epsilon^0$	k_1p_1
26	$q_1^2q_2^2(q_3^2 - M_Z^2)q_4^2q_7^2$ $= (0. + 1.570796\mathbf{3}i)\epsilon^0$	k_1p_1
27	$q_1^2q_2^2(q_3^2 - M_Z^2)q_4^2q_7^2$ $= (0.2909490\mathbf{8} + 2.506812\mathbf{6}i)\epsilon^0$	k_2p_2
28	$q_1^2q_2^2(q_3^2 - M_Z^2)q_7^2q_9^2q_{10}^2$ $= X\epsilon^0 + X\epsilon^{-1} + X\epsilon^{-2}$	1
29	$q_1^2q_2^2(q_3^2 - M_Z^2)q_7^2q_9^2(q_{10}^2 - M_Z^2)$ $= (1.21\mathbf{6} + 4.99\mathbf{9}i)\epsilon^0$	1
30	$q_1^2q_2^2(q_3^2 - M_Z^2)q_7^2q_9^2$ $= (0.3539849\mathbf{8} + 2.2055768\mathbf{1}i)\epsilon^0$	k_1p_1
31	$q_1^2q_2^2(q_3^2 - M_Z^2)q_7^2q_9^2$ $= (0.2909490\mathbf{8} + 2.506812\mathbf{6}i)\epsilon^0$	k_2p_1
32	$(q_1^2 - M_Z^2)q_2^2q_3^2q_9^2q_{12}^2$ $= (1.130277426\mathbf{2} - 2.743372058\mathbf{}i)\epsilon^0$ $(0.322467033\mathbf{4} - 0.606789763\mathbf{5}i)\epsilon^{-1}$	k_2p_1

33	$(q_1^2 - M_Z^2)q_2^2q_3^2(q_9^2 - M_Z^2)q_{12}^2$ $= 0.4505720027\epsilon^0$	k_2p_1
34	$(q_1^2 - M_Z^2)q_2^2q_3^2(q_4^2 - M_Z^2)q_6^2$ $= 0.9474670335\epsilon^0$	k_1p_2
35	$(q_1^2 - M_Z^2)q_2^2q_3^2(q_4^2 - M_Z^2)q_6^2$ $= 0.6974670335\epsilon^0$	k_2p_2
36	$(q_1^2 - M_Z^2)q_2^2q_3^2q_4^2q_5^2$ $= (1.1302774227 + 2.7433720577i)\epsilon^0$ $(0.3224670334 + 0.6067897635i)\epsilon^{-1}$	k_1p_1
37	$(q_1^2 - M_Z^2)q_2^2q_3^2q_4^2q_5^2$ $= (1.1302774262 - 2.7433720588i)\epsilon^0$ $(0.3224670334 - 0.6067897635i)\epsilon^{-1}$	k_2p_2
38	$(q_1^2 - M_Z^2)q_2^2q_3^2(q_4^2 - M_Z^2)q_5^2$ $= 0.9505720025\epsilon^0$	k_1p_1
39	$(q_1^2 - M_Z^2)q_2^2q_3^2(q_4^2 - M_Z^2)q_5^2$ $= 0.4505720027\epsilon^0$	k_2p_2
40	$(q_1^2 - M_Z^2)q_2^2q_3^2q_8^2(q_9^2 - M_Z^2)$ $= 0.9474670335\epsilon^0$	k_1p_1
41	$(q_1^2 - M_Z^2)q_2^2q_3^2q_8^2(q_9^2 - M_Z^2)$ $= 0.6974670335\epsilon^0$	k_2p_1
42	$q_1^2q_2^2q_3^2q_4^2(q_6^2 - M_Z^2)q_7^2$ $= X\epsilon^0 + X\epsilon^{-1} + (1.2 - 0.3i)\epsilon^{-2}$	k_2p_2
43	$q_1^2q_2^2q_3^2(q_6^2 - M_Z^2)q_7^2q_{11}^2$ $= (1.295 + 1.045i)\epsilon^0$	k_2p_1
44	$q_1^2(q_2^2 - M_Z^2)q_3^2(q_6^2 - M_Z^2)q_7^2q_{11}^2$ $= (0.9894 - 0.3807i)\epsilon^0$	k_2p_1
45	$q_1^2q_2^2(q_3^2 - M_Z^2)q_4^2(q_6^2 - M_Z^2)q_7^2$ $= (0.431 - 1.935i)\epsilon^0$	k_2p_2
46	$q_1^2q_2^2q_3^2(q_4^2 - M_Z^2)q_5^2$ $= (3.0601253444 - 1. *^- 10i)\epsilon^0$ $0.546874999975\epsilon^{-1}$ $0.09375\epsilon^{-2}$	$(k_1p_1)(k_1p_1)$
47	$q_1^2q_2^2q_3^2(q_4^2 - M_Z^2)q_5^2$ $= 0.071244804\mathbf{1}\epsilon^0$ $0.02626648328\mathbf{7}\epsilon^{-1}$	$(k_1p_1)(k_2p_2)$
48	$q_1^2q_2^2q_3^2q_4^2(q_5^2 - M_Z^2)$ $= 0.023477185\mathbf{3}\epsilon^0$ $0.0493667583\mathbf{5}\epsilon^{-1}$	$(k_1p_1)(k_1p_1)$
49	$q_1^2q_2^2q_3^2q_4^2(q_5^2 - M_Z^2)$ $= 0.071244804\mathbf{1}\epsilon^0$ $0.02626648328\mathbf{7}\epsilon^{-1}$	$(k_1p_1)(k_2p_2)$

50	$q_1^2q_2^2q_3^2q_7^2(q_8^2-M_Z^2)q_9^2$ $= X\epsilon^0 + X\epsilon^{-1} + (1.\mathbf{2} - 0.\mathbf{3}i)\epsilon^{-2}$	k_2p_1
51	$q_1^2q_2^2(q_3^2-M_Z^2)q_7^2(q_8^2-M_Z^2)q_9^2$ $= (0.43\mathbf{1} - 1.93\mathbf{5}i)\epsilon^0$	k_2p_1
52	$q_1^2q_2^2q_3^2q_4^2q_7^2$ $= (0.664299008\mathbf{7}\mathbf{5} - 1.291928194\mathbf{9}i)\epsilon^0$ $0.205616758\mathbf{3}\mathbf{5}\epsilon^{-1}$	$(k_1p_1)(k_1p_1)$
53	$q_1^2q_2^2q_3^2q_4^2q_7^2$ $= (0.726899724\mathbf{7} - 1.17809724\mathbf{5}i)\epsilon^0$ $0.18750000002\mathbf{5}\epsilon^{-1}$	$(k_1p_1)(k_2p_2)$
54	$q_1^2q_2^2q_3^2q_4^2q_7^2$ $= (1.192499902\mathbf{4} + 1.358790605\mathbf{7}i)\epsilon^0$ $(0.216258241\mathbf{5}\mathbf{5} + 0.589048622\mathbf{5}i)\epsilon^{-1}$ $0.0937\mathbf{5}\epsilon^{-2}$	$(k_2p_2)(k_2p_2)$
55	$q_1^2(q_2^2-M_Z^2)q_3^2q_4^2q_7^2$ $= (0.663427735\mathbf{7} + 0.53552595\mathbf{2}i)\epsilon^0$ $(0.018116758354\mathbf{9} + 0.196349540\mathbf{8}\mathbf{5}i)\epsilon^{-1}$	$(k_1p_1)(k_1p_1)$
56	$q_1^2(q_2^2-M_Z^2)q_3^2q_4^2q_7^2$ $= (0.23987246\mathbf{2} + 0.36514329\mathbf{3}i)\epsilon^0$ $(0.0734764038\mathbf{2} + 0.1394340658\mathbf{7}i)\epsilon^{-1}$	$(k_1p_1)(k_2p_2)$
57	$q_1^2q_2^2q_3^2(q_4^2-M_Z^2)q_7^2$ $= (0.062\mathbf{5} - 0.34804698\mathbf{2}i)\epsilon^0$	$(k_1p_1)(k_1p_1)$
58	$q_1^2q_2^2q_3^2(q_4^2-M_Z^2)q_7^2$ $= (0.217888864 - 0.135123524i)\epsilon^0$ $0.062\mathbf{5}\epsilon^{-1}$	$(k_1p_1)(k_2p_2)$
59	$q_1^2(q_2^2-M_Z^2)q_3^2(q_4^2-M_Z^2)q_7^2$ $= (0.11405643\mathbf{5} - 0.24697909\mathbf{9}i)\epsilon^0$	$(k_1p_1)(k_1p_1)$
60	$q_1^2(q_2^2-M_Z^2)q_3^2(q_4^2-M_Z^2)q_7^2$ $= (0.05730937\mathbf{6} - 0.12267729\mathbf{9}i)\epsilon^0$ $0.062\mathbf{5}\epsilon^{-1}$	$(k_1p_1)(k_2p_2)$
61	$q_1^2q_2^2q_3^2q_7^2q_9^2(q_{10}^2-M_Z^2)$ $= X\epsilon^0 + X\epsilon^{-1} + X\epsilon^{-2}$	k_1p_1
62	$q_1^2q_2^2q_3^2q_7^2q_9^2$ $= (1.316165951\mathbf{5} - 0.383384963\mathbf{4}i)\epsilon^0$ $(0.06101761\mathbf{2} + 0.3101804907\mathbf{5}i)\epsilon^{-1}$ $0.0493667583\mathbf{5}\epsilon^{-2}$	$(k_1p_1)(k_1p_1)$
63	$q_1^2q_2^2q_3^2q_7^2q_9^2$ $= (1.159448980\mathbf{3} + 0.361386722\mathbf{5}i)\epsilon^0$ $(0.057516483\mathbf{3} + 0.3926990817\mathbf{5}i)\epsilon^{-1}$ $0.062\mathbf{5}\epsilon^{-2}$	$(k_1p_1)(k_2p_1)$

64	$q_1^2 q_2^2 q_3^2 q_7^2 q_9^2$ $= (1.192499902\mathbf{4} + 1.358790605\mathbf{7}i)\epsilon^0$ $(0.2162582415\mathbf{5} + 0.589048622\mathbf{5}i)\epsilon^{-1}$ $0.0937\mathbf{5}\epsilon^{-2}$	$(k_2 p_1)(k_2 p_1)$
65	$q_1^2(q_2^2 - M_Z^2) q_3^2 q_7^2 q_9^2$ $= (0.600903211\mathbf{2} + 0.72329293\mathbf{1}i)\epsilon^0$ $(0.035224146324\mathbf{9} + 0.2355238748\mathbf{5}i)\epsilon^{-1}$	$(k_1 p_1)(k_1 p_1)$
66	$q_1^2(q_2^2 - M_Z^2) q_3^2 q_7^2 q_9^2$ $= (0.308944379\mathbf{8} + 0.426060672\mathbf{5}i)\epsilon^0$ $(0.05152359617\mathbf{5} + 0.16396081587\mathbf{5}i)\epsilon^{-1}$	$(k_1 p_1)(k_2 p_1)$
67	$q_1^2 q_2^2 q_3^2 q_7^2 (q_9^2 - M_Z^2)$ $= (0.01055658\mathbf{8} - 0.40896898\mathbf{7}i)\epsilon^0$	$(k_1 p_1)(k_1 p_1)$
68	$q_1^2 q_2^2 q_3^2 q_7^2 (q_9^2 - M_Z^2)$ $= (0.0542417\mathbf{23} - 0.3016684\mathbf{6}i)\epsilon^0$	$(k_1 p_1)(k_2 p_1)$
69	$q_1^2(q_2^2 - M_Z^2) q_3^2 q_7^2 (q_9^2 - M_Z^2)$ $= (0.15675538\mathbf{4} - 0.25661487\mathbf{3}i)\epsilon^0$	$(k_1 p_1)(k_1 p_1)$
70	$q_1^2(q_2^2 - M_Z^2) q_3^2 q_7^2 (q_9^2 - M_Z^2)$ $= (0.1236979\mathbf{7} - 0.1585187\mathbf{81}i)\epsilon^0$	$(k_1 p_1)(k_2 p_1)$
71	$q_1^2 q_2^2 (q_3^2 - M_Z^2) q_4^2 q_7^2$ $= (0.03124999\mathbf{9} - 0.4908738\mathbf{52}i)\epsilon^0$	$(k_1 p_1)(k_1 p_1)$
72	$q_1^2 q_2^2 (q_3^2 - M_Z^2) q_4^2 q_7^2$ $= (0.2759985\mathbf{4} - 0.4384309\mathbf{3}i)\epsilon^0$ $0.062\mathbf{5}\epsilon^{-1}$	$(k_1 p_1)(k_2 p_2)$
73	$q_1^2 q_2^2 (q_3^2 - M_Z^2) q_4^2 q_7^2$ $= (0.0819273\mathbf{4} - 0.9521707\mathbf{2}i)\epsilon^0$	$(k_2 p_2)(k_2 p_2)$
74	$q_1^2 q_2^2 (q_3^2 - M_Z^2) q_7^2 q_9^2 q_{10}^2$ $= X\epsilon^0 + X\epsilon^{-1} + X\epsilon^{-2}$	$k_1 p_1$
75	$q_1^2 q_2^2 (q_3^2 - M_Z^2) q_7^2 q_9^2 (q_{10}^2 - M_Z^2)$ $= (0.285\mathbf{3} - 1.51\mathbf{1}i)\epsilon^0$	$k_1 p_1$
76	$q_1^2 q_2^2 (q_3^2 - M_Z^2) q_7^2 q_9^2$ $= (0.12105911\mathbf{5} - 0.8082640\mathbf{93}i)\epsilon^0$	$(k_1 p_1)(k_1 p_1)$
77	$q_1^2 q_2^2 (q_3^2 - M_Z^2) q_7^2 q_9^2$ $= (0.0908563\mathbf{1} - 0.8149751\mathbf{44}i)\epsilon^0$	$(k_1 p_1)(k_2 p_1)$
78	$q_1^2 q_2^2 (q_3^2 - M_Z^2) q_7^2 q_9^2$ $= (0.0819273\mathbf{4} - 0.9521707\mathbf{2}i)\epsilon^0$	$(k_2 p_1)(k_2 p_1)$
79	$(q_1^2 - M_Z^2) q_2^2 q_3^2 q_9^2 q_{12}^2$ $= (0.6035635\mathbf{88} - 0.5088333\mathbf{71}i)\epsilon^0$ $(0.013271338\mathbf{68} - 0.1394340658\mathbf{7}i)\epsilon^{-1}$	$(k_1 p_2)(k_2 p_1)$
80	$(q_1^2 - M_Z^2) q_2^2 q_3^2 q_9^2 q_{12}^2$ $= (0.384967033\mathbf{4} + 0.883572933\mathbf{7}i)\epsilon^0$ $(0.0937\mathbf{5} + 0.1963495408\mathbf{5}i)\epsilon^{-1}$	$(k_2 p_1)(k_2 p_1)$

81	$(q_1^2 - M_Z^2)q_2^2q_3^2(q_9^2 - M_Z^2)q_{12}^2$ $= \quad 0.196944642\epsilon^0$ $\quad\quad 0.0625\epsilon^{-1}$	$(k_1p_2)(k_2p_1)$
82	$(q_1^2 - M_Z^2)q_2^2q_3^2(q_9^2 - M_Z^2)q_{12}^2$ $= \quad 0.1028083791\mathbf{7}\epsilon^0$	$(k_2p_1)(k_2p_1)$
83	$(q_1^2 - M_Z^2)q_2^2q_3^2q_4^2q_5^2$ $= \quad (0.384967033\mathbf{6} + 0.883572933\mathbf{5}i)\epsilon^0$ $\quad\quad (0.0937\mathbf{5} + 0.1963495408\mathbf{5}i)\epsilon^{-1}$	$(k_1p_1)(k_1p_1)$
84	$(q_1^2 - M_Z^2)q_2^2q_3^2q_4^2q_5^2$ $= \quad (0.60356358\mathbf{8} - 0.50883337\mathbf{1}i)\epsilon^0$ $\quad\quad (0.0132713386\mathbf{8} - 0.1394340658\mathbf{7}i)\epsilon^{-1}$	$(k_1p_1)(k_2p_2)$
85	$(q_1^2 - M_Z^2)q_2^2q_3^2q_4^2q_5^2$ $= \quad (0.384967033\mathbf{4} + 0.883572933\mathbf{8}i)\epsilon^0$ $\quad\quad (0.0937\mathbf{5} + 0.1963495408\mathbf{5}i)\epsilon^{-1}$	$(k_2p_2)(k_2p_2)$
86	$(q_1^2 - M_Z^2)q_2^2q_3^2(q_4^2 - M_Z^2)q_5^2$ $= \quad 0.324050137\mathbf{5}\epsilon^0$	$(k_1p_1)(k_1p_1)$
87	$(q_1^2 - M_Z^2)q_2^2q_3^2(q_4^2 - M_Z^2)q_5^2$ $= \quad 0.196944642\epsilon^0$ $\quad\quad 0.0625\epsilon^{-1}$	$(k_1p_1)(k_2p_2)$
88	$(q_1^2 - M_Z^2)q_2^2q_3^2(q_4^2 - M_Z^2)q_5^2$ $= \quad 0.1028083791\mathbf{7}\epsilon^0$	$(k_2p_2)(k_2p_2)$
89	$q_1^2q_2^2q_3^2q_4^2(q_6^2 - M_Z^2)q_7^2$ $= \quad X\epsilon^0 + X\epsilon^{-1} + X\epsilon^{-2}$	$(k_2p_2)(k_2p_2)$
90	$q_1^2q_2^2q_3^2(q_6^2 - M_Z^2)q_7^2q_{11}^2$ $= \quad (0.438\mathbf{9} - 0.3\mathbf{7}i)\epsilon^0$	$(k_2p_1)(k_2p_1)$
91	$q_1^2(q_2^2 - M_Z^2)q_3^2(q_6^2 - M_Z^2)q_7^2q_{11}^2$ $= \quad (0.330\mathbf{3} + 0.120\mathbf{8}i)\epsilon^0$	$(k_2p_1)(k_2p_1)$
92	$q_1^2q_2^2(q_3^2 - M_Z^2)q_4^2(q_6^2 - M_Z^2)q_7^2$ $= \quad (0.16\mathbf{8} + 0.75\mathbf{5}i)\epsilon^0$	$(k_2p_2)(k_2p_2)$
93	$q_1^2q_2^2q_3^2q_7^2(q_8^2 - M_Z^2)q_9^2$ $= \quad X\epsilon^0 + X\epsilon^{-1} + X\epsilon^{-2}$	$(k_2p_1)(k_2p_1)$
94	$q_1^2q_2^2(q_3^2 - M_Z^2)q_7^2(q_8^2 - M_Z^2)q_9^2$ $= \quad (0.16\mathbf{8} + 0.75\mathbf{5}i)\epsilon^0$	$(k_2p_1)(k_2p_1)$
95	$q_1^2q_2^2q_3^2q_7^2q_9^2(q_{10}^2 - M_Z^2)$ $= \quad X\epsilon^0 + X\epsilon^{-1} + X\epsilon^{-2}$	$(k_1p_1)(k_1p_1)$
96	$q_1^2q_2^2(q_3^2 - M_Z^2)q_7^2q_9^2q_{10}^2$ $= \quad X\epsilon^0 + X\epsilon^{-1} + X\epsilon^{-2}$	$(k_1p_1)(k_1p_1)$
97	$q_1^2q_2^2(q_3^2 - M_Z^2)q_7^2q_9^2(q_{10}^2 - M_Z^2)$ $= \quad (0.093\mathbf{1} + 0.566\mathbf{1}i)\epsilon^0$	$(k_1p_1)(k_1p_1)$
98	$q_1^2q_2^2q_3^2q_7^2q_9^2(q_{10}^2 - M_Z^2)$ $= \quad X\epsilon^0 + X\epsilon^{-1} + X\epsilon^{-2}$	$(k_1p_1)(k_1p_1)(k_1p_1)$

99	$q_1^2 q_2^2 (q_3^2 - M_Z^2) q_7^2 q_9^2 q_{10}^2$ $= X\epsilon^0 + X\epsilon^{-1} + X\epsilon^{-2}$	$(k_1 p_1)(k_1 p_1)(k_1 p_1)$
100	$q_1^2 q_2^2 (q_3^2 - M_Z^2) q_7^2 q_9^2 (q_{10}^2 - M_Z^2)$ $= (0.034\mathbf{6} - 0.230\mathbf{6}i)\epsilon^0$	$(k_1 p_1)(k_1 p_1)(k_1 p_1)$

Table 7.2: Integral definitions and numerical results for the class **0h0w** of $Z \to b\bar{b}$ integrals.

Nr.	denominator	numerator
1	$(q_1^2 - m_t^2)(q_2^2 - M_H^2)(q_3^2 - m_t^2)(q_4^2 - M_W^2)(q_6^2 - M_W^2)(q_7^2 - m_t^2)$ $= 0.0346435798\epsilon^0$	1
2	$(q_1^2 - m_t^2)(q_2^2 - M_H^2)(q_3^2 - m_t^2)(q_4^2 - M_W^2)(q_6^2 - M_W^2)$ $= 0.111103806\mathbf{6}\epsilon^0$	$k_1 p_2$
3	$(q_1^2 - m_t^2)(q_2^2 - M_H^2)(q_3^2 - m_t^2)(q_4^2 - M_W^2)(q_5^2 - M_W^2)$ $= 0.088214399\epsilon^0$	$k_1 p_1$
4	$(q_1^2 - m_t^2)(q_2^2 - M_H^2)(q_3^2 - m_t^2)(q_4^2 - M_W^2)(q_5^2 - M_W^2)$ $= 0.088214399\epsilon^0$	$k_2 p_2$
5	$(q_1^2 - m_t^2)(q_2^2 - M_H^2)(q_3^2 - m_t^2)(q_7^2 - m_t^2)(q_8^2 - M_W^2)(q_9^2 - M_W^2)$ $= 0.0346435798\epsilon^0$	1
6	$(q_1^2 - m_t^2)(q_2^2 - M_H^2)(q_3^2 - m_t^2)(q_8^2 - M_W^2)(q_9^2 - M_W^2)$ $= 0.111103806\mathbf{6}\epsilon^0$	$k_1 p_1$
7	$(q_1^2 - m_t^2)(q_2^2 - M_H^2)(q_3^2 - m_t^2)(q_4^2 - M_W^2)(q_7^2 - m_t^2)$ $= 0.058937015\mathbf{0}5\epsilon^0$	$k_1 p_1$
8	$(q_1^2 - m_t^2)(q_2^2 - M_H^2)(q_3^2 - m_t^2)(q_4^2 - M_W^2)(q_7^2 - m_t^2)$ $= 0.083968199\mathbf{6}\epsilon^0$	$k_2 p_2$
9	$(q_1^2 - m_t^2)(q_2^2 - M_H^2)(q_3^2 - m_t^2)(q_7^2 - m_t^2)(q_9^2 - M_W^2)$ $= 0.079648644\mathbf{9}\epsilon^0$	$k_1 p_1$
10	$(q_1^2 - m_t^2)(q_2^2 - M_H^2)(q_3^2 - m_t^2)(q_7^2 - m_t^2)(q_9^2 - M_W^2)$ $= 0.083968199\mathbf{6}\epsilon^0$	$k_2 p_1$
11	$(q_1^2 - m_t^2)(q_2^2 - M_H^2)(q_3^2 - m_t^2)(q_7^2 - m_t^2)(q_{11}^2 - m_t^2)$ $= 0.061459257\mathbf{0}5\epsilon^0$	$k_1 p_1$
12	$(q_1^2 - M_W^2)(q_2^2 - M_H^2)(q_3^2 - M_W^2)(q_4^2 - m_t^2)(q_6^2 - m_t^2)(q_7^2 - M_W^2)$ $= 0.071440554\mathbf{1}\epsilon^0$	1
13	$(q_1^2 - M_W^2)(q_2^2 - M_H^2)(q_3^2 - M_W^2)(q_4^2 - m_t^2)(q_5^2 - m_t^2)$ $= 0.069402887\mathbf{2}5\epsilon^0$	$k_1 p_1$
14	$(q_1^2 - M_W^2)(q_2^2 - M_H^2)(q_3^2 - M_W^2)(q_4^2 - m_t^2)(q_5^2 - m_t^2)$ $= 0.069402887\mathbf{2}5\epsilon^0$	$k_2 p_2$
15	$(q_1^2 - M_W^2)(q_2^2 - M_H^2)(q_3^2 - M_W^2)(q_7^2 - M_W^2)(q_8^2 - m_t^2)(q_9^2 - m_t^2)$ $= 0.071440554\mathbf{1}\epsilon^0$	1
16	$(q_1^2 - M_W^2)(q_2^2 - M_H^2)(q_3^2 - M_W^2)(q_4^2 - m_t^2)(q_7^2 - M_W^2)$ $= 0.130988606\mathbf{5}\epsilon^0$	$k_1 p_1$
17	$(q_1^2 - M_W^2)(q_2^2 - M_H^2)(q_3^2 - M_W^2)(q_4^2 - m_t^2)(q_7^2 - M_W^2)$ $= 0.141367031\mathbf{3}\epsilon^0$	$k_2 p_2$

18	$(q_1^2-M_W^2)(q_2^2-M_H^2)(q_3^2-M_W^2)(q_7^2-M_W^2)(q_9^2-m_t^2)$ $= \quad 0.153669379\mathbf{4}\epsilon^0$	k_1p_1
19	$(q_1^2-M_W^2)(q_2^2-M_H^2)(q_3^2-M_W^2)(q_7^2-M_W^2)(q_9^2-m_t^2)$ $= \quad 0.141367031\mathbf{3}\epsilon^0$	k_2p_1
20	$(q_1^2-M_W^2)(q_2^2-M_H^2)(q_3^2-M_W^2)(q_7^2-M_W^2)(q_{11}^2-M_W^2)$ $= \quad 0.262153993\mathbf{9}\epsilon^0$	k_1p_1
21	$(q_1^2-m_t^2)(q_2^2-M_H^2)(q_3^2-m_t^2)(q_4^2-M_W^2)(q_6^2-M_W^2)(q_7^2-m_t^2)$ $= \quad 0.010590309\mathbf{93}\epsilon^0$	k_2p_2
22	$(q_1^2-m_t^2)(q_2^2-M_H^2)(q_3^2-m_t^2)(q_6^2-M_W^2)(q_7^2-m_t^2)(q_{11}^2-m_t^2)$ $= \quad 0.00548576035\mathbf{5}\epsilon^0$	k_2p_1
23	$(q_1^2-m_t^2)(q_2^2-M_H^2)(q_3^2-m_t^2)(q_4^2-M_W^2)(q_5^2-M_W^2)$ $= \quad 0.169864447\mathbf{8}\epsilon^0$ $\quad\quad 0.062\mathbf{5}\epsilon^{-1}$	$(k_1p_1)(k_2p_2)$
24	$(q_1^2-m_t^2)(q_2^2-M_H^2)(q_3^2-m_t^2)(q_7^2-m_t^2)(q_8^2-M_W^2)(q_9^2-M_W^2)$ $= \quad 0.010590309\mathbf{93}\epsilon^0$	k_2p_1
25	$(q_1^2-m_t^2)(q_2^2-M_H^2)(q_3^2-m_t^2)(q_4^2-M_W^2)(q_7^2-m_t^2)$ $= \quad 0.0161061223\mathbf{25}\epsilon^0$	$(k_1p_1)(k_1p_1)$
26	$(q_1^2-m_t^2)(q_2^2-M_H^2)(q_3^2-m_t^2)(q_4^2-M_W^2)(q_7^2-m_t^2)$ $= \quad 0.230204763\mathbf{25}\epsilon^0$ $\quad\quad 0.062\mathbf{5}\epsilon^{-1}$	$(k_1p_1)(k_2p_2)$
27	$(q_1^2-m_t^2)(q_2^2-M_H^2)(q_3^2-m_t^2)(q_4^2-M_W^2)(q_7^2-m_t^2)$ $= \quad 0.027736857\mathbf{2}\epsilon^0$	$(k_2p_2)(k_2p_2)$
28	$(q_1^2-m_t^2)(q_2^2-M_H^2)(q_3^2-m_t^2)(q_7^2-m_t^2)(q_9^2-M_W^2)$ $= \quad 0.025173958\mathbf{7}\epsilon^0$	$(k_1p_1)(k_1p_1)$
29	$(q_1^2-m_t^2)(q_2^2-M_H^2)(q_3^2-m_t^2)(q_7^2-m_t^2)(q_9^2-M_W^2)$ $= \quad 0.023920572472\epsilon^0$	$(k_1p_1)(k_2p_1)$
30	$(q_1^2-m_t^2)(q_2^2-M_H^2)(q_3^2-m_t^2)(q_7^2-m_t^2)(q_9^2-M_W^2)$ $= \quad 0.027736857\mathbf{2}\epsilon^0$	$(k_2p_1)(k_2p_1)$
31	$(q_1^2-M_W^2)(q_2^2-M_H^2)(q_3^2-M_W^2)(q_4^2-m_t^2)(q_6^2-m_t^2)(q_7^2-M_W^2)$ $= \quad 0.016869773\mathbf{21}\epsilon^0$	k_2p_2
32	$(q_1^2-M_W^2)(q_2^2-M_H^2)(q_3^2-M_W^2)(q_6^2-m_t^2)(q_7^2-M_W^2)(q_{11}^2-M_W^2)$ $= \quad 0.030941307\mathbf{51}\epsilon^0$	k_2p_1
33	$(q_1^2-M_W^2)(q_2^2-M_H^2)(q_3^2-M_W^2)(q_4^2-m_t^2)(q_5^2-m_t^2)$ $= \quad 0.018141543029\epsilon^0$	$(k_1p_1)(k_1p_1)$
34	$(q_1^2-M_W^2)(q_2^2-M_H^2)(q_3^2-M_W^2)(q_4^2-m_t^2)(q_5^2-m_t^2)$ $= \quad 0.176982466\mathbf{37}\epsilon^0$ $\quad\quad 0.062\mathbf{5}\epsilon^{-1}$	$(k_1p_1)(k_2p_2)$
35	$(q_1^2-M_W^2)(q_2^2-M_H^2)(q_3^2-M_W^2)(q_4^2-m_t^2)(q_5^2-m_t^2)$ $= \quad 0.018141543029\epsilon^0$	$(k_2p_2)(k_2p_2)$
36	$(q_1^2-M_W^2)(q_2^2-M_H^2)(q_3^2-M_W^2)(q_7^2-M_W^2)(q_8^2-m_t^2)(q_9^2-m_t^2)$ $= \quad 0.016869773\mathbf{21}\epsilon^0$	k_2p_1

37	$(q_1^2-M_W^2)(q_2^2-M_H^2)(q_3^2-M_W^2)(q_4^2-m_t^2)(q_7^2-M_W^2)$ $= 0.037776942675\epsilon^0$	$(k_1p_1)(k_1p_1)$
38	$(q_1^2-M_W^2)(q_2^2-M_H^2)(q_3^2-M_W^2)(q_4^2-m_t^2)(q_7^2-M_W^2)$ $= 0.181758246\mathbf{3}7\epsilon^0$ $0.062\mathbf{5}\epsilon^{-1}$	$(k_1p_1)(k_2p_2)$
39	$(q_1^2-M_W^2)(q_2^2-M_H^2)(q_3^2-M_W^2)(q_7^2-M_W^2)(q_9^2-m_t^2)$ $= 0.047517596\mathbf{0}5\epsilon^0$	$(k_1p_1)(k_1p_1)$
40	$(q_1^2-M_W^2)(q_2^2-M_H^2)(q_3^2-M_W^2)(q_7^2-M_W^2)(q_9^2-m_t^2)$ $= 0.038888833\mathbf{6}\epsilon^0$	$(k_1p_1)(k_2p_1)$
41	$(q_1^2-M_W^2)(q_2^2-M_H^2)(q_3^2-M_W^2)(q_7^2-M_W^2)(q_{11}^2-M_W^2)$ $= 0.081486024\mathbf{9}7\epsilon^0$	$(k_1p_1)(k_1p_1)$
42	$(q_1^2-M_W^2)(q_2^2-M_H^2)(q_3^2-M_W^2)(q_7^2-M_W^2)(q_{11}^2-M_W^2)$ $= 0.072097314\mathbf{9}\epsilon^0$	$(k_1p_1)(k_2p_1)$
43	$(q_1^2-m_t^2)(q_2^2-M_H^2)(q_3^2-m_t^2)(q_4^2-M_W^2)(q_6^2-M_W^2)(q_7^2-m_t^2)$ $= 0.003708023\mathbf{7}2\epsilon^0$	$(k_2p_2)(k_2p_2)$
44	$(q_1^2-m_t^2)(q_2^2-M_H^2)(q_3^2-m_t^2)(q_6^2-M_W^2)(q_7^2-m_t^2)(q_{11}^2-m_t^2)$ $= 0.001533241\mathbf{5}9\mathbf{2}\epsilon^0$	$(k_2p_1)(k_2p_1)$
45	$(q_1^2-m_t^2)(q_2^2-M_H^2)(q_3^2-m_t^2)(q_7^2-m_t^2)(q_8^2-M_W^2)(q_9^2-M_W^2)$ $= 0.003708023\mathbf{7}2\epsilon^0$	$(k_2p_1)(k_2p_1)$
46	$(q_1^2-M_W^2)(q_2^2-M_H^2)(q_3^2-M_W^2)(q_6^2-m_t^2)(q_7^2-M_W^2)(q_{11}^2-M_W^2)$ $= 0.009222867\mathbf{5}\epsilon^0$	$(k_2p_1)(k_2p_1)$
47	$(q_1^2-M_W^2)(q_2^2-M_H^2)(q_3^2-M_W^2)(q_6^2-m_t^2)(q_7^2-M_W^2)(q_{11}^2-M_W^2)$ $= 0.003092784\mathbf{2}\mathbf{3}\epsilon^0$	$(k_2p_1)(k_2p_1)$ (k_2p_1)
48	$(q_1^2-m_t^2)(q_2^2-M_H^2)(q_3^2-m_t^2)(q_4^2-M_W^2)(q_5^2-M_W^2)$ $= 0.026584580\mathbf{2}\mathbf{2}\mathbf{5}\epsilon^0$	$(k_1p_1)(k_1p_1)$
49	$(q_1^2-m_t^2)(q_2^2-M_H^2)(q_3^2-m_t^2)(q_4^2-M_W^2)(q_5^2-M_W^2)$ $= 0.026584580\mathbf{2}\mathbf{2}\mathbf{5}\epsilon^0$	$(k_2p_2)(k_2p_2)$
50	$(q_1^2-M_W^2)(q_2^2-M_H^2)(q_3^2-M_W^2)(q_4^2-m_t^2)(q_7^2-M_W^2)$ $= 0.041332331\mathbf{8}7\mathbf{5}\epsilon^0$	$(k_2p_2)(k_2p_2)$
51	$(q_1^2-M_W^2)(q_2^2-M_H^2)(q_3^2-M_W^2)(q_7^2-M_W^2)(q_9^2-m_t^2)$ $= 0.041332331\mathbf{8}7\mathbf{5}\epsilon^0$	$(k_2p_1)(k_2p_1)$
52	$(q_1^2-M_W^2)(q_2^2-M_H^2)(q_3^2-M_W^2)(q_4^2-m_t^2)(q_6^2-m_t^2)(q_7^2-M_W^2)$ $= 0.005007502\mathbf{4}\mathbf{1}\epsilon^0$	$(k_2p_2)(k_2p_2)$
53	$(q_1^2-M_W^2)(q_2^2-M_H^2)(q_3^2-M_W^2)(q_7^2-M_W^2)(q_8^2-m_t^2)(q_9^2-m_t^2)$ $= 0.005007502\mathbf{4}\mathbf{1}\epsilon^0$	$(k_2p_1)(k_2p_1)$

Table 7.3: Integral definitions and numerical results for the class **xhxw0z** of $Z \to b\bar{b}$ integrals.

Nr.	denominator	numerator
1	$(q_1^2-M_H^2)(q_2^2-m_t^2)(q_3^2-m_t^2)(q_4^2-M_W^2)q_6^2(q_7^2-M_Z^2)$ $= 0.133023412\mathbf{3}\epsilon^0$	1

2	$(q_1^2-M_H^2)(q_2^2-M_W^2)(q_3^2-M_W^2)(q_4^2-m_t^2)q_6^2(q_7^2-M_Z^2)$ $= 0.202732523\mathbf{7}\epsilon^0$	1
3	$(q_1^2-M_H^2)(q_2^2-m_t^2)(q_3^2-m_t^2)(q_7^2-M_Z^2)q_8^2(q_9^2-M_W^2)$ $= 0.133023412\mathbf{3}\epsilon^0$	1
4	$(q_1^2-M_H^2)(q_2^2-M_W^2)(q_3^2-M_W^2)(q_7^2-M_Z^2)q_8^2(q_9^2-m_t^2)$ $= 0.202732523\mathbf{7}\epsilon^0$	1
5	$(q_1^2-M_H^2)(q_2^2-m_t^2)(q_3^2-m_t^2)(q_4^2-M_W^2)(q_7^2-M_Z^2)$ $= 0.091169944\mathbf{3}\epsilon^0$	k_1p_1
6	$(q_1^2-M_H^2)(q_2^2-m_t^2)(q_3^2-m_t^2)(q_4^2-M_W^2)(q_7^2-M_Z^2)$ $= 0.117257186\mathbf{85}\epsilon^0$	k_2p_2
7	$(q_1^2-M_H^2)(q_2^2-m_t^2)(q_3^2-m_t^2)(q_7^2-M_Z^2)(q_9^2-M_W^2)(q_{10}^2-M_W^2)$ $= 0.040711635\mathbf{13}\epsilon^0$	1
8	$(q_1^2-M_H^2)(q_2^2-m_t^2)(q_3^2-m_t^2)(q_7^2-M_Z^2)(q_9^2-M_W^2)$ $= 0.113200612\mathbf{05}\epsilon^0$	k_1p_1
9	$(q_1^2-M_H^2)(q_2^2-m_t^2)(q_3^2-m_t^2)(q_7^2-M_Z^2)(q_9^2-M_W^2)$ $= 0.117257186\mathbf{85}\epsilon^0$	k_2p_1
10	$(q_1^2-M_H^2)(q_2^2-M_W^2)(q_3^2-M_W^2)(q_4^2-m_t^2)(q_7^2-M_Z^2)$ $= 0.113495926\mathbf{1}\epsilon^0$	k_1p_1
11	$(q_1^2-M_H^2)(q_2^2-M_W^2)(q_3^2-M_W^2)(q_4^2-m_t^2)(q_7^2-M_Z^2)$ $= 0.124197319\mathbf{95}\epsilon^0$	k_2p_2
12	$(q_1^2-M_H^2)(q_2^2-M_W^2)(q_3^2-M_W^2)(q_7^2-M_Z^2)(q_9^2-m_t^2)(q_{10}^2-m_t^2)$ $= 0.040825985\mathbf{85}\epsilon^0$	1
13	$(q_1^2-M_H^2)(q_2^2-M_W^2)(q_3^2-M_W^2)(q_7^2-M_Z^2)(q_9^2-m_t^2)$ $= 0.137593340\mathbf{05}\epsilon^0$	k_1p_1
14	$(q_1^2-M_H^2)(q_2^2-M_W^2)(q_3^2-M_W^2)(q_7^2-M_Z^2)(q_9^2-m_t^2)$ $= 0.124197319\mathbf{95}\epsilon^0$	k_2p_1
15	$(q_1^2-m_t^2)(q_2^2-M_W^2)q_3^2(q_9^2-M_Z^2)(q_{12}^2-M_W^2)$ $= 0.183107939\mathbf{1}\epsilon^0$	k_1p_2
16	$(q_1^2-m_t^2)(q_2^2-M_W^2)q_3^2(q_4^2-M_Z^2)(q_5^2-M_W^2)$ $= 0.183107939\mathbf{1}\epsilon^0$	k_1p_1
17	$(q_1^2-m_t^2)(q_2^2-M_H^2)(q_3^2-m_t^2)(q_4^2-M_W^2)(q_5^2-M_W^2)$ $= 0.088214399\epsilon^0$	k_1p_1
18	$(q_1^2-m_t^2)(q_2^2-M_Z^2)(q_3^2-m_t^2)(q_4^2-M_W^2)(q_5^2-M_W^2)$ $= 0.094994472\mathbf{2}\epsilon^0$	k_1p_1
19	$(q_1^2-M_W^2)(q_2^2-m_t^2)q_3^2(q_9^2-M_Z^2)(q_{12}^2-m_t^2)$ $= 0.108165638\mathbf{2}\epsilon^0$	k_1p_2
20	$(q_1^2-M_W^2)(q_2^2-m_t^2)q_3^2(q_4^2-M_Z^2)(q_5^2-m_t^2)$ $= 0.108165638\mathbf{2}\epsilon^0$	k_1p_1
21	$(q_1^2-M_W^2)(q_2^2-M_H^2)(q_3^2-M_W^2)(q_4^2-m_t^2)(q_5^2-m_t^2)$ $= 0.069402887\mathbf{25}\epsilon^0$	k_1p_1
22	$(q_1^2-M_W^2)(q_2^2-M_H^2)(q_3^2-M_W^2)(q_4^2-m_t^2)(q_5^2-m_t^2)$ $= 0.069402887\mathbf{25}\epsilon^0$	k_2p_2

23	$(q_1^2-M_W^2)(q_2^2-M_Z^2)(q_3^2-M_W^2)(q_4^2-m_t^2)(q_5^2-m_t^2)$ $= 0.073807384049\epsilon^0$	k_1p_1
24	$(q_1^2-M_W^2)(q_2^2-M_Z^2)(q_3^2-M_W^2)(q_4^2-m_t^2)(q_5^2-m_t^2)$ $= 0.073807384049\epsilon^0$	k_2p_2
25	$(q_1^2-M_W^2)(q_2^2-M_W^2)(q_3^2-M_H^2)(q_7^2-M_W^2)(q_{11}^2-M_Z^2)$ $= 0.229878112\mathbf{7}\epsilon^0$	k_1p_1
26	$(q_1^2-M_W^2)(q_2^2-M_W^2)(q_3^2-M_H^2)(q_7^2-M_W^2)(q_{11}^2-M_Z^2)$ $= 0.237409193\mathbf{45}\epsilon^0$	k_2p_1
27	$(q_1^2-M_Z^2)(q_2^2-m_t^2)(q_3^2-m_t^2)(q_4^2-M_W^2)(q_7^2-M_H^2)$ $= 0.083051243\mathbf{65}\epsilon^0$	k_1p_1
28	$(q_1^2-M_Z^2)(q_2^2-m_t^2)(q_3^2-m_t^2)(q_7^2-M_H^2)(q_9^2-M_W^2)(q_{10}^2-M_W^2)$ $= 0.040825985\mathbf{83}\epsilon^0$	1
29	$(q_1^2-M_Z^2)(q_2^2-m_t^2)(q_3^2-m_t^2)(q_7^2-M_H^2)(q_9^2-M_W^2)$ $= 0.105074155\mathbf{55}\epsilon^0$	k_1p_1
30	$(q_1^2-M_Z^2)(q_2^2-M_W^2)(q_3^2-M_W^2)(q_4^2-m_t^2)(q_7^2-M_H^2)$ $= 0.101951793\mathbf{2}\epsilon^0$	k_1p_1
31	$(q_1^2-M_Z^2)(q_2^2-M_W^2)(q_3^2-M_W^2)(q_7^2-M_H^2)(q_9^2-m_t^2)$ $= 0.126023528\epsilon^0$	k_1p_1
32	$(q_1^2-M_H^2)(q_2^2-m_t^2)(q_3^2-m_t^2)(q_4^2-M_W^2)q_6^2(q_7^2-M_Z^2)$ $= 0.042119388\mathbf{9}\epsilon^0$	k_2p_2
33	$(q_1^2-M_H^2)(q_2^2-M_W^2)(q_3^2-M_W^2)(q_4^2-m_t^2)q_6^2(q_7^2-M_Z^2)$ $= 0.054323600\mathbf{2}\epsilon^0$	k_2p_2
34	$(q_1^2-M_H^2)(q_2^2-m_t^2)(q_3^2-m_t^2)(q_7^2-M_Z^2)q_8^2(q_9^2-M_W^2)$ $= 0.042119388\mathbf{9}\epsilon^0$	k_2p_1
35	$(q_1^2-M_H^2)(q_2^2-M_W^2)(q_3^2-M_W^2)(q_7^2-M_Z^2)q_8^2(q_9^2-m_t^2)$ $= 0.054323600\mathbf{2}\epsilon^0$	k_2p_1
36	$(q_1^2-M_H^2)(q_2^2-m_t^2)(q_3^2-m_t^2)(q_4^2-M_W^2)(q_7^2-M_Z^2)$ $= 0.026841040\mathbf{275}\epsilon^0$	$(k_1p_1)(k_1p_1)$
37	$(q_1^2-M_H^2)(q_2^2-m_t^2)(q_3^2-m_t^2)(q_7^2-M_Z^2)(q_9^2-M_W^2)(q_{10}^2-M_W^2)$ $= 0.011346408\mathbf{29}\epsilon^0$	k_1p_1
38	$(q_1^2-M_H^2)(q_2^2-m_t^2)(q_3^2-m_t^2)(q_7^2-M_Z^2)(q_9^2-M_W^2)$ $= 0.036798180\mathbf{275}\epsilon^0$	$(k_1p_1)(k_1p_1)$
39	$(q_1^2-M_H^2)(q_2^2-M_W^2)(q_3^2-M_W^2)(q_4^2-m_t^2)(q_7^2-M_Z^2)$ $= 0.032799737\mathbf{524}\epsilon^0$	$(k_1p_1)(k_1p_1)$
40	$(q_1^2-M_H^2)(q_2^2-M_W^2)(q_3^2-M_W^2)(q_7^2-M_Z^2)(q_9^2-m_t^2)(q_{10}^2-m_t^2)$ $= 0.010161823\mathbf{76}\epsilon^0$	k_1p_1
41	$(q_1^2-M_H^2)(q_2^2-M_W^2)(q_3^2-M_W^2)(q_7^2-M_Z^2)(q_9^2-m_t^2)$ $= 0.043216067\mathbf{375}\epsilon^0$	$(k_1p_1)(k_1p_1)$
42	$(q_1^2-m_t^2)(q_2^2-m_t^2)(q_3^2-M_H^2)(q_6^2-M_W^2)(q_7^2-m_t^2)(q_{11}^2-M_Z^2)$ $= 0.008648232\mathbf{4}\epsilon^0$	k_2p_1

43	$(q_1^2-m_t^2)(q_2^2-M_H^2)(q_3^2-m_t^2)(q_4^2-M_W^2)(q_5^2-M_W^2)$ $= 0.1698644478\mathbf{7}\epsilon^0$ $\quad 0.062\mathbf{5}\epsilon^{-1}$	$(k_1p_1)(k_2p_2)$
44	$(q_1^2-m_t^2)(q_2^2-M_Z^2)(q_3^2-m_t^2)(q_4^2-M_W^2)(q_5^2-M_W^2)$ $= 0.1466120058\mathbf{7}\epsilon^0$ $\quad 0.062\mathbf{5}\epsilon^{-1}$	$(k_1p_1)(k_2p_2)$
45	$(q_1^2-m_t^2)(q_2^2-m_t^2)(q_3^2-M_H^2)(q_7^2-m_t^2)(q_8^2-M_W^2)(q_{11}^2-M_Z^2)$ $= 0.0104247456\mathbf{6}\epsilon^0$	k_2p_1
46	$(q_1^2-M_W^2)(q_2^2-M_W^2)(q_3^2-M_H^2)(q_6^2-m_t^2)(q_7^2-M_W^2)(q_{11}^2-M_Z^2)$ $= 0.0280044654\mathbf{9}\epsilon^0$	k_2p_1
47	$(q_1^2-M_W^2)(q_2^2-M_H^2)(q_3^2-M_W^2)(q_4^2-m_t^2)(q_5^2-m_t^2)$ $= 0.1769824663\mathbf{7}\epsilon^0$ $\quad 0.062\mathbf{5}\epsilon^{-1}$	$(k_1p_1)(k_2p_2)$
48	$(q_1^2-M_W^2)(q_2^2-M_Z^2)(q_3^2-M_W^2)(q_4^2-m_t^2)(q_5^2-m_t^2)$ $= 0.15452017737\mathbf{5}\epsilon^0$ $\quad 0.062\mathbf{5}\epsilon^{-1}$	$(k_1p_1)(k_2p_2)$
49	$(q_1^2-M_W^2)(q_2^2-M_W^2)(q_3^2-M_H^2)(q_7^2-M_W^2)(q_8^2-m_t^2)(q_{11}^2-M_Z^2)$ $= 0.031233078\mathbf{61}\epsilon^0$	k_2p_1
50	$(q_1^2-M_W^2)(q_2^2-M_W^2)(q_3^2-M_H^2)(q_7^2-M_W^2)(q_{11}^2-M_Z^2)$ $= 0.0664159989\mathbf{5}\epsilon^0$	$(k_1p_1)(k_2p_1)$
51	$(q_1^2-M_W^2)(q_2^2-M_W^2)(q_3^2-M_H^2)(q_7^2-M_W^2)(q_{11}^2-M_Z^2)$ $= 0.075360017\mathbf{6}\epsilon^0$	$(k_2p_1)(k_2p_1)$
52	$(q_1^2-M_Z^2)(q_2^2-m_t^2)(q_3^2-m_t^2)(q_4^2-M_W^2)(q_7^2-M_H^2)$ $= 0.02307470566\mathbf{7}\epsilon^0$	$(k_1p_1)(k_1p_1)$
53	$(q_1^2-M_Z^2)(q_2^2-m_t^2)(q_3^2-m_t^2)(q_7^2-M_H^2)(q_9^2-M_W^2)(q_{10}^2-M_W^2)$ $= 0.010251169\mathbf{15}\epsilon^0$	k_1p_1
54	$(q_1^2-M_Z^2)(q_2^2-m_t^2)(q_3^2-m_t^2)(q_7^2-M_H^2)(q_9^2-M_W^2)$ $= 0.03269668492\mathbf{4}\epsilon^0$	$(k_1p_1)(k_1p_1)$
55	$(q_1^2-M_Z^2)(q_2^2-M_W^2)(q_3^2-M_W^2)(q_4^2-m_t^2)(q_7^2-M_H^2)$ $= 0.027609629\mathbf{15}\epsilon^0$	$(k_1p_1)(k_1p_1)$
56	$(q_1^2-M_Z^2)(q_2^2-M_W^2)(q_3^2-M_W^2)(q_7^2-M_H^2)(q_9^2-m_t^2)$ $= 0.03759159477\mathbf{5}\epsilon^0$	$(k_1p_1)(k_1p_1)$
57	$(q_1^2-M_H^2)(q_2^2-m_t^2)(q_3^2-m_t^2)(q_7^2-M_Z^2)(q_9^2-M_W^2)(q_{10}^2-M_W^2)$ $= 0.00370811793\mathbf{2}\epsilon^0$	$(k_1p_1)(k_1p_1)$
58	$(q_1^2-M_H^2)(q_2^2-M_W^2)(q_3^2-M_W^2)(q_7^2-M_Z^2)(q_9^2-m_t^2)(q_{10}^2-m_t^2)$ $= 0.0030891609\mathbf{3}\epsilon^0$	$(k_1p_1)(k_1p_1)$
59	$(q_1^2-m_t^2)(q_2^2-m_t^2)(q_3^2-M_H^2)(q_6^2-M_W^2)(q_7^2-m_t^2)(q_{11}^2-M_Z^2)$ $= 0.0025938831\mathbf{2}\epsilon^0$	$(k_2p_1)(k_2p_1)$
60	$(q_1^2-m_t^2)(q_2^2-m_t^2)(q_3^2-M_H^2)(q_7^2-m_t^2)(q_8^2-M_W^2)(q_{11}^2-M_Z^2)$ $= 0.003500025852\epsilon^0$	$(k_2p_1)(k_2p_1)$
61	$(q_1^2-M_W^2)(q_2^2-M_W^2)(q_3^2-M_H^2)(q_6^2-m_t^2)(q_7^2-M_W^2)(q_{11}^2-M_Z^2)$ $= 0.0084858581\mathbf{1}\epsilon^0$	$(k_2p_1)(k_2p_1)$

62	$(q_1^2-M_W^2)(q_2^2-M_W^2)(q_3^2-M_H^2)(q_7^2-M_W^2)(q_8^2-m_t^2)(q_{11}^2-M_Z^2)$ $= 0.0101428882\mathbf{2}\epsilon^0$	$(k_2p_1)(k_2p_1)$
63	$(q_1^2-M_Z^2)(q_2^2-m_t^2)(q_3^2-m_t^2)(q_7^2-M_H^2)(q_9^2-M_W^2)(q_{10}^2-M_W^2)$ $= 0.003133833\mathbf{3}6\epsilon^0$	$(k_1p_1)(k_1p_1)$
64	$(q_1^2-M_W^2)(q_2^2-M_W^2)(q_3^2-M_H^2)(q_6^2-m_t^2)(q_7^2-M_W^2)(q_{11}^2-M_Z^2)$ $= 0.002865219\mathbf{5}2\epsilon^0$	$(k_2p_1)(k_2p_1)$ (k_2p_1)
65	$(q_1^2-M_W^2)(q_2^2-M_W^2)(q_3^2-M_H^2)(q_7^2-M_W^2)(q_8^2-m_t^2)(q_{11}^2-M_Z^2)$ $= 0.003603973\mathbf{8}4\epsilon^0$	$(k_2p_1)(k_2p_1)$ (k_2p_1)

Table 7.4: Integral definitions and numerical results for the class **xhxwxz** of $Z \to b\bar{b}$ integrals.

Nr.	denominator	numerator
1	$q_1^2(q_2^2-M_W^2)(q_3^2-m_t^2)(q_4^2-M_W^2)q_7^2$ $= (0.2208525\mathbf{3}+0.2509781\mathbf{4}i)\epsilon^0$	k_1p_1
2	$q_1^2(q_2^2-M_W^2)(q_3^2-m_t^2)q_7^2(q_9^2-M_W^2)$ $= (0.2748390\mathbf{2}+0.2579612\mathbf{5}i)\epsilon^0$	k_1p_1
3	$q_1^2(q_2^2-M_W^2)(q_3^2-m_t^2)q_7^2(q_9^2-M_W^2)$ $= (0.2941198\mathbf{3}+0.2864760\mathbf{7}i)\epsilon^0$	k_2p_1
4	$q_1^2(q_2^2-m_t^2)(q_3^2-M_W^2)(q_4^2-m_t^2)q_7^2$ $= (0.1720932\mathbf{4}+0.1579899\mathbf{5}i)\epsilon^0$	k_1p_1
5	$q_1^2(q_2^2-m_t^2)(q_3^2-M_W^2)q_7^2(q_9^2-m_t^2)$ $= (0.1951475\mathbf{1}+0.1592440\mathbf{2}i)\epsilon^0$	k_1p_1
6	$q_1^2(q_2^2-m_t^2)(q_3^2-M_W^2)q_7^2(q_9^2-m_t^2)$ $= (0.1787946\mathbf{7}+0.1401507\mathbf{7}i)\epsilon^0$	k_2p_1
7	$(q_1^2-m_t^2)(q_2^2-m_t^2)q_3^2q_9^2(q_{12}^2-M_W^2)$ $= 0.116118268\mathbf{2}1\epsilon^0$ $0.043051653\mathbf{1}7\epsilon^{-1}$	k_1p_2
8	$(q_1^2-m_t^2)(q_2^2-m_t^2)q_3^2q_9^2(q_{12}^2-M_W^2)$ $= 0.11583992869\mathbf{5}\epsilon^0$ $0.052559120\mathbf{0}5\epsilon^{-1}$	k_2p_1
9	$(q_1^2-m_t^2)(q_2^2-M_W^2)q_3^2q_9^2(q_{12}^2-M_W^2)$ $= 0.07739723372\mathbf{5}\epsilon^0$ $0.090385639\mathbf{8}\epsilon^{-1}$	k_2p_1
10	$(q_1^2-m_t^2)(q_2^2-m_t^2)q_3^2q_4^2(q_6^2-M_W^2)(q_7^2-m_t^2)$ $= 0.026871949\mathbf{2}\epsilon^0$ $0.024226480\mathbf{7}3\epsilon^{-1}$	1
11	$(q_1^2-m_t^2)(q_2^2-M_W^2)q_3^2q_4^2(q_6^2-M_W^2)(q_7^2-m_t^2)$ $= 0.001735254\mathbf{9}\epsilon^0$ $0.049779177\mathbf{8}\epsilon^{-1}$	1
12	$(q_1^2-m_t^2)q_2^2(q_3^2-m_t^2)(q_4^2-M_W^2)(q_6^2-M_W^2)(q_7^2-m_t^2)$ $= 0.051362401\mathbf{8}\epsilon^0$	1

13	$(q_1^2-m_t^2)(q_2^2-m_t^2)q_3^2q_4^2(q_6^2-M_W^2)$ $= 0.1460509441\epsilon^0$ $0.051095532255\epsilon^{-1}$	k_2p_2
14	$(q_1^2-m_t^2)(q_2^2-m_t^2)q_3^2q_4^2(q_5^2-M_W^2)$ $= 0.116118268219\epsilon^0$ $0.043051653177\epsilon^{-1}$	k_1p_1
15	$(q_1^2-m_t^2)(q_2^2-m_t^2)q_3^2q_4^2(q_5^2-M_W^2)$ $= 0.1158399286955\epsilon^0$ $0.052559120055\epsilon^{-1}$	k_2p_2
16	$(q_1^2-m_t^2)(q_2^2-M_W^2)q_3^2q_4^2(q_5^2-M_W^2)$ $= 0.109330856833\epsilon^0$ $0.067392310755\epsilon^{-1}$	k_1p_1
17	$(q_1^2-m_t^2)(q_2^2-M_W^2)q_3^2q_4^2(q_5^2-M_W^2)$ $= 0.0773972337255\epsilon^0$ $0.090385639\epsilon^{-1}$	k_2p_2
18	$(q_1^2-m_t^2)q_2^2(q_3^2-m_t^2)(q_4^2-M_W^2)(q_5^2-M_W^2)$ $= 0.110880468\epsilon^0$	k_1p_1
19	$(q_1^2-m_t^2)q_2^2(q_3^2-m_t^2)(q_4^2-M_W^2)(q_5^2-M_W^2)$ $= 0.110880468\epsilon^0$	k_2p_2
20	$(q_1^2-m_t^2)(q_2^2-m_t^2)q_3^2(q_7^2-m_t^2)(q_8^2-M_W^2)q_9^2$ $= 0.026871949\epsilon^0$ $0.024226480\epsilon^{-1}$	1
21	$(q_1^2-m_t^2)(q_2^2-M_W^2)q_3^2(q_7^2-m_t^2)(q_8^2-M_W^2)q_9^2$ $= 0.001735259\epsilon^0$ $0.049779177\epsilon^{-1}$	1
22	$(q_1^2-m_t^2)q_2^2(q_3^2-m_t^2)(q_7^2-m_t^2)(q_8^2-M_W^2)(q_9^2-M_W^2)$ $= 0.051362401\epsilon^0$	1
23	$(q_1^2-m_t^2)(q_2^2-m_t^2)q_3^2(q_8^2-M_W^2)q_9^2$ $= 0.1460509441\epsilon^0$ $0.051095532255\epsilon^{-1}$	k_2p_1
24	$(q_1^2-m_t^2)(q_2^2-m_t^2)q_3^2q_4^2(q_7^2-m_t^2)$ $= 0.0938555559555\epsilon^0$ $0.024108559553\epsilon^{-1}$	k_1p_1
25	$(q_1^2-m_t^2)(q_2^2-m_t^2)q_3^2q_4^2(q_7^2-m_t^2)$ $= 0.125543693937\epsilon^0$ $0.035762336144\epsilon^{-1}$	k_2p_2
26	$(q_1^2-m_t^2)(q_2^2-M_W^2)q_3^2q_4^2(q_7^2-m_t^2)$ $= 0.103284784988\epsilon^0$ $0.031816713446\epsilon^{-1}$	k_1p_1
27	$(q_1^2-m_t^2)(q_2^2-M_W^2)q_3^2q_4^2(q_7^2-m_t^2)$ $= 0.134098264465\epsilon^0$ $0.053134477\epsilon^{-1}$	k_2p_2

28	$(q_1^2-m_t^2)(q_2^2-m_t^2)q_3^2(q_7^2-m_t^2)q_9^2$ $= 0.125610656029\mathbf{9}\epsilon^0$ $0.035934429\mathbf{01}\epsilon^{-1}$	k_1p_1
29	$(q_1^2-m_t^2)(q_2^2-m_t^2)q_3^2(q_7^2-m_t^2)q_9^2$ $= 0.125543693\mathbf{97}\epsilon^0$ $0.035762336\mathbf{14}\epsilon^{-1}$	k_2p_1
30	$(q_1^2-m_t^2)(q_2^2-M_W^2)q_3^2(q_7^2-m_t^2)q_9^2$ $= 0.133872926\mathbf{6}\epsilon^0$ $0.053508162\mathbf{7}\epsilon^{-1}$	k_1p_1
31	$(q_1^2-m_t^2)(q_2^2-M_W^2)q_3^2(q_7^2-m_t^2)q_9^2$ $= 0.134098264\mathbf{45}\epsilon^0$ $0.053134477\mathbf{2}\epsilon^{-1}$	k_2p_1
32	$(q_1^2-m_t^2)(q_2^2-M_W^2)q_3^2(q_7^2-m_t^2)q_{11}^2$ $= (0.1937207\mathbf{9}+0.1645789\mathbf{4}i)\epsilon^0$	k_1p_1
33	$(q_1^2-m_t^2)(q_2^2-M_W^2)q_3^2(q_7^2-m_t^2)q_{11}^2$ $= (0.1937207\mathbf{9}+0.1645789\mathbf{3}i)\epsilon^0$	k_2p_1
34	$(q_1^2-m_t^2)q_2^2(q_3^2-m_t^2)(q_4^2-M_W^2)(q_7^2-m_t^2)q_{13}^2$ $= 0.011467179\mathbf{23}\epsilon^0$ $0.024880237\mathbf{52}\epsilon^{-1}$	1
35	$(q_1^2-m_t^2)q_2^2(q_3^2-m_t^2)(q_4^2-M_W^2)(q_7^2-m_t^2)$ $= 0.068835790\mathbf{1}\epsilon^0$	k_1p_1
36	$(q_1^2-m_t^2)q_2^2(q_3^2-m_t^2)(q_4^2-M_W^2)(q_7^2-m_t^2)$ $= 0.103623536\mathbf{6}\epsilon^0$	k_2p_2
37	$(q_1^2-m_t^2)q_2^2(q_3^2-m_t^2)(q_7^2-m_t^2)(q_9^2-M_W^2)$ $= 0.098607574\mathbf{4}\epsilon^0$	k_1p_1
38	$(q_1^2-m_t^2)q_2^2(q_3^2-m_t^2)(q_7^2-m_t^2)(q_9^2-M_W^2)$ $= 0.103623536\mathbf{6}\epsilon^0$	k_2p_1
39	$(q_1^2-m_t^2)q_2^2(q_3^2-m_t^2)(q_7^2-m_t^2)(q_{11}^2-m_t^2)$ $= 0.072968501\mathbf{35}\epsilon^0$	k_1p_1
40	$(q_1^2-m_t^2)q_2^2(q_3^2-M_W^2)(q_4^2-m_t^2)(q_7^2-m_t^2)$ $= 0.069081323\mathbf{35}\epsilon^0$	k_1p_1
41	$(q_1^2-m_t^2)q_2^2(q_3^2-M_W^2)(q_4^2-m_t^2)(q_7^2-m_t^2)$ $= 0.086003523\mathbf{9}\epsilon^0$	k_2p_2
42	$(q_1^2-m_t^2)q_2^2(q_3^2-M_W^2)(q_7^2-m_t^2)(q_9^2-m_t^2)q_{10}^2$ $= 0.011467179\mathbf{25}\epsilon^0$ $0.024880237\mathbf{52}\epsilon^{-1}$	1
43	$(q_1^2-m_t^2)q_2^2(q_3^2-M_W^2)(q_7^2-m_t^2)(q_9^2-m_t^2)$ $= 0.091380363\mathbf{5}\epsilon^0$	k_1p_1
44	$(q_1^2-m_t^2)q_2^2(q_3^2-M_W^2)(q_7^2-m_t^2)(q_9^2-m_t^2)$ $= 0.086003523\mathbf{9}\epsilon^0$	k_2p_1

45	$(q_1^2 - M_W^2)(q_2^2 - m_t^2)q_3^2q_9^2(q_{12}^2 - m_t^2)$ $= 0.103608656075\epsilon^0$ $0.030598760665\epsilon^{-1}$	k_1p_2
46	$(q_1^2 - M_W^2)(q_2^2 - m_t^2)q_3^2q_9^2(q_{12}^2 - m_t^2)$ $= 0.116727719047\epsilon^0$ $0.051948179785\epsilon^{-1}$	k_2p_1
47	$(q_1^2 - M_W^2)(q_2^2 - M_W^2)q_3^2q_9^2(q_{12}^2 - m_t^2)$ $= 0.110826941\mathbf{8}\epsilon^0$ $0.043051653\mathbf{17}\epsilon^{-1}$	k_1p_2
48	$(q_1^2 - M_W^2)(q_2^2 - M_W^2)q_3^2q_9^2(q_{12}^2 - m_t^2)$ $= 0.086809120845\epsilon^0$ $0.087189441\mathbf{1}\epsilon^{-1}$	k_2p_1
49	$(q_1^2 - M_W^2)(q_2^2 - m_t^2)q_3^2q_4^2(q_6^2 - m_t^2)(q_7^2 - M_W^2)$ $= 0.019207090\mathbf{1}\epsilon^0$ $0.055503424\mathbf{92}\epsilon^{-1}$	1
50	$(q_1^2 - M_W^2)(q_2^2 - M_W^2)q_3^2q_4^2(q_6^2 - m_t^2)(q_7^2 - M_W^2)$ $= 0.131479996\mathbf{7}\epsilon^0$ $0.134019190\mathbf{8}\epsilon^{-1}$	1
51	$(q_1^2 - M_W^2)q_2^2(q_3^2 - M_W^2)(q_4^2 - m_t^2)(q_6^2 - m_t^2)(q_7^2 - M_W^2)$ $= 0.114727530\mathbf{4}\epsilon^0$	1
52	$(q_1^2 - M_W^2)(q_2^2 - m_t^2)q_3^2q_4^2(q_5^2 - m_t^2)$ $= 0.103608656075\epsilon^0$ $0.030598760665\epsilon^{-1}$	k_1p_1
53	$(q_1^2 - M_W^2)(q_2^2 - m_t^2)q_3^2q_4^2(q_5^2 - m_t^2)$ $= 0.116727719047\epsilon^0$ $0.051948179785\epsilon^{-1}$	k_2p_2
54	$(q_1^2 - M_W^2)(q_2^2 - M_W^2)q_3^2q_4^2(q_5^2 - m_t^2)$ $= 0.110826941\mathbf{8}\epsilon^0$ $0.043051653\mathbf{17}\epsilon^{-1}$	k_1p_1
55	$(q_1^2 - M_W^2)(q_2^2 - M_W^2)q_3^2q_4^2(q_5^2 - m_t^2)$ $= 0.086809120845\epsilon^0$ $0.087189441\mathbf{1}\epsilon^{-1}$	k_2p_2
56	$(q_1^2 - M_W^2)q_2^2(q_3^2 - M_W^2)(q_4^2 - m_t^2)(q_5^2 - m_t^2)$ $= 0.083273578\mathbf{4}\epsilon^0$	k_1p_1
57	$(q_1^2 - M_W^2)q_2^2(q_3^2 - M_W^2)(q_4^2 - m_t^2)(q_5^2 - m_t^2)$ $= 0.083273578\mathbf{4}\epsilon^0$	k_2p_2
58	$(q_1^2 - M_W^2)(q_2^2 - m_t^2)q_3^2(q_7^2 - M_W^2)(q_8^2 - m_t^2)q_9^2$ $= 0.019207090\mathbf{1}\epsilon^0$ $0.055503424\mathbf{92}\epsilon^{-1}$	1
59	$(q_1^2 - M_W^2)(q_2^2 - M_W^2)q_3^2(q_7^2 - M_W^2)(q_8^2 - m_t^2)q_9^2$ $= 0.131479996\mathbf{7}\epsilon^0$ $0.134019190\mathbf{8}\epsilon^{-1}$	1

60	$(q_1^2 - M_W^2)q_2^2(q_3^2 - M_W^2)(q_7^2 - M_W^2)(q_8^2 - m_t^2)(q_9^2 - m_t^2)$ $= 0.1147275304\epsilon^0$	1
61	$(q_1^2 - M_W^2)(q_2^2 - m_t^2)q_3^2q_4^2(q_7^2 - M_W^2)$ $= 0.1274132736\mathbf{3}7\epsilon^0$ $0.0740872148\mathbf{5}\epsilon^{-1}$	k_1p_1
62	$(q_1^2 - M_W^2)(q_2^2 - m_t^2)q_3^2q_4^2(q_7^2 - M_W^2)$ $= 0.1586562899\mathbf{0}5\epsilon^0$ $0.095333688\epsilon^{-1}$	k_2p_2
63	$(q_1^2 - M_W^2)(q_2^2 - M_W^2)q_3^2q_4^2(q_7^2 - M_W^2)$ $= 0.058404906\mathbf{7}\epsilon^0$ $0.1341163767499\epsilon^{-1}$	k_1p_1
64	$(q_1^2 - M_W^2)(q_2^2 - M_W^2)q_3^2q_4^2(q_7^2 - M_W^2)$ $= 0.038107739\mathbf{65}\epsilon^0$ $0.189584358\mathbf{7}\epsilon^{-1}$	k_2p_2
65	$(q_1^2 - M_W^2)(q_2^2 - m_t^2)q_3^2(q_7^2 - M_W^2)q_9^2$ $= 0.15700936275\mathbf{5}\epsilon^0$ $0.096482609\mathbf{7}\epsilon^{-1}$	k_1p_1
66	$(q_1^2 - M_W^2)(q_2^2 - m_t^2)q_3^2(q_7^2 - M_W^2)q_9^2$ $= 0.1586562899\mathbf{0}5\epsilon^0$ $0.095333688\epsilon^{-1}$	k_2p_1
67	$(q_1^2 - M_W^2)(q_2^2 - M_W^2)q_3^2(q_7^2 - M_W^2)q_9^2$ $= 0.022893166\mathbf{35}\epsilon^0$ $0.194622658\mathbf{9}\epsilon^{-1}$	k_1p_1
68	$(q_1^2 - M_W^2)(q_2^2 - M_W^2)q_3^2(q_7^2 - M_W^2)q_9^2$ $= 0.038107739\mathbf{65}\epsilon^0$ $0.189584358\mathbf{7}\epsilon^{-1}$	k_2p_1
69	$(q_1^2 - M_W^2)(q_2^2 - m_t^2)q_3^2(q_7^2 - M_W^2)q_{11}^2$ $= (0.325515\mathbf{8} + 0.2945986\mathbf{3}i)\epsilon^0$	k_1p_1
70	$(q_1^2 - M_W^2)(q_2^2 - m_t^2)q_3^2(q_7^2 - M_W^2)q_{11}^2$ $= (0.325515\mathbf{8} + 0.2945986\mathbf{3}i)\epsilon^0$	k_2p_1
71	$(q_1^2 - M_W^2)q_2^2(q_3^2 - m_t^2)(q_4^2 - M_W^2)(q_7^2 - M_W^2)q_{13}^2$ $= 0.187286487\mathbf{1}\epsilon^0$ $0.137692261\mathbf{8}\epsilon^{-1}$	1
72	$(q_1^2 - M_W^2)q_2^2(q_3^2 - m_t^2)(q_4^2 - M_W^2)(q_7^2 - M_W^2)$ $= 0.174134842\mathbf{7}\epsilon^0$	k_1p_1
73	$(q_1^2 - M_W^2)q_2^2(q_3^2 - m_t^2)(q_4^2 - M_W^2)(q_7^2 - M_W^2)$ $= 0.2421197038\mathbf{5}\epsilon^0$	k_2p_2
74	$(q_1^2 - M_W^2)q_2^2(q_3^2 - m_t^2)(q_7^2 - M_W^2)(q_9^2 - M_W^2)q_{10}^2$ $= 0.187286487\mathbf{1}\epsilon^0$ $0.137692261\mathbf{8}\epsilon^{-1}$	1
75	$(q_1^2 - M_W^2)q_2^2(q_3^2 - m_t^2)(q_7^2 - M_W^2)(q_9^2 - M_W^2)$ $= 0.2271318206\mathbf{5}\epsilon^0$	k_1p_1

76	$(q_1^2 - M_W^2)q_2^2(q_3^2 - m_t^2)(q_7^2 - M_W^2)(q_9^2 - M_W^2)$ $= 0.24211970385\epsilon^0$	k_2p_1
77	$(q_1^2 - M_W^2)q_2^2(q_3^2 - m_t^2)(q_7^2 - M_W^2)(q_{11}^2 - m_t^2)$ $= 0.154456303\mathbf{4}\epsilon^0$	k_1p_1
78	$(q_1^2 - M_W^2)q_2^2(q_3^2 - m_t^2)(q_7^2 - M_W^2)(q_{11}^2 - m_t^2)$ $= 0.154456303\mathbf{4}\epsilon^0$	k_2p_1
79	$(q_1^2 - M_W^2)q_2^2(q_3^2 - M_W^2)(q_4^2 - m_t^2)(q_7^2 - M_W^2)q_{13}^2$ $= 0.187286487\mathbf{1}\epsilon^0$ $0.137692261\mathbf{8}\epsilon^{-1}$	1
80	$(q_1^2 - M_W^2)q_2^2(q_3^2 - M_W^2)(q_4^2 - m_t^2)(q_7^2 - M_W^2)$ $= 0.176495994\mathbf{9}\epsilon^0$	k_1p_1
81	$(q_1^2 - M_W^2)q_2^2(q_3^2 - M_W^2)(q_4^2 - m_t^2)(q_7^2 - M_W^2)$ $= 0.195895107\mathbf{3}\mathbf{5}\epsilon^0$	k_2p_2
82	$(q_1^2 - M_W^2)q_2^2(q_3^2 - M_W^2)(q_7^2 - M_W^2)(q_9^2 - m_t^2)q_{10}^2$ $= 0.187286487\mathbf{1}\epsilon^0$ $0.137692261\mathbf{8}\epsilon^{-1}$	1
83	$(q_1^2 - M_W^2)q_2^2(q_3^2 - M_W^2)(q_7^2 - M_W^2)(q_9^2 - m_t^2)$ $= 0.212904021\mathbf{5}\epsilon^0$	k_1p_1
84	$(q_1^2 - M_W^2)q_2^2(q_3^2 - M_W^2)(q_7^2 - M_W^2)(q_9^2 - m_t^2)$ $= 0.195895107\mathbf{3}\mathbf{5}\epsilon^0$	k_2p_1
85	$(q_1^2 - M_W^2)q_2^2(q_3^2 - M_W^2)(q_7^2 - M_W^2)(q_{11}^2 - M_W^2)$ $= 0.422761740\mathbf{9}\epsilon^0$	k_1p_1
86	$q_1^2(q_2^2 - M_W^2)(q_3^2 - m_t^2)(q_4^2 - M_W^2)q_7^2$ $= (0.0685937\mathbf{6} - 0.0830938\mathbf{9}i)\epsilon^0$	$(k_1p_1)(k_1p_1)$
87	$q_1^2(q_2^2 - M_W^2)(q_3^2 - m_t^2)(q_4^2 - M_W^2)q_7^2$ $= (0.1219\mathbf{3} - 0.06254\mathbf{5}i)\epsilon^0$ $0.062\mathbf{5}\epsilon^{-1}$	$(k_1p_1)(k_2p_2)$
88	$q_1^2(q_2^2 - M_W^2)(q_3^2 - m_t^2)q_7^2(q_9^2 - M_W^2)$ $= (0.0933139\mathbf{3} - 0.0865854\mathbf{5}i)\epsilon^0$	$(k_1p_1)(k_1p_1)$
89	$q_1^2(q_2^2 - M_W^2)(q_3^2 - m_t^2)q_7^2(q_9^2 - M_W^2)$ $= (0.0858179\mathbf{6} - 0.0806874\mathbf{1}i)\epsilon^0$	$(k_1p_1)(k_2p_1)$
90	$q_1^2(q_2^2 - m_t^2)(q_3^2 - M_W^2)(q_4^2 - m_t^2)q_7^2$ $= (0.19388370\mathbf{3} - 0.03097990\mathbf{6}i)\epsilon^0$ $0.062\mathbf{5}\epsilon^{-1}$	$(k_1p_1)(k_2p_2)$
91	$q_1^2(q_2^2 - m_t^2)(q_3^2 - M_W^2)q_7^2(q_9^2 - m_t^2)$ $= (0.0500310\mathbf{79} - 0.0390954\mathbf{78}i)\epsilon^0$	$(k_1p_1)(k_2p_1)$
92	$(q_1^2 - m_t^2)(q_2^2 - m_t^2)q_3^2q_9^2(q_{12}^2 - M_W^2)$ $= 0.136357174\mathbf{02}\epsilon^0$ $0.05164073257\mathbf{5}\epsilon^{-1}$	$(k_1p_2)(k_2p_1)$
93	$(q_1^2 - m_t^2)(q_2^2 - M_W^2)q_3^2q_9^2(q_{12}^2 - M_W^2)$ $= 0.050678121\mathbf{67}\epsilon^0$ $0.045309803958\mathbf{7}\epsilon^{-1}$	$(k_1p_2)(k_2p_1)$

94	$(q_1^2-m_t^2)(q_2^2-m_t^2)q_3^2q_4^2(q_6^2-M_W^2)(q_7^2-m_t^2)$ $= 0.00808652447\epsilon^0$ $0.00602841044\epsilon^{-1}$	k_2p_2
95	$(q_1^2-m_t^2)(q_2^2-M_W^2)q_3^2q_4^2(q_6^2-M_W^2)(q_7^2-m_t^2)$ $= 0.002706151240\epsilon^0$ $0.0123302747750\epsilon^{-1}$	k_2p_2
96	$(q_1^2-m_t^2)(q_2^2-M_W^2)q_3^2(q_6^2-M_W^2)(q_7^2-m_t^2)q_{11}^2$ $= (0.025407\mathbf{2}-0.035438\mathbf{5}i)\epsilon^0$	k_2p_1
97	$(q_1^2-m_t^2)q_2^2(q_3^2-m_t^2)(q_4^2-M_W^2)(q_6^2-M_W^2)(q_7^2-m_t^2)$ $= 0.016236941\mathbf{5}3\epsilon^0$	k_2p_2
98	$(q_1^2-m_t^2)q_2^2(q_3^2-m_t^2)(q_6^2-M_W^2)(q_7^2-m_t^2)(q_{11}^2-m_t^2)$ $= 0.007301506\mathbf{5}9\epsilon^0$	k_2p_1
99	$(q_1^2-m_t^2)q_2^2(q_3^2-M_W^2)(q_6^2-M_W^2)(q_7^2-m_t^2)(q_{11}^2-M_W^2)$ $= 0.022398101\mathbf{6}1\epsilon^0$	k_2p_1
100	$(q_1^2-m_t^2)(q_2^2-m_t^2)q_3^2q_4^2(q_5^2-M_W^2)$ $= 0.03354632575\mathbf{2}\epsilon^0$ $0.0123377547750\epsilon^{-1}$	$(k_1p_1)(k_1p_1)$
101	$(q_1^2-m_t^2)(q_2^2-m_t^2)q_3^2q_4^2(q_5^2-M_W^2)$ $= 0.1363571740\mathbf{2}\epsilon^0$ $0.05164073257\mathbf{5}\epsilon^{-1}$	$(k_1p_1)(k_2p_2)$
102	$(q_1^2-m_t^2)(q_2^2-M_W^2)q_3^2q_4^2(q_5^2-M_W^2)$ $= 0.032990278378\epsilon^0$ $0.0182161585\mathbf{5}5\epsilon^{-1}$	$(k_1p_1)(k_1p_1)$
103	$(q_1^2-m_t^2)(q_2^2-M_W^2)q_3^2q_4^2(q_5^2-M_W^2)$ $= 0.050678121\mathbf{6}7\epsilon^0$ $0.045309803958\mathbf{7}\epsilon^{-1}$	$(k_1p_1)(k_2p_2)$
104	$(q_1^2-m_t^2)q_2^2(q_3^2-m_t^2)(q_4^2-M_W^2)(q_5^2-M_W^2)$ $= 0.097710450\mathbf{0}6\epsilon^0$ $0.06\mathbf{2}5\epsilon^{-1}$	$(k_1p_1)(k_2p_2)$
105	$(q_1^2-m_t^2)(q_2^2-m_t^2)q_3^2(q_7^2-m_t^2)(q_8^2-M_W^2)q_9^2$ $= 0.008086524\mathbf{4}7\epsilon^0$ $0.00602841044\epsilon^{-1}$	k_2p_1
106	$(q_1^2-m_t^2)(q_2^2-M_W^2)q_3^2(q_7^2-m_t^2)(q_8^2-M_W^2)q_9^2$ $= 0.002706151240\epsilon^0$ $0.0123302747750\epsilon^{-1}$	k_2p_1
107	$(q_1^2-m_t^2)q_2^2(q_3^2-m_t^2)(q_7^2-m_t^2)(q_8^2-M_W^2)(q_9^2-M_W^2)$ $= 0.016236941\mathbf{5}3\epsilon^0$	k_2p_1
108	$(q_1^2-m_t^2)(q_2^2-m_t^2)q_3^2q_4^2(q_7^2-m_t^2)$ $= 0.025283649342\mathbf{5}\epsilon^0$ $0.006027139882\mathbf{5}\epsilon^{-1}$	$(k_1p_1)(k_1p_1)$
109	$(q_1^2-m_t^2)(q_2^2-m_t^2)q_3^2q_4^2(q_7^2-m_t^2)$ $= 0.2129662347\mathbf{1}\epsilon^0$ $0.068498197437\mathbf{5}\epsilon^{-1}$	$(k_1p_1)(k_2p_2)$

110	$(q_1^2-m_t^2)(q_2^2-m_t^2)q_3^2q_4^2(q_7^2-m_t^2)$ $= 0.039843570\mathbf{41}\epsilon^0$ $0.011896974432\mathbf{5}\epsilon^{-1}$	$(k_2p_2)(k_2p_2)$
111	$(q_1^2-m_t^2)(q_2^2-M_W^2)q_3^2q_4^2(q_7^2-m_t^2)$ $= 0.027823787202\mathbf{5}\epsilon^0$ $0.007438751387\mathbf{5}\epsilon^{-1}$	$(k_1p_1)(k_1p_1)$
112	$(q_1^2-m_t^2)(q_2^2-M_W^2)q_3^2q_4^2(q_7^2-m_t^2)$ $= 0.141807100\mathbf{87}\epsilon^0$ $0.070391096\mathbf{5}\epsilon^{-1}$	$(k_1p_1)(k_2p_2)$
113	$(q_1^2-m_t^2)(q_2^2-m_t^2)q_3^2(q_7^2-m_t^2)q_9^2$ $= 0.038851566\mathbf{96}\epsilon^0$ $0.010963947017\mathbf{5}\epsilon^{-1}$	$(k_1p_1)(k_1p_1)$
114	$(q_1^2-m_t^2)(q_2^2-m_t^2)q_3^2(q_7^2-m_t^2)q_9^2$ $= 0.03486611040\mathbf{5}\epsilon^0$ $0.009930715432\mathbf{5}\epsilon^{-1}$	$(k_1p_1)(k_2p_1)$
115	$(q_1^2-m_t^2)(q_2^2-m_t^2)q_3^2(q_7^2-m_t^2)q_9^2$ $= 0.039843570\mathbf{41}\epsilon^0$ $0.011896974432\mathbf{5}\epsilon^{-1}$	$(k_2p_1)(k_2p_1)$
116	$(q_1^2-m_t^2)(q_2^2-M_W^2)q_3^2(q_7^2-m_t^2)q_9^2$ $= 0.041329543237\mathbf{5}\epsilon^0$ $0.016228494772\mathbf{5}\epsilon^{-1}$	$(k_1p_1)(k_1p_1)$
117	$(q_1^2-m_t^2)(q_2^2-M_W^2)q_3^2(q_7^2-m_t^2)q_9^2$ $= 0.037104562575\epsilon^0$ $0.015089003895\epsilon^{-1}$	$(k_1p_1)(k_2p_1)$
118	$(q_1^2-m_t^2)q_2^2(q_3^2-m_t^2)(q_4^2-M_W^2)(q_7^2-m_t^2)q_{13}^2$ $= 0.002837419\mathbf{95}\epsilon^0$ $0.006228844\mathbf{84}\epsilon^{-1}$	k_1p_1
119	$(q_1^2-m_t^2)q_2^2(q_3^2-m_t^2)(q_4^2-M_W^2)(q_7^2-m_t^2)q_{13}^2$ $= 0.002556650\mathbf{44}\epsilon^0$ $0.007118871\mathbf{14}\epsilon^{-1}$	k_2p_2
120	$(q_1^2-m_t^2)q_2^2(q_3^2-m_t^2)(q_4^2-M_W^2)(q_7^2-m_t^2)$ $= 0.018277513\mathbf{712}\epsilon^0$	$(k_1p_1)(k_1p_1)$
121	$(q_1^2-m_t^2)q_2^2(q_3^2-m_t^2)(q_4^2-M_W^2)(q_7^2-m_t^2)$ $= 0.176815\mathbf{864}\epsilon^0$ $0.06\mathbf{25}\epsilon^{-1}$	$(k_1p_1)(k_2p_2)$
122	$(q_1^2-m_t^2)q_2^2(q_3^2-m_t^2)(q_7^2-m_t^2)(q_9^2-M_W^2)$ $= 0.031215213\mathbf{5}\epsilon^0$	$(k_1p_1)(k_1p_1)$
123	$(q_1^2-m_t^2)q_2^2(q_3^2-m_t^2)(q_7^2-m_t^2)(q_9^2-M_W^2)$ $= 0.030041797\mathbf{9}\epsilon^0$	$(k_1p_1)(k_2p_1)$
124	$(q_1^2-m_t^2)q_2^2(q_3^2-M_W^2)(q_4^2-m_t^2)(q_7^2-m_t^2)$ $= 0.018334930409\epsilon^0$	$(k_1p_1)(k_1p_1)$

125	$(q_1^2-m_t^2)q_2^2(q_3^2-M_W^2)(q_4^2-m_t^2)(q_7^2-m_t^2)$ $= 0.17376503725\epsilon^0$ $0.0625\epsilon^{-1}$	$(k_1p_1)(k_2p_2)$
126	$(q_1^2-m_t^2)q_2^2(q_3^2-M_W^2)(q_7^2-m_t^2)(q_9^2-m_t^2)q_{10}^2$ $= 0.00385017703\mathbf{6}\epsilon^0$ $0.0053212476\mathbf{2}\epsilon^{-1}$	k_1p_1
127	$(q_1^2-m_t^2)q_2^2(q_3^2-M_W^2)(q_7^2-m_t^2)(q_9^2-m_t^2)$ $= 0.027528747\mathbf{45}\epsilon^0$	$(k_1p_1)(k_1p_1)$
128	$(q_1^2-m_t^2)q_2^2(q_3^2-M_W^2)(q_7^2-m_t^2)(q_9^2-m_t^2)$ $= 0.023754168277\mathbf{5}\epsilon^0$	$(k_1p_1)(k_2p_1)$
129	$(q_1^2-M_W^2)(q_2^2-m_t^2)q_3^2q_9^2(q_{12}^2-m_t^2)$ $= 0.138005591\mathbf{3}\epsilon^0$ $0.054810968063\mathbf{7}\epsilon^{-1}$	$(k_1p_2)(k_2p_1)$
130	$(q_1^2-M_W^2)(q_2^2-m_t^2)q_3^2q_9^2(q_{12}^2-m_t^2)$ $= 0.03314754480\mathbf{5}\epsilon^0$ $0.01735220908\mathbf{5}\epsilon^{-1}$	$(k_2p_1)(k_2p_1)$
131	$(q_1^2-M_W^2)(q_2^2-M_W^2)q_3^2q_9^2(q_{12}^2-m_t^2)$ $= 0.0471603755\mathbf{8}\epsilon^0$ $0.05164073257\mathbf{5}\epsilon^{-1}$	$(k_1p_2)(k_2p_1)$
132	$(q_1^2-M_W^2)(q_2^2-m_t^2)q_3^2q_4^2(q_6^2-m_t^2)(q_7^2-M_W^2)$ $= 0.0065125076\mathbf{9}\epsilon^0$ $0.01374221978\mathbf{5}\epsilon^{-1}$	k_2p_2
133	$(q_1^2-M_W^2)(q_2^2-M_W^2)q_3^2q_4^2(q_6^2-m_t^2)(q_7^2-M_W^2)$ $= 0.0265530567\mathbf{9}\epsilon^0$ $0.03265189641\mathbf{5}\epsilon^{-1}$	k_2p_2
134	$(q_1^2-M_W^2)(q_2^2-m_t^2)q_3^2(q_6^2-m_t^2)(q_7^2-M_W^2)q_{11}^2$ $= (0.03771\mathbf{7}-0.04170\mathbf{6}i)\epsilon^0$	k_2p_1
135	$(q_1^2-M_W^2)q_2^2(q_3^2-m_t^2)(q_6^2-m_t^2)(q_7^2-M_W^2)(q_{11}^2-m_t^2)$ $= 0.016878229\epsilon^0$	k_2p_1
136	$(q_1^2-M_W^2)q_2^2(q_3^2-M_W^2)(q_4^2-m_t^2)(q_6^2-m_t^2)(q_7^2-M_W^2)$ $= 0.027030538\mathbf{41}\epsilon^0$	k_2p_2
137	$(q_1^2-M_W^2)q_2^2(q_3^2-M_W^2)(q_6^2-m_t^2)(q_7^2-M_W^2)(q_{11}^2-M_W^2)$ $= 0.058659933\mathbf{7}\epsilon^0$	k_2p_1
138	$(q_1^2-M_W^2)(q_2^2-m_t^2)q_3^2q_4^2(q_5^2-m_t^2)$ $= 0.02737539051\mathbf{5}\epsilon^0$ $0.007165432527\mathbf{5}\epsilon^{-1}$	$(k_1p_1)(k_1p_1)$
139	$(q_1^2-M_W^2)(q_2^2-m_t^2)q_3^2q_4^2(q_5^2-m_t^2)$ $= 0.138005591\mathbf{3}\epsilon^0$ $0.054810968063\mathbf{7}\epsilon^{-1}$	$(k_1p_1)(k_2p_2)$
140	$(q_1^2-M_W^2)(q_2^2-m_t^2)q_3^2q_4^2(q_5^2-m_t^2)$ $= 0.03314754480\mathbf{5}\epsilon^0$ $0.01735220908\mathbf{5}\epsilon^{-1}$	$(k_2p_2)(k_2p_2)$

141	$(q_1^2 - M_W^2)(q_2^2 - M_W^2)q_3^2 q_4^2(q_5^2 - m_t^2)$ $= 0.0299733467325\epsilon^0$ $0.009188071811\epsilon^{-1}$	$(k_1p_1)(k_1p_1)$
142	$(q_1^2 - M_W^2)(q_2^2 - M_W^2)q_3^2 q_4^2(q_5^2 - m_t^2)$ $= 0.0471603755587\epsilon^0$ $0.051640732575\epsilon^{-1}$	$(k_1p_1)(k_2p_2)$
143	$(q_1^2 - M_W^2)q_2^2(q_3^2 - M_W^2)(q_4^2 - m_t^2)(q_5^2 - m_t^2)$ $= 0.107680829806\epsilon^0$ $0.0625\epsilon^{-1}$	$(k_1p_1)(k_2p_2)$
144	$(q_1^2 - M_W^2)(q_2^2 - m_t^2)q_3^2(q_7^2 - M_W^2)(q_8^2 - m_t^2)q_9^2$ $= 0.006512507609\epsilon^0$ $0.0137422197785\epsilon^{-1}$	k_2p_1
145	$(q_1^2 - M_W^2)(q_2^2 - M_W^2)q_3^2(q_7^2 - M_W^2)(q_8^2 - m_t^2)q_9^2$ $= 0.026553056709\epsilon^0$ $0.0326518964155\epsilon^{-1}$	k_2p_1
146	$(q_1^2 - M_W^2)q_2^2(q_3^2 - M_W^2)(q_7^2 - M_W^2)(q_8^2 - m_t^2)(q_9^2 - m_t^2)$ $= 0.027030538401\epsilon^0$	k_2p_1
147	$(q_1^2 - M_W^2)(q_2^2 - m_t^2)q_3^2 q_4^2(q_7^2 - M_W^2)$ $= 0.0367472890006\epsilon^0$ $0.020054122139909\epsilon^{-1}$	$(k_1p_1)(k_1p_1)$
148	$(q_1^2 - M_W^2)(q_2^2 - m_t^2)q_3^2 q_4^2(q_7^2 - M_W^2)$ $= 0.146514007\epsilon^0$ $0.080824761487\epsilon^{-1}$	$(k_1p_1)(k_2p_2)$
149	$(q_1^2 - M_W^2)(q_2^2 - M_W^2)q_3^2 q_4^2(q_7^2 - M_W^2)$ $= 0.024192574\epsilon^0$ $0.033529094\epsilon^{-1}$	$(k_1p_1)(k_1p_1)$
150	$(q_1^2 - M_W^2)(q_2^2 - M_W^2)q_3^2 q_4^2(q_7^2 - M_W^2)$ $= 0.00654369106\epsilon^0$ $0.095149130275\epsilon^{-1}$	$(k_1p_1)(k_2p_2)$
151	$(q_1^2 - M_W^2)(q_2^2 - m_t^2)q_3^2(q_7^2 - M_W^2)q_9^2$ $= 0.049465417\epsilon^0$ $0.029720666\epsilon^{-1}$	$(k_1p_1)(k_1p_1)$
152	$(q_1^2 - M_W^2)(q_2^2 - m_t^2)q_3^2(q_7^2 - M_W^2)q_9^2$ $= 0.04467666853\epsilon^0$ $0.025754944\epsilon^{-1}$	$(k_1p_1)(k_2p_1)$
153	$(q_1^2 - M_W^2)(q_2^2 - M_W^2)q_3^2(q_7^2 - M_W^2)q_9^2$ $= 0.01046763857\epsilon^0$ $0.05898940517\epsilon^{-1}$	$(k_1p_1)(k_1p_1)$
154	$(q_1^2 - M_W^2)(q_2^2 - M_W^2)q_3^2(q_7^2 - M_W^2)q_9^2$ $= 0.010713553\epsilon^0$ $0.0525573889\epsilon^{-1}$	$(k_1p_1)(k_2p_1)$

155	$(q_1^2 - M_W^2)q_2^2(q_3^2 - m_t^2)(q_4^2 - M_W^2)(q_7^2 - M_W^2)q_{13}^2$ $= 0.04688817179\epsilon^0$ $0.0344061595\mathbf{6}9\epsilon^{-1}$	k_1p_1
156	$(q_1^2 - M_W^2)q_2^2(q_3^2 - m_t^2)(q_4^2 - M_W^2)(q_7^2 - M_W^2)q_{13}^2$ $= 0.0536749712\epsilon^0$ $0.0391244038\mathbf{8}\epsilon^{-1}$	k_2p_2
157	$(q_1^2 - M_W^2)q_2^2(q_3^2 - m_t^2)(q_4^2 - M_W^2)(q_7^2 - M_W^2)$ $= 0.048667959675\epsilon^0$	$(k_1p_1)(k_1p_1)$
158	$(q_1^2 - M_W^2)q_2^2(q_3^2 - m_t^2)(q_4^2 - M_W^2)(q_7^2 - M_W^2)$ $= 0.1120075920\mathbf{2}\epsilon^0$ $0.062\mathbf{5}\epsilon^{-1}$	$(k_1p_1)(k_2p_2)$
159	$(q_1^2 - M_W^2)q_2^2(q_3^2 - m_t^2)(q_7^2 - M_W^2)(q_9^2 - M_W^2)q_{10}^2$ $= 0.058929748\mathbf{7}\epsilon^0$ $0.0391244038\mathbf{8}\epsilon^{-1}$	k_1p_1
160	$(q_1^2 - M_W^2)q_2^2(q_3^2 - m_t^2)(q_7^2 - M_W^2)(q_9^2 - M_W^2)$ $= 0.072342831\mathbf{4}5\epsilon^0$	$(k_1p_1)(k_1p_1)$
161	$(q_1^2 - M_W^2)q_2^2(q_3^2 - m_t^2)(q_7^2 - M_W^2)(q_9^2 - M_W^2)$ $= 0.069928123\mathbf{7}\epsilon^0$	$(k_1p_1)(k_2p_1)$
162	$(q_1^2 - M_W^2)q_2^2(q_3^2 - M_W^2)(q_4^2 - m_t^2)(q_7^2 - M_W^2)q_{13}^2$ $= 0.046755071\mathbf{3}\epsilon^0$ $0.0344399713\mathbf{0}4\epsilon^{-1}$	k_1p_1
163	$(q_1^2 - M_W^2)q_2^2(q_3^2 - M_W^2)(q_4^2 - m_t^2)(q_7^2 - M_W^2)q_{13}^2$ $= 0.039968272\mathbf{3}5\epsilon^0$ $0.02972172\mathbf{7}\epsilon^{-1}$	k_2p_2
164	$(q_1^2 - M_W^2)q_2^2(q_3^2 - M_W^2)(q_4^2 - m_t^2)(q_7^2 - M_W^2)$ $= 0.049302631\mathbf{4}2\mathbf{5}\epsilon^0$	$(k_1p_1)(k_1p_1)$
165	$(q_1^2 - M_W^2)q_2^2(q_3^2 - M_W^2)(q_4^2 - m_t^2)(q_7^2 - M_W^2)$ $= 0.102747678\mathbf{2}7\epsilon^0$ $0.062\mathbf{5}\epsilon^{-1}$	$(k_1p_1)(k_2p_2)$
166	$(q_1^2 - M_W^2)q_2^2(q_3^2 - M_W^2)(q_7^2 - M_W^2)(q_9^2 - m_t^2)q_{10}^2$ $= 0.034713494\mathbf{8}4\epsilon^0$ $0.02972172\mathbf{7}\epsilon^{-1}$	k_1p_1
167	$(q_1^2 - M_W^2)q_2^2(q_3^2 - M_W^2)(q_7^2 - M_W^2)(q_9^2 - m_t^2)$ $= 0.064653957\mathbf{6}\epsilon^0$	$(k_1p_1)(k_1p_1)$
168	$(q_1^2 - M_W^2)q_2^2(q_3^2 - M_W^2)(q_7^2 - M_W^2)(q_9^2 - m_t^2)$ $= 0.054189265875\epsilon^0$	$(k_1p_1)(k_2p_1)$
169	$(q_1^2 - M_W^2)q_2^2(q_3^2 - M_W^2)(q_7^2 - M_W^2)(q_{11}^2 - M_W^2)$ $= 0.12934827132\mathbf{5}\epsilon^0$	$(k_1p_1)(k_1p_1)$
170	$(q_1^2 - m_t^2)(q_2^2 - m_t^2)q_3^2q_4^2(q_6^2 - M_W^2)(q_7^2 - m_t^2)$ $= 0.00259992813\mathbf{8}\epsilon^0$ $0.00200480655\mathbf{6}\epsilon^{-1}$	$(k_2p_2)(k_2p_2)$

171	$(q_1^2-m_t^2)(q_2^2-M_W^2)q_3^2(q_6^2-M_W^2)(q_7^2-m_t^2)q_{11}^2$ $= (0.0079888\mathbf{7}+0.0117117\mathbf{7}i)\epsilon^0$	$(k_2p_1)(k_2p_1)$
172	$(q_1^2-m_t^2)q_2^2(q_3^2-m_t^2)(q_6^2-M_W^2)(q_7^2-m_t^2)(q_{11}^2-m_t^2)$ $= 0.001978727307\epsilon^0$	$(k_2p_1)(k_2p_1)$
173	$(q_1^2-m_t^2)q_2^2(q_3^2-M_W^2)(q_6^2-M_W^2)(q_7^2-m_t^2)(q_{11}^2-M_W^2)$ $= 0.006303341\mathbf{1}3\epsilon^0$	$(k_2p_1)(k_2p_1)$
174	$(q_1^2-m_t^2)(q_2^2-m_t^2)q_3^2(q_7^2-m_t^2)(q_8^2-M_W^2)q_9^2$ $= 0.00259992813\mathbf{8}\epsilon^0$ $0.002004806556\epsilon^{-1}$	$(k_2p_1)(k_2p_1)$
175	$(q_1^2-m_t^2)q_2^2(q_3^2-m_t^2)(q_4^2-M_W^2)(q_7^2-m_t^2)q_{13}^2$ $= 0.00083309635\mathbf{4}\epsilon^0$ $0.0018707481412\mathbf{5}\epsilon^{-1}$	$(k_1p_1)(k_1p_1)$
176	$(q_1^2-m_t^2)q_2^2(q_3^2-m_t^2)(q_4^2-M_W^2)(q_7^2-m_t^2)q_{13}^2$ $= 0.031787668\mathbf{0}4\epsilon^0$ $0.01369517564\mathbf{5}\epsilon^{-1}$	$(k_1p_1)(k_2p_2)$
177	$(q_1^2-m_t^2)q_2^2(q_3^2-M_W^2)(q_7^2-m_t^2)(q_9^2-m_t^2)q_{10}^2$ $= 0.00127772990\mathbf{3}\epsilon^0$ $0.00144804948\mathbf{2}\epsilon^{-1}$	$(k_1p_1)(k_1p_1)$
178	$(q_1^2-M_W^2)(q_2^2-m_t^2)q_3^2(q_6^2-m_t^2)(q_7^2-M_W^2)q_{11}^2$ $= (0.012288\mathbf{3}+0.013875\mathbf{4}i)\epsilon^0$	$(k_2p_1)(k_2p_1)$
179	$(q_1^2-M_W^2)q_2^2(q_3^2-m_t^2)(q_6^2-m_t^2)(q_7^2-M_W^2)(q_{11}^2-m_t^2)$ $= 0.0047892854\mathbf{2}\epsilon^0$	$(k_2p_1)(k_2p_1)$
180	$(q_1^2-M_W^2)q_2^2(q_3^2-M_W^2)(q_6^2-m_t^2)(q_7^2-M_W^2)(q_{11}^2-M_W^2)$ $= 0.016996762\mathbf{4}3\epsilon^0$	$(k_2p_1)(k_2p_1)$
181	$(q_1^2-M_W^2)q_2^2(q_3^2-m_t^2)(q_4^2-M_W^2)(q_7^2-M_W^2)q_{13}^2$ $= 0.013622145\mathbf{0}5\epsilon^0$ $0.010229740\mathbf{3}4\epsilon^{-1}$	$(k_1p_1)(k_1p_1)$
182	$(q_1^2-M_W^2)q_2^2(q_3^2-m_t^2)(q_4^2-M_W^2)(q_7^2-M_W^2)q_{13}^2$ $= 0.028157999\mathbf{2}8\epsilon^0$ $0.024467234932\mathbf{5}\epsilon^{-1}$	$(k_1p_1)(k_2p_2)$
183	$(q_1^2-M_W^2)q_2^2(q_3^2-m_t^2)(q_7^2-M_W^2)(q_9^2-M_W^2)q_{10}^2$ $= 0.020162453\mathbf{3}3\epsilon^0$ $0.01274674018\mathbf{5}\epsilon^{-1}$	$(k_1p_1)(k_1p_1)$
184	$(q_1^2-M_W^2)q_2^2(q_3^2-M_W^2)(q_4^2-m_t^2)(q_7^2-M_W^2)q_{13}^2$ $= 0.024698049\mathbf{5}4\epsilon^0$ $0.02680945122\mathbf{5}\epsilon^{-1}$	$(k_1p_1)(k_2p_2)$
185	$(q_1^2-M_W^2)q_2^2(q_3^2-M_W^2)(q_7^2-M_W^2)(q_9^2-m_t^2)q_{10}^2$ $= 0.008054326\mathbf{4}2\epsilon^0$ $0.00804540174\mathbf{5}\epsilon^{-1}$	$(k_1p_1)(k_1p_1)$
186	$(q_1^2-m_t^2)q_2^2(q_3^2-m_t^2)(q_4^2-M_W^2)(q_7^2-m_t^2)q_{13}^2$ $= 0.016021046\mathbf{7}8\epsilon^0$ $0.0072051895737\mathbf{5}\epsilon^{-1}$	$(k_1p_1)(k_1p_1)(k_2p_2)$

187	$(q_1^2-m_t^2)q_2^2(q_3^2-m_t^2)(q_4^2-M_W^2)(q_7^2-m_t^2)q_{13}^2$ $= 0.0161165077\mathbf{7}\epsilon^0$ $0.007646966767\mathbf{5}\epsilon^{-1}$	$(k_1p_1)(k_2p_2)(k_2p_2)$
188	$(q_1^2-m_t^2)q_2^2(q_3^2-M_W^2)(q_7^2-m_t^2)(q_9^2-m_t^2)q_{10}^2$ $= 0.000446055492\mathbf{5}\epsilon^0$ $0.0004517077987\mathbf{5}\epsilon^{-1}$	$(k_1p_1)(k_1p_1)(k_1p_1)$
189	$(q_1^2-M_W^2)q_2^2(q_3^2-M_W^2)(q_6^2-m_t^2)(q_7^2-M_W^2)(q_{11}^2-M_W^2)$ $= 0.005523816\mathbf{6}\epsilon^0$	$(k_2p_1)(k_2p_1)(k_2p_1)$
190	$(q_1^2-M_W^2)q_2^2(q_3^2-m_t^2)(q_4^2-M_W^2)(q_7^2-M_W^2)q_{13}^2$ $= 0.011259076\mathbf{2}\epsilon^0$ $0.014215601837\mathbf{5}\epsilon^{-1}$	$(k_1p_1)(k_1p_1)(k_2p_2)$
191	$(q_1^2-M_W^2)q_2^2(q_3^2-m_t^2)(q_7^2-M_W^2)(q_9^2-M_W^2)q_{10}^2$ $= 0.007321121\mathbf{2}7\epsilon^0$ $0.004504456298\mathbf{7}\epsilon^{-1}$	$(k_1p_1)(k_1p_1)(k_1p_1)$
192	$(q_1^2-m_t^2)(q_2^2-M_W^2)q_3^2q_9^2(q_{12}^2-M_W^2)$ $= 0.1093308568\mathbf{3}\epsilon^0$ $0.0673923107\mathbf{5}\epsilon^{-1}$	k_1p_2
193	$(q_1^2-m_t^2)(q_2^2-M_W^2)q_3^2q_4^2(q_6^2-M_W^2)$ $= 0.14083107250\mathbf{4}\epsilon^0$ $0.084500127\mathbf{8}\epsilon^{-1}$	k_2p_2
194	$(q_1^2-m_t^2)q_2^2(q_3^2-m_t^2)(q_4^2-M_W^2)(q_6^2-M_W^2)$ $= 0.1453282089\mathbf{5}\epsilon^0$	k_1p_2
195	$(q_1^2-m_t^2)(q_2^2-M_W^2)q_3^2(q_8^2-M_W^2)q_9^2$ $= 0.14083107250\mathbf{4}\epsilon^0$ $0.084500127\mathbf{8}\epsilon^{-1}$	k_2p_1
196	$(q_1^2-m_t^2)q_2^2(q_3^2-m_t^2)(q_8^2-M_W^2)(q_9^2-M_W^2)$ $= 0.1453282089\mathbf{5}\epsilon^0$	k_1p_1
197	$(q_1^2-M_W^2)q_2^2(q_3^2-M_W^2)(q_7^2-M_W^2)(q_{11}^2-M_W^2)$ $= 0.422761740\mathbf{9}\epsilon^0$	k_2p_1
198	$(q_1^2-m_t^2)(q_2^2-m_t^2)q_3^2q_9^2(q_{12}^2-M_W^2)$ $= 0.032754688017\mathbf{5}\epsilon^0$ $0.017582652317\mathbf{5}\epsilon^{-1}$	$(k_2p_1)(k_2p_1)$
199	$(q_1^2-m_t^2)(q_2^2-M_W^2)q_3^2q_9^2(q_{12}^2-M_W^2)$ $= 0.0152318412\mathbf{8}\epsilon^0$ $0.030394618\mathbf{6}5\epsilon^{-1}$	$(k_2p_1)(k_2p_1)$
200	$(q_1^2-m_t^2)(q_2^2-m_t^2)q_3^2q_4^2(q_5^2-M_W^2)$ $= 0.03275468801\mathbf{7}\epsilon^0$ $0.017582652317\mathbf{5}\epsilon^{-1}$	$(k_2p_2)(k_2p_2)$
201	$(q_1^2-m_t^2)(q_2^2-M_W^2)q_3^2q_4^2(q_5^2-M_W^2)$ $= 0.0152318412\mathbf{8}\epsilon^0$ $0.030394618\mathbf{6}5\epsilon^{-1}$	$(k_2p_2)(k_2p_2)$
202	$(q_1^2-m_t^2)q_2^2(q_3^2-m_t^2)(q_4^2-M_W^2)(q_5^2-M_W^2)$ $= 0.032692999\mathbf{2}\epsilon^0$	$(k_1p_1)(k_1p_1)$

203	$(q_1^2-m_t^2)q_2^2(q_3^2-m_t^2)(q_4^2-M_W^2)(q_5^2-M_W^2)$ $= 0.0326929992\epsilon^0$	$(k_2p_2)(k_2p_2)$
204	$(q_1^2-m_t^2)(q_2^2-M_W^2)q_3^2q_4^2(q_7^2-m_t^2)$ $= 0.041780579692\mathbf{5}\epsilon^0$ $0.017647880777\mathbf{5}\epsilon^{-1}$	$(k_2p_2)(k_2p_2)$
205	$(q_1^2-m_t^2)(q_2^2-M_W^2)q_3^2(q_7^2-m_t^2)q_9^2$ $= 0.041780579692\mathbf{5}\epsilon^0$ $0.017647880777\mathbf{5}\epsilon^{-1}$	$(k_2p_1)(k_2p_1)$
206	$(q_1^2-m_t^2)q_2^2(q_3^2-m_t^2)(q_4^2-M_W^2)(q_7^2-m_t^2)$ $= 0.03421363739\mathbf{9}\epsilon^0$	$(k_2p_2)(k_2p_2)$
207	$(q_1^2-m_t^2)q_2^2(q_3^2-m_t^2)(q_7^2-m_t^2)(q_9^2-M_W^2)$ $= 0.03421363739\mathbf{9}\epsilon^0$	$(k_2p_1)(k_2p_1)$
208	$(q_1^2-M_W^2)(q_2^2-m_t^2)q_3^2q_9^2(q_{12}^2-m_t^2)$ $= 0.02737539051\mathbf{5}\epsilon^0$ $0.007165432527\mathbf{5}\epsilon^{-1}$	$(k_1p_2)(k_1p_2)$
209	$(q_1^2-M_W^2)(q_2^2-M_W^2)q_3^2q_9^2(q_{12}^2-m_t^2)$ $= 0.029973346732\mathbf{5}\epsilon^0$ $0.009188071\mathbf{8}\epsilon^{-1}$	$(k_1p_2)(k_1p_2)$
210	$(q_1^2-M_W^2)(q_2^2-M_W^2)q_3^2q_9^2(q_{12}^2-m_t^2)$ $= 0.019122565\mathbf{4}\epsilon^0$ $0.02917897642\mathbf{5}\epsilon^{-1}$	$(k_2p_1)(k_2p_1)$
211	$(q_1^2-M_W^2)(q_2^2-M_W^2)q_3^2q_4^2(q_5^2-m_t^2)$ $= 0.019122565\mathbf{4}\epsilon^0$ $0.02917897642\mathbf{5}\epsilon^{-1}$	$(k_2p_2)(k_2p_2)$
212	$(q_1^2-M_W^2)q_2^2(q_3^2-M_W^2)(q_4^2-m_t^2)(q_5^2-m_t^2)$ $= 0.02093851087\mathbf{2}\epsilon^0$	$(k_1p_1)(k_1p_1)$
213	$(q_1^2-M_W^2)q_2^2(q_3^2-M_W^2)(q_4^2-m_t^2)(q_5^2-m_t^2)$ $= 0.02093851087\mathbf{2}\epsilon^0$	$(k_2p_2)(k_2p_2)$
214	$(q_1^2-M_W^2)(q_2^2-m_t^2)q_3^2q_4^2(q_7^2-M_W^2)$ $= 0.04768685551\mathbf{2}\epsilon^0$ $0.03164490152\mathbf{5}\epsilon^{-1}$	$(k_2p_2)(k_2p_2)$
215	$(q_1^2-M_W^2)(q_2^2-M_W^2)q_3^2q_4^2(q_7^2-M_W^2)$ $= 0.00395157932\mathbf{5}\epsilon^0$ $0.062511518\mathbf{3}\epsilon^{-1}$	$(k_2p_2)(k_2p_2)$
216	$(q_1^2-M_W^2)(q_2^2-m_t^2)q_3^2(q_7^2-M_W^2)q_9^2$ $= 0.04768685551\mathbf{2}\epsilon^0$ $0.03164490152\mathbf{5}\epsilon^{-1}$	$(k_2p_1)(k_2p_1)$
217	$(q_1^2-M_W^2)(q_2^2-M_W^2)q_3^2(q_7^2-M_W^2)q_9^2$ $= 0.00395157932\mathbf{5}\epsilon^0$ $0.062511518\mathbf{3}\epsilon^{-1}$	$(k_2p_1)(k_2p_1)$
218	$(q_1^2-M_W^2)q_2^2(q_3^2-M_W^2)(q_4^2-m_t^2)(q_7^2-M_W^2)$ $= 0.056134634\mathbf{65}\epsilon^0$	$(k_2p_2)(k_2p_2)$

219	$(q_1^2 - M_W^2)q_2^2(q_3^2 - M_W^2)(q_7^2 - M_W^2)(q_9^2 - m_t^2)$ $= 0.05613463465\epsilon^0$	$(k_2p_1)(k_2p_1)$
220	$(q_1^2 - M_W^2)q_2^2(q_3^2 - M_W^2)(q_7^2 - M_W^2)(q_{11}^2 - M_W^2)$ $= 0.11818500547\mathbf{5}\epsilon^0$	$(k_1p_1)(k_2p_1)$
221	$(q_1^2 - m_t^2)(q_2^2 - M_W^2)q_3^2q_4^2(q_6^2 - M_W^2)(q_7^2 - m_t^2)$ $= 0.00076346344\epsilon^0$ $0.0040913063925\epsilon^{-1}$	$(k_2p_2)(k_2p_2)$
222	$(q_1^2 - m_t^2)q_2^2(q_3^2 - m_t^2)(q_4^2 - M_W^2)(q_6^2 - M_W^2)(q_7^2 - m_t^2)$ $= 0.005778651\mathbf{2}\epsilon^0$	$(k_2p_2)(k_2p_2)$
223	$(q_1^2 - m_t^2)(q_2^2 - M_W^2)q_3^2(q_7^2 - m_t^2)(q_8^2 - M_W^2)q_9^2$ $= 0.00076346344\epsilon^0$ $0.0040913063925\epsilon^{-1}$	$(k_2p_1)(k_2p_1)$
224	$(q_1^2 - m_t^2)q_2^2(q_3^2 - m_t^2)(q_7^2 - m_t^2)(q_8^2 - M_W^2)(q_9^2 - M_W^2)$ $= 0.005778651\mathbf{2}\epsilon^0$	$(k_2p_1)(k_2p_1)$
225	$(q_1^2 - M_W^2)(q_2^2 - m_t^2)q_3^2q_4^2(q_6^2 - m_t^2)(q_7^2 - M_W^2)$ $= 0.001652859\mathbf{6}\epsilon^0$ $0.004558827847\epsilon^{-1}$	$(k_2p_2)(k_2p_2)$
226	$(q_1^2 - M_W^2)(q_2^2 - M_W^2)q_3^2q_4^2(q_6^2 - m_t^2)(q_7^2 - M_W^2)$ $= 0.009785369\mathbf{7}\epsilon^0$ $0.010748065782\mathbf{5}\epsilon^{-1}$	$(k_2p_2)(k_2p_2)$
227	$(q_1^2 - M_W^2)q_2^2(q_3^2 - M_W^2)(q_4^2 - m_t^2)(q_6^2 - m_t^2)(q_7^2 - M_W^2)$ $= 0.007889007\mathbf{2}\epsilon^0$	$(k_2p_2)(k_2p_2)$
228	$(q_1^2 - M_W^2)(q_2^2 - m_t^2)q_3^2(q_7^2 - M_W^2)(q_8^2 - m_t^2)q_9^2$ $= 0.001652859\mathbf{6}\epsilon^0$ $0.004558827847\epsilon^{-1}$	$(k_2p_1)(k_2p_1)$
229	$(q_1^2 - M_W^2)(q_2^2 - M_W^2)q_3^2(q_7^2 - M_W^2)(q_8^2 - m_t^2)q_9^2$ $= 0.009785369\mathbf{7}\epsilon^0$ $0.010748065782\mathbf{5}\epsilon^{-1}$	$(k_2p_1)(k_2p_1)$
230	$(q_1^2 - M_W^2)q_2^2(q_3^2 - M_W^2)(q_7^2 - M_W^2)(q_8^2 - m_t^2)(q_9^2 - m_t^2)$ $= 0.007889007\mathbf{2}\epsilon^0$	$(k_2p_1)(k_2p_1)$
231	$(q_1^2 - M_W^2)q_2^2(q_3^2 - m_t^2)(q_4^2 - M_W^2)(q_7^2 - M_W^2)q_{13}^2$ $= 0.017508305\mathbf{8}\epsilon^0$ $0.012746740185\epsilon^{-1}$	$(k_2p_2)(k_2p_2)$
232	$(q_1^2 - M_W^2)q_2^2(q_3^2 - m_t^2)(q_4^2 - M_W^2)(q_7^2 - M_W^2)q_{13}^2$ $= 0.010355198\mathbf{3}\epsilon^0$ $0.015343555575\epsilon^{-1}$	$(k_1p_1)(k_2p_2)(k_2p_2)$

Table 7.5: Integral definitions and numerical results for the class **0hxwxt0z** of $Z \to b\bar{b}$ integrals.

Nr.	denominator	numerator
1	$q_1^2(q_2^2 - M_W^2)(q_3^2 - m_t^2)(q_4^2 - M_W^2)(q_6^2 - M_Z^2)q_7^2$ $= X\epsilon^0$	1

2	$q_1^2(q_2^2-m_t^2)(q_3^2-M_W^2)(q_4^2-m_t^2)(q_6^2-M_Z^2)q_7^2$ $= X\epsilon^0$	1
3	$q_1^2(q_2^2-M_W^2)(q_3^2-m_t^2)q_7^2(q_8^2-M_Z^2)(q_9^2-M_W^2)$ $= X\epsilon^0$	1
4	$q_1^2(q_2^2-m_t^2)(q_3^2-M_W^2)q_7^2(q_8^2-M_Z^2)(q_9^2-m_t^2)$ $= X\epsilon^0$	1
5	$q_1^2(q_2^2-M_W^2)(q_3^2-m_t^2)(q_4^2-M_W^2)q_7^2$ $= (0.22085253 + 0.25097814i)\epsilon^0$	k_1p_1
6	$q_1^2(q_2^2-M_W^2)(q_3^2-m_t^2)(q_4^2-M_W^2)q_7^2$ $= (0.29411983 + 0.28647607i)\epsilon^0$	k_2p_2
7	$q_1^2(q_2^2-M_W^2)(q_3^2-m_t^2)q_7^2(q_9^2-M_W^2)$ $= (0.27483902 + 0.25796125i)\epsilon^0$	k_1p_1
8	$q_1^2(q_2^2-M_W^2)(q_3^2-m_t^2)q_7^2(q_9^2-M_W^2)$ $= (0.29411983 + 0.28647607i)\epsilon^0$	k_2p_1
9	$q_1^2(q_2^2-m_t^2)(q_3^2-M_W^2)(q_4^2-m_t^2)q_7^2$ $= (0.17209324 + 0.15798995i)\epsilon^0$	k_1p_1
10	$q_1^2(q_2^2-m_t^2)(q_3^2-M_W^2)(q_4^2-m_t^2)q_7^2$ $= (0.17879467 + 0.14015077i)\epsilon^0$	k_2p_2
11	$q_1^2(q_2^2-m_t^2)(q_3^2-M_W^2)q_7^2(q_9^2-m_t^2)$ $= (0.19514751 + 0.15924402i)\epsilon^0$	k_1p_1
12	$q_1^2(q_2^2-m_t^2)(q_3^2-M_W^2)q_7^2(q_9^2-m_t^2)$ $= (0.17879467 + 0.14015077i)\epsilon^0$	k_2p_1
13	$(q_1^2-m_t^2)(q_2^2-M_W^2)q_3^2(q_9^2-M_Z^2)(q_{12}^2-M_W^2)$ $= 0.150253544\mathbf{7}\epsilon^0$	k_2p_1
14	$(q_1^2-m_t^2)(q_2^2-M_W^2)q_3^2(q_4^2-M_Z^2)(q_6^2-M_W^2)(q_7^2-m_t^2)$ $= 0.095369979\mathbf{6}\epsilon^0$	1
15	$(q_1^2-m_t^2)(q_2^2-M_Z^2)(q_3^2-m_t^2)(q_4^2-M_W^2)(q_6^2-M_W^2)(q_7^2-m_t^2)$ $= 0.039141888\mathbf{6}\epsilon^0$	1
16	$(q_1^2-m_t^2)(q_2^2-m_t^2)(q_3^2-M_Z^2)q_4^2(q_6^2-M_W^2)(q_7^2-m_t^2)$ $= 0.059962597\mathbf{6}\epsilon^0$	1
17	$(q_1^2-m_t^2)(q_2^2-M_W^2)q_3^2(q_4^2-M_Z^2)(q_6^2-M_W^2)$ $= 0.226733182\mathbf{3}\epsilon^0$	k_1p_2
18	$(q_1^2-m_t^2)(q_2^2-M_W^2)q_3^2(q_4^2-M_Z^2)(q_6^2-M_W^2)$ $= 0.187370513\mathbf{8}\epsilon^0$	k_2p_2
19	$(q_1^2-m_t^2)(q_2^2-M_Z^2)(q_3^2-m_t^2)(q_4^2-M_W^2)(q_6^2-M_W^2)$ $= 0.120965809\mathbf{4}\epsilon^0$	k_1p_2
20	$(q_1^2-m_t^2)(q_2^2-M_W^2)q_3^2(q_4^2-M_Z^2)(q_5^2-M_W^2)$ $= 0.183107939\mathbf{1}\epsilon^0$	k_1p_1
21	$(q_1^2-m_t^2)(q_2^2-M_W^2)q_3^2(q_4^2-M_Z^2)(q_5^2-M_W^2)$ $= 0.150253544\mathbf{7}\epsilon^0$	k_2p_2
22	$(q_1^2-m_t^2)(q_2^2-M_Z^2)(q_3^2-m_t^2)(q_4^2-M_W^2)(q_5^2-M_W^2)$ $= 0.094994472\mathbf{2}\epsilon^0$	k_1p_1

23	$(q_1^2-m_t^2)(q_2^2-M_Z^2)(q_3^2-m_t^2)(q_4^2-M_W^2)(q_5^2-M_W^2)$ $= 0.0949944722\epsilon^0$	k_2p_2
24	$(q_1^2-m_t^2)(q_2^2-M_W^2)q_3^2(q_7^2-m_t^2)(q_8^2-M_W^2)(q_9^2-M_Z^2)$ $= 0.0953699796\epsilon^0$	1
25	$(q_1^2-m_t^2)(q_2^2-M_Z^2)(q_3^2-m_t^2)(q_7^2-m_t^2)(q_8^2-M_W^2)(q_9^2-M_W^2)$ $= 0.0391418896\epsilon^0$	1
26	$(q_1^2-m_t^2)(q_2^2-m_t^2)(q_3^2-M_Z^2)(q_7^2-m_t^2)(q_8^2-M_W^2)q_9^2$ $= 0.0599625976\epsilon^0$	1
27	$(q_1^2-m_t^2)(q_2^2-M_W^2)q_3^2(q_8^2-M_W^2)(q_9^2-M_Z^2)$ $= 0.22673318235\epsilon^0$	k_1p_1
28	$(q_1^2-m_t^2)(q_2^2-M_W^2)q_3^2(q_8^2-M_W^2)(q_9^2-M_Z^2)$ $= 0.187370513855\epsilon^0$	k_2p_1
29	$(q_1^2-m_t^2)(q_2^2-M_Z^2)(q_3^2-m_t^2)(q_8^2-M_W^2)(q_9^2-M_W^2)$ $= 0.120965809\mathbf{4}\epsilon^0$	k_1p_1
30	$(q_1^2-m_t^2)(q_2^2-M_W^2)q_3^2(q_4^2-M_Z^2)(q_7^2-m_t^2)$ $= 0.109873298855\epsilon^0$	k_1p_1
31	$(q_1^2-m_t^2)(q_2^2-M_W^2)q_3^2(q_4^2-M_Z^2)(q_7^2-m_t^2)$ $= 0.133500640455\epsilon^0$	k_2p_2
32	$(q_1^2-m_t^2)(q_2^2-M_W^2)q_3^2(q_7^2-m_t^2)(q_9^2-M_Z^2)$ $= 0.147836550255\epsilon^0$	k_1p_1
33	$(q_1^2-m_t^2)(q_2^2-M_W^2)q_3^2(q_7^2-m_t^2)(q_9^2-M_Z^2)$ $= 0.133500640455\epsilon^0$	k_2p_1
34	$(q_1^2-m_t^2)(q_2^2-M_W^2)q_3^2(q_7^2-m_t^2)q_{11}^2$ $= (0.1937207\mathbf{9}+0.1645789\mathbf{4}i)\epsilon^0$	k_1p_1
35	$(q_1^2-m_t^2)(q_2^2-M_W^2)q_3^2(q_7^2-m_t^2)q_{11}^2$ $= (0.1937207\mathbf{9}+0.1645789\mathbf{3}i)\epsilon^0$	k_2p_1
36	$(q_1^2-m_t^2)(q_2^2-M_Z^2)(q_3^2-m_t^2)(q_4^2-M_W^2)(q_7^2-m_t^2)$ $= 0.062191766255\epsilon^0$	k_1p_1
37	$(q_1^2-m_t^2)(q_2^2-M_Z^2)(q_3^2-m_t^2)(q_4^2-M_W^2)(q_7^2-m_t^2)$ $= 0.09000477\mathbf{1}\epsilon^0$	k_2p_2
38	$(q_1^2-m_t^2)(q_2^2-M_Z^2)(q_3^2-m_t^2)(q_7^2-m_t^2)(q_9^2-M_W^2)$ $= 0.085421494\mathbf{9}\epsilon^0$	k_1p_1
39	$(q_1^2-m_t^2)(q_2^2-M_Z^2)(q_3^2-m_t^2)(q_7^2-m_t^2)(q_9^2-M_W^2)$ $= 0.09000477\mathbf{1}\epsilon^0$	k_2p_1
40	$(q_1^2-m_t^2)(q_2^2-M_Z^2)(q_3^2-m_t^2)(q_7^2-m_t^2)(q_{11}^2-m_t^2)$ $= 0.065133321\mathbf{6}\epsilon^0$	k_1p_1
41	$(q_1^2-m_t^2)q_2^2(q_3^2-M_W^2)(q_4^2-m_t^2)(q_7^2-m_t^2)$ $= 0.069081323\mathbf{3}5\epsilon^0$	k_1p_1
42	$(q_1^2-m_t^2)q_2^2(q_3^2-M_W^2)(q_7^2-m_t^2)(q_9^2-m_t^2)(q_{10}^2-M_Z^2)$ $= 0.048611728\mathbf{8}8\epsilon^0$	1
43	$(q_1^2-m_t^2)q_2^2(q_3^2-M_W^2)(q_7^2-m_t^2)(q_9^2-m_t^2)$ $= 0.091380363\mathbf{5}\epsilon^0$	k_1p_1

44	$(q_1^2-m_t^2)q_2^2(q_3^2-M_W^2)(q_7^2-m_t^2)(q_9^2-m_t^2)$ $= 0.0860035239\epsilon^0$	k_2p_1
45	$(q_1^2-m_t^2)(q_2^2-m_t^2)(q_3^2-M_Z^2)q_4^2(q_7^2-m_t^2)$ $= 0.0904900990\mathbf{5}\epsilon^0$	k_1p_1
46	$(q_1^2-m_t^2)(q_2^2-m_t^2)(q_3^2-M_Z^2)q_4^2(q_7^2-m_t^2)$ $= 0.137620946\epsilon^0$	k_2p_2
47	$(q_1^2-m_t^2)(q_2^2-m_t^2)(q_3^2-M_Z^2)(q_7^2-m_t^2)q_9^2(q_{10}^2-M_W^2)$ $= 0.0486117289\mathbf{1}\epsilon^0$	1
48	$(q_1^2-m_t^2)(q_2^2-m_t^2)(q_3^2-M_Z^2)(q_7^2-m_t^2)q_9^2$ $= 0.127050962\mathbf{5}\epsilon^0$	k_1p_1
49	$(q_1^2-m_t^2)(q_2^2-m_t^2)(q_3^2-M_Z^2)(q_7^2-m_t^2)q_9^2$ $= 0.137620946\epsilon^0$	k_2p_1
50	$(q_1^2-M_W^2)(q_2^2-m_t^2)q_3^2(q_9^2-M_Z^2)(q_{12}^2-m_t^2)$ $= 0.116024242\mathbf{0}\epsilon^0$	k_2p_1
51	$(q_1^2-M_W^2)(q_2^2-m_t^2)q_3^2(q_4^2-M_Z^2)(q_6^2-m_t^2)(q_7^2-M_W^2)$ $= 0.1267665\mathbf{4}\epsilon^0$	1
52	$(q_1^2-M_W^2)(q_2^2-M_Z^2)(q_3^2-M_W^2)(q_4^2-m_t^2)(q_6^2-m_t^2)(q_7^2-M_W^2)$ $= 0.082234549\mathbf{6}\epsilon^0$	1
53	$(q_1^2-M_W^2)(q_2^2-M_W^2)(q_3^2-M_Z^2)q_4^2(q_6^2-m_t^2)(q_7^2-M_W^2)$ $= 0.213763027\mathbf{4}\epsilon^0$	1
54	$(q_1^2-M_W^2)(q_2^2-m_t^2)q_3^2(q_4^2-M_Z^2)(q_6^2-m_t^2)$ $= 0.137844062\mathbf{8}\epsilon^0$	k_1p_2
55	$(q_1^2-M_W^2)(q_2^2-m_t^2)q_3^2(q_4^2-M_Z^2)(q_6^2-m_t^2)$ $= 0.134514131\mathbf{6}\epsilon^0$	k_2p_2
56	$(q_1^2-M_W^2)(q_2^2-m_t^2)q_3^2(q_4^2-M_Z^2)(q_5^2-m_t^2)$ $= 0.108165638\mathbf{2}\epsilon^0$	k_1p_1
57	$(q_1^2-M_W^2)(q_2^2-m_t^2)q_3^2(q_4^2-M_Z^2)(q_5^2-m_t^2)$ $= 0.116024242\mathbf{0}\epsilon^0$	k_2p_2
58	$(q_1^2-M_W^2)(q_2^2-M_Z^2)(q_3^2-M_W^2)(q_4^2-m_t^2)(q_5^2-m_t^2)$ $= 0.073807384\mathbf{0}\epsilon^0$	k_1p_1
59	$(q_1^2-M_W^2)(q_2^2-M_Z^2)(q_3^2-M_W^2)(q_4^2-m_t^2)(q_5^2-m_t^2)$ $= 0.073807384\mathbf{0}\epsilon^0$	k_2p_2
60	$(q_1^2-M_W^2)(q_2^2-m_t^2)q_3^2(q_7^2-M_W^2)(q_8^2-m_t^2)(q_9^2-M_Z^2)$ $= 0.1267665\mathbf{4}\epsilon^0$	1
61	$(q_1^2-M_W^2)(q_2^2-M_Z^2)(q_3^2-M_W^2)(q_7^2-M_W^2)(q_8^2-m_t^2)(q_9^2-m_t^2)$ $= 0.082234549\mathbf{6}\epsilon^0$	1
62	$(q_1^2-M_W^2)(q_2^2-M_W^2)(q_3^2-M_Z^2)(q_7^2-M_W^2)(q_8^2-m_t^2)q_9^2$ $= 0.213763027\mathbf{4}\epsilon^0$	1
63	$(q_1^2-M_W^2)(q_2^2-m_t^2)q_3^2(q_8^2-m_t^2)(q_9^2-M_Z^2)$ $= 0.137844062\mathbf{8}\epsilon^0$	k_1p_1
64	$(q_1^2-M_W^2)(q_2^2-m_t^2)q_3^2(q_8^2-m_t^2)(q_9^2-M_Z^2)$ $= 0.134514131\mathbf{6}\epsilon^0$	k_2p_1

65	$(q_1^2-M_W^2)(q_2^2-m_t^2)q_3^2(q_4^2-M_Z^2)(q_7^2-M_W^2)$ $= 0.215587435\mathbf{95}\epsilon^0$	k_1p_1
66	$(q_1^2-M_W^2)(q_2^2-m_t^2)q_3^2(q_4^2-M_Z^2)(q_7^2-M_W^2)$ $= 0.221748765\mathbf{2}\epsilon^0$	k_2p_2
67	$(q_1^2-M_W^2)(q_2^2-m_t^2)q_3^2(q_7^2-M_W^2)(q_9^2-M_Z^2)$ $= 0.254210572\mathbf{65}\epsilon^0$	k_1p_1
68	$(q_1^2-M_W^2)(q_2^2-m_t^2)q_3^2(q_7^2-M_W^2)(q_9^2-M_Z^2)$ $= 0.221748765\mathbf{2}\epsilon^0$	k_2p_1
69	$(q_1^2-M_W^2)(q_2^2-m_t^2)q_3^2(q_7^2-M_W^2)q_{11}^2$ $= (0.325515\mathbf{8}+0.294598\mathbf{6}\mathbf{3}i)\epsilon^0$	k_1p_1
70	$(q_1^2-M_W^2)(q_2^2-m_t^2)q_3^2(q_7^2-M_W^2)q_{11}^2$ $= (0.325515\mathbf{8}+0.294598\mathbf{6}\mathbf{3}i)\epsilon^0$	k_2p_1
71	$(q_1^2-M_W^2)q_2^2(q_3^2-m_t^2)(q_4^2-M_W^2)(q_7^2-M_W^2)(q_{13}^2-M_Z^2)$ $= 0.181368892\mathbf{6}\epsilon^0$	1
72	$(q_1^2-M_W^2)q_2^2(q_3^2-m_t^2)(q_4^2-M_W^2)(q_7^2-M_W^2)$ $= 0.174134842\mathbf{7}\epsilon^0$	k_1p_1
73	$(q_1^2-M_W^2)q_2^2(q_3^2-m_t^2)(q_7^2-M_W^2)(q_9^2-M_W^2)(q_{10}^2-M_Z^2)$ $= 0.181368892\mathbf{6}\epsilon^0$	1
74	$(q_1^2-M_W^2)q_2^2(q_3^2-m_t^2)(q_7^2-M_W^2)(q_9^2-M_W^2)$ $= 0.227131820\mathbf{65}\epsilon^0$	k_1p_1
75	$(q_1^2-M_W^2)(q_2^2-M_Z^2)(q_3^2-M_W^2)(q_4^2-m_t^2)(q_7^2-M_W^2)$ $= 0.143719276\mathbf{8}\epsilon^0$	k_1p_1
76	$(q_1^2-M_W^2)(q_2^2-M_Z^2)(q_3^2-M_W^2)(q_4^2-m_t^2)(q_7^2-M_W^2)$ $= 0.156035821\mathbf{65}\epsilon^0$	k_2p_2
77	$(q_1^2-M_W^2)(q_2^2-M_Z^2)(q_3^2-M_W^2)(q_7^2-M_W^2)(q_9^2-m_t^2)$ $= 0.169839065\mathbf{1}\epsilon^0$	k_1p_1
78	$(q_1^2-M_W^2)(q_2^2-M_Z^2)(q_3^2-M_W^2)(q_7^2-M_W^2)(q_9^2-m_t^2)$ $= 0.156035821\mathbf{65}\epsilon^0$	k_2p_1
79	$(q_1^2-M_W^2)(q_2^2-M_Z^2)(q_3^2-M_W^2)(q_7^2-M_W^2)(q_{11}^2-M_W^2)$ $= 0.300337556\mathbf{6}\epsilon^0$	k_1p_1
80	$(q_1^2-M_W^2)(q_2^2-M_W^2)(q_3^2-M_Z^2)q_4^2(q_7^2-M_W^2)(q_{13}^2-m_t^2)$ $= 0.181368892\mathbf{6}\epsilon^0$	1
81	$(q_1^2-M_W^2)(q_2^2-M_W^2)(q_3^2-M_Z^2)q_4^2(q_7^2-M_W^2)$ $= 0.302430184\mathbf{95}\epsilon^0$	k_1p_1
82	$(q_1^2-M_W^2)(q_2^2-M_W^2)(q_3^2-M_Z^2)q_4^2(q_7^2-M_W^2)$ $= 0.455461102\mathbf{2}\epsilon^0$	k_2p_2
83	$(q_1^2-M_W^2)(q_2^2-M_W^2)(q_3^2-M_Z^2)(q_7^2-M_W^2)q_9^2(q_{10}^2-m_t^2)$ $= 0.181368892\mathbf{6}\epsilon^0$	1
84	$(q_1^2-M_W^2)(q_2^2-M_W^2)(q_3^2-M_Z^2)(q_7^2-M_W^2)q_9^2$ $= 0.409684584\mathbf{95}\epsilon^0$	k_1p_1
85	$(q_1^2-M_W^2)(q_2^2-M_W^2)(q_3^2-M_Z^2)(q_7^2-M_W^2)q_9^2$ $= 0.455461102\mathbf{2}\epsilon^0$	k_2p_1

86	$(q_1^2 - M_Z^2)(q_2^2 - m_t^2)(q_3^2 - m_t^2)(q_9^2 - M_W^2)q_{12}^2$ $= \quad 0.16252798845\epsilon^0$	k_1p_2
87	$(q_1^2 - M_Z^2)(q_2^2 - m_t^2)(q_3^2 - m_t^2)(q_9^2 - M_W^2)q_{12}^2$ $= \quad 0.14067475285\epsilon^0$	k_2p_1
88	$(q_1^2 - M_Z^2)(q_2^2 - M_W^2)(q_3^2 - M_W^2)(q_9^2 - m_t^2)q_{12}^2$ $= \quad 0.21998209975\epsilon^0$	k_1p_2
89	$(q_1^2 - M_Z^2)(q_2^2 - M_W^2)(q_3^2 - M_W^2)(q_9^2 - m_t^2)q_{12}^2$ $= \quad 0.13580057099\epsilon^0$	k_2p_1
90	$(q_1^2 - M_Z^2)(q_2^2 - m_t^2)(q_3^2 - m_t^2)(q_4^2 - M_W^2)q_5^2$ $= \quad 0.16252798845\epsilon^0$	k_1p_1
91	$(q_1^2 - M_Z^2)(q_2^2 - m_t^2)(q_3^2 - m_t^2)(q_4^2 - M_W^2)q_5^2$ $= \quad 0.14067475285\epsilon^0$	k_2p_2
92	$(q_1^2 - M_Z^2)(q_2^2 - M_W^2)(q_3^2 - M_W^2)(q_4^2 - m_t^2)q_5^2$ $= \quad 0.21998209975\epsilon^0$	k_1p_1
93	$(q_1^2 - M_Z^2)(q_2^2 - M_W^2)(q_3^2 - M_W^2)(q_4^2 - m_t^2)q_5^2$ $= \quad 0.13580057099\epsilon^0$	k_2p_2
94	$q_1^2(q_2^2 - M_W^2)(q_3^2 - m_t^2)(q_4^2 - M_W^2)(q_6^2 - M_Z^2)q_7^2$ $= \quad X\epsilon^0$	k_2p_2
95	$q_1^2(q_2^2 - M_W^2)(q_3^2 - m_t^2)(q_6^2 - M_Z^2)q_7^2(q_{11}^2 - m_t^2)$ $= \quad (0.023446\mathbf{8} - 0.108759\mathbf{6}i)\epsilon^0$	k_2p_1
96	$q_1^2(q_2^2 - m_t^2)(q_3^2 - M_W^2)(q_4^2 - m_t^2)(q_6^2 - M_Z^2)q_7^2$ $= \quad X\epsilon^0$	k_2p_2
97	$q_1^2(q_2^2 - m_t^2)(q_3^2 - M_W^2)(q_6^2 - M_Z^2)q_7^2(q_{11}^2 - M_W^2)$ $= \quad (0.045562\mathbf{1} - 0.198713\mathbf{6}i)\epsilon^0$	k_2p_1
98	$q_1^2(q_2^2 - M_W^2)(q_3^2 - m_t^2)q_7^2(q_8^2 - M_Z^2)(q_9^2 - M_W^2)$ $= \quad X\epsilon^0$	k_2p_1
99	$q_1^2(q_2^2 - m_t^2)(q_3^2 - M_W^2)q_7^2(q_8^2 - M_Z^2)(q_9^2 - m_t^2)$ $= \quad X\epsilon^0$	k_2p_1
100	$q_1^2(q_2^2 - M_W^2)(q_3^2 - m_t^2)(q_4^2 - M_W^2)q_7^2$ $= \quad (0.121908 - 0.0625\mathbf{3}i)\epsilon^0$ $\quad 0.0625\epsilon^{-1}$	$(k_1p_1)(k_2p_2)$
101	$q_1^2(q_2^2 - M_W^2)(q_3^2 - m_t^2)(q_4^2 - M_W^2)q_7^2$ $= \quad (0.098177\mathbf{57} - 0.094730\mathbf{77}i)\epsilon^0$	$(k_2p_2)(k_2p_2)$
102	$q_1^2(q_2^2 - M_W^2)(q_3^2 - m_t^2)q_7^2(q_9^2 - M_W^2)$ $= \quad (0.085817\mathbf{96} - 0.080687\mathbf{41}i)\epsilon^0$	$(k_1p_1)(k_2p_1)$
103	$q_1^2(q_2^2 - M_W^2)(q_3^2 - m_t^2)q_7^2(q_9^2 - M_W^2)$ $= \quad (0.098177\mathbf{57} - 0.094730\mathbf{77}i)\epsilon^0$	$(k_2p_1)(k_2p_1)$
104	$q_1^2(q_2^2 - m_t^2)(q_3^2 - M_W^2)(q_4^2 - m_t^2)q_7^2$ $= \quad (0.054390\mathbf{61} - 0.052559\mathbf{75}i)\epsilon^0$	$(k_1p_1)(k_1p_1)$
105	$q_1^2(q_2^2 - m_t^2)(q_3^2 - M_W^2)(q_4^2 - m_t^2)q_7^2$ $= \quad (0.193706 - 0.031023i)\epsilon^0$ $\quad 0.0625\epsilon^{-1}$	$(k_1p_1)(k_2p_2)$

106	$q_1^2(q_2^2-m_t^2)(q_3^2-M_W^2)(q_4^2-m_t^2)q_7^2$ $= (0.052852618-0.040114052i)\epsilon^0$	$(k_2p_2)(k_2p_2)$
107	$q_1^2(q_2^2-m_t^2)(q_3^2-M_W^2)q_7^2(q_9^2-m_t^2)$ $= (0.064527507-0.053186613i)\epsilon^0$	$(k_1p_1)(k_1p_1)$
108	$q_1^2(q_2^2-m_t^2)(q_3^2-M_W^2)q_7^2(q_9^2-m_t^2)$ $= (0.050031079-0.039095478i)\epsilon^0$	$(k_1p_1)(k_2p_1)$
109	$q_1^2(q_2^2-m_t^2)(q_3^2-M_W^2)q_7^2(q_9^2-m_t^2)$ $= (0.052852618-0.040114052i)\epsilon^0$	$(k_2p_1)(k_2p_1)$
110	$(q_1^2-m_t^2)(q_2^2-M_W^2)q_3^2(q_9^2-M_Z^2)(q_{12}^2-M_W^2)$ $= 0.072972505410\epsilon^0$ $0.06250\epsilon^{-1}$	$(k_1p_2)(k_2p_1)$
111	$(q_1^2-m_t^2)(q_2^2-M_W^2)q_3^2(q_4^2-M_Z^2)(q_6^2-M_W^2)(q_7^2-m_t^2)$ $= 0.021241458680\epsilon^0$	k_2p_2
112	$(q_1^2-m_t^2)(q_2^2-M_Z^2)(q_3^2-m_t^2)(q_4^2-M_W^2)(q_6^2-M_W^2)(q_7^2-m_t^2)$ $= 0.012075556650\epsilon^0$	k_2p_2
113	$(q_1^2-m_t^2)(q_2^2-M_Z^2)(q_3^2-m_t^2)(q_6^2-M_W^2)(q_7^2-m_t^2)(q_{11}^2-m_t^2)$ $= 0.0060244697450\epsilon^0$	k_2p_1
114	$(q_1^2-m_t^2)(q_2^2-m_t^2)(q_3^2-M_Z^2)q_4^2(q_6^2-M_W^2)(q_7^2-m_t^2)$ $= 0.018514746070\epsilon^0$	k_2p_2
115	$(q_1^2-m_t^2)(q_2^2-M_W^2)q_3^2(q_4^2-M_Z^2)(q_5^2-M_W^2)$ $= 0.053232106750\epsilon^0$	$(k_1p_1)(k_1p_1)$
116	$(q_1^2-m_t^2)(q_2^2-M_W^2)q_3^2(q_4^2-M_Z^2)(q_5^2-M_W^2)$ $= 0.072972505410\epsilon^0$ $0.06250\epsilon^{-1}$	$(k_1p_1)(k_2p_2)$
117	$(q_1^2-m_t^2)(q_2^2-M_Z^2)(q_3^2-m_t^2)(q_4^2-M_W^2)(q_5^2-M_W^2)$ $= 0.146612005870\epsilon^0$ $0.06250\epsilon^{-1}$	$(k_1p_1)(k_2p_2)$
118	$(q_1^2-m_t^2)(q_2^2-M_W^2)q_3^2(q_7^2-m_t^2)(q_8^2-M_W^2)(q_9^2-M_Z^2)$ $= 0.021241458680\epsilon^0$	k_2p_1
119	$(q_1^2-m_t^2)(q_2^2-M_Z^2)(q_3^2-m_t^2)(q_7^2-m_t^2)(q_8^2-M_W^2)(q_9^2-M_W^2)$ $= 0.012075556650\epsilon^0$	k_2p_1
120	$(q_1^2-m_t^2)(q_2^2-m_t^2)(q_3^2-M_Z^2)(q_7^2-m_t^2)(q_8^2-M_W^2)q_9^2$ $= 0.018514746070\epsilon^0$	k_2p_1
121	$(q_1^2-m_t^2)(q_2^2-M_W^2)q_3^2(q_4^2-M_Z^2)(q_7^2-m_t^2)$ $= 0.028466059325\epsilon^0$	$(k_1p_1)(k_1p_1)$
122	$(q_1^2-m_t^2)(q_2^2-M_W^2)q_3^2(q_4^2-M_Z^2)(q_7^2-m_t^2)$ $= 0.167514166\epsilon^0$ $0.06250\epsilon^{-1}$	$(k_1p_1)(k_2p_2)$
123	$(q_1^2-m_t^2)(q_2^2-M_W^2)q_3^2(q_7^2-m_t^2)(q_9^2-M_Z^2)$ $= 0.043972280625\epsilon^0$	$(k_1p_1)(k_1p_1)$
124	$(q_1^2-m_t^2)(q_2^2-M_W^2)q_3^2(q_7^2-m_t^2)(q_9^2-M_Z^2)$ $= 0.036558278\epsilon^0$	$(k_1p_1)(k_2p_1)$

125	$(q_1^2-m_t^2)(q_2^2-M_Z^2)(q_3^2-m_t^2)(q_4^2-M_W^2)(q_7^2-m_t^2)$ $= 0.016849912472\epsilon^0$	$(k_1p_1)(k_1p_1)$
126	$(q_1^2-m_t^2)(q_2^2-M_Z^2)(q_3^2-m_t^2)(q_4^2-M_W^2)(q_7^2-m_t^2)$ $= 0.212353653120\epsilon^0$ $0.06250\epsilon^{-1}$	$(k_1p_1)(k_2p_2)$
127	$(q_1^2-m_t^2)(q_2^2-M_Z^2)(q_3^2-m_t^2)(q_4^2-M_W^2)(q_7^2-m_t^2)$ $= 0.029726438350\epsilon^0$	$(k_2p_2)(k_2p_2)$
128	$(q_1^2-m_t^2)(q_2^2-M_Z^2)(q_3^2-m_t^2)(q_7^2-m_t^2)(q_9^2-M_W^2)$ $= 0.026999738250\epsilon^0$	$(k_1p_1)(k_1p_1)$
129	$(q_1^2-m_t^2)(q_2^2-M_Z^2)(q_3^2-m_t^2)(q_7^2-m_t^2)(q_9^2-M_W^2)$ $= 0.025769447\mathbf{4}\epsilon^0$	$(k_1p_1)(k_2p_1)$
130	$(q_1^2-m_t^2)(q_2^2-M_Z^2)(q_3^2-m_t^2)(q_7^2-m_t^2)(q_9^2-M_W^2)$ $= 0.029726438350\epsilon^0$	$(k_2p_1)(k_2p_1)$
131	$(q_1^2-m_t^2)q_2^2(q_3^2-M_W^2)(q_4^2-m_t^2)(q_7^2-m_t^2)$ $= 0.018334930409\epsilon^0$	$(k_1p_1)(k_1p_1)$
132	$(q_1^2-m_t^2)q_2^2(q_3^2-M_W^2)(q_4^2-m_t^2)(q_7^2-m_t^2)$ $= 0.173765037250\epsilon^0$ $0.06250\epsilon^{-1}$	$(k_1p_1)(k_2p_2)$
133	$(q_1^2-m_t^2)q_2^2(q_3^2-M_W^2)(q_7^2-m_t^2)(q_9^2-m_t^2)(q_{10}^2-M_Z^2)$ $= 0.011010855507\epsilon^0$	k_1p_1
134	$(q_1^2-m_t^2)q_2^2(q_3^2-M_W^2)(q_7^2-m_t^2)(q_9^2-m_t^2)$ $= 0.027528747450\epsilon^0$	$(k_1p_1)(k_1p_1)$
135	$(q_1^2-m_t^2)q_2^2(q_3^2-M_W^2)(q_7^2-m_t^2)(q_9^2-m_t^2)$ $= 0.0237541682775\epsilon^0$	$(k_1p_1)(k_2p_1)$
136	$(q_1^2-m_t^2)(q_2^2-m_t^2)(q_3^2-M_Z^2)q_4^2(q_7^2-m_t^2)$ $= 0.024292587\mathbf{6}\epsilon^0$	$(k_1p_1)(k_1p_1)$
137	$(q_1^2-m_t^2)(q_2^2-m_t^2)(q_3^2-M_Z^2)q_4^2(q_7^2-m_t^2)$ $= 0.233133395\mathbf{6}2\epsilon^0$ $0.06250\epsilon^{-1}$	$(k_1p_1)(k_2p_2)$
138	$(q_1^2-m_t^2)(q_2^2-m_t^2)(q_3^2-M_Z^2)q_4^2(q_7^2-m_t^2)$ $= 0.047733428750\epsilon^0$	$(k_2p_2)(k_2p_2)$
139	$(q_1^2-m_t^2)(q_2^2-m_t^2)(q_3^2-M_Z^2)(q_7^2-m_t^2)q_9^2(q_{10}^2-M_W^2)$ $= 0.013484019\mathbf{7}7\epsilon^0$	k_1p_1
140	$(q_1^2-m_t^2)(q_2^2-m_t^2)(q_3^2-M_Z^2)(q_7^2-m_t^2)q_9^2$ $= 0.040406387250\epsilon^0$	$(k_1p_1)(k_1p_1)$
141	$(q_1^2-m_t^2)(q_2^2-m_t^2)(q_3^2-M_Z^2)(q_7^2-m_t^2)q_9^2$ $= 0.039412211425\epsilon^0$	$(k_1p_1)(k_2p_1)$
142	$(q_1^2-m_t^2)(q_2^2-m_t^2)(q_3^2-M_Z^2)(q_7^2-m_t^2)q_9^2$ $= 0.047733428750\epsilon^0$	$(k_2p_1)(k_2p_1)$
143	$(q_1^2-M_W^2)(q_2^2-m_t^2)q_3^2(q_9^2-M_Z^2)(q_{12}^2-m_t^2)$ $= 0.161673002\mathbf{5}\epsilon^0$ $0.06250\epsilon^{-1}$	$(k_1p_2)(k_2p_1)$

144	$(q_1^2-M_W^2)(q_2^2-m_t^2)q_3^2(q_9^2-M_Z^2)(q_{12}^2-m_t^2)$ $= \quad 0.03188551332\mathbf{5}\epsilon^0$	$(k_2p_1)(k_2p_1)$
145	$(q_1^2-M_W^2)(q_2^2-m_t^2)q_3^2(q_4^2-M_Z^2)(q_6^2-m_t^2)(q_7^2-M_W^2)$ $= \quad 0.027203280\mathbf{1}\epsilon^0$	k_2p_2
146	$(q_1^2-M_W^2)(q_2^2-M_Z^2)(q_3^2-M_W^2)(q_4^2-m_t^2)(q_6^2-m_t^2)(q_7^2-M_W^2)$ $= \quad 0.019388606\mathbf{1}7\epsilon^0$	k_2p_2
147	$(q_1^2-M_W^2)(q_2^2-M_Z^2)(q_3^2-M_W^2)(q_6^2-m_t^2)(q_7^2-M_W^2)(q_{11}^2-M_W^2)$ $= \quad 0.037033338\mathbf{2}5\epsilon^0$	k_2p_1
148	$(q_1^2-M_W^2)(q_2^2-M_W^2)(q_3^2-M_Z^2)q_4^2(q_6^2-m_t^2)(q_7^2-M_W^2)$ $= \quad 0.066266\mathbf{1}90\mathbf{3}\epsilon^0$	k_2p_2
149	$(q_1^2-M_W^2)(q_2^2-m_t^2)q_3^2(q_4^2-M_Z^2)(q_5^2-m_t^2)$ $= \quad 0.02765820\mathbf{4}92\mathbf{5}\epsilon^0$	$(k_1p_1)(k_1p_1)$
150	$(q_1^2-M_W^2)(q_2^2-m_t^2)q_3^2(q_4^2-M_Z^2)(q_5^2-m_t^2)$ $= \quad 0.161673002\mathbf{5}\epsilon^0$ $\quad\quad 0.062\mathbf{5}\epsilon^{-1}$	$(k_1p_1)(k_2p_2)$
151	$(q_1^2-M_W^2)(q_2^2-m_t^2)q_3^2(q_4^2-M_Z^2)(q_5^2-m_t^2)$ $= \quad 0.03188551332\mathbf{5}\epsilon^0$	$(k_2p_2)(k_2p_2)$
152	$(q_1^2-M_W^2)(q_2^2-M_Z^2)(q_3^2-M_W^2)(q_4^2-m_t^2)(q_5^2-m_t^2)$ $= \quad 0.01907680362\mathbf{5}\epsilon^0$	$(k_1p_1)(k_1p_1)$
153	$(q_1^2-M_W^2)(q_2^2-M_Z^2)(q_3^2-M_W^2)(q_4^2-m_t^2)(q_5^2-m_t^2)$ $= \quad 0.154520177\mathbf{3}7\mathbf{5}\epsilon^0$ $\quad\quad 0.062\mathbf{5}\epsilon^{-1}$	$(k_1p_1)(k_2p_2)$
154	$(q_1^2-M_W^2)(q_2^2-M_Z^2)(q_3^2-M_W^2)(q_4^2-m_t^2)(q_5^2-m_t^2)$ $= \quad 0.01907680362\mathbf{5}\epsilon^0$	$(k_2p_2)(k_2p_2)$
155	$(q_1^2-M_W^2)(q_2^2-m_t^2)q_3^2(q_7^2-M_W^2)(q_8^2-m_t^2)(q_9^2-M_Z^2)$ $= \quad 0.027203280\mathbf{1}\epsilon^0$	k_2p_1
156	$(q_1^2-M_W^2)(q_2^2-M_Z^2)(q_3^2-M_W^2)(q_7^2-M_W^2)(q_8^2-m_t^2)(q_9^2-m_t^2)$ $= \quad 0.019388606\mathbf{1}7\epsilon^0$	k_2p_1
157	$(q_1^2-M_W^2)(q_2^2-M_W^2)(q_3^2-M_Z^2)(q_7^2-M_W^2)(q_8^2-m_t^2)q_9^2$ $= \quad 0.066266\mathbf{1}90\mathbf{3}\epsilon^0$	k_2p_1
158	$(q_1^2-M_W^2)(q_2^2-m_t^2)q_3^2(q_4^2-M_Z^2)(q_7^2-M_W^2)$ $= \quad 0.06138304537\mathbf{5}\epsilon^0$	$(k_1p_1)(k_1p_1)$
159	$(q_1^2-M_W^2)(q_2^2-m_t^2)q_3^2(q_4^2-M_Z^2)(q_7^2-M_W^2)$ $= \quad 0.188168427\mathbf{1}2\epsilon^0$ $\quad\quad 0.062\mathbf{5}\epsilon^{-1}$	$(k_1p_1)(k_2p_2)$
160	$(q_1^2-M_W^2)(q_2^2-m_t^2)q_3^2(q_7^2-M_W^2)(q_9^2-M_Z^2)$ $= \quad 0.077891750\mathbf{6}5\epsilon^0$	$(k_1p_1)(k_1p_1)$
161	$(q_1^2-M_W^2)(q_2^2-m_t^2)q_3^2(q_7^2-M_W^2)(q_9^2-M_Z^2)$ $= \quad 0.060028079\mathbf{4}75\epsilon^0$	$(k_1p_1)(k_2p_1)$
162	$(q_1^2-M_W^2)q_2^2(q_3^2-m_t^2)(q_4^2-M_W^2)(q_7^2-M_W^2)(q_{13}^2-M_Z^2)$ $= \quad 0.041158591\mathbf{9}9\epsilon^0$	k_1p_1

163	$(q_1^2-M_W^2)q_2^2(q_3^2-m_t^2)(q_4^2-M_W^2)(q_7^2-M_W^2)(q_{13}^2-M_Z^2)$ $= 0.0518233222\epsilon^0$	k_2p_2
164	$(q_1^2-M_W^2)q_2^2(q_3^2-m_t^2)(q_7^2-M_W^2)(q_9^2-M_W^2)(q_{10}^2-M_Z^2)$ $= 0.049072194\mathbf{9}\epsilon^0$	k_1p_1
165	$(q_1^2-M_W^2)q_2^2(q_3^2-m_t^2)(q_7^2-M_W^2)(q_9^2-M_W^2)$ $= 0.072342831\mathbf{45}\epsilon^0$	$(k_1p_1)(k_1p_1)$
166	$(q_1^2-M_W^2)(q_2^2-M_Z^2)(q_3^2-M_W^2)(q_4^2-m_t^2)(q_7^2-M_W^2)$ $= 0.041114023\mathbf{425}\epsilon^0$	$(k_1p_1)(k_1p_1)$
167	$(q_1^2-M_W^2)(q_2^2-M_Z^2)(q_3^2-M_W^2)(q_4^2-m_t^2)(q_7^2-M_W^2)$ $= 0.157218595\mathbf{87}\epsilon^0$ $0.0\mathbf{625}\epsilon^{-1}$	$(k_1p_1)(k_2p_2)$
168	$(q_1^2-M_W^2)(q_2^2-M_Z^2)(q_3^2-M_W^2)(q_7^2-M_W^2)(q_9^2-m_t^2)$ $= 0.052285461\mathbf{075}\epsilon^0$	$(k_1p_1)(k_1p_1)$
169	$(q_1^2-M_W^2)(q_2^2-M_Z^2)(q_3^2-M_W^2)(q_7^2-M_W^2)(q_9^2-m_t^2)$ $= 0.043022290\mathbf{175}\epsilon^0$	$(k_1p_1)(k_2p_1)$
170	$(q_1^2-M_W^2)(q_2^2-M_Z^2)(q_3^2-M_W^2)(q_7^2-M_W^2)(q_{11}^2-M_W^2)$ $= 0.092988543\mathbf{2}\epsilon^0$	$(k_1p_1)(k_1p_1)$
171	$(q_1^2-M_W^2)(q_2^2-M_Z^2)(q_3^2-M_W^2)(q_7^2-M_W^2)(q_{11}^2-M_W^2)$ $= 0.082951819775\epsilon^0$	$(k_1p_1)(k_2p_1)$
172	$(q_1^2-M_W^2)(q_2^2-M_W^2)(q_3^2-M_Z^2)q_4^2(q_7^2-M_W^2)(q_{13}^2-m_t^2)$ $= 0.041612251\mathbf{37}\epsilon^0$	k_1p_1
173	$(q_1^2-M_W^2)(q_2^2-M_W^2)(q_3^2-M_Z^2)q_4^2(q_7^2-M_W^2)(q_{13}^2-m_t^2)$ $= 0.055819201\mathbf{3}\epsilon^0$	k_2p_2
174	$(q_1^2-M_W^2)(q_2^2-M_W^2)(q_3^2-M_Z^2)q_4^2(q_7^2-M_W^2)$ $= 0.082984648\mathbf{35}\epsilon^0$	$(k_1p_1)(k_1p_1)$
175	$(q_1^2-M_W^2)(q_2^2-M_W^2)(q_3^2-M_Z^2)q_4^2(q_7^2-M_W^2)$ $= 0.130593316\mathbf{2}\epsilon^0$ $0.0\mathbf{625}\epsilon^{-1}$	$(k_1p_1)(k_2p_2)$
176	$(q_1^2-M_W^2)(q_2^2-M_W^2)(q_3^2-M_Z^2)(q_7^2-M_W^2)q_9^2(q_{10}^2-m_t^2)$ $= 0.049525854\mathbf{31}\epsilon^0$	k_1p_1
177	$(q_1^2-M_W^2)(q_2^2-M_W^2)(q_3^2-M_Z^2)(q_7^2-M_W^2)q_9^2$ $= 0.13132850557\mathbf{5}\epsilon^0$	$(k_1p_1)(k_1p_1)$
178	$(q_1^2-M_W^2)(q_2^2-M_W^2)(q_3^2-M_Z^2)(q_7^2-M_W^2)q_9^2$ $= 0.131271995\mathbf{65}\epsilon^0$	$(k_1p_1)(k_2p_1)$
179	$(q_1^2-M_Z^2)(q_2^2-m_t^2)(q_3^2-m_t^2)(q_9^2-M_W^2)q_{12}^2$ $= 0.146376231\mathbf{37}\epsilon^0$ $0.0\mathbf{625}\epsilon^{-1}$	$(k_1p_2)(k_2p_1)$
180	$(q_1^2-M_Z^2)(q_2^2-m_t^2)(q_3^2-m_t^2)(q_9^2-M_W^2)q_{12}^2$ $= 0.041978093\mathbf{175}\epsilon^0$	$(k_2p_1)(k_2p_1)$
181	$(q_1^2-M_Z^2)(q_2^2-M_W^2)(q_3^2-M_W^2)(q_9^2-m_t^2)q_{12}^2$ $= 0.071214405\mathbf{02}\epsilon^0$ $0.0\mathbf{625}\epsilon^{-1}$	$(k_1p_2)(k_2p_1)$

182	$(q_1^2 - M_Z^2)(q_2^2 - M_W^2)(q_3^2 - M_W^2)(q_9^2 - m_t^2)q_{12}^2$ $= \quad 0.033106109425\epsilon^0$	$(k_2p_1)(k_2p_1)$
183	$(q_1^2 - M_Z^2)(q_2^2 - m_t^2)(q_3^2 - m_t^2)(q_4^2 - M_W^2)q_5^2$ $= \quad 0.054292973\epsilon^0$	$(k_1p_1)(k_1p_1)$
184	$(q_1^2 - M_Z^2)(q_2^2 - m_t^2)(q_3^2 - m_t^2)(q_4^2 - M_W^2)q_5^2$ $= \quad 0.146376231\mathbf{3}\epsilon^0$ $\quad 0.0625\epsilon^{-1}$	$(k_1p_1)(k_2p_2)$
185	$(q_1^2 - M_Z^2)(q_2^2 - m_t^2)(q_3^2 - m_t^2)(q_4^2 - M_W^2)q_5^2$ $= \quad 0.041978093175\epsilon^0$	$(k_2p_2)(k_2p_2)$
186	$(q_1^2 - M_Z^2)(q_2^2 - M_W^2)(q_3^2 - M_W^2)(q_4^2 - m_t^2)q_5^2$ $= \quad 0.071214405\mathbf{2}\epsilon^0$ $\quad 0.0625\epsilon^{-1}$	$(k_1p_1)(k_2p_2)$
187	$(q_1^2 - M_Z^2)(q_2^2 - M_W^2)(q_3^2 - M_W^2)(q_4^2 - m_t^2)q_5^2$ $= \quad 0.033106109425\epsilon^0$	$(k_2p_2)(k_2p_2)$
188	$q_1^2(q_2^2 - M_W^2)(q_3^2 - m_t^2)(q_4^2 - M_W^2)(q_6^2 - M_Z^2)q_7^2$ $= \quad X\epsilon^0$	$(k_2p_2)(k_2p_2)$
189	$q_1^2(q_2^2 - M_W^2)(q_3^2 - m_t^2)(q_6^2 - M_Z^2)q_7^2(q_{11}^2 - m_t^2)$ $= \quad (0.005967\mathbf{4} + 0.032054\mathbf{1}i)\epsilon^0$	$(k_2p_1)(k_2p_1)$
190	$q_1^2(q_2^2 - m_t^2)(q_3^2 - M_W^2)(q_4^2 - m_t^2)(q_6^2 - M_Z^2)q_7^2$ $= \quad X\epsilon^0$	$(k_2p_2)(k_2p_2)$
191	$q_1^2(q_2^2 - m_t^2)(q_3^2 - M_W^2)(q_6^2 - M_Z^2)q_7^2(q_{11}^2 - M_W^2)$ $= \quad (0.012922\mathbf{7} + 0.060145\mathbf{1}i)\epsilon^0$	$(k_2p_1)(k_2p_1)$
192	$q_1^2(q_2^2 - M_W^2)(q_3^2 - m_t^2)q_7^2(q_8^2 - M_Z^2)(q_9^2 - M_W^2)$ $= \quad X\epsilon^0$	$(k_2p_1)(k_2p_1)$
193	$q_1^2(q_2^2 - m_t^2)(q_3^2 - M_W^2)q_7^2(q_8^2 - M_Z^2)(q_9^2 - m_t^2)$ $= \quad X\epsilon^0$	$(k_2p_1)(k_2p_1)$
194	$(q_1^2 - m_t^2)(q_2^2 - M_Z^2)(q_3^2 - m_t^2)(q_4^2 - M_W^2)(q_6^2 - M_W^2)(q_7^2 - m_t^2)$ $= \quad 0.004245331\mathbf{2}8\epsilon^0$	$(k_2p_2)(k_2p_2)$
195	$(q_1^2 - m_t^2)(q_2^2 - M_Z^2)(q_3^2 - m_t^2)(q_6^2 - M_W^2)(q_7^2 - m_t^2)(q_{11}^2 - m_t^2)$ $= \quad 0.001668988\mathbf{3}2\epsilon^0$	$(k_2p_1)(k_2p_1)$
196	$(q_1^2 - m_t^2)(q_2^2 - m_t^2)(q_3^2 - M_Z^2)q_4^2(q_6^2 - M_W^2)(q_7^2 - m_t^2)$ $= \quad 0.006690037\mathbf{2}1\epsilon^0$	$(k_2p_2)(k_2p_2)$
197	$(q_1^2 - m_t^2)(q_2^2 - M_Z^2)(q_3^2 - m_t^2)(q_7^2 - m_t^2)(q_8^2 - M_W^2)(q_9^2 - M_W^2)$ $= \quad 0.004245331\mathbf{2}8\epsilon^0$	$(k_2p_1)(k_2p_1)$
198	$(q_1^2 - m_t^2)(q_2^2 - m_t^2)(q_3^2 - M_Z^2)(q_7^2 - m_t^2)(q_8^2 - M_W^2)q_9^2$ $= \quad 0.006690037\mathbf{2}1\epsilon^0$	$(k_2p_1)(k_2p_1)$
199	$(q_1^2 - m_t^2)q_2^2(q_3^2 - M_W^2)(q_7^2 - m_t^2)(q_9^2 - m_t^2)(q_{10}^2 - M_Z^2)$ $= \quad 0.003106760\mathbf{0}4\epsilon^0$	$(k_1p_1)(k_1p_1)$
200	$(q_1^2 - m_t^2)(q_2^2 - m_t^2)(q_3^2 - M_Z^2)(q_7^2 - m_t^2)q_9^2(q_{10}^2 - M_W^2)$ $= \quad 0.004370176\mathbf{2}5\epsilon^0$	$(k_1p_1)(k_1p_1)$
201	$(q_1^2 - M_W^2)(q_2^2 - M_Z^2)(q_3^2 - M_W^2)(q_6^2 - m_t^2)(q_7^2 - M_W^2)(q_{11}^2 - M_W^2)$ $= \quad 0.010961668\mathbf{7}4\epsilon^0$	$(k_2p_1)(k_2p_1)$

202	$(q_1^2-M_W^2)q_2^2(q_3^2-m_t^2)(q_4^2-M_W^2)(q_7^2-M_W^2)(q_{13}^2-M_Z^2)$ $= 0.01175492532\epsilon^0$	$(k_1p_1)(k_1p_1)$
203	$(q_1^2-M_W^2)q_2^2(q_3^2-m_t^2)(q_4^2-M_W^2)(q_7^2-M_W^2)(q_{13}^2-M_Z^2)$ $= 0.049513696685\epsilon^0$	$(k_1p_1)(k_2p_2)$
204	$(q_1^2-M_W^2)q_2^2(q_3^2-m_t^2)(q_7^2-M_W^2)(q_9^2-M_W^2)(q_{10}^2-M_Z^2)$ $= 0.015648943\mathbf{2}3\epsilon^0$	$(k_1p_1)(k_1p_1)$
205	$(q_1^2-M_W^2)(q_2^2-M_W^2)(q_3^2-M_Z^2)q_4^2(q_7^2-M_W^2)(q_{13}^2-m_t^2)$ $= 0.022532281\mathbf{1}7\epsilon^0$	$(k_1p_1)(k_2p_2)$
206	$(q_1^2-M_W^2)(q_2^2-M_W^2)(q_3^2-M_Z^2)(q_7^2-M_W^2)q_9^2(q_{10}^2-m_t^2)$ $= 0.015938556\mathbf{4}7\epsilon^0$	$(k_1p_1)(k_1p_1)$
207	$(q_1^2-m_t^2)q_2^2(q_3^2-M_W^2)(q_7^2-m_t^2)(q_9^2-m_t^2)(q_{10}^2-M_Z^2)$ $= 0.0009934943\mathbf{1}6\epsilon^0$	$(k_1p_1)(k_1p_1)$ (k_1p_1)
208	$(q_1^2-m_t^2)(q_2^2-m_t^2)(q_3^2-M_Z^2)(q_7^2-m_t^2)q_9^2(q_{10}^2-M_W^2)$ $= 0.00154809541\mathbf{2}\epsilon^0$	$(k_1p_1)(k_1p_1)$ (k_1p_1)
209	$(q_1^2-M_W^2)(q_2^2-M_Z^2)(q_3^2-M_W^2)(q_6^2-m_t^2)(q_7^2-M_W^2)(q_{11}^2-M_W^2)$ $= 0.003647918\mathbf{2}9\epsilon^0$	$(k_2p_1)(k_2p_1)$ (k_2p_1)
210	$(q_1^2-M_W^2)q_2^2(q_3^2-m_t^2)(q_4^2-M_W^2)(q_7^2-M_W^2)(q_{13}^2-M_Z^2)$ $= 0.024487096\mathbf{4}7\epsilon^0$	$(k_1p_1)(k_1p_1)$ (k_2p_2)
211	$(q_1^2-M_W^2)q_2^2(q_3^2-m_t^2)(q_7^2-M_W^2)(q_9^2-M_W^2)(q_{10}^2-M_Z^2)$ $= 0.005477946\mathbf{7}9\epsilon^0$	$(k_1p_1)(k_1p_1)$ (k_1p_1)
212	$(q_1^2-m_t^2)(q_2^2-M_W^2)q_3^2(q_9^2-M_Z^2)(q_{12}^2-M_W^2)$ $= 0.183107939\mathbf{1}\epsilon^0$	k_1p_2
213	$(q_1^2-M_W^2)q_2^2(q_3^2-m_t^2)(q_7^2-M_W^2)(q_9^2-M_W^2)$ $= 0.242119703\mathbf{8}5\epsilon^0$	k_2p_1
214	$(q_1^2-m_t^2)(q_2^2-M_W^2)q_3^2(q_9^2-M_Z^2)(q_{12}^2-M_W^2)$ $= 0.040058834\mathbf{5}5\epsilon^0$	$(k_2p_1)(k_2p_1)$
215	$(q_1^2-m_t^2)(q_2^2-M_W^2)q_3^2(q_4^2-M_Z^2)(q_5^2-M_W^2)$ $= 0.040058834\mathbf{5}5\epsilon^0$	$(k_2p_2)(k_2p_2)$
216	$(q_1^2-m_t^2)(q_2^2-M_Z^2)(q_3^2-m_t^2)(q_4^2-M_W^2)(q_5^2-M_W^2)$ $= 0.028463512\mathbf{7}75\epsilon^0$	$(k_1p_1)(k_1p_1)$
217	$(q_1^2-m_t^2)(q_2^2-M_Z^2)(q_3^2-m_t^2)(q_4^2-M_W^2)(q_5^2-M_W^2)$ $= 0.028463512\mathbf{7}75\epsilon^0$	$(k_2p_2)(k_2p_2)$
218	$(q_1^2-m_t^2)(q_2^2-M_W^2)q_3^2(q_4^2-M_Z^2)(q_7^2-m_t^2)$ $= 0.039638\mathbf{2}01\epsilon^0$	$(k_2p_2)(k_2p_2)$
219	$(q_1^2-m_t^2)(q_2^2-M_W^2)q_3^2(q_7^2-m_t^2)(q_9^2-M_Z^2)$ $= 0.039638\mathbf{2}01\epsilon^0$	$(k_2p_1)(k_2p_1)$
220	$(q_1^2-M_W^2)(q_2^2-m_t^2)q_3^2(q_4^2-M_Z^2)(q_7^2-M_W^2)$ $= 0.065350074\mathbf{1}\epsilon^0$	$(k_2p_2)(k_2p_2)$
221	$(q_1^2-M_W^2)(q_2^2-m_t^2)q_3^2(q_7^2-M_W^2)(q_9^2-M_Z^2)$ $= 0.065350074\mathbf{1}\epsilon^0$	$(k_2p_1)(k_2p_1)$
222	$(q_1^2-M_W^2)q_2^2(q_3^2-m_t^2)(q_7^2-M_W^2)(q_9^2-M_W^2)$ $= 0.069928123\mathbf{7}\epsilon^0$	$(k_1p_1)(k_2p_1)$

223	$(q_1^2-M_W^2)(q_2^2-M_Z^2)(q_3^2-M_W^2)(q_4^2-m_t^2)(q_7^2-M_W^2)$ $= 0.045351680625\epsilon^0$	$(k_2p_2)(k_2p_2)$
224	$(q_1^2-M_W^2)(q_2^2-M_Z^2)(q_3^2-M_W^2)(q_7^2-M_W^2)(q_9^2-m_t^2)$ $= 0.045351680625\epsilon^0$	$(k_2p_1)(k_2p_1)$
225	$(q_1^2-M_W^2)(q_2^2-M_W^2)(q_3^2-M_Z^2)q_4^2(q_7^2-M_W^2)$ $= 0.160202659575\epsilon^0$	$(k_2p_2)(k_2p_2)$
226	$(q_1^2-M_W^2)(q_2^2-M_W^2)(q_3^2-M_Z^2)(q_7^2-M_W^2)q_9^2$ $= 0.160202659575\epsilon^0$	$(k_2p_1)(k_2p_1)$
227	$(q_1^2-M_Z^2)(q_2^2-m_t^2)(q_3^2-m_t^2)(q_9^2-M_W^2)q_{12}^2$ $= 0.054292973\epsilon^0$	$(k_1p_2)(k_1p_2)$
228	$(q_1^2-M_Z^2)(q_2^2-M_W^2)(q_3^2-M_W^2)(q_9^2-m_t^2)q_{12}^2$ $= 0.0735039633\epsilon^0$	$(k_1p_2)(k_1p_2)$
229	$(q_1^2-M_Z^2)(q_2^2-M_W^2)(q_3^2-M_W^2)(q_4^2-m_t^2)q_5^2$ $= 0.0735039633\epsilon^0$	$(k_1p_1)(k_1p_1)$
230	$(q_1^2-m_t^2)(q_2^2-M_W^2)q_3^2(q_4^2-M_Z^2)(q_6^2-M_W^2)(q_7^2-m_t^2)$ $= 0.006454302177\epsilon^0$	$(k_2p_2)(k_2p_2)$
231	$(q_1^2-m_t^2)(q_2^2-M_W^2)q_3^2(q_7^2-m_t^2)(q_8^2-M_W^2)(q_9^2-M_Z^2)$ $= 0.006454302177\epsilon^0$	$(k_2p_1)(k_2p_1)$
232	$(q_1^2-M_W^2)(q_2^2-m_t^2)q_3^2(q_4^2-M_Z^2)(q_6^2-m_t^2)(q_7^2-M_W^2)$ $= 0.008060136477\epsilon^0$	$(k_2p_2)(k_2p_2)$
233	$(q_1^2-M_W^2)(q_2^2-M_Z^2)(q_3^2-M_W^2)(q_4^2-m_t^2)(q_6^2-m_t^2)(q_7^2-M_W^2)$ $= 0.005724933422\epsilon^0$	$(k_2p_2)(k_2p_2)$
234	$(q_1^2-M_W^2)(q_2^2-M_W^2)(q_3^2-M_Z^2)q_4^2(q_6^2-m_t^2)(q_7^2-M_W^2)$ $= 0.023855451455\epsilon^0$	$(k_2p_2)(k_2p_2)$
235	$(q_1^2-M_W^2)(q_2^2-m_t^2)q_3^2(q_7^2-M_W^2)(q_8^2-m_t^2)(q_9^2-M_Z^2)$ $= 0.008060136477\epsilon^0$	$(k_2p_1)(k_2p_1)$
236	$(q_1^2-M_W^2)(q_2^2-M_Z^2)(q_3^2-M_W^2)(q_7^2-M_W^2)(q_8^2-m_t^2)(q_9^2-m_t^2)$ $= 0.005724933422\epsilon^0$	$(k_2p_1)(k_2p_1)$
237	$(q_1^2-M_W^2)(q_2^2-M_W^2)(q_3^2-M_Z^2)(q_7^2-M_W^2)(q_8^2-m_t^2)q_9^2$ $= 0.023855451455\epsilon^0$	$(k_2p_1)(k_2p_1)$
238	$(q_1^2-M_W^2)q_2^2(q_3^2-m_t^2)(q_4^2-M_W^2)(q_7^2-M_W^2)(q_{13}^2-M_Z^2)$ $= 0.017024873885\epsilon^0$	$(k_2p_2)(k_2p_2)$
239	$(q_1^2-M_W^2)q_2^2(q_3^2-m_t^2)(q_4^2-M_W^2)(q_7^2-M_W^2)(q_{13}^2-M_Z^2)$ $= 0.028642336\epsilon^0$	$(k_1p_1)(k_2p_2)$ (k_2p_2)

Table 7.6: Integral definitions and numerical results for the class **0hxwxtxz** of $Z \to b\bar{b}$ integrals.

Bibliography

[1] A. Salam, Weak and Electromagnetic Interactions, originally printed in: Svartholm (ed.), Elementary Particle Theory, Proceedings of the Nobel Symposium held 1968 at Lerum, Sweden (Stockholm 1968), p. 367-377; see also: spires (1968).

[2] S. Glashow, Partial Symmetries of Weak Interactions, Nucl. Phys. 22 (1961) 579–588, doi:10.1016/0029–5582(61)90469–2. doi:10.1016/0029-5582(61)90469-2.

[3] S. Glashow, J. Iliopoulos, L. Maiani, Weak Interactions with Lepton-Hadron Symmetry, Phys. Rev. D2 (1970) 1285–1292, doi:10.1103/PhysRevD.2.1285. doi:10.1103/PhysRevD.2.1285.

[4] S. Weinberg, A Model of Leptons, Phys. Rev. Lett. 19 (1967) 1264–1266. doi:10.1103/PhysRevLett.19.1264.

[5] S. Chatrchyan, et al., Observation of a new boson at a mass of 125 GeV with the CMS experiment at the LHC, Phys. Lett. B716 (2012) 30–61. arXiv:1207.7235, doi:10.1016/j.physletb.2012.08.021.

[6] G. Aad, et al., Observation of a new particle in the search for the Standard Model Higgs boson with the ATLAS detector at the LHC, Phys. Lett. B716 (2012) 1–29. arXiv:1207.7214, doi:10.1016/j.physletb.2012.08.020.

[7] S. S. Schweber, QED and the men who made it: Dyson, Feynman, Schwinger, and Tomonaga, Princeton, USA, Univ. Pr. (1994) 732 p.

[8] D. Kaiser, Drawing theories apart: the dispersion of Feynman diagrams in postwar physics, Chicago Univ. Press, Chicago, IL, 2005.
URL http://cds.cern.ch/record/941915

[9] W. E. Lamb, R. C. Retherford, Fine Structure of the Hydrogen Atom by a Microwave Method, Phys. Rev. 72 (1947) 241–243. doi:10.1103/PhysRev.72.241.

[10] H. A. Bethe, The Electromagnetic shift of energy levels, Phys. Rev. 72 (1947) 339–341. doi:10.1103/PhysRev.72.339.

[11] J. S. Schwinger, On Quantum electrodynamics and the magnetic moment of the electron, Phys. Rev. 73 (1948) 416–417. doi:10.1103/PhysRev.73.416.

[12] M. Veltman, Limit on Mass Differences in the Weinberg Model, Nucl. Phys. B123 (1977) 89. doi:10.1016/0550-3213(77)90342-X.

[13] A. Akhundov, D. Bardin, T. Riemann, Electroweak one loop corrections to the decay of the neutral vector boson, Nucl. Phys. B276 (1986) 1, Dubna preprint JINR-E2-85-617 (Aug 1985). doi:10.1016/0550-3213(86)90014-3.

[14] W. Beenakker, W. Hollik, The width of the Z Boson, Z. Phys. C40 (1988) 141. doi:10.1007/BF01559728.

[15] F. Jegerlehner, Precision tests of electroweak interaction parameters, In: R. Manka, M. Zralek (eds.), proceedings of the 11th Int. School of Theoretical Physics, Testing the standard model, Szczyrk, Poland, Sep 18-22, 1987 (Singapore, World Scientific, 1988), pp. 33-108, Bielefeld preprint BI-TP-87/16, https://lib-extopc.kek.jp/preprints/PDF/1988/8801/8801263.pdf.

[16] J. Bernabeu, A. Pich, A. Santamaria, $\Gamma(Z \to b\bar{b})$: A signature of hard mass terms for a heavy top, Phys. Lett. B200 (1988) 569–574. doi:10.1016/0370-2693(88)90173-6.

[17] K. Hikasa, et al., Review of particle properties. Particle Data Group, Phys. Rev. D45 (1992) S1, [Erratum: Phys. Rev.D46,5210(1992)]. doi:10.1103/PhysRevD.46.5210,10.1103/PhysRevD.45.S1.

[18] S. Schael, et al., Precision electroweak measurements on the Z resonance, Phys. Rept. 427 (2006) 257–454. arXiv:hep-ex/0509008, doi:10.1016/j.physrep.2005.12.006.

[19] D. Bardin, W. Beenakker, M. Bilenky, W. Hollik, M. Martinez, G. Montagna, O. Nicrosini, V. Novikov, L. Okun, A. Olshevsky, G. Passarino, F. Piccinini, S. Riemann, T. Riemann, A. Rozanov, F. Teubert, M. Vysotsky, Electroweak working group report (1997) 7–162, CERN 95–03A. In: D. Bardin, W. Hollik, G. Passarino (eds.), Reports of the working group on precision calculations for the Z resonance, CERN 95-03, p. 7-162 (31 March 1995). arXiv:hep-ph/9709229.

[20] D. Yu. Bardin, et al., Electroweak working group report, in: Workshop Group on Precision Calculations for the Z Resonance (2nd meeting held Mar 31, 3rd meeting held Jun 13) Geneva, Switzerland, January 14, 1994, 1997, pp. 7–162. arXiv:hep-ph/9709229.
URL http://doc.cern.ch/cernrep/1995/95-03/95-03.html

[21] F. Abe, et al., Observation of top quark production in $\bar{p}p$ collisions, Phys. Rev. Lett. 74 (1995) 2626–2631. arXiv:hep-ex/9503002, doi:10.1103/PhysRevLett.74.2626.

[22] S. Abachi, et al., Observation of the top quark, Phys. Rev. Lett. 74 (1995) 2632–2637. arXiv:hep-ex/9503003, doi:10.1103/PhysRevLett.74.2632.

[23] A. Akhundov, D. Bardin, T. Riemann, Hunting the hidden standard Higgs, Phys. Lett. B166 (1986) 111. doi:10.1016/0370-2693(86)91166-4.

[24] A. Blondel, J. Gluza, P. Janot (org.), Mini workshop on precision EW and QCD calculations for the FCC studies: methods and techniques, 12-13 Jan 2018, CERN. Webpage https://indico.cern.ch/event/669224/. J. Gluza, S. Jadach and T. Riemann (eds.), submitted as CERN Yellow Report.

[25] R. H. Mellin, Om definita integraler, Acta Soc. Sci. Fenn. 20(7) , 1 (1895).

[26] E. W. Barnes, The theory of the gamma function, Messenger Math. 29(2), 64 (1900).

[27] V. Smirnov, "Feynman integral calculus", (Springer Verlag, Berlin, 2006).

[28] M. Prausa, epsilon: A tool to find a canonical basis of master integrals, Comput. Phys. Commun. 219 (2017) 361–376. arXiv:1701.00725, doi:10.1016/j.cpc.2017.05.026.

[29] A. Freitas, Y.-C. Huang, On the Numerical Evaluation of Loop Integrals With Mellin-Barnes Representations, JHEP 04 (2010) 074. arXiv:1001.3243, doi:10.1007/JHEP04(2010)074.

[30] G. Somogyi, Angular integrals in d dimensions, J. Math. Phys. 52 (2011) 083501. arXiv:1101.3557, doi:10.1063/1.3615515.

[31] V. Del Duca, G. Somogyi, Z. Trocsanyi, Integration of collinear-type doubly unresolved counterterms in NNLO jet cross sections, JHEP 06 (2013) 079. arXiv:1301.3504, doi:10.1007/JHEP06(2013)079.

[32] G. Somogyi, A subtraction scheme for computing QCD jet cross sections at NNLO: integrating the doubly unresolved subtraction terms, JHEP 04 (2013) 010. arXiv:1301.3919, doi:10.1007/JHEP04(2013)010.

[33] C. Anastasiou, C. Duhr, F. Dulat, B. Mistlberger, Soft triple-real radiation for Higgs production at N3LO, JHEP 07 (2013) 003. arXiv:1302.4379, doi:10.1007/JHEP07(2013)003.

[34] MBtools webpage, http://projects.hepforge.org/mbtools/.

[35] I. Dubovyk, A. Freitas, J. Gluza, T. Riemann, J. Usovitsch, 30 years, some 700 integrals, and 1 dessert, or: Electroweak two-loop corrections to the $Z\bar{b}b$ vertex, PoS LL2016 (2016) 075, https://pos.sissa.it/archive/conferences/260/034/LL2016_075.pdf. arXiv:1610.07059.

[36] I. Dubovyk, J. Gluza, T. Riemann, J. Usovitsch, Numerical integration of massive two-loop Mellin-Barnes integrals in Minkowskian regions, PoS LL2016 (2016) 034, https://pos.sissa.it/260/034/pdf. arXiv:1607.07538.

[37] I. Dubovyk, A. Freitas, J. Gluza, T. Riemann, J. Usovitsch, The two-loop electroweak bosonic corrections to $\sin^2\theta^{\rm b}_{\rm eff}$, Phys. Lett. B762 (2016) 184–189. arXiv:1607.08375, doi:10.1016/j.physletb.2016.09.012.

[38] I. Dubovyk, A. Freitas, J. Gluza, T. Riemann, J. Usovitsch, Complete electroweak two-loop corrections to Z boson production and decay, Phys. Lett. B783 (2018) 86–94. arXiv:1804.10236, doi:10.1016/j.physletb.2018.06.037.

[39] European Strategy for Particle Physics by the European Strategy Group for Particle Physics, CERN's white paper for the 15th European Strategy Session of the Council, http://prac.us.edu.pl/~/gluza/pdf/fccstrat.pdf.

[40] A. Blondel, et al., Standard Model Theory for the FCC-ee: The Tera-Z, in: Mini Workshop on Precision EW and QCD Calculations for the FCC Studies : Methods and Techniques CERN, Geneva, Switzerland, January 12-13, 2018, 2018. arXiv:1809.01830.

[41] I. Dubovyk, J. Gluza, A. Freitas, K. Grzanka, S. Jadach, T. Riemann, J. Usovitsch, Precision calculations for FCC, poster presented by S. Jadach at the FCC weak 2018, 9-13 April 2018, Amsterdam. https://indico.cern.ch/event/656491/contributions/2947663/attachments/1622685/2582801/Poster-FCC-Amsterdam_SJadach_et_al.pdf.

[42] H. Baer, T. Barklow, K. Fujii, Y. Gao, A. Hoang, S. Kanemura, J. List, H. E. Logan, A. Nomerotski, M. Perelstein, et al., The International Linear Collider Technical Design Report - Volume 2: Physics, arXiv:1306.6352.

[43] M. Bicer, et al., First Look at the Physics Case of TLEP, JHEP 01 (2014) 164. arXiv:1308.6176, doi:10.1007/JHEP01(2014)164.

[44] CEPC-SPPC Study Group, CEPC-SPPC Preliminary Conceptual Design Report. 1. Physics and Detector, IHEP-CEPC-DR-2015-01, IHEP-TH-2015-01, IHEP-EP-2015-01.

[45] D. d'Enterria, Physics at the FCC-ee, in: Proceedings, 17th Lomonosov Conference on Elementary Particle Physics: Moscow, Russia, August 20-26, 2015, 2017, pp. 182–191. arXiv:1602.05043, doi:10.1142/9789813224568_0028.
URL https://inspirehep.net/record/1421932/files/arXiv:1602.05043.pdf

[46] M. Benedikt, et al., *Future Circular Collider, Vol. 2, The Lepton Collider (FCC-ee)*, https://cds.cern.ch/record/2651299, Submitted for publication to Eur. Phys. J. ST. (Dec 2018).

[47] A. Blondel, A. Freitas, J. Gluza, T. Riemann, S. Heinemeyer, S. Jadach, P. Janot, Theory Requirements and Possibilities for the FCC-ee and other Future High Energy and Precision Frontier Lepton Colliders, arXiv:1901.02648.

[48] SM50: *The Standard Model At 50 Years*, 1-4 June 2018, Case Western Reserve University Department of Physics Cleveland, Ohio, webpage http://artsci.case.edu/smat50/.

[49] G. 't Hooft, M. Veltman, Regularization and Renormalization of Gauge Fields, Nucl. Phys. B44 (1972) 189–213, doi:10.1016/0550–3213(72)90279–9. doi:10.1016/0550-3213(72)90279-9.

[50] G. 't Hooft, M. Veltman, Combinatorics of gauge fields, Nucl. Phys. B50 (1972) 318–353. doi:10.1016/S0550-3213(72)80021-X.

[51] F. J. Hasert, et al., Observation of Neutrino Like Interactions Without Muon Or Electron in the Gargamelle Neutrino Experiment, Phys. Lett. B46 (1973) 138–140, [,5.15(1973)]. doi:10.1016/0370-2693(73)90499-1.

[52] G. Arnison, et al., Experimental Observation of Isolated Large Transverse Energy Electrons with Associated Missing Energy at $\sqrt{s} = 540$ GeV, Phys. Lett. B122 (1983) 103–116, [611(1983)]. doi:10.1016/0370-2693(83)91177-2.

[53] M. Banner, et al., Observation of Single Isolated Electrons of High Transverse Momentum in Events with Missing Transverse Energy at the CERN $\bar{p}p$ Collider, Phys. Lett. B122 (1983) 476–485, [7.45(1983)]. doi:10.1016/0370-2693(83)91605-2.

[54] G. Arnison, et al., Experimental Observation of Lepton Pairs of Invariant Mass Around 95 GeV/c^2 at the CERN SPS Collider, Phys. Lett. B126 (1983) 398–410, [7.55(1983)]. doi:10.1016/0370-2693(83)90188-0.

[55] P. Bagnaia, et al., Evidence for $Z^0 \to e^+e^-$ at the CERN $\bar{p}p$ Collider, Phys. Lett. B129 (1983) 130–140, [7.69(1983)]. doi:10.1016/0370-2693(83)90744-X.

[56] The Nobel Prize in Physics 1984, press release, https://www.nobelprize.org/prizes/physics/1984/press-release/".

[57] LEP Design Report: Vol.2. The LEP Main Ring, CERN-LEP-84-01.

[58] The Large Electron-Positron Collider, https://home.cern/about/accelerators/large-electron-positron-collider.

[59] SLAC Linear Collider Conceptual Design Report.
URL http://inspirehep.net/record/154130/files/slac-r-229.pdf

[60] ALEPH collab., DELPHI collab., L3 collab., OPAL collab., SLD collab., LEP Electroweak Working Group, SLD Electroweak Group, SLD Heavy Flavour Group, S. Schael, et al., Precision electroweak measurements on the Z resonance, Phys. Rept. 427 (2006) 257–454. arXiv:hep-ex/0509008, doi:10.1016/j.physrep.2005.12.006.

[61] A. Sirlin, Radiative Corrections in the $SU(2)_L xU(1)$ Theory: A Simple Renormalization Framework, Phys. Rev. D22 (1980) 971–981. doi:10.1103/PhysRevD.22.971.

[62] D. Bardin, P. Khristova, O. Fedorenko, On the lowest order electroweak corrections to spin 1/2 fermion scattering. 1. The one loop diagrammar, Nucl. Phys. B175 (1980) 435. doi:10.1016/0550-3213(80)90021-8.

[63] D. Y. Bardin, P. K. Khristova, O. Fedorenko, On the Lowest Order Electroweak Corrections to Spin 1/2 Fermion Scattering. 2. The One Loop Amplitudes, Nucl. Phys. B197 (1982) 1. doi:10.1016/0550-3213(82)90152-3.

[64] W. J. Marciano, A. Sirlin, Radiative Corrections to Neutrino Induced Neutral Current Phenomena in the $SU(2)_L x U(1)$ Theory, Phys. Rev. D22 (1980) 2695. doi:10.1103/PhysRevD.22.2695.

[65] D. Bardin, C. Burdik, P. Khristova, T. Riemann, Electroweak radiative corrections to deep inelastic scattering at HERA. Neutral current scattering, Z. Phys. C42 (1989) 679, https://lib-extopc.kek.jp/preprints/PDF/1989/8904/8904210.pdf. doi:10.1007/BF01557676.

[66] D. Bardin, M. Bilenky, G. Mitselmakher, T. Riemann, M. Sachwitz, A Realistic Approach to the Standard Z Peak, Z. Phys. C44 (1989) 493, https://lib-extopc.kek.jp/preprints/PDF/1989/8906/8906215.pdf. doi:10.1007/BF01415565.

[67] W. J. Marciano, A. Sirlin, Testing the Standard Model by Precise Determinations of W+- and Z Masses, Phys. Rev. D29 (1984) 945, [Erratum: Phys. Rev.D31,213(1985)]. doi:10.1103/PhysRevD.29.945,10.1103/PhysRevD.31.213.3.

[68] D. Bardin, S. Riemann, T. Riemann, Electroweak one loop corrections to the decay of the charged vector boson, Z. Phys. C32 (1986) 121, https://lib-extopc.kek.jp/preprints/PDF/1986/8607/8607019.pdf. doi:10.1007/BF01441360.

[69] A. Denner, T. Sack, The W boson width, Z. Phys. C46 (1990) 653–663. doi:10.1007/BF01560267.

[70] S. Jadach, B. F. L. Ward, Z. Was, The Precision Monte Carlo event generator KK for two fermion final states in e^+e^- collisions, Comput. Phys. Commun. 130 (2000) 260–325, up to date source available from http://home.cern.ch/jadach/. arXiv:hep-ph/9912214, doi:10.1016/S0010-4655(00)00048-5.

[71] D. Y. Bardin, M. S. Bilenky, T. Riemann, M. Sachwitz, H. Vogt, P. C. Christova, DIZET: A program package for the calculation of electroweak one loop corrections for the process $e^+e^- \to f^+f^-$ around the Z^0 peak, Comput. Phys. Commun. 59 (1990) 303–312. doi:10.1016/0010-4655(90)90179-5.

[72] D. Bardin, M. Bilenky, P. Christova, M. Jack, L. Kalinovskaya, A. Olchevski, S. Riemann, T. Riemann, ZFITTER 6.21: A semi-analytical program for fermion pair production in e^+e^- annihilation, Comput. Phys. Commun. 133 (2001) 229–395. arXiv:hep-ph/9908433, doi:10.1016/S0010-4655(00)00152-1.

[73] A. Arbuzov, M. Awramik, M. Czakon, A. Freitas, M. Grünewald, K. Mönig, S. Riemann, T. Riemann, ZFITTER: A Semi-analytical program for fermion pair production in e^+e^- annihilation, from version 6.21 to version 6.42, Comput. Phys. Commun. 174 (2006) 728–758. arXiv:hep-ph/0507146, doi:10.1016/j.cpc.2005.12.009.

[74] The ZFITTER homepage, http://sanc.jinr.ru/users/zfitter.

[75] S. Riemann, *Suche nach einem Z'-Boson auf der Z-Resonanz mit dem L3-Detektor am LEP-Beschleuniger*, Dissertation, Technische Hochschule Aachen (1994), 94 S., Internal Report: DESY-Zeuthen 94-01, September 1994.

[76] A. Leike, S. Riemann, T. Riemann, Z Z' mixing and radiative corrections at LEP-1, Phys. Lett. B291 (1992) 187–194. arXiv:hep-ph/9507436, doi:10.1016/0370-2693(92)90142-Q.

[77] D. Yu. Bardin, M. Grünewald, G. Passarino, Precision calculation project report. arXiv:hep-ph/9902452.

[78] M. Awramik, M. Czakon, A. Freitas, Bosonic corrections to the effective weak mixing angle at $O(\alpha^2)$, Phys. Lett. B642 (2006) 563–566. arXiv:hep-ph/0605339, doi:10.1016/j.physletb.2006.07.035.

[79] M. Awramik, M. Czakon, A. Freitas, B. Kniehl, Two-loop electroweak fermionic corrections to $\sin^2\theta^{b\bar{b}}_{\rm eff}$, Nucl. Phys. B813 (2009) 174–187. arXiv:0811.1364, doi:10.1016/j.nuclphysb.2008.12.031.

[80] A. Freitas, Higher-order electroweak corrections to the partial widths and branching ratios of the Z boson, JHEP 1404 (2014) 070. arXiv:1401.2447, doi:10.1007/JHEP04(2014)070.

[81] S. Weinzierl, Computer algebra in particle physics, in: 11th National Seminar of Theoretical Physics (In Italian) Parma, Italy, September 2-13, 2002, 2002. arXiv:hep-ph/0209234.

[82] V. Smirnov, Evaluating Feynman integrals, Springer Tracts Mod. Phys. 211 (2004) 1–244.

[83] C. Anastasiou, A. Daleo, Numerical evaluation of loop integrals, JHEP 0610 (2006) 031. arXiv:hep-ph/0511176, doi:10.1088/1126-6708/2006/10/031.

[84] J. Gluza, T. Riemann, Massive Feynman integrals and electroweak corrections, Nucl. Part. Phys. Proc. 261-262 (2015) 140–154. arXiv:1412.3311, doi:10.1016/j.nuclphysbps.2015.03.012.

[85] A. Freitas, Numerical multi-loop integrals and applications, Prog. Part. Nucl. Phys. 90 (2016) 201–240. arXiv:1604.00406, doi:10.1016/j.ppnp.2016.06.004.

[86] A. Kotikov, Differential equations method: New technique for massive Feynman diagrams calculation, Phys. Lett. B254 (1991) 158–164. doi:10.1016/0370-2693(91)90413-K.

[87] A. Kotikov, Differential equations method: The Calculation of vertex type Feynman diagrams, Phys. Lett. B259 (1991) 314–322.

[88] A. V. Kotikov, Differential equation method: The Calculation of N point Feynman diagrams, Phys. Lett. B267 (1991) 123–127.

[89] E. Remiddi, Differential equations for Feynman graph amplitudes, Nuovo Cim. A110 (1997) 1435–1452. arXiv:hep-th/9711188.

[90] J. M. Henn, Multiloop integrals in dimensional regularization made simple, Phys. Rev. Lett. 110 (25) (2013) 251601. arXiv:1304.1806, doi:10.1103/PhysRevLett.110.251601.

[91] J. Ablinger, A. Behring, J. Blumlein, A. De Freitas, A. von Manteuffel, C. Schneider, Calculating Three Loop Ladder and V-Topologies for Massive Operator Matrix Elements by Computer Algebra, Comput. Phys. Commun. 202 (2016) 33–112. arXiv:1509.08324, doi:10.1016/j.cpc.2016.01.002.

[92] O. Gituliar, V. Magerya, Fuchsia: a tool for reducing differential equations for Feynman master integrals to epsilon form, Comput. Phys. Commun. 219 (2017) 329–338. arXiv:1701.04269, doi:10.1016/j.cpc.2017.05.004.

[93] A. von Manteuffel, L. Tancredi, A non-planar two-loop three-point function beyond multiple polylogarithms, JHEP 06 (2017) 127. arXiv:1701.05905, doi:10.1007/JHEP06(2017)127.

[94] L. Adams, E. Chaubey, S. Weinzierl, Simplifying Differential Equations for Multiscale Feynman Integrals beyond Multiple Polylogarithms, Phys. Rev. Lett. 118 (14) (2017) 141602. arXiv:1702.04279, doi:10.1103/PhysRevLett.118.141602.

[95] C. Meyer, Algorithmic transformation of multi-loop master integrals to a canonical basis with CANONICA, Comput. Phys. Commun. 222 (2018) 295–312. arXiv:1705.06252, doi:10.1016/j.cpc.2017.09.014.

[96] A. Georgoudis, K. J. Larsen, Y. Zhang, Azurite: An algebraic geometry based package for finding bases of loop integrals, Comput. Phys. Commun. 221 (2017) 203–215. arXiv:1612.04252, doi:10.1016/j.cpc.2017.08.013.

[97] P. Maierhofer, J. Usovitsch, P. Uwer, Kira–A Feynman integral reduction program, Comput. Phys. Commun. 230 (2018) 99–112. arXiv:1705.05610, doi:10.1016/j.cpc.2018.04.012.

[98] T. Hahn, Generating Feynman diagrams and amplitudes with FeynArts 3, Comput. Phys. Commun. 140 (2001) 418–431. arXiv:hep-ph/0012260.

[99] B. Chokoufe Nejad, T. Hahn, J. N. Lang, E. Mirabella, FormCalc 8: Better Algebra and Vectorization, J. Phys. Conf. Ser. 523 (2014) 012050. arXiv:1310.0274, doi:10.1088/1742-6596/523/1/012050.

[100] G. Ossola, C. G. Papadopoulos, R. Pittau, CutTools: A program implementing the OPP reduction method to compute one-loop amplitudes, JHEP 03 (2008) 042. arXiv:0711.3596, doi:10.1088/1126-6708/2008/03/042.

[101] C. F. Berger, Z. Bern, L. J. Dixon, F. Febres Cordero, D. Forde, H. Ita, D. A. Kosower, D. Maitre, An Automated Implementation of On-Shell Methods for One-Loop Amplitudes, Phys. Rev. D78 (2008) 036003. arXiv:0803.4180, doi:10.1103/PhysRevD.78.036003.

[102] A. van Hameren, C. G. Papadopoulos, R. Pittau, Automated one-loop calculations: A proof of concept, JHEP 09 (2009) 106. arXiv:0903.4665, doi:10.1088/1126-6708/2009/09/106.

[103] S. Badger, B. Biedermann, P. Uwer, NGluon: A package to Calculate One-loop Multi-gluon Amplitudes, Comput. Phys. Commun. 182 (2011) 1674–1692. arXiv:1011.2900, doi:10.1016/j.cpc.2011.04.008.

[104] P. Mastrolia, G. Ossola, T. Reiter, F. Tramontano, Scattering AMplitudes from Unitarity-based Reduction Algorithm at the Integrand-level, JHEP 08 (2010) 080. arXiv:1006.0710, doi:10.1007/JHEP08(2010)080.

[105] V. Hirschi, R. Frederix, S. Frixione, M. V. Garzelli, F. Maltoni, R. Pittau, Automation of one-loop QCD corrections, JHEP 05 (2011) 044. arXiv:1103.0621, doi:10.1007/JHEP05(2011)044.

[106] G. Cullen, J. P. Guillet, G. Heinrich, T. Kleinschmidt, E. Pilon, T. Reiter, M. Rodgers, Golem95C: A library for one-loop integrals with complex masses, Comput. Phys. Commun. 182 (2011) 2276–2284. arXiv:1101.5595, doi:10.1016/j.cpc.2011.05.015.

[107] G. Cullen, N. Greiner, G. Heinrich, G. Luisoni, P. Mastrolia, G. Ossola, T. Reiter, F. Tramontano, Automated One-Loop Calculations with GoSam, Eur. Phys. J. C72 (2012) 1889. arXiv:1111.2034, doi:10.1140/epjc/s10052-012-1889-1.

[108] F. Cascioli, P. Maierhofer, S. Pozzorini, Scattering Amplitudes with Open Loops, Phys. Rev. Lett. 108 (2012) 111601. arXiv:1111.5206, doi:10.1103/PhysRevLett.108.111601.

[109] J. Fleischer, T. Riemann, V. Yundin, New developments in PJFry, PoS LL2012 (2012) 020, http://pos.sissa.it/...151/020/LL2012_020.pdf. arXiv:1210.4095.

[110] G. van Oldenborgh, FF: A package to evaluate one loop Feynman diagrams, Comput. Phys. Commun. 66 (1991) 1–15. doi:10.1016/0010-4655(91)90002-3.

[111] A. van Hameren, OneLOop: For the evaluation of one-loop scalar functions, Comput. Phys. Commun. 182 (2011) 2427–2438. arXiv:1007.4716, doi:10.1016/j.cpc.2011.06.011.

[112] R. K. Ellis, G. Zanderighi, Scalar one-loop integrals for QCD, JHEP 02 (2008) 002. arXiv:0712.1851, doi:10.1088/1126-6708/2008/02/002.

[113] A. Denner, S. Dittmaier, L. Hofer, Collier: a fortran-based Complex One-Loop LIbrary in Extended Regularizations, Comput. Phys. Commun. 212 (2017) 220–238. arXiv:1604.06792, doi:10.1016/j.cpc.2016.10.013.

[114] A. Freitas, Numerical evaluation of multi-loop integrals using subtraction terms, JHEP 1207 (2012) 132. arXiv:1205.3515, doi:10.1007/JHEP07(2012)132,10.1007/JHEP09(2012)129.

[115] S. P. Martin, D. G. Robertson, TSIL: A program for the calculation of two-loop self-energy integrals, Comput. Phys. Commun. 174 (2006) 133–151. arXiv:hep-ph/0501132, doi:10.1016/j.cpc.2005.08.005.

[116] M. Caffo, H. Czyz, M. Gunia, E. Remiddi, BOKASUN: A Fast and precise numerical program to calculate the Master Integrals of the two-loop sunrise diagrams, Comput. Phys. Commun. 180 (2009) 427–430. arXiv:0807.1959, doi:10.1016/j.cpc.2008.10.011.

[117] K. Hepp, Proof of the Bogolyubov-Parasiuk theorem on renormalization, Commun. Math. Phys. 2 (1966) 301–326, http://www.projecteuclid.org/euclid.cmp/1103815087. doi:10.1007/BF01773358.

[118] T. Binoth, G. Heinrich, An automatized algorithm to compute infrared divergent multi-loop integrals, Nucl. Phys. B585 (2000) 741–759. arXiv:hep-ph/0004013v.2.

[119] A. V. Smirnov, FIESTA 3: cluster-parallelizable multiloop numerical calculations in physical regions, Comput. Phys. Commun. 185 (2014) 2090–2100. arXiv:1312.3186, doi:10.1016/j.cpc.2014.03.015.

[120] S. Borowka, J. Carter, G. Heinrich, Numerical Evaluation of Multi-Loop Integrals for Arbitrary Kinematics with SecDec 2.0, Comput. Phys. Commun. 184 (2013) 396–408. arXiv:1204.4152, doi:10.1016/j.cpc.2012.09.020.

[121] S. Borowka, G. Heinrich, S. Jahn, S. P. Jones, M. Kerner, J. Schlenk, T. Zirke, pySecDec: a toolbox for the numerical evaluation of multi-scale integralsarXiv:1703.09692.

[122] J. Gluza, K. Kajda, T. Riemann, AMBRE - a Mathematica package for the construction of Mellin-Barnes representations for Feynman integrals, Comput. Phys. Commun. 177 (2007) 879–893. arXiv:0704.2423, doi:10.1016/j.cpc.2007.07.001.

[123] J. Gluza, K. Kajda, T. Riemann, V. Yundin, Numerical Evaluation of Tensor Feynman Integrals in Euclidean Kinematics, Eur. Phys. J. C71 (2011) 1516. arXiv:1010.1667, doi:10.1140/epjc/s10052-010-1516-y.

[124] AMBRE webpage: http://prac.us.edu.pl/~gluza/ambre.

[125] K. Bielas, I. Dubovyk, PlanarityTest 1.1 (January 2014), a Mathematica package for testing the planarity of Feynman diagrams, http://us.edu.pl/~gluza/ambre/planarity/, [126].

[126] K. Bielas, I. Dubovyk, J. Gluza, T. Riemann, Some Remarks on Non-planar Feynman Diagrams, Acta Phys. Polon. B44 (11) (2013) 2249–2255. arXiv:1312.5603, doi:10.5506/APhysPolB.44.2249.

[127] M. Czakon, Automatized analytic continuation of Mellin-Barnes integrals, Comput. Phys. Commun. 175 (2006) 559–571. arXiv:hep-ph/0511200, doi:10.1016/j.cpc.2006.07.002.

[128] A. Smirnov, V. Smirnov, On the Resolution of Singularities of Multiple Mellin-Barnes Integrals, Eur. Phys. J. C62 (2009) 445–449. arXiv:0901.0386, doi:10.1140/epjc/s10052-009-1039-6.

[129] J. Usovitsch, I. Dubovyk, T. Riemann, Numerical calculation of multiple MB-integral representations for Feynman integrals. J. Usovitsch, MBnumerics, a Mathematica/Fortran package, to be made available at http://prac.us.edu.pl/~gluza/ambre/.

[130] J. Usovitsch, I. Dubovyk, T. Riemann, MBnumerics: Numerical integration of Mellin-Barnes integrals in physical regions, PoS LL2018 (2018) 046. arXiv:1810.04580, doi:10.22323/1.303.0046.

[131] R. Pittau, A four-dimensional approach to quantum field theories, JHEP 11 (2012) 151. arXiv:1208.5457, doi:10.1007/JHEP11(2012)151.

[132] B. Page, R. Pittau, Two-loop off-shell QCD amplitudes in FDR, JHEP 11 (2015) 183. arXiv:1506.09093, doi:10.1007/JHEP11(2015)183.

[133] R. Pittau, QCD corrections to $H \to gg$ in FDR, Eur. Phys. J. C74 (1) (2014) 2686. arXiv:1307.0705, doi:10.1140/epjc/s10052-013-2686-1.

[134] G. F. R. Sborlini, F. Driencourt-Mangin, G. Rodrigo, Four-dimensional unsubtraction with massive particles, JHEP 10 (2016) 162. arXiv:1608.01584, doi:10.1007/JHEP10(2016)162.

[135] G. F. R. Sborlini, F. Driencourt-Mangin, R. Hernandez-Pinto, G. Rodrigo, Four-dimensional unsubtraction from the loop-tree duality, JHEP 08 (2016) 160. arXiv:1604.06699, doi:10.1007/JHEP08(2016)160.

[136] S. Buchta, G. Chachamis, P. Draggiotis, G. Rodrigo, Numerical implementation of the loop-tree duality method, Eur. Phys. J. C77 (5) (2017) 274. arXiv:1510.00187, doi:10.1140/epjc/s10052-017-4833-6.

[137] B. Page, S. Abreu, F. Febres Cordero, H. Ita, M. Jaquier, M. Zeng, First two-loop amplitudes with the numerical unitarity method, PoS RADCOR2017 (2018) 012. doi:10.22323/1.290.0012.

[138] S. Abreu, F. Febres Cordero, H. Ita, B. Page, M. Zeng, Five-Point Two-Loop Amplitudes from Numerical Unitarity, in: 14th DESY Workshop on Elementary Particle

Physics: Loops and Legs in Quantum Field Theory 2018 (LL2018) St Goar, Germany, April 29-May 4, 2018, 2018. arXiv:1807.09447.

[139] A. Blondel, et al., Theory report on the 11th FCC-ee workshop, 2019. arXiv:1905.05078.

[140] M. C. Bergere, Y.-M. P. Lam, Asymptotic expansion of Feynman amplitudes. Part 1: The convergent case, Commun. Math. Phys. 39 (1974) 1. doi:10.1007/BF01609168.

[141] N. I. Usyukina, On a Representation for Three Point Function, Teor. Mat. Fiz. 22 (1975) 300–306, http://www.mathnet.ru/php/getFT.phtml?jrnid=tmf&paperid=3683&what=fullt&option_lang=eng. doi:10.1007/BF01037795.

[142] V. A. Smirnov, Analytical result for dimensionally regularized massless on shell double box, Phys. Lett. B460 (1999) 397–404. arXiv:hep-ph/9905323, doi:10.1016/S0370-2693(99)00777-7.

[143] J. Tausk, Nonplanar massless two loop Feynman diagrams with four on-shell legs, Phys. Lett. B469 (1999) 225–234. arXiv:hep-ph/9909506, doi:10.1016/S0370-2693(99)01277-0.

[144] E. W. Barnes, A new development of the theory of the hypergeometric functions, Proc. Lond. Math. Soc. (2) 6 (1908) 141–177. doi:10.1112/plms/s2-6.1.141.

[145] E. Boos, A. I. Davydychev, A Method of evaluating massive Feynman integrals, Theor. Math. Phys. 89 (1991) 1052–1063. doi:10.1007/BF01016805.

[146] J. Gluza, T. Jelinski, D. A. Kosower, Efficient Evaluation of Massive Mellin-Barnes Integrals, Phys. Rev. D95 (7) (2017) 076016. arXiv:1609.09111, doi:10.1103/PhysRevD.95.076016.

[147] M. Czakon (MB, MBasymptotics), D. Kosower (barnesroutines), A. Smirnov, V. Smirnov (MBresolve), K. Bielas, I. Dubovyk, J. Gluza, K. Kajda, T. Riemann (AMBRE, PlanarityTest), MBtools webpage, https://mbtools.hepforge.org/.

[148] J. Blümlein, I. Dubovyk, J. Gluza, M. Ochman, C. G. Raab, T. Riemann, C. Schneider, Non-planar Feynman integrals, Mellin-Barnes representations, multiple sums, PoS LL2014 (2014) 052. arXiv:1407.7832.

[149] G. Heinrich, V. Smirnov, Analytical evaluation of dimensionally regularized massive on-shell double boxes, Phys. Lett. B598 (2004) 55–66. arXiv:hep-ph/0406053.

[150] M. Czakon, A. Mitov, S. Moch, Heavy-quark production in gluon fusion at two loops in QCD, Nucl. Phys. B798 (2008) 210–250. arXiv:0707.4139, doi:10.1016/j.nuclphysb.2008.02.001.

[151] K. Bielas, I. Dubovyk, PlanarityTest 1.2.1 (Aug 2017), a Mathematica package for testing the planarity of Feynman diagrams, http://us.edu.pl/~gluza/ambre/planarity/, [126].

[152] K. Kajda, I. Dubovyk, AMBRE 2.2 (12 Sep 2015), a Mathematica package representing Feynman integrals by Mellin-Barnes integrals, available at http://prac.us.edu.pl/~gluza/ambre/, [123].

[153] I. Dubovyk, AMBRE 3.0 (1 Sep 2015), a Mathematica package representing Feynman integrals by Mellin-Barnes integrals, available at http://prac.us.edu.pl/~gluza/ambre/, [123, 163].

[154] A. Smirnov, Mathematica program MBresolve.m version 1.0 (Jan 2009), available at the MB Tools webpage http://projects.hepforge.org/mbtools/, [128].

[155] D. Kosower, Mathematica program barnesroutines.m version 1.1.1 (July 23, 2009), available at the MB Tools webpage, http://projects.hepforge.org/mbtools/.

[156] M. Ochman, T. Riemann, MBsums - a Mathematica package for the representation of Mellin-Barnes integrals by multiple sums, Acta Phys. Polon. B46 (11) (2015) 2117. arXiv:1511.01323, doi:10.5506/APhysPolB.46.2117.

[157] Silesia U., Katowice, webpage http://prac.us.edu.pl/~gluza/ambre.

[158] I. Dubovyk, T. Riemann, J. Usovitsch, MBnumerics, a Mathematica-Fortran package, to be made available at http://prac.us.edu.pl/~gluza/ambre/.

[159] T. Hahn, CUBA: A Library for multidimensional numerical integration, Comput. Phys. Commun. 168 (2005) 78–95. arXiv:hep-ph/0404043, doi:10.1016/j.cpc.2005.01.010.

[160] J. Gluza, F. Haas, K. Kajda, T. Riemann, Automatizing the application of Mellin-Barnes representations for Feynman integrals, PoS ACAT2007 (2007) 081, https://cds.cern.ch/record/1048613/files/ACAT-081.pdf. arXiv:0707.3567.

[161] J. Gluza, K. Kajda, T. Riemann, V. Yundin, New results for loop integrals: AMBRE, CSectors, hexagon, PoS ACAT08 (2008) 124, https://pos.sissa.it/070/124/pdf. arXiv:0902.4830.

[162] J. Gluza, K. Kajda, T. Riemann, V. Yundin, News on Ambre and CSectors, Nucl. Phys. Proc. Suppl. 205-206 (2010) 147–151. arXiv:1006.4728, doi:10.1016/j.nuclphysbps.2010.08.034.

[163] I. Dubovyk, J. Gluza, T. Riemann, Non-planar Feynman diagrams and Mellin-Barnes representations with *AMBRE* 3.0, J. Phys. Conf. Ser. 608 (1) (2015) 012070. doi:10.1088/1742-6596/608/1/012070.

[164] I. Dubovyk, J. Gluza, T. Jelinski, T. Riemann, J. Usovitsch, New prospects for the numerical calculation of Mellin-Barnes integrals in Minkowskian kinematics, Acta Phys. Polon. B48 (2017) 995. arXiv:1704.02288, doi:10.5506/APhysPolB.48.995.

[165] M. Prausa, Mellin-Barnes meets Method of Brackets: a novel approach to Mellin-Barnes representations of Feynman integrals, Eur. Phys. J. C77 (9) (2017) 594. arXiv:1706.09852, doi:10.1140/epjc/s10052-017-5150-9.

[166] A. Freitas, Y.-C. Huang, Electroweak two-loop corrections to $sin^2\theta^{b\bar{b}}_{\rm eff}$ and R_b using numerical Mellin-Barnes integrals, JHEP 1208 (2012) 050. arXiv:1205.0299, doi:10.1007/JHEP08(2012)050.

[167] I. Gonzalez, I. Schmidt, Optimized negative dimensional integration method (NDIM) and multiloop Feynman diagram calculation, Nucl. Phys. B769 (2007) 124–173. arXiv:hep-th/0702218, doi:10.1016/j.nuclphysb.2007.01.031.

[168] I. Gonzalez, V. H. Moll, Definite integrals by the method of brackets. Part 1. arXiv:0812.3356.

[169] I. Gonzalez, Method of Brackets and Feynman diagrams evaluation, Nucl. Phys. Proc. Suppl. 205-206 (2010) 141–146. arXiv:1008.2148, doi:10.1016/j.nuclphysbps.2010.08.033.

[170] P. Cvitanovic, T. Kinoshita, Feynman-Dyson rules in parametric space, Phys. Rev. D10 (1974) 3978–3991. doi:10.1103/PhysRevD.10.3978.

[171] C. Bogner, S. Weinzierl, Feynman graph polynomials, Int. J. Mod. Phys. A25 (2010) 2585–2618. arXiv:1002.3458, doi:10.1142/S0217751X10049438.

[172] N. Nakanishi, Graph theory and Feynman integrals, Mathematics and its applications, Gordon and Breach, 1971.
URL https://books.google.ch/books?id=5f7uAAAAMAAJ

[173] S. Wolfram, the Mathematica book, Wolfram media/Cambridge University Press, 2003.

[174] V. Smirnov, "Applied Asymptotic Expansions in Momenta and Masses" (Springer Verlag, Berlin, 2002).

[175] R. Boels, B. A. Kniehl, G. Yang, Master integrals for the four-loop Sudakov form factor, Nucl. Phys. B902 (2016) 387–414. arXiv:1508.03717, doi:10.1016/j.nuclphysb.2015.11.016.

[176] U. Aglietti, R. Bonciani, Master integrals with 2 and 3 massive propagators for the 2 loop electroweak form-factor - planar case, Nucl. Phys. B698 (2004) 277–318. arXiv:hep-ph/0401193, doi:10.1016/j.nuclphysb.2004.07.018.

[177] U. Aglietti, R. Bonciani, Master integrals with one massive propagator for the two-loop electroweak form factor, Nucl. Phys. B668 (2003) 3–76. arXiv:hep-ph/0304028.

[178] A. Djouadi, C. Verzegnassi, Virtual very heavy top effects in LEP/SLC precision measurements, Phys. Lett. B195 (1987) 265.

[179] A. Djouadi, ($\alpha\alpha_f$) Vacuum Polarization Functions of the Standard Model Gauge Bosons, Nuovo Cim. A100 (1988) 357. doi:10.1007/BF02812964.

[180] B. A. Kniehl, Two loop corrections to the vacuum polarizations in perturbative QCD, Nucl. Phys. B347 (1990) 86–104. doi:10.1016/0550-3213(90)90552-O.

[181] B. A. Kniehl, A. Sirlin, Dispersion relations for vacuum polarization functions in electroweak physics, Nucl. Phys. B371 (1992) 141–148. doi:10.1016/0550-3213(92)90232-Z.

[182] A. Djouadi, P. Gambino, Electroweak gauge bosons selfenergies: Complete QCD corrections, Phys. Rev. D49 (1994) 3499–3511, Erratum: Phys. Rev. D53 (1996) 4111. arXiv:hep-ph/9309298, doi:10.1103/PhysRevD.49.3499,10.1103/PhysRevD.53.4111.

[183] R. Barbieri, M. Beccaria, P. Ciafaloni, G. Curci, A. Vicere, Radiative correction effects of a very heavy top, Phys. Lett. B288 (1992) 95–98, [Erratum: Phys. Lett.B312,511(1993)]. arXiv:hep-ph/9205238, doi:10.1016/0370-2693(93)90990-Y,10.1016/0370-2693(92)91960-H.

[184] R. Barbieri, M. Beccaria, P. Ciafaloni, G. Curci, A. Vicere, Two loop heavy top effects in the Standard Model, Nucl. Phys. B409 (1993) 105–127, doi:10.1016/0550–3213(93)90448–X. doi:10.1016/0550-3213(93)90448-X.

[185] J. Fleischer, O. V. Tarasov, F. Jegerlehner, Two loop heavy top corrections to the rho parameter: A Simple formula valid for arbitrary Higgs mass, Phys. Lett. B319 (1993) 249–256. doi:10.1016/0370-2693(93)90810-5.

[186] J. Fleischer, O. V. Tarasov, F. Jegerlehner, Two loop large top mass corrections to electroweak parameters: Analytic results valid for arbitrary Higgs mass, Phys. Rev. D51 (1995) 3820–3837. doi:10.1103/PhysRevD.51.3820.

[187] G. Degrassi, P. Gambino, A. Vicini, Two loop heavy top effects on the m(Z) - m(W) interdependence, Phys. Lett. B383 (1996) 219–226. arXiv:hep-ph/9603374, doi:10.1016/0370-2693(96)00720-4.

[188] G. Degrassi, P. Gambino, A. Sirlin, Precise calculation of m_w, $\sin^2\hat{\theta}_w$, m_z, and $\sin^2\theta_{eff}^{lept}$, Phys. Lett. B394 (1997) 188–194. arXiv:hep-ph/9611363, doi:10.1016/S0370-2693(96)01677-2.

[189] G. Degrassi, P. Gambino, Two loop heavy top corrections to the Z^0 boson partial widths, Nucl. Phys. B567 (2000) 3–31. arXiv:hep-ph/9905472, doi:10.1016/S0550-3213(99)00729-4.

[190] A. Freitas, W. Hollik, W. Walter, G. Weiglein, Complete fermionic two loop results for the $M_W - M_Z$ interdependence, Phys. Lett. B495 (2000) 338–346, , Erratum–ibid. B570 (2003) 260–264, hep–ph/0007091v3. doi:10.1016/S0370-2693(00)01263-6.

[191] A. Freitas, W. Hollik, W. Walter, G. Weiglein, Electroweak two loop corrections to the $M_W - M_Z$ mass correlation in the Standard Model, Nucl. Phys. B632 (2002) 189–218, E: B666 (2003) 305–307, hep–ph/0202131v4. doi:10.1016/S0550-3213(02)00243-2.

[192] M. Awramik, M. Czakon, A. Freitas, G. Weiglein, Complete two-loop electroweak fermionic corrections to $\sin^2\theta^{\rm lept}_{\rm eff}$ and indirect determination of the Higgs boson mass, Phys. Rev. Lett. 93 (2004) 201805. arXiv:hep-ph/0407317, doi:10.1103/PhysRevLett.93.201805.

[193] W. Hollik, U. Meier, S. Uccirati, The effective electroweak mixing angle $\sin^2\theta^{\rm eff}$ with two-loop fermionic contributions, Nucl. Phys. B731 (2005) 213–224. arXiv:hep-ph/0507158, doi:10.1016/j.nuclphysb.2005.10.015.

[194] A. Freitas, Two-loop fermionic electroweak corrections to the Z-boson width and production rate, Phys. Lett. B730 (2014) 50–52. arXiv:1310.2256, doi:10.1016/j.physletb.2014.01.017.

[195] L. Avdeev, J. Fleischer, S. Mikhailov, O. Tarasov, $O(\alpha\alpha_s^2)$ correction to the electroweak ρ parameter, Phys. Lett. B336 (1994) 560–566, doi:10.1016/0370–2693(94)90573–8, Erratum–ibid. B349 (1995) 597–598, hep–ph/9406363v2. doi:10.1016/0370-2693(94)90573-8.

[196] K. Chetyrkin, J. H. Kühn, M. Steinhauser, Corrections of order $O(G_F M_t^2 \alpha_s^2)$ to the ρ parameter, Phys. Lett. B351 (1995) 331–338, doi:10.1016/0370–2693(95)00380–4. arXiv:hep-ph/9502291, doi:10.1016/0370-2693(95)00380-4.

[197] J. J. van der Bij, K. G. Chetyrkin, M. Faisst, G. Jikia, T. Seidensticker, Three loop leading top mass contributions to the ρ parameter, Phys. Lett. B498 (2001) 156–162. arXiv:hep-ph/0011373, doi:10.1016/S0370-2693(01)00002-8.

[198] M. Faisst, J. H. Kühn, T. Seidensticker, O. Veretin, Three loop top quark contributions to the ρ parameter, Nucl. Phys. B665 (2003) 649–662. arXiv:hep-ph/0302275, doi:10.1016/S0550-3213(03)00450-4.

[199] Y. Schröder, M. Steinhauser, Four-loop singlet contribution to the ρ parameter, Phys. Lett. B622 (2005) 124–130. arXiv:hep-ph/0504055, doi:10.1016/j.physletb.2005.06.085.

[200] K. G. Chetyrkin, M. Faisst, J. H. Kühn, P. Maierhofer, C. Sturm, Four-loop QCD corrections to the rho parameter, Phys. Rev. Lett. 97 (2006) 102003. arXiv:hep-ph/0605201, doi:10.1103/PhysRevLett.97.102003.

[201] R. Boughezal, M. Czakon, Single scale tadpoles and $O(G_F m_t^2 \alpha(s)^3)$ corrections to the ρ parameter, Nucl. Phys. B755 (2006) 221–238. arXiv:hep-ph/0606232, doi:10.1016/j.nuclphysb.2006.08.007.

[202] M. Awramik, M. Czakon, Complete two loop bosonic contributions to the muon lifetime in the standard model, Phys. Rev. Lett. 89 (2002) 241801. arXiv:hep-ph/0208113, doi:10.1103/PhysRevLett.89.241801.

[203] M. Awramik, M. Czakon, Complete two loop electroweak contributions to the muon lifetime in the standard model, Phys. Lett. B568 (2003) 48–54. arXiv:hep-ph/0305248, doi:10.1016/j.physletb.2003.06.007.

[204] A. Onishchenko, O. Veretin, Two loop bosonic electroweak corrections to the muon lifetime and $M_Z - M_W$ interdependence, Phys. Lett. B551 (2003) 111–114. arXiv:hep-ph/0209010, doi:10.1016/S0370-2693(02)03004-6.

[205] M. Awramik, M. Czakon, A. Freitas, G. Weiglein, Precise prediction for the W boson mass in the Standard Model, Phys. Rev. D69 (2004) 053006. arXiv:hep-ph/0311148, doi:10.1103/PhysRevD.69.053006.

[206] W. Hollik, U. Meier, S. Uccirati, The effective electroweak mixing angle $\sin^2\theta^{\rm eff}$ with two-loop bosonic contributions, Nucl. Phys. B765 (2007) 154–165. arXiv:hep-ph/0610312, doi:10.1016/j.nuclphysb.2006.12.001.

[207] M. Awramik, M. Czakon, A. Freitas, Electroweak two-loop corrections to the effective weak mixing angle, JHEP 0611 (2006) 048. arXiv:hep-ph/0608099, doi:10.1088/1126-6708/2006/11/048.

[208] K. Olive, et al., Review of Particle Physics, Chin. Phys. C38 (2014) 090001. doi:10.1088/1674-1137/38/9/090001.

[209] D. Y. Bardin, A. Leike, T. Riemann, M. Sachwitz, Energy Dependent Width Effects in e^+e^- Annihilation Near the Z Boson Pole, Phys. Lett. B206 (1988) 539–542. doi:10.1016/0370-2693(88)91625-5.

[210] K. G. Chetyrkin, J. H. Kuhn, A. Kwiatkowski, QCD corrections to the e^+e^- cross-section and the Z boson decay rate, CERN 95-03. See also: QCD corrections to the e^+e^- cross-section and the Z boson decay rate: Concepts and results, LBL-36678-REV and Phys. Rept. 277 (1996) 189-281. arXiv:hep-ph/9503396, doi:10.1016/S0370-1573(96)00012-9.

[211] P. Baikov, K. Chetyrkin, J. Kühn, Order α_s^4 QCD Corrections to Z and τ Decays, Phys. Rev. Lett. 101 (2008) 012002. arXiv:0801.1821, doi:10.1103/PhysRevLett.101.012002.

[212] A. Kataev, Higher order $O(\alpha^2)$ and $O(\alpha\alpha_s)$ corrections to $\sigma_{tot}(e^+e^- \to hadrons)$ and Z-boson decay rate, Phys. Lett. B287 (1992) 209–212. doi:10.1016/0370-2693(92)91901-K.

[213] M. Steinhauser, Leptonic contribution to the effective electromagnetic coupling constant up to three loops, Phys. Lett. B429 (1998) 158–161. arXiv:hep-ph/9803313, doi:10.1016/S0370-2693(98)00503-6.

[214] M. Davier, A. Hoecker, B. Malaescu, Z. Zhang, Reevaluation of the hadronic vacuum polarisation contributions to the Standard Model predictions of the muon $g-2$ and $\alpha(m_Z^2)$ using newest hadronic cross-section data, Eur. Phys. J. C77 (12) (2017) 827. arXiv:1706.09436, doi:10.1140/epjc/s10052-017-5161-6.

[215] F. Jegerlehner, Variations on Photon Vacuum Polarization, arXiv:1711.06089.

[216] A. Keshavarzi, D. Nomura, T. Teubner, The muon $g-2$ and $\alpha(M_Z^2)$: a new data-based analysis, Phys. Rev. D97 (11) (2018) 114025. arXiv:1802.02995, doi:10.1103/PhysRevD.97.114025.

[217] C. Patrignani, et al., Review of Particle Physics, Chin. Phys. C40 (10) (2016) 100001. doi:10.1088/1674-1137/40/10/100001.

[218] M. Davier, A. Hoecker, B. Malaescu, Z. Zhang, Reevaluation of the Hadronic Contributions to the Muon g-2 and to $\alpha(M_Z)$, Eur. Phys. J. C71 (2011) 1515, [Erratum: Eur. Phys. J. C72,1874(2012)]. arXiv:1010.4180, doi:10.1140/epjc/s10052-012-1874-8,10.1140/epjc/s10052-010-1515-z.

[219] J. Fleischer, O. V. Tarasov, F. Jegerlehner, P. Raczka, Two loop $O(\alpha_s G_\mu m_t^2)$ corrections to the partial decay width of the Z^0 into $b\bar{b}$ final states in the large top mass limit, Phys. Lett. B293 (1992) 437–444. doi:10.1016/0370-2693(92)90909-N.

[220] G. Buchalla, A. J. Buras, QCD corrections to the $\bar{s}dZ$ vertex for arbitrary top quark mass, Nucl. Phys. B398 (1993) 285–300. doi:10.1016/0550-3213(93)90110-B.

[221] G. Degrassi, Current algebra approach to heavy top effects in $Z \to b + \bar{b}$, Nucl. Phys. B407 (1993) 271–289. arXiv:hep-ph/9302288, doi:10.1016/0550-3213(93)90058-W.

[222] K. Chetyrkin, A. Kwiatkowski, M. Steinhauser, Leading top mass corrections of order $O(\alpha\alpha_s m_t^2/M_W^2)$ to partial decay rate $\Gamma(Z \to b\bar{b})$, Mod. Phys. Lett. A8 (1993) 2785–2792, doi:10.1142/S0217732393003172. doi:10.1142/S0217732393003172.

[223] A. Czarnecki, J. H. Kühn, Nonfactorizable QCD and electroweak corrections to the hadronic Z boson decay rate, Phys. Rev. Lett. 77 (1996) 3955–3958. arXiv:hep-ph/9608366.

[224] R. Harlander, T. Seidensticker, M. Steinhauser, Complete corrections of order $O(\alpha\alpha_s)$ to the decay of the Z boson into bottom quarks, Phys. Lett. B426 (1998) 125–132. arXiv:hep-ph/9712228, doi:10.1016/S0370-2693(98)00220-2.

[225] S. Bauberger, F. A. Berends, M. Böhm, M. Buza, Analytical and numerical methods for massive two loop selfenergy diagrams, Nucl. Phys. B434 (1995) 383–407. arXiv:hep-ph/9409388, doi:10.1016/0550-3213(94)00475-T.

[226] S. Bauberger, M. Böhm, Simple one-dimensional integral representations for two loop selfenergies: The master diagram, Nucl. Phys. B445 (1995) 25–48. arXiv:hep-ph/9501201, doi:10.1016/0550-3213(95)00199-3.

[227] M. Czakon, M. Awramik, A. Freitas, Bosonic corrections to the effective leptonic weak mixing angle at the two-loop level, Nucl. Phys. Proc. Suppl. 157 (2006) 58–62. arXiv:hep-ph/0602029, doi:10.1016/j.nuclphysbps.2006.03.036.

[228] A. Freitas, K. Hagiwara, S. Heinemeyer, P. Langacker, K. Moenig, M. Tanabashi, G. W. Wilson, Exploring Quantum Physics at the ILC, in: Proceedings, 2013 Community Summer Study on the Future of U.S. Particle Physics: Snowmass on the Mississippi (CSS2013): Minneapolis, MN, USA, July 29-August 6, 2013, 2013. arXiv:1307.3962.
URL http://inspirehep.net/record/1242667/files/arXiv:1307.3962.pdf

[229] A. Freitas, Electroweak precision tests in the LHC era and Z-decay form factors at two-loop level, in: Proceedings, 12th DESY Workshop on Elementary Particle Physics: Loops and Legs in Quantum Field Theory (LL2014): Weimar, Germany, April 27-May 2, 2014, 2014. arXiv:1406.6980.

[230] "Motivation: Experimental capabilities and requirements", talk held by A. Blondel at [24], https://indico.cern.ch/event/669224/contributions/2805398/attachments/1581811/2499870/Blondel-FCC-ee-physics_case_and_theory_errors-v2.pdf.

[231] S. Borowka, G. Heinrich, S. P. Jones, M. Kerner, J. Schlenk, T. Zirke, SecDec-3.0: numerical evaluation of multi-scale integrals beyond one loop, Comput. Phys. Commun. 196 (2015) 470–491. arXiv:1502.06595, doi:10.1016/j.cpc.2015.05.022.

[232] S. Actis, M. Czakon, J. Gluza, T. Riemann, Virtual hadronic and leptonic contributions to Bhabha scattering, Phys. Rev. Lett. 100 (2008) 131602. arXiv:0711.3847, doi:10.1103/PhysRevLett.100.131602.

[233] S. Actis, M. Czakon, J. Gluza, T. Riemann, Virtual Hadronic and Heavy-Fermion $O(\alpha^2)$ Corrections to Bhabha Scattering, Phys. Rev. D78 (2008) 085019. arXiv:0807.4691, doi:10.1103/PhysRevD.78.085019.